UNITED STATES AIR FORCE

SUMMER RESEARCH PROGRAM -- 1997

SUMMER FACULTY RESEARCH PROGRAM FINAL REPORTS

VOLUME 2A

ARMSTRONG LABORATORY

RESEARCH & DEVELOPMENT LABORATORIES

5800 Uplander Way

Culver City, CA 90230-6608

Program Director, RDL
Gary Moore

Program Manager, AFOSR
Major Linda Steel-Goodwin

Program Manager, RDL
Scott Licoscos

Program Administrator, RDL
Johnetta Thompson

Program Administrator, RDL
Rebecca Kelly-Clemmons

Submitted to:

AIR FORCE OFFICE OF SCIENTIFIC RESEARCH

Bolling Air Force Base

Washington, D.C.

December 1997

20010319 065

AQM01-06-1195

REPORT DOCUMENTATION PAGE

AFRL-SR-BL-TR-00-

0751

Public reporting burden for this collection of information is estimated to average 1 hour per response, including the time for reviewing instructions, s
the collection of information. Send comments regarding this burden estimate or any other aspect of this collection of information, including su
Operations and Reports, 1215 Jefferson Davis Highway, Suite 1204, Arlington, VA 22202-4302, and to the Office of Management and Budget, Pa,
d reviewing
Information

1. AGENCY USE ONLY *(Leave blank)*	2. REPORT DATE	3. REPORT TYPE AND DATES COVERED
	December, 1997	

4. TITLE AND SUBTITLE
1997 Summer Research Program (SRP), Summer Faculty Research Program (SFRP), Final Reports, Volume 2A, Armstrong Laboratory

5. FUNDING NUMBERS
F49620-93-C-0063

6. AUTHOR(S)
Gary Moore

7. PERFORMING ORGANIZATION NAME(S) AND ADDRESS(ES)
Research & Development Laboratories (RDL)
5800 Uplander Way
Culver City, CA 90230-6608

8. PERFORMING ORGANIZATION REPORT NUMBER

9. SPONSORING/MONITORING AGENCY NAME(S) AND ADDRESS(ES)
Air Force Office of Scientific Research (AFOSR)
801 N. Randolph St.
Arlington, VA 22203-1977

10. SPONSORING/MONITORING AGENCY REPORT NUMBER

11. SUPPLEMENTARY NOTES

12a. DISTRIBUTION AVAILABILITY STATEMENT
Approved for Public Release

12b. DISTRIBUTION CODE

13. ABSTRACT *(Maximum 200 words)*

The United States Air Force Summer Research Program (USAF-SRP) is designed to introduce university, college, and technical institute faculty members, graduate students, and high school students to Air Force research. This is accomplished by the faculty members (Summer Faculty Research Program, (SFRP)), graduate students (Graduate Student Research Program (GSRP)), and high school students (High School Apprenticeship Program (HSAP)) being selected on a nationally advertised competitive basis during the summer intersession period to perform research at Air Force Research Laboratory (AFRL) Technical Directorates, Air Force Air Logistics Centers (ALC), and other AF Laboratories. This volume consists of a program overview, program management statistics, and the final technical reports from the SFRP participants at the Armstrong Laboratory.

14. SUBJECT TERMS
Air Force Research, Air Force, Engineering, Laboratories, Reports, Summer, Universities, Faculty, Graduate Student, High School Student

15. NUMBER OF PAGES

16. PRICE CODE

17. SECURITY CLASSIFICATION OF REPORT	18. SECURITY CLASSIFICATION OF THIS PAGE	19. SECURITY CLASSIFICATION OF ABSTRACT	20. LIMITATION OF ABSTRACT
Unclassified	Unclassified	Unclassified	UL

SFRP FINAL REPORT TABLE OF CONTENTS i-xviii

1. INTRODUCTION 1
2. PARTICIPATION IN THE SUMMER RESEARCH PROGRAM 2
3. RECRUITING AND SELECTION 3
4. SITE VISITS 4
5. HBCU/MI PARTICIPATION 4
6. SRP FUNDING SOURCES 5
7. COMPENSATION FOR PARTICIPATIONS 5
8. CONTENTS OF THE 1996 REPORT 6

APPENDICIES:

A. PROGRAM STATISTICAL SUMMARY A-1
B. SRP EVALUATION RESPONSES B-1

SFRP FINAL REPORTS

PREFACE

Reports in this volume are numbered consecutively beginning with number 1. Each report is paginated with the report number followed by consecutive page numbers, e.g., 1-1, 1-2, 1-3; 2-1, 2-2, 2-3.

Due to its length, Volume 2 is bound in two parts, 2A and 2B. Volume 2A contains #1-20. Volume 2B contains reports #21-36. The Table of Contents for Volume 2 is included in both parts.

This document is one of a set of 16 volumes describing the 1997 AFOSR Summer Research Program. The following volumes comprise the set:

VOLUME	TITLE
1	Program Management Report
	Summer Faculty Research Program (SFRP) Reports
2A & 2B	Armstrong Laboratory
3A & 3B	Phillips Laboratory
4A & 4B	Rome Laboratory
5A, 5B & 5C	Wright Laboratory
6	Arnold Engineering Development Center, U.S. Air Force Academy, Air Logistic Centers, and Wilford Hall Medical Center
	Graduate Student Research Program (GSRP) Reports
7	Armstrong Laboratory
8	Phillips Laboratory
9	Rome Laboratory
10A & 10B	Wright Laboratory
11	Arnold Engineering Development Center, U.S. Air Force Academy, Air Logistic Centers, and Wilford Hall Medical Center
	High School Apprenticeship Program (HSAP) Reports
12A & 12B	Armstrong Laboratory
13	Phillips Laboratory
14	Rome Laboratory
15A&15B	Wright Laboratory
16	Arnold Engineering Development Center

SRP Final Report Table of Contents

Author	University/Institution Report Title	Armstrong Laboratory Directorate	Vol-Page
DR Jean M Andino	University of Florida , Gainesville , FL Atmospheric Reactions of Volatille Paint Components a Modeling Approach	AL/EQL	2- 1
DR Anthony R Andrews	Ohio University , Athens , OH Novel Electrochemiluminescence Reactions and Instrumentation	AL/EQL	2- 2
DR Stephan B Bach	Univ of Texas at San Antonio , San Antonio , TX Investigation of Sampling Interfaces for Portable Mass Spectormetry and a survery of field Portable	AL/OEA	2- 3
DR Marilyn Barger	Florida A&M-FSU College of Engineering , Tallahassee , FL Analysis for The Anaerobic Metabolites of Toulene at Fire Training Area 23 Tyndall AFB, Florida	AL/EQL	2- 4
DR Dulal K Bhaumik	University of South Alabama , Mobile , AL The Net Effect of a Covariate in Analysis of Covariance	AL/AOEP	2- 5
DR Marc L Carter, PhD, PA	Hofstra University , Hempstead , NY Assessment of the Reliability of Ground Based Observeres for the Detecton of Aircraft	AL/OEO	2- 6
DR Huseyin M Cekirge	Florida State University , Tallahassee , FL Developing a Relational Database for Natural Attenuation Field Data	AL/EQL	2- 7
DR Cheng Cheng	Johns Hopkins University , Baltimore , MD Investigation of Two Statistical Issues in Building a Classification System	AL/HRM	2- 8
DR Gerald P Chubb	Ohio State University , Columbus , OH Use of Air Synthetic Forces For GCI Training Exercises	AL/HR1	2- 9
DR Sneed B Collard, Jr.	University of West Florida , Pensacola , FL Suitability of Ascidians as Trace Metal Biosenosrs-Biomonitors In Marine Environments An Assessment	AL/EQL	2- 10
DR Catherine A Cornwell	Syracuse University , Syracuse , NY Rat Ultrasoud Vocalization Development and Neurochemistry in Stress-Sensitive Brain Regions	AL/OER	2- 11

SRP Final Report Table of Contents

Author	University/Institution Report Title	Armstrong Laboratory Directorate	Vol-Pag
DR Baolin Deng	New Mexico Tech , Socorro , NM Effect of Iron Corrosion Inhibitors on Reductive Degradation of Chlorinated Solvents	AL/EQL	2- 1
DR Micheal P Dooley	Iowa State University , Ames , IA Copulatory Response Fertilizing Potential, and Sex Ratio of Offsprings Sired by male rats Ecposed in	AL/OER	2- 1
DR Itiel E Dror	Miami University , Oxford , OH The Effect of Visual Similarity and Reference Frame Alignment on the Recognition of Military Aircraf	AL/HRT	2- 1
DR Brent D Foy	Wright State University , Dayton , OH Advances in Biologivcally-Based Kinetic Modeling for Toxicological Applications	AFRL/HES	2- 1
DR Irwin S Goldberg	St. Mary's Univ , San Antonio , TX Mixing and Streaming of a Fluid Near the Entrance of a Tube During Oscillatory Flow	AL/OES	2- 16
DR Ramesh C Gupta	University of Maine at Orono , Orono , ME A Dynamical system approach in Biomedical Research	ALOES	2- 17
DR John R Herbold	Univ of Texas at San Antonio , San Antonio , TX A Protocol for Development of Amplicons for a Rapid and Efficient Methoiid of Genotyping Hepatitis C	AL/AOEL	2- 18
DR Andrew E Jackson	Arizona State University , Mesa , AZ Development fo a Conceptual Design for an Information Systems Infrastructure To Support the Squadron	AL/HRA	2- 19
DR Charles E Lance	Univ of Georgia Res Foundation , Athens , GA Replication and Extension of the Schmidt, Hunter, and Outerbridge (1986) Model of Job Performance R	AL/HRT	2- 20
DR David A Ludwig	Univ of N.C. at Greensboro , Greensboro , NC Mediating effect of onset rate on the relationship between+ Gz and LBNP Tolerance	AL/AOCY	2- 21
DR Robert P Mahan	University of Georgia , Athens , GA The Effects of Task Structure on Cognitive Organizing Principles Implaicating for Complex Display	AL/CFTO	2- 22

SRP Final Report Table of Contents

Author	University/Institution Report Title	Armstrong Laboratory Directorate	Vol-Page
DR Phillip H Marshall	Texas Tech University , Lubbock , TX Preliminary report on the effects of varieties of feedback training on single target time-to-contac	AL/HRM	2- 23
DR Bruce V Mutter	Bluefield State College , Bluefield , WV	AL/EQP	2- 24
DR Allen L Nagy	Wright State University , Dayton , OH The Detection of Color Breakup In Field Sequential Color Displays	AL/CFHV	2- 25
DR Brent L Nielsen	Auburn University , Auburn , AL Rapid PCR Detection of Vancomycin Resistance of Enteroccus Species in infected Urine and Blood	AL/AOEL	2- 26
DR Thomas E Nygren	Ohio State University , Columbus , OH Group Differences in perceived importance of swat workload dimensions: Effects on judgment and perf	AL/CFHP	2- 27
DR Edward H Piepmeier	Oregon State University , Corvallis , OR	AL/AOHR	2- 28
DR Judy L Ratliff	Murray State Univ , Murray , KY Accumulation of Storntium and Calcium by Didemnum Conchyliatum	AL/EQL	2- 29
DR Joan R Rentsch	Wright State University , Dayton , OH the Effects of Individual Differences and Team Processed on Team Member Schema Similarity and task P	AL/CFHI	2- 30
DR Paul D Retzlaff	Univ of Northern Colorado , Greeley , CO The Armstrong Laboratory Aviation Personality Survey (ALAPS) Norming and Cross - Validation	AL/AOCN	2- 31
DR David B Reynolds	Wright State University , Dayton , OH Modeling Heat Flux Through Fabrics Exposed to a Radiant Souurce and Analysis of Hot Air Burns	AL/CFBE	2- 32
DR Barth F Smets	University of Connecticut , Storrs , CT Desorption and Biodegradation of Dinitrotoluenes in aged soils	AL/EQL	2- 33

Author	University/Institution Report Title	Phillips Laboratory Directorate	Vol-Page
DR Graham R Allan	National Avenue , Las Vegas , NM Temporal and Spatial Characterisation of a Synchronously-Pumped Periodically-Poled Lithium Niobate O	PL/LIDD	3- 1
DR Mark J Balas	Univ of Colorado at Boulder , Boulder , CO Nonlinear Tracking Control for a Precision Deployable Structure Using a Partitioned Filter Approach	PL/SX	3- 2
DR Mikhail S Belen'kii	Georgia Inst of Technology , Atlanta , GA Multiple Aperture Averaging Technique for Measurment Full Aperture Tilt with a Laser Guide Star and	PL/LIG	3- 3
DR Gajanan S Bhat	Univ of Tennessee , Knoxville , TN Spinning Hollow Fibers From High Performance Polymers	PL/RK	3- 4
DR David B Choate	Transylvania Univ , Lexington , KY Blackhole Analysis	PL/VTMR	3- 5
DR Neb Duric	University of New Mexico , Albuquerque , NM Image Recovery Using Phase Diversity	AFRL/DEB	3- 6
DR Arthur B Edwards	9201 University City Blvd. , Charlotte , NC Theory of Protons in Buried Oxides	PL/VTMR	3- 7
DR Gary M Erickson	Boston University , Boston , MA Modeling The Magnetospheric Magnetic Field	PL/GPSG	3- 8
DR Hany A Ghoneim	Rochester Inst of Technol , Rochester , NY Focal Point Accuracy Assessement of an Off-Axis Solar Caoncentrator	PL/RKES	3- 9
DR Subir Ghosh	Univ of Calif, Riverside , Riverside , CA Designing Propulsion Reliability of Space Launch Vehicles	PL/RKBA	3- 10
DR George W Hanson	Univ of Wisconsin - Milwaukee , Milwaukee , WI Asymptotic analysis of the Natural system modes of coupled bodies in the large separatin, Low-Freque	AFRL/DEH	3- 11

SRP Final Report Table of Contents

Author	University/Institution Report Title	Phillips Laboratory Directorate	Vol-Page
DR Brian D Jeffs	Brigham Young University , Provo , UT Blind Bayyesian Restoration of Adaptive Optics Images Using Generalized Gaussian Markov Random Field	AFRL/DES	3- 12
DR Christopher H Jenkins	S Dakota School of Mines/Tech , Rapid City , SD Mechnics of Surface Precosion for Membrane Reflectors	PL/VTVS	3- 13
DR Dikshitulu K Kalluri	University of Lowell , Lowell , MA Mode Conversion in a Time-Varying Magnetoplasma Medium	PL/GPID	3- 14
DR Aravinda Kar	University of Central Florida , Orlando , FL Measurement of the Cutting Performance of a High Beam Quality Chemical Oxygen-Iodine Laser on Aerosp	AFRL/DEO	3- 15
DR Bernard Kirtman	Univ of Calif, Santa Barbara , Santa Barbara , CA Quantum Chemical Characterization of the elkectronic Structure and Reactions of Silicon Dangling Bon	PL/VTMR	3- 16
DR Spencer P Kuo	Polytechnic University , Farmingdale , NY Excitation of Oscillating Two Stream Instability by Upper Hybrid Pump Waves in Ionospheric Heating	PL.GPI	3- 17
DR Henry A Kurtz	Memphis State University , Memphis , TN H2 Reactions at Dangling Bonds in SIO2	PL/VTMR	3- 18
DR Min-Chang Lee	Massachusetts Inst of Technology , Cambridge , MA Laboratory Studies of Ionospheric Plasma Effects Produced by Lightning-induced Whistler Waves	PL/GPSG	3- 19
DR Donald J Leo	University of Toledo , Toledo , OH Microcontroller-Based Implementation of Adaptive Structural Control	AFRL/VSD	3- 20
DR Hua Li	University of New Mexico , Albuquerque , NM	PL/LIDD	3- 21
DR Hanli Liu	Univ of Texas at Arlington , Arlington , TX Experimental Validation of Three-Dimensional Reconstruction of Inhomogenety Images in Turbid Media	AFRL/DEB	3- 22

SRP Final Report Table of Contents

Author	University/Institution Report Title	Phillips Laboratory Directorate	Vol-Pag
DR M. Arfin K Lodhi	Texas Tech University , Lubbock , TX Thermoelectric Energy Conversion with solid Electolytes	PL/VTRP	3- 2
DR Tim C Newell	University of New Mexico , Albuquerque , NM Study of Nonlineaar Dynamics in a Diode Pumped Nd:YAG laser	PL/LIGR	3- 2-
DR Michael J Pangia	Georgia College & State University , Milledgeville , GA Preparatory Work Towards a Computer Simulation of Electron beam Operations on TSS 1	PL/GPSG	3- 2
DR Vladimir O Papitashvili	Univ of Michigan , Ann Arbor , MI Modeling of Ionospheric Convectin from the IMF and Solar Wind Data	PL/GPSG	3- 26
DR Jaime Ramirez-Angulo	New Mexico State University , Las Cruces , NM	PL/VTMR	3- 27
DR Louis F Rossi	University of Lowell , Lowell , MA Analysis of Turbulent Mixing in the Stratosphere & Troposphere	PL/GPOL	3- 28
DR David P Stapleton	University of Central Oklahoma , Edmond , OK Atmospheric Effects Upon Sub-Orbital Boost glide Spaceplane Trajectories	PL/RKBA	3- 29
DR Jenn-Ming Yang	Univ of Calif, Los Angeles , Los Angeles , CA Thermodynamic Stability and Oxidation Behavior of Refractory (Hf, Ta, Zr) Carbide/boride Composites	PL/RKS	3- 30

SRP Final Report Table of Contents

Author	University/Institution Report Title	Rome Laboratory Directorate	Vol-Page
DR A. F Anwar	University of Connecticut , Storrs , CT Properties of Quantum Wells Formed In AlGaN/GaN Heterostructures	RL/ERAC	4- 1
DR Milica Barjaktarovic	Wilkes University , Wilkes Barre , PA Assured Software Design: Privacy Enhanced Mail (PEM) and X.509 Certificate Specification	AFRL/IFG	4- 2
DR Stella N Batalama	SUNY Buffalo , Buffalo , NY Adaptive Robust Spread-Spectrum Receivers	AFRL/IFG	4- 3
DR Adam W Bojanczyk	Cornell Univesity , Ithaca , NY Lowering the Computational Complexity of Stap Radar Systems	RL/OCSS	4- 4
DR Nazeih M Botros	So. Illinois Univ-Carbondale , Carbondale , IL A PC-Based Speech Synthesizing Using Sinusoidal Transform Coding (STC)	RL/ERC-1	4- 5
DR Nikolaos G Bourbakis	SUNY Binghamton , Binghamton , NY Eikones-An Object-Oriented Language Forimage Analysis & Process	AFRL/IF	4- 6
DR Peter P Chen	Louisiana State University , Baton Rouge , LA Reconstructing the information Warfare Attack Scenario Guessing what Actually Had Happened Based on	RL/CA-II	4- 7
DR Everett E Crisman	Brown University , Providence , RI A Three-Dimensional, Dielectric Antenna Array Re-Configurable By Optical Wavelength Multiplexing	RL/ERAC	4- 8
DR Digendra K Das	SUNYIT , Utica , NY A Study of the Emerging Dianostic Techniques in Avionics	RL/ERSR	4- 9
DR Venugopala R Dasigi	Southern Polytechnic State Univ , Marietta , GA Information Fusion for text Classification-an Expjerimental Comparison	AFRL/IFT	4- 10
DR Richard R Eckert	SUNY Binghamton , Binghamton , NY Enhancing the rome Lab ADII virtual environment system	AFRL/IFSA	4- 11

Author	University/Institution Report Title	Rome Laboratory Directorate	Vol-Pag
DR Micheal A Fiddy	University of Lowell , Lowell , MA Target Identification from Limited Backscattered Field Data	RL/ERCS	4- 1
DR Lili He	Nothern Illinois University , Dekalb , IL the Study of Caaractreistics of CdS Passivation on InP	RL/EROC	4- 1
DR Edem Ibragimov	Michigan Tech University , Houghton , MI Effects of Surface Scattering in 3-D Optical Mass Storage	RL/IRAP	4- 1
DR Phillip G Kornreich	Syracuse University , Syracuse , NY Analysis of Optically Active Material Layer Fibers	RL/OCPA	4- 15
DR Kuo-Chi Lin	University of Central Florida , Orlando , FL A Study on The Crowded Airspace Self Organized Criticality	AFRL/IFSB	4- 16
Dr. Beth L Losiewicz	Colorado College , Colorado Spring , CO The Miami Corpus Latin American Dialect Database continued Research and Documentation	RL/IRAA	4- 17
DR John D Norgard	Univ of Colorado at Colorado Springs , Colorado Spring , CO Microwave Holography using Infrared Thermograms of Electromagnetic Fields	RL/ERST	4- 18
DR Jeffrey B Norman	Vassar College , Poughkeepsie , NY Gain Spectra of Beam-Coupling In Photorefractive Semiconductors	RL/OCPA	4- 19
DR Dimitrios N Pados	State Univ. of New York Buffalo , Buffalo , NY Joint Domain Space-Time Adaptive Processing w/Small Training Data Sets	AFRL/SNR	4- 21
DR Brajendra N Panda	University of North Dakota , Grand Forks , ND A Model to Attain Data Integrity After System Invasion	AFRL/IFG	4- 22
DR Michael A Pittarelli	SUNY OF Tech Utica , Utica , NY Phase Transitions in probability Estimation and Constraint Satisfaction Problems	AFRL/IFT	4- 23

Author	University/Institution Report Title	Rome Laboratory Directorate	Vol-Page
DR Salahuddin Qazi	SUNY OF Tech Utica , Utica , NY Low Data rate Multimedia Communication Using Wireless Links	RL/IWT	4- 24
DR Arindam Saha	Mississippi State University , Mississippi State , MS An Implementationa of the message passing Interface on Rtems	RL/OCSS	4- 25
DR Ravi Sankar	University of South Florida , Tampa , FL A Study ofIntegrated and Intelligent Network Management	RL/C3BC	4- 26
DR Mark S Schmalz	University of Florida , Gainesville , FL Errors inherent in Reconstruction of Targets From multi-Look Imagery	AFRL/IF	4- 27
DR John L Stensby	Univ of Alabama at Huntsville , Huntsville , AL Simple Real-time Tracking Indicator for a Frequrncy Feedback Demodulator	RL/IRAP	4- 28
DR Micheal C Stinson	Central Michigan University , Mt. Pleasant , MI Destructive Objects	RL/CAII	4- 29
DR Donald R Ucci	Illinois Inst of Technology , Chicago , IL Simulation of a Robust Locally Optimum Receiver in correlated Noise Using Autoregressive Modeling	RL/C3BB	4- 30
DR Nong Ye	Arizona State University , Tempe , AZ A Process Engineering Approach to Continuous Command and Control on Security-Aware Computer Networks	AFRL/IFSA	4- 31

SRP Final Report Table of Contents

Author	University/Institution Report Title	Wright Laboratory Directorate	Vol-Pag
DR William A Baeslack	Ohio State University , Columbus , OH	WL/MLLM	5-
DR Bhavik R Bakshi	Ohio State University , Columbus , OH Modeling of Materials Manufacturing Processes by NonlinearContimuum Regression	WL/MLIM	5-
DR Brian P Beecken	Bethel College , St. Paul , MN Contribution of a Scene Projector's Non-Uniformity to a Test Article's Output Image Non-Uniformity	AFRL/MN	5-
DR John H Beggs	Mississippi State University , Mississippi State , MS The Finite Element Method in Electromagnetics For Multidisciplinary Design	AFRL/VA	5- 4
DR Kevin D Belfield	University of Detroit Mercy , Detroit , MI Synthesis of Novel Organic Compounds and Polymers for two Photon Asorption, NLO, and Photorefractive	WL/MLBP	5- 5
DR Raj K Bhatnagar	University of Cincinnati , Cincinnati , OH A Study of Intra-Class Variability in ATR Systems	AFRL/SN	5- 6
DR Victor M Birman	Univ of Missouri - St. Louis , St Louis , MO Theoretical Foundations for Detection of Post-Processing Cracks in Ceramic Matrix Composites Based o	WL/FIBT	5- 7
DR Gregory A Blaisdell	Purdue University , West Lafayette , IN A Review of Benchmark Flows for Large EddySimulation	AFRL/VA	5- 8
DR Octavia I Camps	Pennsylvania State University , University Park , PA MDL Texture Segmentation Compressed Images	WL/MNGA	5- 9
DR Yiding Cao	Florida International Univ , Miami , FL A Feasibility Study of Turbine Disk Cooling by Employing Radially Rotating Heat Pipes	WL/POTT	5- 10
DR Reaz A Chaudhuri	University of Utah , Salt Lake City , UT A Novel Compatibility/Equilibrium Based Interative Post-Processing Approach For Axisymmetric brittle	WL/MLBM	5- 11

SRP Final Report Table of Contents

Author	University/Institution Report Title	Wright Laboratory Directorate	Vol-Page
DR Mohamed F Chouikha	Howard University , Washington , DC Detection Techniques Use in Forward-Looking Radar Signal Procesing a Literature Review	WL/AAMR	5- 12
DR Milton L Cone	Embry-Riddle Aeronautical University , Prescott , AZ Scheduling in the Dynamic System Simulation Testbed	WL/AACF	5- 13
DR Robert C Creese	West Virginia University , Morgantown , WV Feature Based Cost Modeling	WL/MTI	5- 14
DR William Crossley	Purdue University , West Lafayette , IN Objects and Methods for Aircraft Conceptual Design and Optimization in a Knowledge-Based Environment	WL/FIBD	5- 15
DR Gene A Crowder	Tulane University , New Orleans , LA Vibrational Analysis of some High-Energy Compounds	WL/MNM	5- 16
DR Richard W Darling	University of South Florida , Tampa , FL Geometrically Invariant NonLinear recursive Filters, with Applicaation to Target Tracking	WL/MNAG	5- 17
DR Robert J DeAngelis	Univ of Nebraska - Lincoln , Lincoln , NE Quantitative Description of Wire Tecxtures In Cubic Metals	WL/MNM	5- 18
DR Bill M Diong	Pan American University , Edinburg , TX Analysis and Control Design for a Novel Resonant DC-DC Converter	WL/POOC	5- 19
DR John K Douglass	University of Arizona , Tucson , AZ Guiding Missiles "On The Fly:" Applications of Neurobiologica Princioles to Machine Vision For Arma	AFRL/MN	5- 20
DR Mark E Eberhart	Colorado School of Mines , Golden , CO Modeling The Charge Redistribution Associated with Deformation and Fracture	WL/MLLM	5- 21
DR Gregory S Elliott	Rutgers:State Univ of New Jersey , Piscataway , NJ On the Development of Planar Doppler Velocimetry	WL/POPT	5- 22

Author	University/Institution Report Title	Wright Laboratory Directorate	Vol-Pac
DR Elizabeth A Ervin	University of Dayton , Dayton , OH Eval of the Pointwise K-2 Turbulence Model to Predict Transition & Separtion in a Low Pressure	WL/POTT	5- 2
DR Altan M Ferendeci	University of Cincinnati , Cincinnati , OH Vertically Interconnected 3D MMICs with Active Interlayer Elements	WL/AADI	5- 2
DR Dennis R Flentge	Cedarville College , Cedarville , OH Kinetic Study of the Thermal Decomposition of t-Butylphenyl Phosphate Using the System for Thermal D	WL/POSL	5- 2
DR George N Frantziskonis	University of Arizona , Tuson , AZ Multiscale Material Characterization and Applications	WL/MLLP	5- 2
DR Zewdu Gebeyehu	Tuskegee University , Tuskegee , AL Synthesis and Characterization of Metal-Xanthic Acid and -Amino Acid Com[lexes Useful Ad Nonlinear	WL/MLPO	5- 2
DR Richard D Gould	North Carolina State U-Raleigh , Raleigh , NC Reduction and Analysis of LDV and Analog Raw Data	WL/POPT	5- 28
DR Michael S Grace	University of Virginia , Charlottesville , VA Structure and Function of an Extremely Sensitive Biological Infrared Detector	WL/MLPJ	5- 29
DR Gary M Graham	Ohio University , Athens , OH Indicial Response Model for Roll Rate Effects on A 65-Degree Delta wing	WL/FIGC	5- 30
DR Allen G Greenwood	Mississippi State University , Mississippi Sta , MS An Object-Based approach for Integrating Cost Assessment into Product/Process Design	WL/MTI	5- 31
DR Rita A Gregory	Georgia Inst of Technology , Atlanta , GA Range Estimating for Research and Development Alternatives	WL/FIVC	5- 32
DR Mark T Hanson	University of Kentucky , Lexington , KY Anisotropy in Epic 96&97: Implementation and Effects	WL/MNM	5- 33

SRP Final Report Table of Contents

Author	University/Institution Report Title	Wright Laboratory Directorate	Vol-Page
DR Majeed M Hayat	University of Dayton , Dayton , OH A Model for Turbulence and Photodetection Noise in Imaging	WL/AAJT	5- 34
DR Larry S Helmick	Cedarville College , Cedarville , OH NMA Study of the Decomposition Reaction Path of Demnum fluid under Tribological Conditions	WL/MLBT	5- 35
DR William F Hosford	Univ of Michigan , Ann Arbor , MI INTENSITY OF [111]AND [100] TEXTURAL COMPONENTS IN COMPRESSION-FORGED TANTALUM	AFRL/MN	5- 36
DR David E Hudak	Ohio Northern University , Ada , OH A Study fo a Data-Parallel Imlementation of An Implicit Solution fo the 3D Navier-Stokes Equations	WL/FIMC	5- 37
DR David P Johnson	Mississippi State University , Mississippi , MS An Innovative Segmented Tugsten Penetrating Munition	WL/MNAZ	5- 38
DR Ismail I Jouny	Lafayette College , Easton , PA	WL/AACT	5- 39
DR Edward T Knobbe	Oklahoma State University , Stillwater , OK Organically Modified silicate Films as Corrosion Resistant Treatments for 2024-T3 Alumium Alloy	WL/MLBT	5- 40
DR Seungug Koh	University of Dayton , Dayton , OH Numerically Efficinet Direct Ray Tracing Algorithms for Automatic Target Recognition using FPGAs	WL/AAST	5- 41
DR Ravi Kothari	University of Cincinnati , Cincinnati , OH A Function Approximation Approach for Region of Interest Selection in synthetic Aperture Radar Image	WL/AACA	5- 42
DR Douglas A Lawrence	Ohio University , Athens , OH On the Analysis and Design of Gain scheduled missile Autopilots	WL/MNAG	5- 43
DR Robert Lee	Ohio State University , Columbus , OH Boundary Conditions applied to the Finite Vlume Time Domain Method for the Solution of Maxwell's Equ	WL/FIM	5- 44

Author	University/Institution Report Title	Wright Laboratory Directorate	Vol-Pag
DR Junghsen Lieh	Wright State University , Dayton , OH Develop an Explosive Simulated Testing Apparatus for Impact Physics Research at Wright Laboratory	WL/FIV	5- 1
DR James S Marsh	University of West Florida , Pensacola , FL Distortion Compensation and Elimination in Holographic Reocnstruction	WL/MNSI	5- 4
DR Mark D McClain	Cedarville College , Cedarville , OH A Molecular Orbital Theory Analysis of Oligomers of 2,2'-Bithiazole and Partially Reduced 3,3'-Dimet	WL/MLBP	5- 4
DR William S McCormick	Wright State University , Dayton , OH Some Observations of Target Recognition Using High Range Resolution Radar	WL/AACR	5- 48
DR Richard O Mines	University of South Florida , Tampa , FL Testing Protocol for the Demilitarization System at the Eglin AFB Herd Facility	WLMN/M	5- 49
DR Dakshina V Murty	University of Portland , Portland , OR A Useful Benchmarking Method in Computational Mechanics, CFD, adn Heat Tansfer	WL/FIBT	5- 50
DR Krishna Naishadham	Wright State University , Dayton , OH	WL/MLPO	5- 51
DR Serguei Ostapenko	University of South Florida , Tampa , FL	WL/MLPO	5- 52
DR Yi Pan	University of Dayton , Dayton , OH Improvement of Cache Utilization and Parallel Efficiency of a Time-Dependnet Maxwell Equation Solver	AFRL/VA	5- 53
DR Rolfe G Petschek	Case Western Reserve Univ , Cleveland , OH AB INITIO AUANTUM CHEMICAL STUDIES OF NICKEL DITHIOLENE COMPLEX	WL/MLPJ	5- 54
DR Kishore V Pochiraju	Stevens Inst of Technology , Hoboken , NJ Refined Reissner's Variational Solution in the Vicinity of Stress Singularities	AFRL/ML	5- 55

SRP Final Report Table of Contents

Author	University/Institution Report Title	Wright Laboratory Directorate	Vol-Page
DR Muhammad M Rahman	University of South Florida , Tampa , FL Computation of Free Surface Flows with Applications in Capillary Pumped Loops. Heat Pipes, and Jet I	WL/POOB	5- 56
DR Mateen M Rizki	Wright State University , Dayton , OH Classification of High Range Resolution Radar Signatures Using Evolutionary Computation	WL/AACA	5- 57
DR Shankar M Sastry	Washington University , St Louis , MO	WL/MLLM	5- 58
DR Martin Schwartz	University of North Texas , Denton , TX Computational Studies of Hydrogen Abstraction From Haloalkanes by the Hydroxyl Radical	WL/MLBT	5- 59
DR Rathinam P Selvam	Univ of Arkansas , Fayetteville , AR Computation of Nonlenear Viscous Panel Flutter Using a Full-Implicit Aeroelastic Solver	WL/FIMC	5- 60
DR Yuri B Shtessel	Univ of Alabama at Huntsville , Huntsville , AL Smoothed Sliding Mode control Approach For Addressing Actuator Deflection and Deflection Rate Satura	AFRL/VA	5- 61
DR Mario Sznaier	Pennsylvania State University , University Park , PA Suboptimal Control of Nonlenear Systems via Receding Horizon State Dependent Riccati Equations	WL/MNAG	5- 62
DR Barney E Taylor	Miami Univ. - Hamilton , Hamilton , OH Photoconductivity Studies of the Polymer 6FPBO	WLMLBP	5- 63
DR Joseph W Tedesco	Auburn University , Auburn , AL high Velocity Penetration of Layered Concrete Targets with Small Scale Ogive-nose Steel projectiles	WL/MNSA	5- 64
DR Krishnaprasad Thirunarayan	Wright State University , Dayton , OH A VHDL MODEL SYNTHESIS APPLET IN TCL/TK	WL/AAST	5- 65

Author	University/Institution Report Title	Wright Laboratory Directorate	Vol-Pag
DR Karen A Tomko	Wright State University , Dayton , OH Grid Level Parallelization of an Implicit Solution of the 3D Navier-Stokes Equations	WL/FIMC	5- 6
DR Max B Trueblood	University of Missouri-Rolla , Rolla , MO AStudy of the Particulate Emissions of a Well-Stirred Reactor	WL/POSC	5- 6
DR Chi-Tay Tsai	Florida Atlantic University , Boca Raton , FL Dislocation Dynamics in Heterojunction Bipolar Transistor Under Current Induced Thermal St	WL/AA	5- 6
DR John L Valasek	Texas A&M University , College Station , TX Two Axis Pneumatic Vortex Control at High Speed and Low Angle-of-Attack	WL/FIMT	5- 6
DR Mitch J Wolff	Wright State University , Dayton , OH An Experimaental and Computational Analysis of the Unsteady Blade Row Potential Interaction in a Tr	WL/POTF	5- 7
DR Rama K Yedavalli	Ohio State University , Columbus , OH Improved Aircraft Roll Maneuver Performance Using Smart Deformable Wings	WL/FIBD	5- 71

SRP Final Report Table of Contents

Author	University/Institution Report Title	Arnold Engineering Development Center Directorate	Vol-Page
DR Csaba A Biegl	Vanderbilt University , Nashville , TN Parallel processing for Tubine Engine Modeling and Test Data validation	AEDC/SVT	6- 1
DR Frank G Collins	Tennessee Univ Space Institute , Tullahoma , TN Design of a Mass Spectrometer Sampling Probe for The AEDC Impulse Facility	AEDC	6- 2
DR Kenneth M Jones	N Carolina A&T State Univ , Greensboro , NC	AEDC/SVT	6- 3
DR Kevin M Lyons	North Carolina State U-Raleigh , Raleigh , NC Velocity Field Measurements Using Filtered-Rayleigh Scattering	AEDC/SVT	6- 4
DR Gerald J Micklow	Univ of Alabama at Tuscaloosa , Tucasloosa , AL	AEDC/SVT	6- 5
DR Michael S Moore	Vanderbilt University , Nashville , TN Extension and Installation of the Model-Integrated Real-Time Imaging System (Mirtis)	AEDC/SVT	6- 6
DR Robert L Roach	Tennessee Univ Space Institute , Tullahoma , TN Investigation of Fluid Mechanical Phenomena Relating to Air Injection Between the Segments of an Arc	AEDC	6- 7
DR Nicholas S Winowich	University of Tennessee , Knoxville , TN	AEDC	6- 8
DR Daniel M Knauss	Colorado School of Mines , Golden , CO Synthesis of salts With Delocalized Anions For Use as Third Order Nonlinear Optical Materials	USAFA/DF	6- 9
DR Jeffrey M Bigelow	Oklahoma Christian Univ of Science & Art , Oklahoma City , OK Raster-To-Vector Conversion of Circuit Diagrams: Software Requirements	OCALC/TI	6- 10

Author	University/Institution Report Title	Arnold Engineering Development Center Directorate	Vol-Pa
DR Paul W Whaley	Oklahoma Christian Univ of Science & Art , Oklahoma City , OK A Probabilistic framework for the Analysis of corrosion Damage in Aging Aircraft	OCALC/L	6- 1
DR Bjong W Yeigh	Oklahoma State University , Stillwater , OK Logistics Asset Management : Models and Simulations	OCALC/TI	6- 1
DR Michael J McFarland	Utah State University , Logan , UT Delisting of Hill Air Force Base's Industrial Wastewater Treatment Plant Sludge	OC-ALC/E	6- 1
DR William E Sanford	Colorado State University , Fort Collins , CO Nucrical Modeling of Physical Constraints on in-SItu Cosolvent Flushing as a Groundwater Remedial Op	OO-ALC/E	6- 1
DR Sophia Hassiotis	University of South Florida , Tampa , FL Fracture Analysis of the F-5, 15%-Spar Bolt	SAALC/TI	6- 1
DR Devendra Kumar	CUNY-City College , New York , NY A Simple, Multiversion Concurrency Control Protocol For Internet Databases	SAALC/LD	6- 1
DR Ernest L McDuffie	Florida State University , Tallahassee , FL A Propossed Exjpert System for ATS Capability Analysis	SAALC/TI	6- 1
DR Prabhaker Mateti	Wright State University , Dayton , OH How to Provide and Evaluate Computer Network Security	SMALC/TI	6- 1
DR Mansur Rastani	N Carolina A&T State Univ , Greensboro , NC Optimal Structural Design of Modular Composite bare base Shelters	SMALC/L	6- 19
DR Joe G Chow	Florida International Univ , Miami , FL Re-engineer and Re-Manufacture Aircraft Sstructural Components Using Laser Scanning	WRALC/TI	6- 2

1. INTRODUCTION

The Summer Research Program (SRP), sponsored by the Air Force Office of Scientific Research (AFOSR), offers paid opportunities for university faculty, graduate students, and high school students to conduct research in U.S. Air Force research laboratories nationwide during the summer.

Introduced by AFOSR in 1978, this innovative program is based on the concept of teaming academic researchers with Air Force scientists in the same disciplines using laboratory facilities and equipment not often available at associates' institutions.

The Summer Faculty Research Program (SFRP) is open annually to approximately 150 faculty members with at least two years of teaching and/or research experience in accredited U.S. colleges, universities, or technical institutions. SFRP associates must be either U.S. citizens or permanent residents.

The Graduate Student Research Program (GSRP) is open annually to approximately 100 graduate students holding a bachelor's or a master's degree; GSRP associates must be U.S. citizens enrolled full time at an accredited institution.

The High School Apprentice Program (HSAP) annually selects about 125 high school students located within a twenty mile commuting distance of participating Air Force laboratories.

AFOSR also offers its research associates an opportunity, under the Summer Research Extension Program (SREP), to continue their AFOSR-sponsored research at their home institutions through the award of research grants. In 1994 the maximum amount of each grant was increased from $20,000 to $25,000, and the number of AFOSR-sponsored grants decreased from 75 to 60. A separate annual report is compiled on the SREP.

The numbers of projected summer research participants in each of the three categories and SREP "grants" are usually increased through direct sponsorship by participating laboratories.

AFOSR's SRP has well served its objectives of building critical links between Air Force research laboratories and the academic community, opening avenues of communications and forging new research relationships between Air Force and academic technical experts in areas of national interest, and strengthening the nation's efforts to sustain careers in science and engineering. The success of the SRP can be gauged from its growth from inception (see Table 1) and from the favorable responses the 1997 participants expressed in end-of-tour SRP evaluations (Appendix B).

AFOSR contracts for administration of the SRP by civilian contractors. The contract was first awarded to Research & Development Laboratories (RDL) in September 1990. After completion of the

1990 contract, RDL (in 1993) won the recompetition for the basic year and four 1-year options.

2. PARTICIPATION IN THE SUMMER RESEARCH PROGRAM

The SRP began with faculty associates in 1979; graduate students were added in 1982 and high school students in 1986. The following table shows the number of associates in the program each year.

YEAR	SRP Participation, by Year			TOTAL
	SFRP	GSRP	HSAP	
1979	70			70
1980	87			87
1981	87			87
1982	91	17		108
1983	101	53		154
1984	152	84		236
1985	154	92		246
1986	158	100	42	300
1987	159	101	73	333
1988	153	107	101	361
1989	168	102	103	373
1990	165	121	132	418
1991	170	142	132	444
1992	185	121	159	464
1993	187	117	136	440
1994	192	117	133	442
1995	190	115	137	442
1996	188	109	138	435
1997	148	98	140	427

Beginning in 1993, due to budget cuts, some of the laboratories weren't able to afford to fund as many associates as in previous years. Since then, the number of funded positions has remained fairly constant at a slightly lower level.

3. RECRUITING AND SELECTION

The SRP is conducted on a nationally advertised and competitive-selection basis. The advertising for faculty and graduate students consisted primarily of the mailing of 8,000 52-page SRP brochures to chairpersons of departments relevant to AFOSR research and to administrators of grants in accredited universities, colleges, and technical institutions. Historically Black Colleges and Universities (HBCUs) and Minority Institutions (MIs) were included. Brochures also went to all participating USAF laboratories, the previous year's participants, and numerous individual requesters (over 1000 annually).

RDL placed advertisements in the following publications: *Black Issues in Higher Education, Winds of Change,* and *IEEE Spectrum.* Because no participants list either *Physics Today* or *Chemical & Engineering News* as being their source of learning about the program for the past several years, advertisements in these magazines were dropped, and the funds were used to cover increases in brochure printing costs.

High school applicants can participate only in laboratories located no more than 20 miles from their residence. Tailored brochures on the HSAP were sent to the head counselors of 180 high schools in the vicinity of participating laboratories, with instructions for publicizing the program in their schools. High school students selected to serve at Wright Laboratory's Armament Directorate (Eglin Air Force Base, Florida) serve eleven weeks as opposed to the eight weeks normally worked by high school students at all other participating laboratories.

Each SFRP or GSRP applicant is given a first, second, and third choice of laboratory. High school students who have more than one laboratory or directorate near their homes are also given first, second, and third choices.

Laboratories make their selections and prioritize their nominees. AFOSR then determines the number to be funded at each laboratory and approves laboratories' selections.

Subsequently, laboratories use their own funds to sponsor additional candidates. Some selectees do not accept the appointment, so alternate candidates are chosen. This multi-step selection procedure results in some candidates being notified of their acceptance after scheduled deadlines. The total applicants and participants for 1997 are shown in this table.

1997 Applicants and Participants			
PARTICIPANT CATEGORY	TOTAL APPLICANTS	SELECTEES	DECLINING SELECTEES
SFRP	490	188	32
(HBCU/MI)	(0)	(0)	(0)
GSRP	202	98	9
(HBCU/MI)	(0)	(0)	(0)
HSAP	433	140	14
TOTAL	1125	426	55

4. SITE VISITS

During June and July of 1997, representatives of both AFOSR/NI and RDL visited each participating laboratory to provide briefings, answer questions, and resolve problems for both laboratory personnel and participants. The objective was to ensure that the SRP would be as constructive as possible for all participants. Both SRP participants and RDL representatives found these visits beneficial. At many of the laboratories, this was the only opportunity for all participants to meet at one time to share their experiences and exchange ideas.

5. HISTORICALLY BLACK COLLEGES AND UNIVERSITIES AND MINORITY INSTITUTIONS (HBCU/MIs)

Before 1993, an RDL program representative visited from seven to ten different HBCU/MIs annually to promote interest in the SRP among the faculty and graduate students. These efforts were marginally effective, yielding a doubling of HBCI/MI applicants. In an effort to achieve AFOSR's goal of 10% of all applicants and selectees being HBCU/MI qualified, the RDL team decided to try other avenues of approach to increase the number of qualified applicants. Through the combined efforts of the AFOSR Program Office at Bolling AFB and RDL, two very active minority groups were found, HACU (Hispanic American Colleges and Universities) and AISES (American Indian Science and Engineering Society). RDL is in communication with representatives of each of these organizations on a monthly basis to keep up with the their activities and special events. Both organizations have widely-distributed magazines quarterlies in which RDL placed ads.

Since 1994 the number of both SFRP and GSRP HBCU/MI applicants and participants has increased ten-fold, from about two dozen SFRP applicants and a half dozen selectees to over 100 applicants and two dozen selectees, and a half-dozen GSRP applicants and two or three selectees to 18 applicants and 7 or 8 selectees. Since 1993, the SFRP had a two-fold applicant increase and a two-fold selectee increase. Since 1993, the GSRP had a three-fold applicant increase and a three to four-fold increase in selectees.

In addition to RDL's special recruiting efforts, AFOSR attempts each year to obtain additional funding or use leftover funding from cancellations the past year to fund HBCU/MI associates. This year, 5 HBCU/MI SFRPs declined after they were selected (and there was no one qualified to replace them with). The following table records HBCU/MI participation in this program.

SRP HBCU/MI Participation, By Year				
YEAR	SFRP		GSRP	
	Applicants	Participants	Applicants	Participants
1985	76	23	15	11
1986	70	18	20	10
1987	82	32	32	10
1988	53	17	23	14
1989	39	15	13	4
1990	43	14	17	3
1991	42	13	8	5
1992	70	13	9	5
1993	60	13	6	2
1994	90	16	11	6
1995	90	21	20	8
1996	119	27	18	7

6. SRP FUNDING SOURCES

Funding sources for the 1997 SRP were the AFOSR-provided slots for the basic contract and laboratory funds. Funding sources by category for the 1997 SRP selected participants are shown here.

1997 SRP FUNDING CATEGORY	SFRP	GSRP	HSAP
AFOSR Basic Allocation Funds	141	89	123
USAF Laboratory Funds	48	9	17
HBCU/MI By AFOSR (Using Procured Addn'l Funds)	0	0	N/A
TOTAL	9	98	140

SFRP - 188 were selected, but thirty two canceled too late to be replaced.
GSRP - 98 were selected, but nine canceled too late to be replaced.
HSAP - 140 were selected, but fourteen canceled too late to be replaced.

7. COMPENSATION FOR PARTICIPANTS

Compensation for SRP participants, per five-day work week, is shown in this table.

1997 SRP Associate Compensation

PARTICIPANT CATEGORY	1991	1992	1993	1994	1995	1996	1997
Faculty Members	$690	$718	$740	$740	$740	$770	$770
Graduate Student (Master's Degree)	$425	$442	$455	$455	$455	$470	$470
Graduate Student (Bachelor's Degree)	$365	$380	$391	$391	$391	$400	$400
High School Student (First Year)	$200	$200	$200	$200	$200	$200	$200
High School Student (Subsequent Years)	$240	$240	$240	$240	$240	$240	$240

The program also offered associates whose homes were more than 50 miles from the laboratory an expense allowance (seven days per week) of $50/day for faculty and $40/day for graduate students. Transportation to the laboratory at the beginning of their tour and back to their home destinations at the end was also reimbursed for these participants. Of the combined SFRP and GSRP associates, 65 % (194 out of 286) claimed travel reimbursements at an average round-trip cost of $776.

Faculty members were encouraged to visit their laboratories before their summer tour began. All costs of these orientation visits were reimbursed. Forty-three percent (85 out of 188) of faculty associates took orientation trips at an average cost of $388. By contrast, in 1993, 58 % of SFRP associates took

orientation visits at an average cost of $685; that was the highest percentage of associates opting to take an orientation trip since RDL has administered the SRP, and the highest average cost of an orientation trip. These 1993 numbers are included to show the fluctuation which can occur in these numbers for planning purposes.

Program participants submitted biweekly vouchers countersigned by their laboratory research focal point, and RDL issued paychecks so as to arrive in associates' hands two weeks later.

This is the second year of using direct deposit for the SFRP and GSRP associates. The process went much more smoothly with respect to obtaining required information from the associates, only 7% of the associates' information needed clarification in order for direct deposit to properly function as opposed to 10% from last year. The remaining associates received their stipend and expense payments via checks sent in the US mail.

HSAP program participants were considered actual RDL employees, and their respective state and federal income tax and Social Security were withheld from their paychecks. By the nature of their independent research, SFRP and GSRP program participants were considered to be consultants or independent contractors. As such, SFRP and GSRP associates were responsible for their own income taxes, Social Security, and insurance.

8. CONTENTS OF THE 1997 REPORT

The complete set of reports for the 1997 SRP includes this program management report (Volume 1) augmented by fifteen volumes of final research reports by the 1997 associates, as indicated below:

1997 SRP Final Report Volume Assignments

LABORATORY	SFRP	GSRP	HSAP
Armstrong	2	7	12
Phillips	3	8	13
Rome	4	9	14
Wright	5A, 5B	10	15
AEDC, ALCs, WHMC	6	11	16

APPENDIX A -- PROGRAM STATISTICAL SUMMARY

A. Colleges/Universities Represented

Selected SFRP associates represented 169 different colleges, universities, and institutions, GSRP associates represented 95 different colleges, universities, and institutions.

B. States Represented

SFRP -Applicants came from 47 states plus Washington D.C. Selectees represent 44 states.

GSRP - Applicants came from 44 states. Selectees represent 32 states.

HSAP - Applicants came from thirteen states. Selectees represent nine states.

Total Number of Participants	
SFRP	189
GSRP	97
HSAP	140
TOTAL	426

Degrees Represented			
	SFRP	GSRP	TOTAL
Doctoral	184	0	184
Master's	2	41	43
Bachelor's	0	56	56
TOTAL	186	97	298

SFRP Academic Titles	
Assistant Professor	64
Associate Professor	70
Professor	40
Instructor	0
Chairman	1
Visiting Professor	1
Visiting Assoc. Prof.	1
Research Associate	9
TOTAL	186

Source of Learning About the SRP		
Category	Applicants	Selectees
Applied/participated in prior years	28%	34%
Colleague familiar with SRP	19%	16%
Brochure mailed to institution	23%	17%
Contact with Air Force laboratory	17%	23%
IEEE Spectrum	2%	1%
BIIHE	1%	1%
Other source	10%	8%
TOTAL	100%	100%

APPENDIX B – SRP EVALUATION RESPONSES

1. OVERVIEW

Evaluations were completed and returned to RDL by four groups at the completion of the SRP. The number of respondents in each group is shown below.

Table B-1. Total SRP Evaluations Received

Evaluation Group	Responses
SFRP & GSRPs	275
HSAPs	113
USAF Laboratory Focal Points	84
USAF Laboratory HSAP Mentors	6

All groups indicate unanimous enthusiasm for the SRP experience.

The summarized recommendations for program improvement from both associates and laboratory personnel are listed below:

A. Better preparation on the labs' part prior to associates' arrival (i.e., office space, computer assets, clearly defined scope of work).

B. Faculty Associates suggest higher stipends for SFRP associates.

C. Both HSAP Air Force laboratory mentors and associates would like the summer tour extended from the current 8 weeks to either 10 or 11 weeks; the groups state it takes 4-6 weeks just to get high school students up-to-speed on what's going on at laboratory. (Note: this same argument was used to raise the faculty and graduate student participation time a few years ago.)

2. 1997 USAF LABORATORY FOCAL POINT (LFP) EVALUATION RESPONSES

The summarized results listed below are from the 84 LFP evaluations received.

1. LFP evaluations received and associate preferences:

Table B-2. Air Force LFP Evaluation Responses (By Type)

		How Many Associates Would You Prefer To Get ? (% Response)											
		SFRP				GSRP (w/Univ Professor)				GSRP (w/o Univ Professor)			
Lab	Evals Recv'd	0	1	2	3+	0	1	2	3+	0	1	2	3+
AEDC	0	-	-	-	-	-	-	-	-	-	-	-	-
WHMC	0	-	-	-	-	-	-	-	-	-	-	-	-
AL	7	28	28	28	14	54	14	28	0	86	0	14	0
USAFA	1	0	100	0	0	100	0	0	0	0	100	0	0
PL	25	40	40	16	4	88	12	0	0	84	12	4	0
RL	5	60	40	0	0	80	10	0	0	100	0	0	0
WL	46	30	43	20	6	78	17	4	0	93	4	2	0
Total	84	32%	50%	13%	5%	80%	11%	6%	0%	73%	23%	4%	0%

LFP Evaluation Summary. The summarized responses, by laboratory, are listed on the following page. LFPs were asked to rate the following questions on a scale from 1 (below average) to 5 (above average).

2. LFPs involved in SRP associate application evaluation process:
   a. Time available for evaluation of applications:
   b. Adequacy of applications for selection process:
3. Value of orientation trips:
4. Length of research tour:
5. a. Benefits of associate's work to laboratory:
   b. Benefits of associate's work to Air Force:
6. a. Enhancement of research qualifications for LFP and staff:
   b. Enhancement of research qualifications for SFRP associate:
   c. Enhancement of research qualifications for GSRP associate:
7. a. Enhancement of knowledge for LFP and staff:
   b. Enhancement of knowledge for SFRP associate:
   c. Enhancement of knowledge for GSRP associate:
8. Value of Air Force and university links:
9. Potential for future collaboration:
10. a. Your working relationship with SFRP:
    b. Your working relationship with GSRP:
11. Expenditure of your time worthwhile:

(Continued on next page)

12. Quality of program literature for associate:
13. a. Quality of RDL's communications with you:
    b. Quality of RDL's communications with associates:
14. Overall assessment of SRP:

Table B-3. Laboratory Focal Point Reponses to above questions

	AEDC	*AL*	*USAFA*	*PL*	*RL*	*WHMC*	*WL*
# Evals Recv'd	0	7	1	14	5	0	46
Question #							
2	-	86 %	0 %	88 %	80 %	-	85 %
2a	-	4.3	n/a	3.8	4.0	-	3.6
2b	-	4.0	n/a	3.9	4.5	-	4.1
3	-	4.5	n/a	4.3	4.3	-	3.7
4	-	4.1	4.0	4.1	4.2	-	3.9
5a	-	4.3	5.0	4.3	4.6	-	4.4
5b	-	4.5	n/a	4.2	4.6	-	4.3
6a	-	4.5	5.0	4.0	4.4	-	4.3
6b	-	4.3	n/a	4.1	5.0	-	4.4
6c	-	3.7	5.0	3.5	5.0	-	4.3
7a	-	4.7	5.0	4.0	4.4	-	4.3
7b	-	4.3	n/a	4.2	5.0	-	4.4
7c	-	4.0	5.0	3.9	5.0	-	4.3
8	-	4.6	4.0	4.5	4.6	-	4.3
9	-	4.9	5.0	4.4	4.8	-	4.2
10a	-	5.0	n/a	4.6	4.6	-	4.6
10b	-	4.7	5.0	3.9	5.0	-	4.4
11	-	4.6	5.0	4.4	4.8	-	4.4
12	-	4.0	4.0	4.0	4.2	-	3.8
13a	-	3.2	4.0	3.5	3.8	-	3.4
13b	-	3.4	4.0	3.6	4.5	-	3.6
14	-	4.4	5.0	4.4	4.8	-	4.4

3. 1997 SFRP & GSRP EVALUATION RESPONSES

The summarized results listed below are from the 257 SFRP/GSRP evaluations received.

Associates were asked to rate the following questions on a scale from 1 (below average) to 5 (above average) - by Air Force base results and over-all results of the 1997 evaluations are listed after the questions.

1. The match between the laboratories research and your field:
2. Your working relationship with your LFP:
3. Enhancement of your academic qualifications:
4. Enhancement of your research qualifications:
5. Lab readiness for you: LFP, task, plan:
6. Lab readiness for you: equipment, supplies, facilities:
7. Lab resources:
8. Lab research and administrative support:
9. Adequacy of brochure and associate handbook:
10. RDL communications with you:
11. Overall payment procedures:
12. Overall assessment of the SRP:
13. a. Would you apply again?
    b. Will you continue this or related research?
14. Was length of your tour satisfactory?
15. Percentage of associates who experienced difficulties in finding housing:
16. Where did you stay during your SRP tour?
    a. At Home:
    b. With Friend:
    c. On Local Economy:
    d. Base Quarters:
17. Value of orientation visit:
    a. Essential:
    b. Convenient:
    c. Not Worth Cost:
    d. Not Used:

SFRP and GSRP associate's responses are listed in tabular format on the following page.

Table B-4. 1997 SFRP & GSRP Associate Responses to SRP Evaluation

	Arnold	Brooks	Edwards	Eglin	Griffis	Hanscom	Kelly	Kirtland	Lackland	Robins	Tyndall	WPAFB	average
# res	6	48	6	14	31	19	3	32	1	2	10	85	257
1	4.8	4.4	4.6	4.7	4.4	4.9	4.6	4.6	5.0	5.0	4.0	4.7	4.6
2	5.0	4.6	4.1	4.9	4.7	4.7	5.0	4.7	5.0	5.0	4.6	4.8	4.7
3	4.5	4.4	4.0	4.6	4.3	4.2	4.3	4.4	5.0	5.0	4.5	4.3	4.4
4	4.3	4.5	3.8	4.6	4.4	4.4	4.3	4.6	5.0	4.0	4.4	4.5	4.5
5	4.5	4.3	3.3	4.8	4.4	4.5	4.3	4.2	5.0	5.0	3.9	4.4	4.4
6	4.3	4.3	3.7	4.7	4.4	4.5	4.0	3.8	5.0	5.0	3.8	4.2	4.2
7	4.5	4.4	4.2	4.8	4.5	4.3	4.3	4.1	5.0	5.0	4.3	4.3	4.4
8	4.5	4.6	3.0	4.9	4.4	4.3	4.3	4.5	5.0	5.0	4.7	4.5	4.5
9	4.7	4.5	4.7	4.5	4.3	4.5	4.7	4.3	5.0	5.0	4.1	4.5	4.5
10	4.2	4.4	4.7	4.4	4.1	4.1	4.0	4.2	5.0	4.5	3.6	4.4	4.3
11	3.8	4.1	4.5	4.0	3.9	4.1	4.0	4.0	3.0	4.0	3.7	4.0	4.0
12	5.7	4.7	4.3	4.9	4.5	4.9	4.7	4.6	5.0	4.5	4.6	4.5	4.6
Numbers below are percentages													
13a	83	90	83	93	87	75	100	81	100	100	100	86	87
13b	100	89	83	100	94	98	100	94	100	100	100	94	93
14	83	96	100	90	87	80	100	92	100	100	70	84	88
15	17	6	0	33	20	76	33	25	0	100	20	8	39
16a	-	26	17	9	38	23	33	4	-	-	-	30	
16b	100	33	-	40	-	8	-	-	-	-	36	2	
16c	-	41	83	40	62	69	67	96	100	100	64	68	
16d	-	-	-	-	-	-	-	-	-	-	-	0	
17a	-	33	100	17	50	14	67	39	-	50	40	31	35
17b	-	21	-	17	10	14	-	24	-	50	20	16	16
17c	-	-	-	-	10	7	-	-	-	-	-	2	3
17d	100	46	-	66	30	69	33	37	100	-	40	51	46

4. 1997 USAF LABORATORY HSAP MENTOR EVALUATION RESPONSES

Not enough evaluations received (5 total) from Mentors to do useful summary.

5. 1997 HSAP EVALUATION RESPONSES

The summarized results listed below are from the 113 HSAP evaluations received.

HSAP apprentices were asked to rate the following questions on a scale from 1 (below average) to 5 (above average)

1. Your influence on selection of topic/type of work.
2. Working relationship with mentor, other lab scientists.
3. Enhancement of your academic qualifications.
4. Technically challenging work.
5. Lab readiness for you: mentor, task, work plan, equipment.
6. Influence on your career.
7. Increased interest in math/science.
8. Lab research & administrative support.
9. Adequacy of RDL's Apprentice Handbook and administrative materials.
10. Responsiveness of RDL communications.
11. Overall payment procedures.
12. Overall assessment of SRP value to you.
13. Would you apply again next year? Yes (92 %)
14. Will you pursue future studies related to this research? Yes (68 %)
15. Was Tour length satisfactory? Yes (82 %)

	Arnold	Brooks	Edwards	Eglin	Griffiss	Hanscom	Kirtland	Tyndall	WPAFB	Totals
# resp	5	19	7	15	13	2	7	5	40	113
1	2.8	3.3	3.4	3.5	3.4	4.0	3.2	3.6	3.6	3.4
2	4.4	4.6	4.5	4.8	4.6	4.0	4.4	4.0	4.6	4.6
3	4.0	4.2	4.1	4.3	4.5	5.0	4.3	4.6	4.4	4.4
4	3.6	3.9	4.0	4.5	4.2	5.0	4.6	3.8	4.3	4.2
5	4.4	4.1	3.7	4.5	4.1	3.0	3.9	3.6	3.9	4.0
6	3.2	3.6	3.6	4.1	3.8	5.0	3.3	3.8	3.6	3.7
7	2.8	4.1	4.0	3.9	3.9	5.0	3.6	4.0	4.0	3.9
8	3.8	4.1	4.0	4.3	4.0	4.0	4.3	3.8	4.3	4.2
9	4.4	3.6	4.1	4.1	3.5	4.0	3.9	4.0	3.7	3.8
10	4.0	3.8	4.1	3.7	4.1	4.0	3.9	2.4	3.8	3.8
11	4.2	4.2	3.7	3.9	3.8	3.0	3.7	2.6	3.7	3.8
12	4.0	4.5	4.9	4.6	4.6	5.0	4.6	4.2	4.3	4.5
Numbers below are percentages										
13	60%	95%	100%	100%	85%	100%	100%	100%	90%	92%
14	20%	80%	71%	80%	54%	100%	71%	80%	65%	68%
15	100%	70%	71%	100%	100%	50%	86%	60%	80%	82%

ATMOSPHERIC REACTIONS OF VOLATILE PAINT COMPONENTS: A MODELING APPROACH

Jean M.Andino, Ph.D.
Associate Professor
Department of Environmental Engineering Sciences

University of Florida
P.O. Box 116450
Gainesville, FL 32611-6450

Final Report for:
Summer Research Program
Rome Laboratory

Sponsored by:
Air Force Office of Scientific Research
Bolling Air Force Base, Washington, DC

And

Rome Laboratory

September 1997

ATMOSPHERIC REACTIONS OF VOLATILE PAINT COMPONENTS: A MODELING APPROACH

Jean M. Andino, Ph.D.
Assistant Professor
Department of Environmental Engineering Sciences
University of Florida

Abstract

In order to determine effective air pollution control strategies, the reactions of pollutants must be known. The primary mechanism of destruction for oxygenated compounds in the atmosphere is reaction with hydroxyl radicals. In the presence of oxygen and NO, these radicals form alkoxy radicals. To predict the yields of stable products from the reactions of organics, one must be able to accurately estimate the relative importance of the decomposition, isomerization, and O_2 reaction pathways of these alkoxy radicals. The work presented examines the decomposition and O_2 reaction pathways for alkoxy radicals of the general type, R_1-O-C(O)-R_2. Experimental yields for the OH initiated photooxidation of selected oxygenated compounds that are typically used in Air Force operations were compared to yields predicted from computer based chemical modeling. New estimates for the rate constants for the decomposition and O_2 reaction pathways for alkoxy radicals of the general form R_1-O-C(O)-R_2 have been determined to be 2.2×10^{4} s^{-1} and 4.6×10^{-16} $cm^3 molecule^{-1}$ s^{-1}, respectively. These new rate constant estimates will allow Air Force personnel to accurately assess the air quality impacts of operations involving oxygenated compounds.

ATMOSPHERIC REACTIONS OF VOLATILE PAINT COMPONENTS: A MODELING APPROACH

Jean M. Andino, Ph.D.

Introduction

The atmospheric chemistry of oxygenated compounds has received increased attention because of the use of these compounds as fuel additives and solvents. Once emitted into the atmosphere, these compounds can react to eventually form ozone, a nationally regulated pollutant. Traditionally, air quality models have been used by researchers in order to evaluate ozone controlling strategies. To make accurate predictions, these models must, among other things, accurately represent the chemistry taking place in a given region. The research sponsored by the Air Force Summer Faculty program was aimed at improving the chemical kinetic representations of key intermediates formed from oxygenated compounds through the use of computer modeling. Many of the species that were used as test compounds included volatile components of paints used in typical Air Force operations. It has been found that the paints used by the Air Force contain a wide variety of acetates, alcohols, and ketones, among other classes of compounds[1]. Therefore, in order for the Air Force to evaluate the air quality impact of proposed changes in operations involving the emissions of volatile

components, the chemistry of oxygenated compounds must be accurately represented in air quality models.

The kinetics of the OH, NO_3, and ozone reactions with selected oxygenated species have been reasonably well investigated, and compilations of these values are available in the literature [2]. Based on these values, and considering the average atmospheric concentrations of OH, NO_3, and ozone in the atmosphere, it is clear that the major loss process for oxygenated compounds in the atmosphere is reaction with OH radicals. From structure activity calculations[3] and product studies available in the literature [4-8] , it is known that the most likely mode of hydroxyl radical attack on oxygenated compounds that are of interest to Air Force operations is hydrogen atom abstraction from a carbon center to form a highly reactive radical. Oxygen quickly adds to the initial radical to form a peroxy radical, which, in the presence of nitric oxide, is subsequently reduced to an alkoxy radical. It is the fate of this alkoxy radical that is in question. It is known that the alkoxy radical can decompose, react with oxygen, or isomerize, depending on the nature (primary, secondary, tertiary) and size of the radical [2] . However, the kinetics associated with each of these pathways are uncertain. Atkinson [2] has reported equations that can be used to determine rate constants for the alkoxy radical decomposition and oxygen reactions. Both equations are

based on the enthalpies of the particular reaction- either the enthalpy of decomposition (ΔH_d) or the enthalpy of alkoxy radical reaction with oxygen(ΔH_{O2}). The equations are:

$$k_{O_2 Reaction} = 1.3 \times 10^{-19} n d e^{-0.32 \Delta H_{O_2}} \qquad \text{(Equation 1)}$$

$$k_{Decomposition} = 2.4 x 10^{14} e^{-E_d / RT} \qquad \text{(Equation 2)}$$

where "n" is the number of abstractable hydrogen atoms, "d" is the degeneracy, "A" is the preexponential factor, "E_d" is defined as:

$$E_d = 11.2 + 0.79\ \Delta H_d ,$$

"R" is the ideal gas constant, and "T" is the temperature in Kelvin. The equations represented above have been tested against a small database of alkoxy radicals, and seem to be adequate for endothermic reactions [2]. However, these equations do not adequately predict the rate constants associated with alkoxy radical reactions that are exothermic in nature. In addition, the equations do not adequately represent alkoxy radicals formed from oxygenated compounds. Much of the difficulty associated with developing equations to predict the rate constants of the reactions of various types of alkoxy radicals has been due to the paucity of experimental product data. In recent years, several experimentally based product studies have been conducted both at Tyndall AFB and elsewhere

on oxygenated compounds [4-8]. These new results formed the basis of the modeling studies conducted this summer, and have led to new estimates for the decomposition and O_2 reaction pathways for alkoxy radicals of the general form R_1-O-C(O)-R_2 that originate from oxygenated compounds.

Methods

One of the major volatile components of paints used in Air Force operations is 2-ethoxy ethyl acetate (EEA) [1]. This compound has been investigated experimentally by the Air Team at Tyndall AFB [4], and therefore served as the perfect test compound. The initial goal was to determine if a computer model of the reactions of EEA could adequately predict the products seen in experimental studies. A mechanism was devised based on the work of Wells et al. [4] (see Figure 1), and was implemented in the *"Atmospheric Photochemical Mechanism Preparation and Emissions Processing Program"* [9] . The rate constants for the initial OH radical abstraction steps were determined using the relative rate study of Wells et al. [4] in conjunction with the structure activity formulation of Kwok and Atkinson[3] . Rate constants for the reactions of the initial radical with O_2 and the

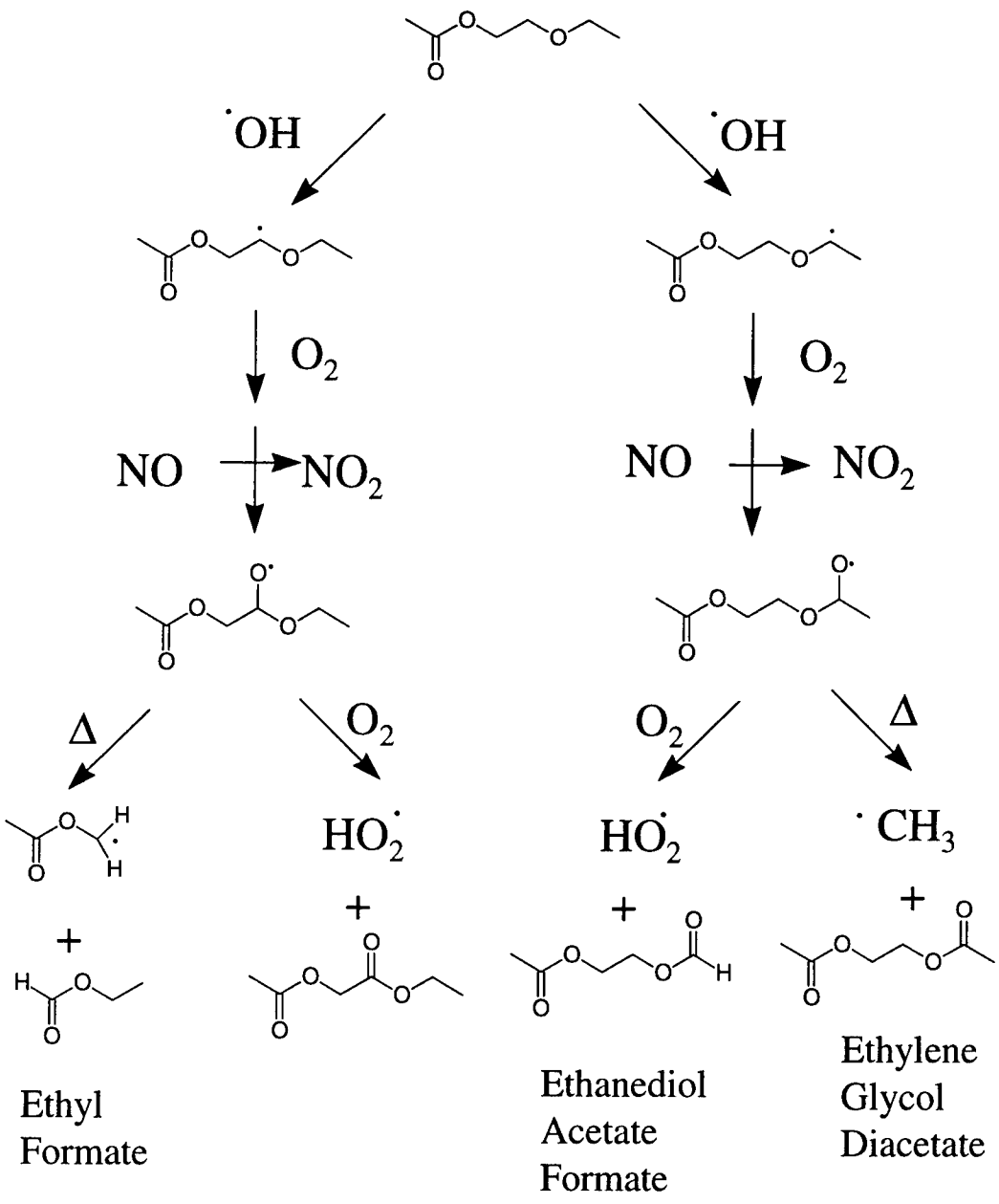

Figure 1: Mechanism of hydroxyl radical reaction with 2-ethoxy ethyl acetate in air.

subsequent peroxy/alkoxy radical reactions with NO or NO_2 were estimated using the recommendations in Atkinson [2]. The rate constants for alkoxy radical decomposition and O_2 reaction pathways in the initial mechanism used were determined by calculating the corresponding enthalpies of reaction and using Equations 1 and 2 (the method of Atkinson[2]). The enthalpies of reaction were determined using *the "National Institute of Standards and Technology (NIST) Structures and Properties Database Estimation Program"*[10] which is based on Benson group additivity principles. It should be noted that some of the enthalpies could not be calculated because of a lack of Benson group information, and therefore had to be estimated using a bond additivity principle. As an example, the enthalpy of formation of one of the initial radicals formed in the EEA photooxidation mechanism,

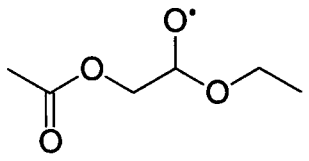

could not be calculated using the NIST program. However, the enthalpy of formation of the corresponding protenated compound could be determined. Thus, using the available database in the NIST program, the contribution of the hydrogen atom to the overall enthalpy of formation of a compound was determined. Several test compounds for which data

were available both for the stable species and the hydrogen atom abstracted radical were used to determine the contribution of the hydrogen atom to the enthalpy of formation. As just one example, the following two compounds were input into the NIST program:

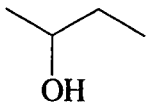

A

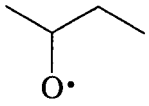

B

The enthalpies of formation for structures A and B were calculated using the NIST program as -70.4 kcal/mol and -17.5 kcal/mol, respectively. The difference between the two enthalpies (52.9 kcal/mol) represents the contribution of the hydrogen atom to the overall enthalpy of formation. This value was consistent regardless of what structures were input, and was used to correct for the contribution of the hydrogen atom to the enthalpy of formation. Presented in Table I are the enthalpies of formation for individual species and overall reactions in the EEA + OH mechanism along with the corresponding rate constants. Those structures whose enthalpies were estimated using the above mentioned technique are clearly noted.

The completed mechanism was executed in the Carter modeling program [9], which gives concentration versus time profiles as the output. Reactions which modeled the loss of the major products EF, EAF, and

Table I: Calculated enthalpies and rate constants for EEA photooxidation by OH radicals.

Parent Cmpd	*Radical*	*Δ/ O_2*	*ΣH_f reactant(s)* [a]	*Products*	*H_f products* [b]	*ΔH_{rxn}*	*k*
EEA	(Rad1-O) 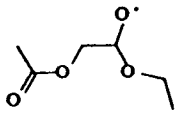	Δ	-139.2	Ethyl Formate 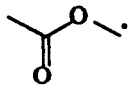	-92.0 -45.7 [c]	-1.5	9.0×10^{6}
		Δ	-139.2	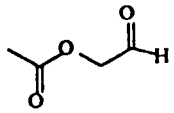 $C_2H_3O^{\bullet}$	-125.6 -4.1	-9 5	3.9×10^{11}
		O_2	-139.2	$HO_2^{\bullet}$ 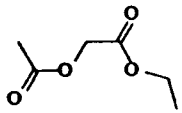	2.5 -192.9	-51 2	1.7×10^{-12}
	(Rad2-O) 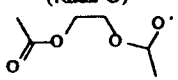	O_2	-139.2	HO_2 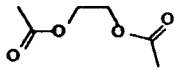	2.5 -192.9	-51 2	1.7×10^{-12}
		Δ	-139.2	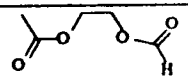 $^{\bullet}CH_3$	-179.7 34.8	-5.7	2.45×10^{9}
		Δ	-139.2	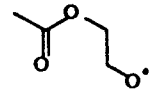 CH_3CHO	-90.4 -39 6	9.2	5.7

[a, b] Units of kcal/mol. Calculated using the NIST program [10].

[c] The enthalpy of the protenated compound was compound was calculated using the NIST program [10], and 52.9 kcal/mol was added to the enthalpy to take into account the contribution of the abstracted hydrogen atom.

EGD were not included in the mechanism in order to directly compare corrected experimental and predicted yields. The yield for a given product was determined as the ratio of the concentration of the product to the change in the concentration of the reactant organic.

Once the mechanism for EEA was developed, corrected, and tested, additional compounds were also tested to see if predicted results matched experimental results using the formulation of Atkinson [2] to determine the rate constants for the alkoxy radical reactions. Full mechanisms were prepared for the additional oxygenated compounds. Table II indicates the compounds tested and their structure. Presented in Table III are the product yields resulting from laboratory studies of the OH initiated photooxidation of each of the compounds.

Table II: Names and structures of test compounds used in this study.

Compound	*Structure*
Ethyl-3-Ethoxy Propionate	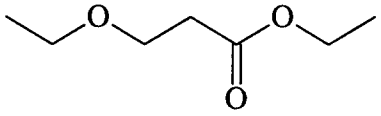
2-Ethoxy Ethanol	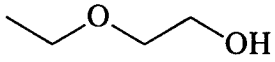
2-Butoxy Ethanol	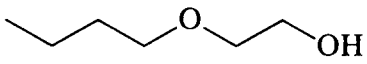
Diethyl Ether	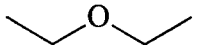
Ethyl-t-Butyl Ether	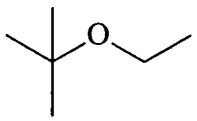

Table III: Experimentally determined molar yields for the products of the OH initiated photooxidation of several oxygenated compounds.

Parent Compound	*Product Name*	*Yield*	*Reaction Pathway*	*Source*
2-Ethoxy Ethyl Acetate	Ethyl Formate	0.328	Decomp.	[4]
	Ethylene Glycol Diacetate	0.04	O_2	
	Ethanediol Acetate Formate	0.37	O_2	
Ethyl-2-Ethoxy Propionate	Ethyl (3-Formoloxy) Propionate	0.30	Decomp.	[11]
	Ethyl Glyoxate	0.25	Decomp.	
	Ethyl Formate	0.37	Decomp.	
	Diethyl Malonate		O_2	
	Ethyl (2-Formyl) Acetate	0.048	Decomp./ O_2	
	Acetaldehyde	0.049	Decomp./ O_2	
2-Ethoxy Ethanol	Ethyl Formate	0.37	Decomp. Decomp./ O_2	[12]
2-Butoxy Ethanol	Butyl Formate	0.35	Decomp.	[8]
	Ethylene Glycol Monoformate	0.39	Decomp.	
	Butoxyacetaldehyde	0.12	O_2	
	3-Hydroxy Butyl Formate	0.20	O_2	
	Propionaldehyde	0.2	Decomp./ O_2	
Diethyl Ether	Ethyl Formate	0.95 (0.84)	Decomp.	[6] ([5])
	Ethyl Acetate	< 0.05 (0.06)	O_2	[6] ([5])
Ethyl-t-Butyl Ether	t-Butyl Formate	0.64 (0.77)	Decomp.	[7] ([6])
	t-Butyl Acetate	0.13 (0)	O_2	[7] ([6])

Results

The yields of the three major products of EEA photooxidation, ethanediol acetate formate (EAF), ethyl formate (EF), and ethylene glycol diacetate (EGD), were determined using a mechanism that implemented the rate constants derived from Equations 1 and 2. These yields were 0.0003, 0.0451, and 0.453, respectively. The experimentally derived product yields reported by Wells et al. [4] were 0.37, 0.328, and 0.04, respectively. It was therefore clear that the rate constants used in the initial mechanism did not adequately represent experimental conditions, and therefore could not be used to properly assess the impact of EEA emissions from painting operations on ozone formation. In addition, upon careful examination of the structure of the alkoxy radicals, it was evident that alkoxy radicals of the form R_1-O-C(O)-R_2 were influential in the production of the products of interest. The rate constants for the alkoxy radical decomposition and O_2 reaction pathways in the EEA mechanism were subsequently adjusted so that predicted yields matched experimental yields. Note that the rate constants of other reactions in the EEA mechanism were not adjusted, since they were relatively well known, or had been studied experimentally. The results indicated that rate constants for the decomposition and oxygen reaction pathways for the R_1-O-C(O)-R_2 alkoxy radical of 2.2×10^4 s^{-1} and 4.6×10^{-16} cm^3 $molecule^{-1}$

s^{-1}, respectively, produced predicted yields for the products of EEA photooxidation that closely matched experimentally determined yields. Figures 2-4 indicate the agreement between the experimental data points for EEA and the predicted yields. The dotted lines represent the predictions made using the older alkoxy radical reaction rate constant formulation (based on enthalpies) by Atkinson [2], and the solid lines represent the predictions made using the two newly developed rate constants (independent of reaction enthalpies). The points are actual data points from the study of Wells et al. [4].

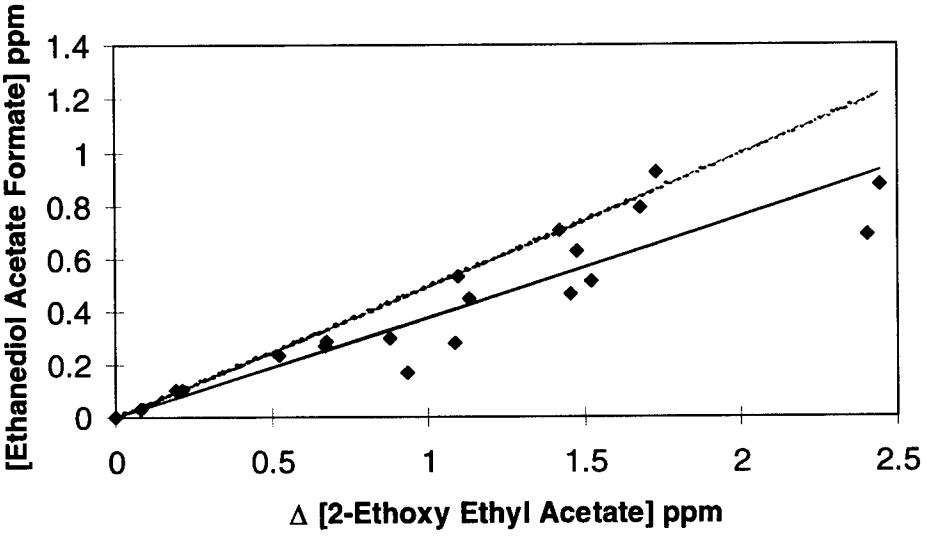

Figure 2: Predicted and experimental results for the production of ethanediol acetate formate (EAF) from EEA + OH photooxidation.

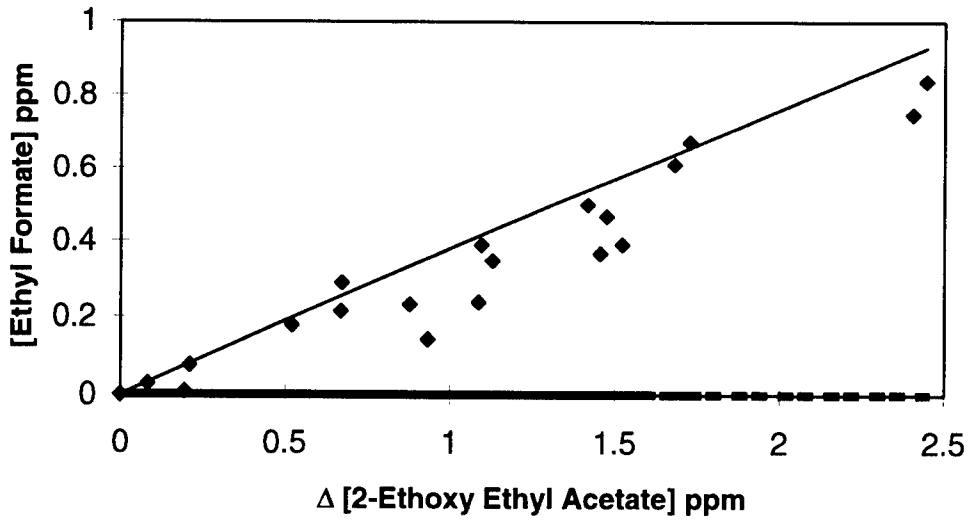

Figure 3: Predicted and experimental results for the production of ethyl formate (EF) from EEA + OH photooxidation.

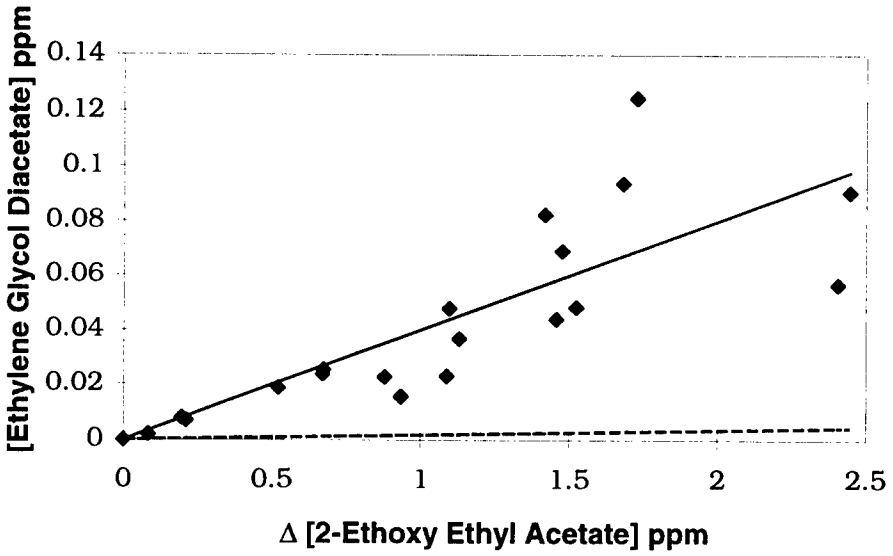

Figure 4: Predicted and experimental results for the production of ethylene glycol diacetate (EGD) from EEA + OH photooxidation.

The modeling studies were also conducted on the oxygenated compounds appearing in Table II. Use of the older, enthalpy based equations (Equations 1 and 2) to determine rate constants for the alkoxy radical reaction pathways produced yields of the major products of photooxidation that were not consistent with experimental results. Table IV clearly illustrates the discrepancies between the predicted and experimental results. Once the rate constants determined in the EEA study were applied to the reactions of alkoxy radicals of the form: R_1-O-C(O)-R_2, the match between the predicted and experimental yields improved. Again, Table IV indicates the agreement between the predicted and experimental yields. It is important to note that the rate constants developed in the EEA modeling study were directly applied to the alkoxy radical reactions of the additional oxygenated compounds studied. The rate constants were not adjusted further. Examination of Table IV gives a clear indication that mechanisms that use the new, enthalpy-independent alkoxy radical rate constants are able to more accurately reproduce experimentally observed product yields than mechanisms based on the enthalpy dependent alkoxy radical reaction rate constants.

Table IV: Comparison between experimental and predicted molar yields of products formed in the hydroxyl radical initiated photooxidation of selected oxygenated compounds.

Parent Compound	Product Name	Expt'l Yield	Predicted Yield [a]	Predicted Yield [b]
2-Ethoxy Ethyl Acetate	Ethyl Formate	0.328	0.38	0.0451
	Ethylene Glycol Diacetate	0.04	0.04	0.453
	Ethanediol Acetate Formate	0.37	0.38	0.0003
Ethyl-2-Ethoxy Propionate	Ethyl (3-Formoloxy) Propionate	0.30	0.23	$9x10^{-5}$
	Ethyl Glyoxate	0.25	0.32	0.05
	Ethyl Formate	0.37	0.32	0.05
	Diethyl Malonate		0.03	0.15
	Ethyl (2-Formyl) Acetate	0.048	0.11	0.37
	Acetaldehyde	0.049	0.11	0.38
2-Ethoxy Ethanol	Ethyl Formate	0.37	0.34	0.04
2-Butoxy Ethanol	Butyl Formate	0.35	0.32	0.41
Diethyl Ether	Ethyl Formate	0.95 (0.84)	0.90	1.00
	Ethyl Acetate	< 0.05 (0.06)	0.09	0.00007
Ethyl-t-Butyl Ether	t-Butyl Formate	0.64 (0.77)	0.76	0.0006
	t-Butyl Acetate	0.13 (0)	0.08	0.90

[a] Predictions made using the rate constants developed in this work for the R_1-O-C(O·)-R_2 radical.

[b] Predictions made using the rate constant formulations (Equations 1 and 2) by Atkinson [2].

Discussion

The newly developed rate constants provide a better estimate to the oxygenated alkoxy radical decomposition and O_2 reaction pathways than previous estimates. It is clear that based on the results obtained with tests against six different oxygenated compounds, an enthalpy based relationship is not needed to adequately model the product distributions expected from the reactions of alkoxy radicals of the form R_1-O-C(O)-R_2. Instead, the decomposition and O_2 reaction pathways for these specific alkoxy radicals can be well represented by rate constants of 2.2×10^{4} s^{-1} and 4.6×10^{-16} cm^3 $molecule^{-1}$ s^{-1}, respectively. In order to further test the rate constants derived in this study, additional experimental and modeling work on the OH initiated photooxidation of oxygenated compounds will have to be performed. However, in the near future, the newly derived rate constants can provide much needed improvement to the representations of oxygenated species in air quality models, thus allowing the Air Force to more accurately predict the air quality impact of operations that involve the release of volatile oxygenated organic compounds.

References

[1] Wells,J.R., Baxley,J.S., Winner,D.A., *"Atmospheric Chemistry of Coating Systems"*, United States Air Force Armstrong Laboratory Report No. AL/EQ-TR-1996-0041, October, 1996.

[2] Atkinson,R., *J Phys. Chem. Ref Data*, **Monograph 2**, 1992.

[3] Kwok,E. and Atkinson,R., *Atm. Env.* , **29**, 1996, 1685-1695.

[4] Wells,J.R., Wiseman,F.L., Williams,D.C., Baxley,J.S., Smith,D.F., *Int. J. Chem. Kinet.* , **28**, 1996, 475-480.

[5] Eberhard,J. , Muller,C., Stocker,D.W., Kerr, J.A., *Int. J. Chem. Kinet.*, **25**, 1993, 639-649.

[6] Wallington,T.J., Japar,S.M., *Env. Sci. Tech.* , **25**, 1991, 410-415.

[7] Smith,D.F., Kleindienst,T.E., Hudgens,E.E., McIver,C.D., Bufalini,J.J., *Int. J. Chem. Kinet.* , **24**, 1992, 199-215.

[8] Stemmler,K., Mengon,W., Kinnison,D.J., Kerr,J.A., *Env. Sci. Tech.*, **31**, 1997, 1496-1504.

[9] Carter,W.P.L., *"Documentation for the SAPRC Atmospheric Photochemical Mechanism Preparation and Emissions Processing Program for Implementation in Airshed Models"*, California Air Resources Board, Contract No. A5-122-32, October, 1988.

[10] Stein,S.E., Rukkers,J.M., Brown,R.L., *"NIST Standard Reference Database 25: NIST Structures and Properties Database Estimation Program"*, 1991.

[11] Baxley, J.S., Henley,M.V., Wells, J.R., *Int. J. Chem. Kinet.*, In press, 1997.

[12] Based on studies conducted by the Air Team at Tyndall AFB. Results are to be published.

NOVEL ELECTROCHEMILUMINESCENCE REACTIONS AND INSTRUMENTATION

Anthony Andrews
Assistant Professor
Centre for Intelligent Chemical Instrumentation

Clippinger Laboratories
Ohio University
Athens, OH, 45701-2979

Final Report for:
Summer Faculty Research Program
Armstrong Laboratory

Sponsored by:
Air Force Office of Scientific Research
Bolling Air Force Base, DC

and

Armstrong Laboratory

August 1997

NOVEL ELECTROCHEMILUMINESCENCE REACTIONS AND INSTRUMENTATION

Anthony Andrews
Assistant Professor
Centre for Intelligent Chemical Instrumentation
Ohio University

Abstract

A number of compounds whose structure indicated that they might bind to cations were screened for their electrochemiluminescence (ECL) properties. Screening was carried out in the presence of tripropylamine as a co-reactant. The organic compounds were screened both with and without a cation present by using a batch ECL instrument in two modes, solution and bead capture.

The three compounds which showed a large increase in ECL in the presence of cadmium ions were examined further. Conditions for the ECL reaction were optimised and a calibration graph for cadmium constructed. Limits of detection for cadmium were found to be in the low parts per billion region.

An ECL system which operates in both stop-flow and flow-through modes was constructed. A data acquisition program for acquisition of both the electrode voltage and photomultiplier tube output was written. A preliminary characterisation of the home-built flow-through ECL system was carried out using tris(2,2'-bipyridyl)ruthenium(II), a well known electrochemiluminescent compound.

NOVEL ELECTROCHEMILUMINESCENCE REACTIONS AND INSTRUMENTATION

Anthony Andrews

Introduction

ECL is the generation of light during a chemical reaction with at least one of the reagents being generated *in situ* at an electrode. This has the advantage of allowing the reaction to be controlled and managed by adjustments to the applied potential. The occurrence, mechanisms and analytical applications of ECL are well covered in a recent review (1). Probably the most common electrochemiluminescent reagent is tris(2,2'-bipyridinyl)ruthenium(II) [$Ru(bpy)_3^{2+}$] which has been used to determine a number of different compounds including aliphatic amines (2), drugs (3,4), amino acids (5,6), oxalate in urine (7), pyruvate (8) and ß-lactam antibiotics (9).

Perhaps the greatest potential for ECL lies in the area of sensors. Electrochemical sensors have the potential for analytical measurement to move from the laboratory to the field, and to perform these measurements rapidly, inexpensively and reliably.

By utilising the additional selectivity of ECL it is feasible that a major disadvantage of field electrochemical sensors could be overcome, that is, their lack of selectivity. This is because the addition of a chemiluminescence step adds extra selectivity to the sensor in addition to the discrimination provided by the electrochemical stage.

In order for ECL sensors to become a reality, more fundamental electrochemiluminescent reactions must be discovered and characterised.(10). Preliminary work in this area has been undertaken by Bruno and co-workers who have reported on a number of novel ECL reactions (11-13). This work indicated that ECL can be modified in the presence of metal ions (cations). The determination of metal ions in the field is a topic of interest to both the US Air Force and agencies such as the US EPA.

A logical extension of the previous work would be to continue screening organic ligands for intrinsic ECL and a modification of that ECL in the presence of cations. This work has focussed on this area and another critical area for ECL development, that of instrumentation design.

ORGANIC LIGAND SCREENING

Experimental

The instrument used to screen compounds for ECL activity was a Origen Analyzer (Igen, Inc.). Solutions for the Origen were ECL assay buffer which consisted of disodium hydrogen phosphate (0.15 M, Fisher Scientific), Triton X-100 (0.5 %, Sigma) and tripropylamine (TPA, 0.2 M, Aldrich) pH adjusted to 7.5 with concentrated hydrochloric acid. Cell cleaner solution consisted of potassium hydroxide (0.71 M, Sigma) and Triton X-100 (0.5 %). All water used was 18 MΩ water obtained from a Barnstead E-pure system. Ions were obtained as atomic absorption standards from Fisher Scientific or Spex Corp. A list of ions examined for their effect upon ECL is given in Table 1. Organic compounds whose structure indicated that they might form complexes with cations, thus changing their ECL, were obtained from Aldrich or Alfa ÆSAR. Figure 1 shows the structures of these twelve compounds. Solutions of the individual compounds (1 mg/mL) were prepared in methanol (HPLC grade, Aldrich).

Samples for screening were prepared with organic ligand (200 µL), ion of interest (100 µL) and assay buffer (700 µL). Samples were screened using the default setting on the Origen in bead capture and solution modes.

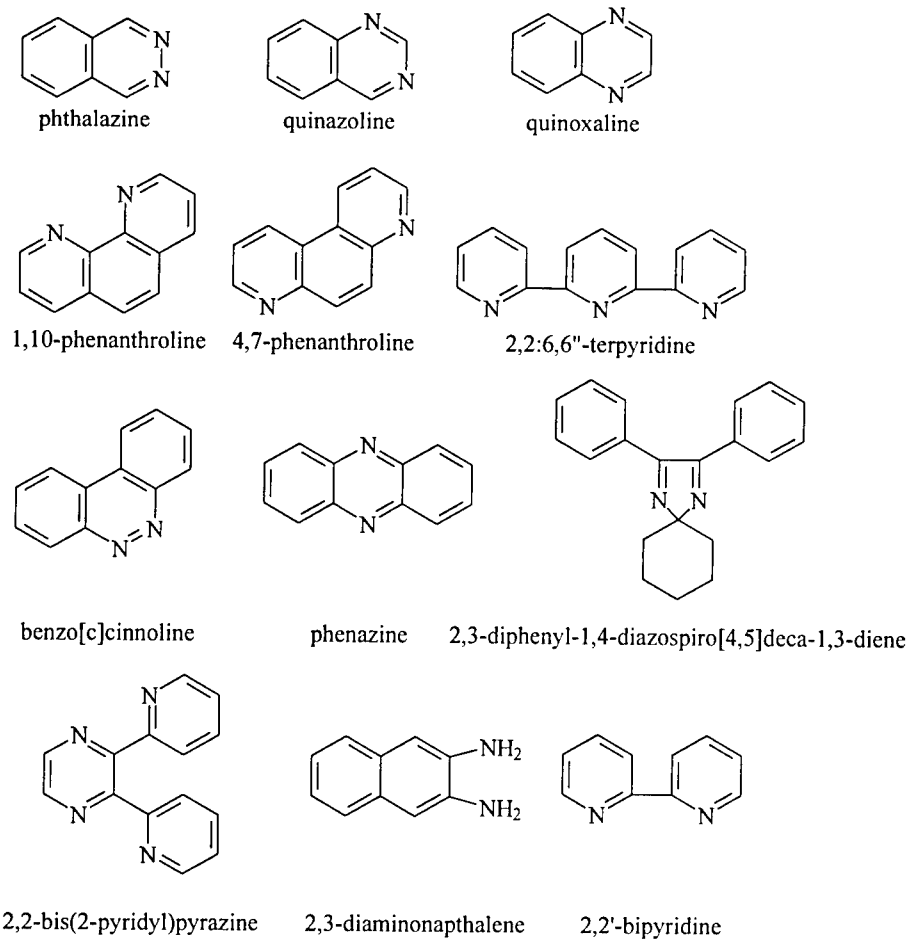

Figure 1. Structure and names of the 12 organic ligands screened for ECL.

Table 1 Ions tested for effect upon ECL

Ag^{+}	Ba^{2+}	Cu^{2+}	K^{+}	Ni^{2+}	Se^{4+}	Tl^{+}
Al^{3+}	Ca^{2+}	Eu^{3+}	Li^{+}	Pb^{2+}	Si^{4+}	V^{5+}
As^{3+}	Cd^{2+}	Fe^{3+}	Mg^{2+}	Re^{3+}	Sn^{2+}	W^{4+}
Au^{+}	Cr^{6+}	Ga^{3+}	Mn^{2+}	Ru^{3+}	Sr^{2+}	Zn^{2+}
B	Co^{2+}	Hg^{2+}	Na^{+}	Sb^{2+}	Tb^{3+}	

Results

Initial ECL screen

The results of the ECL screening are shown in Figures 2-14.

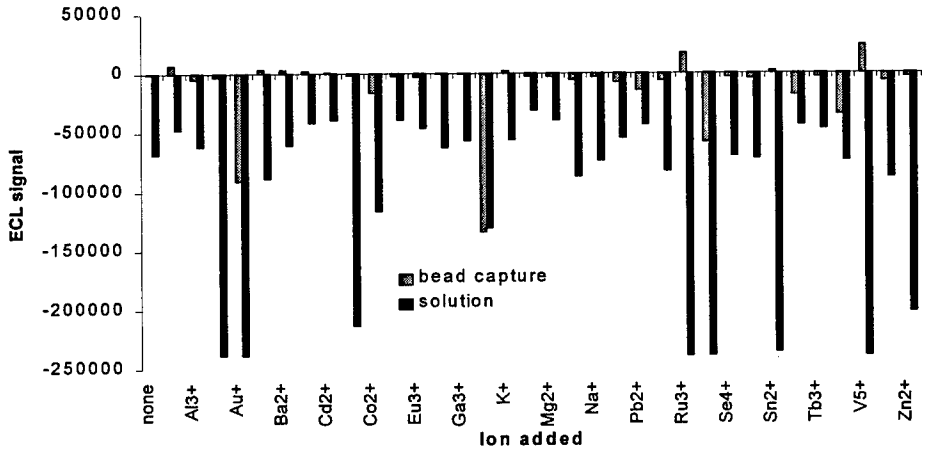

Figure 2. Results of the ECL screen with no organic ligand.

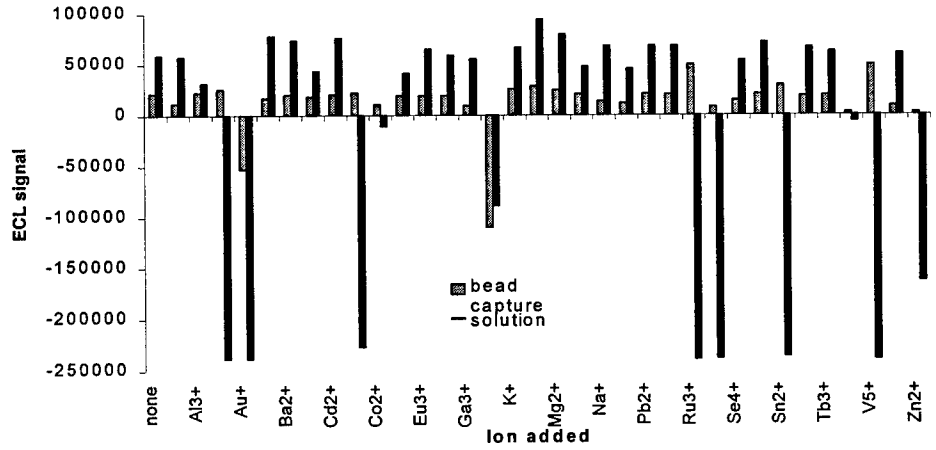

Figure 3. Results of the ECL screen with phthalazine.

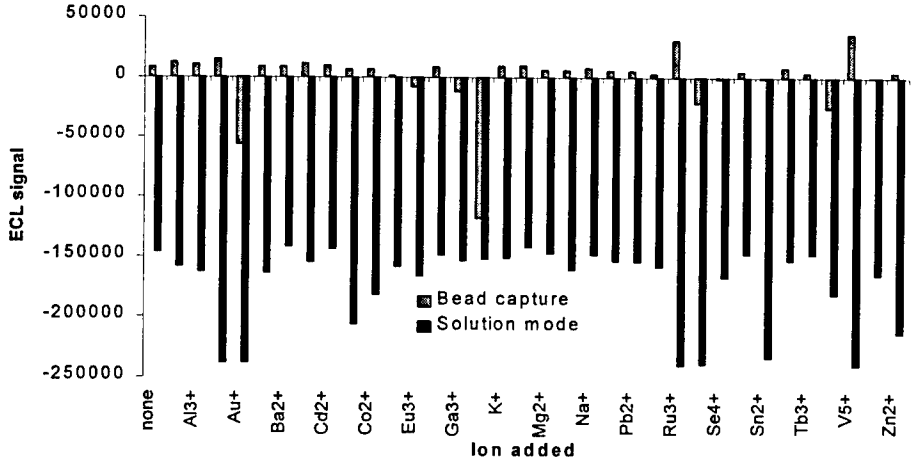

Figure 4. Results of the ECL screen with quinazoline.

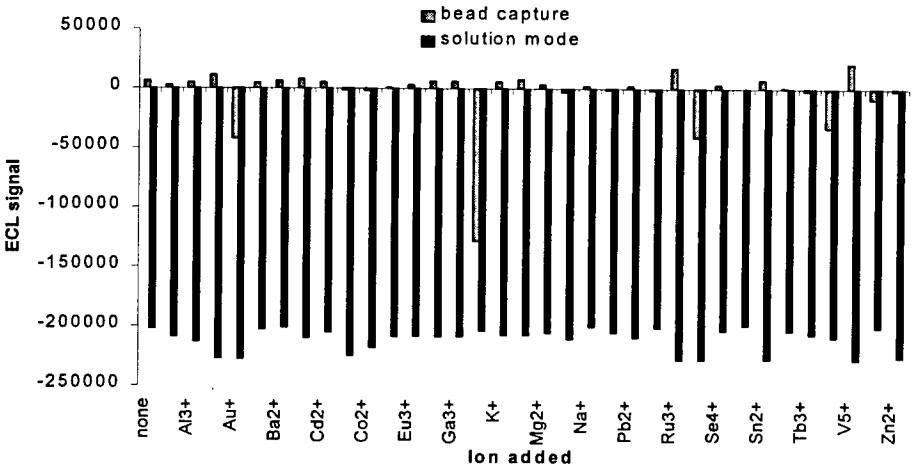

Figure 5. Results of the ECL screen with quinoxaline.

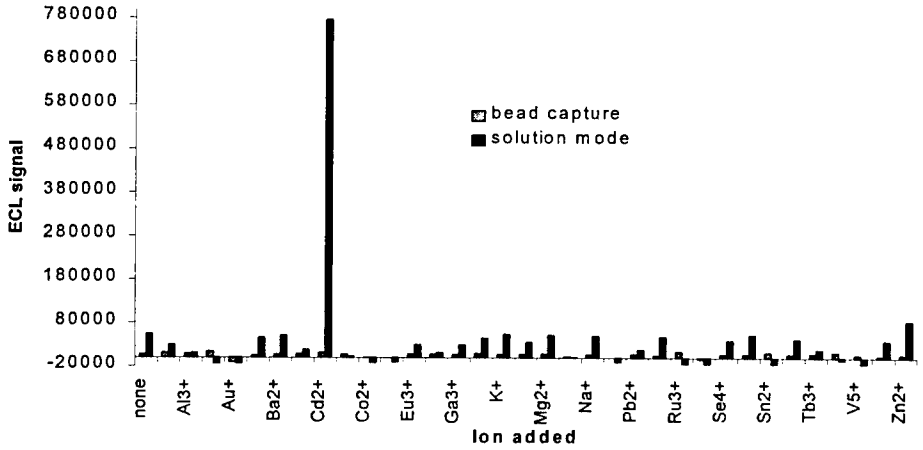

Figure 6. Results of the ECL screen with 1,10-phenanthroline.

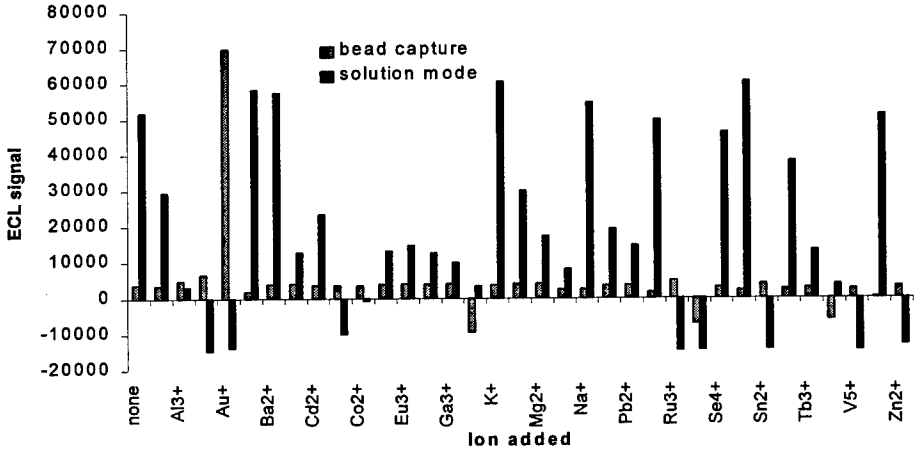

Figure 7. Results of the ECL screen with 4,7-phenanthroline.

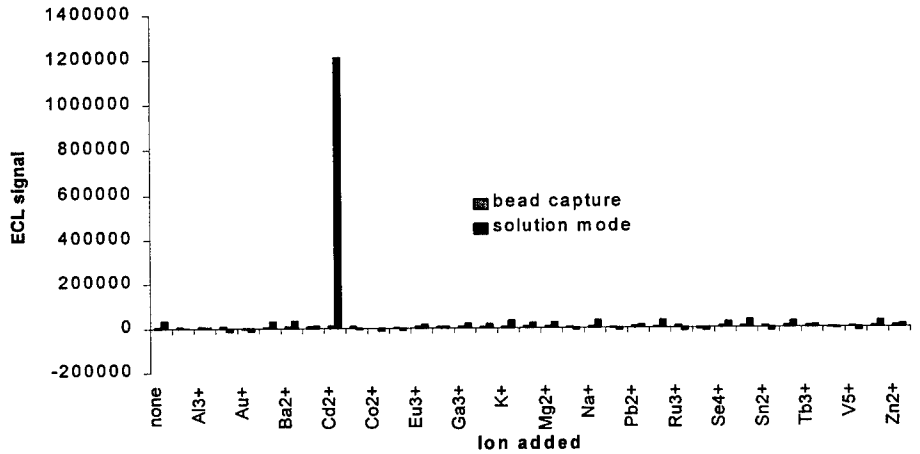

Figure 8. Results of the ECL screen with terpyridine.

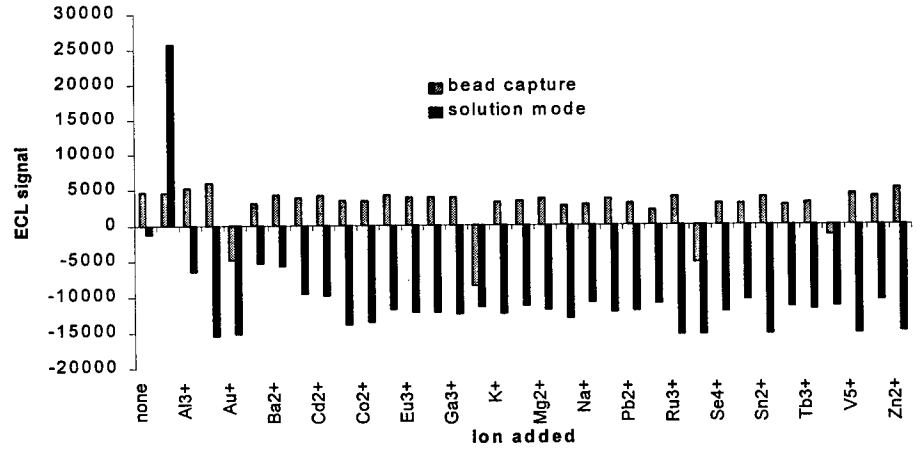

Figure 9. Results of the ECL screen with phenazine.

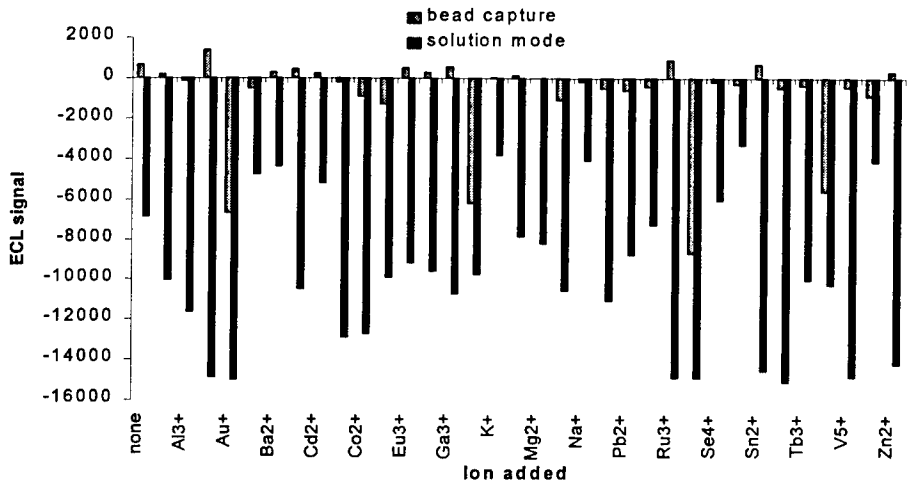

Figure 10. Results of the ECL screen with 2,3-bis(2-pyridyl)pyrazine.

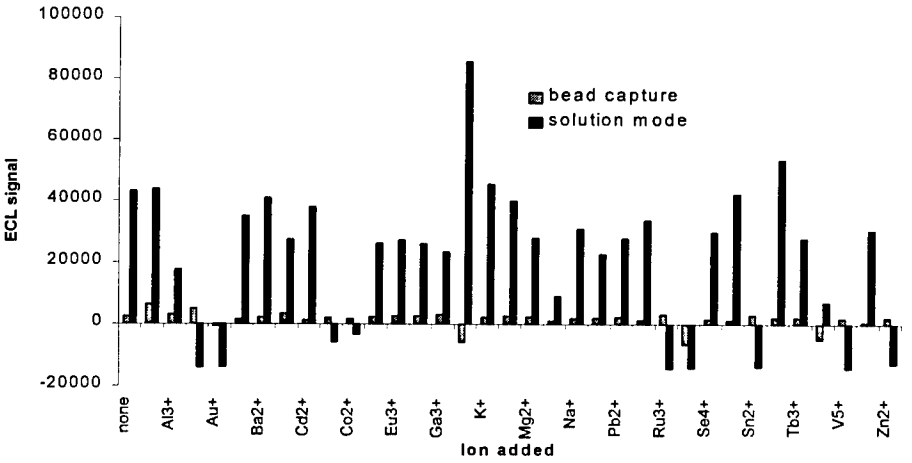

Figure 11. Results of the ECL screen with 2,3-diphenyl-1,4-diazospiro[4,5]deca-1,3-diene.

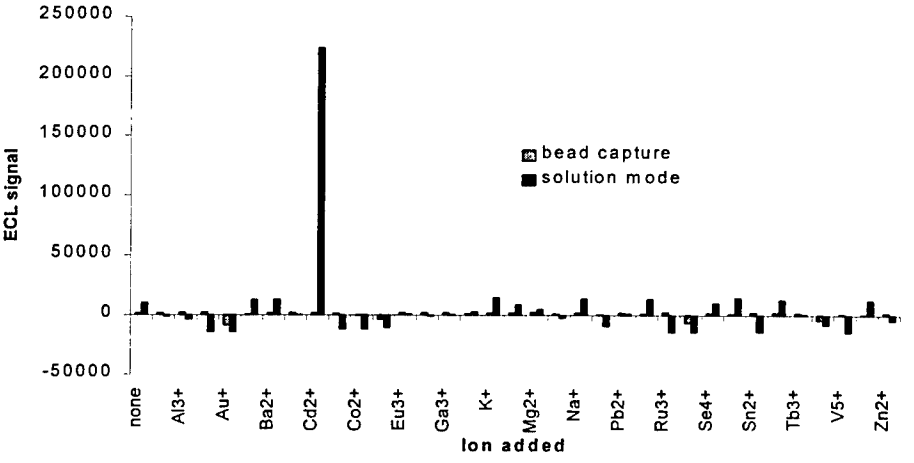

Figure 12. Results of the ECL screen with 2,2'-bipyridine.

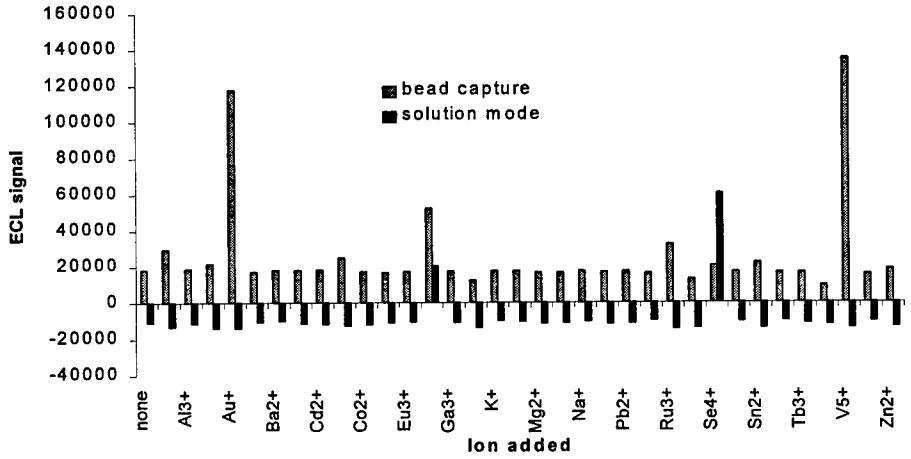

Figure 13. Results of the ECL screen with 2,3-diaminonapthalene.

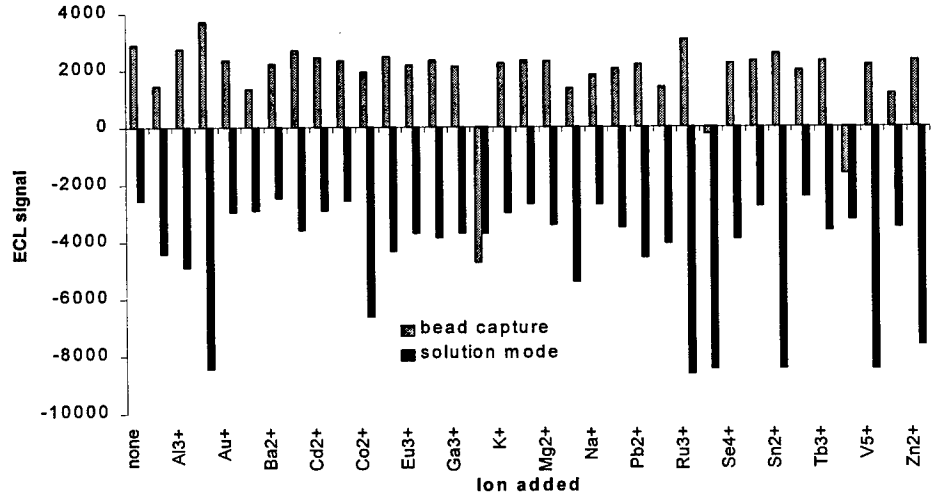

Figure 14. Results of the ECL screen with benzo[c]cinnoline.

The following reactions were found to give enhanced ECL: In the bead capture mode; Au with 4,7-phenathroline and 2,3-DAN, Fe with 2,3-DAN, V with 2,3-DAN and phthalazine, and Ru with phthalazine. In solution mode; Cd with 1,10-phenanhroline, terpyridine and bipyridine, Hg with diazaspiro, Se with 2,3-DAN, Fe with 2,3-DAN and Ag with phenazine.

Reaction Optimisation

Three compounds were found to give greatly increased ECL in the presence of cadmium ions. To optimise the reaction conditions for ECL generation between cadmium ions and these compounds the following parameters were studied; organic ligand concentration, TPA assay buffer pH, TPA assay buffer concentration, order of mixing of solutions, and the time after mixing at which the ECL is generated. The parameters were optimised using a

univariate approach. Exact optimisation details are given in the 1997 Final Report for the Summer Faculty Research Program at Armstrong Laboratory of Paul Taverna (14).

Calibration graphs for cadmium were generated under the optimum reaction conditions. Figures 15, 16 and 17 are the linear portions of calibration graphs for cadmium with 1,10-phenanthroline, terpyridine and bipyridine respectively. It was found that above 1 ppm for 1,10-phenanthroline, 750 ppb for terpyridine and 5 ppm for bipyridine the emission levelled off.

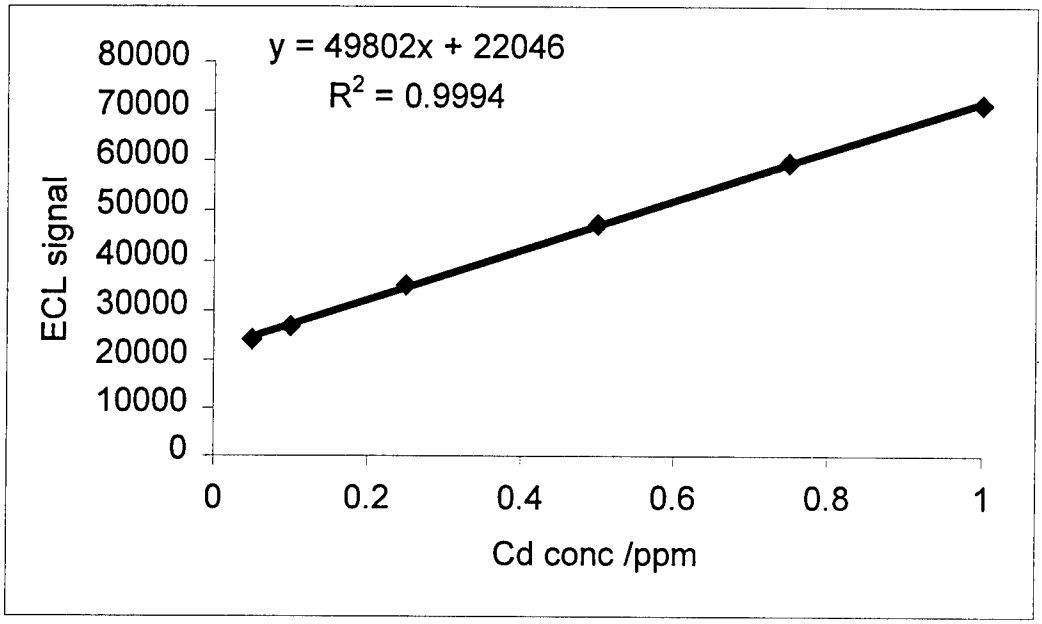

Figure 15. Cadmium ion calibration graph (linear region) with 1,10-phenanthroline.

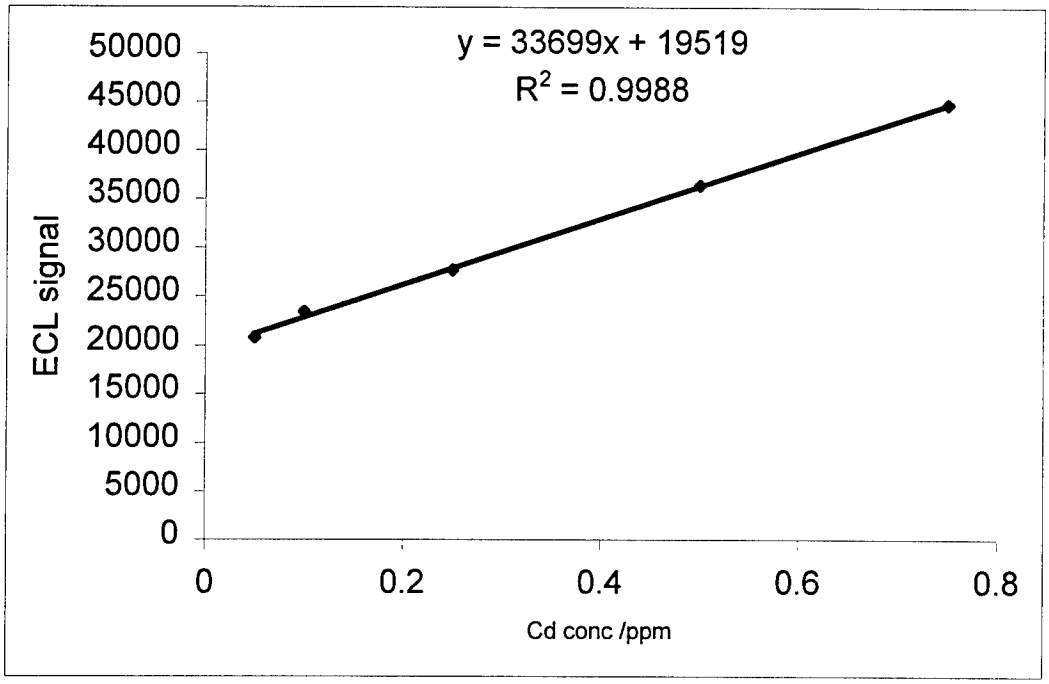

Figure 16. Cadmium ion calibration graph (linear region) with terpyridine.

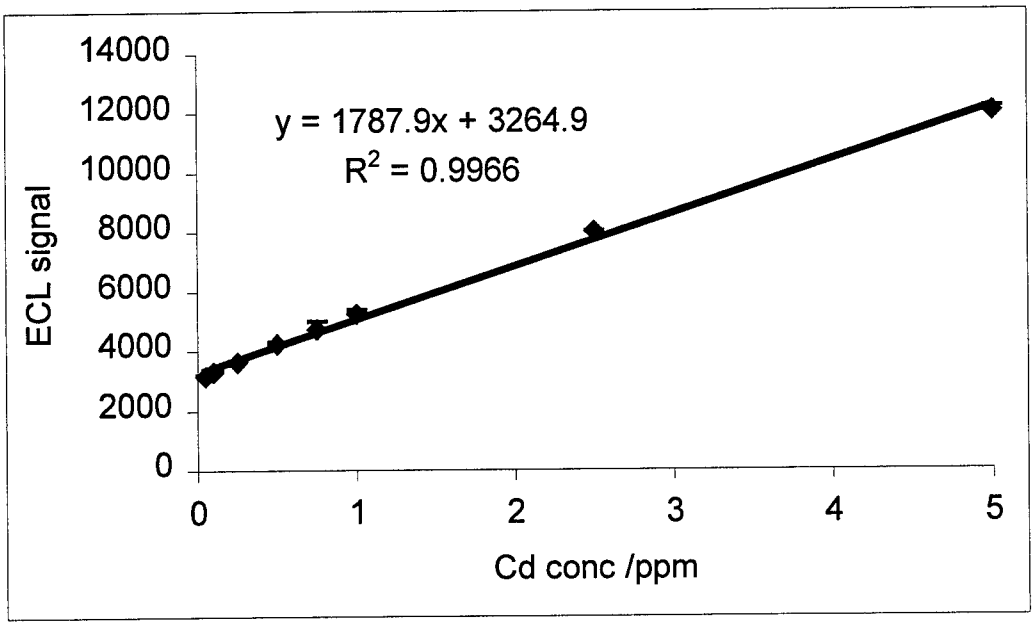

Figure 17. Cadmium ion calibration graph (linear region) with bipyridine.

Limits of detection (blank signal plus three times standard deviation of blank) calculated from the graphs are 6, 8, and 50 ppb cadmium ion with 1,10-phenanthroline, terpyridine and bipyridine respectively. Interference from other metal ions present in solution was also examined and is reported on in the report of Paul Taverna as described earlier.

Discussion

An interesting point to note is the presence of enhanced ECL in the bead capture mode. The theory behind the bead capture mode of operation is that the magnetic field supplied by the magnet attracts magnetic material in the ECL cell (normally coated beads) to the electrode surface. The rest of the sample is washed out of the cell with TPA assay buffer. When the voltage is applied the ECL material is at the electrode surface and gives rise to a larger signal than would have been seen had the ECL material been distributed throughout the ECL cell.

Ions such as Au^{+}, V^{5+} and Ru^{3+} are not ferromagnetic and so a sample containing these ions and a ligand should not have anything that can be attracted top the electrode surface. Hence, all the sample should be swept out of the cell by the TPA assay buffer. An examination of the electron configuration of Au^{+} and Ru^{3+} indicates that they have an unpaired electron. This means that they will be paramagnetic. This may explain how material is attracted to the electrode surface and the enhanced signal seen. V^{5+} has no unpaired electrons though and will not be paramagnetic. For this reason the enhanced signal seen with V^{5+} in the bead capture mode cannot be explained at this time. If some of the V^{5+} was in fact V^{2+} however this would exhibit paramagnetic behaviour and could explain the results seen. No experiments were conducted to test this hypothesis.

Emission in the $Ru(bpy)_3^{2+}$ reaction occurs via the following mechanism (1):

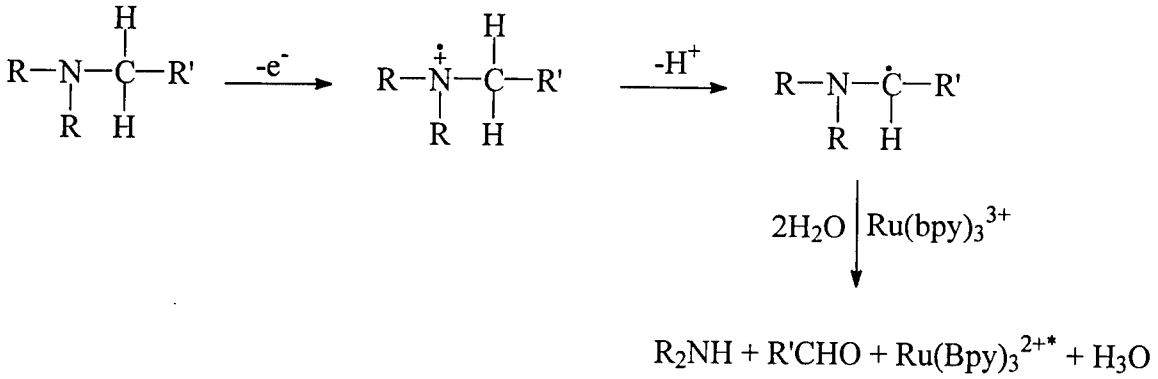

$$R_2NH + R'CHO + Ru(Bpy)_3^{2+*} + H_3O$$

It is presumed that the emission seen in the sample mode in this research occurs via a similar mechanism. However, there is no evidence to support this supposition at this time. Further studies are required to validate this statement.

ECL EQUIPMENT CHARACTERISATION

Experimental

Voltage waveforms were to generated by using a Model 660 electrochemical workstation (CH Instruments). The workstation was controlled by CH 660 software (Version 1.03 CH Instruments). The working electrode was either platinum, gold, silver or glassy carbon, the reference electrode an silver/silver chloride electrode (all from CH Instruments) and the auxiliary electrode was stainless steel tubing used on the exit port of the flow cell. Solutions were pumped through Teflon tubing (0.8 mm id) with a Minipuls 2 pump (Gilson) fitted with black/black silicone tubing. Light emitted was detected using an integrated photon counting head (Hamamatsu, H 5920-01). The power supply for the photomultiplier (PMT) head was a ± 5 V output AC to DC power module (Acopian). A diagram of the ECL flow cell is given in Figure 18. The output from the PMT was acquired using the counter on an AT-MIO-16XE-50 board (National Instruments) controlled by Labview software (Version 4.1, National Instruments). The software was set up to simultaneously acquire the voltage of the working electrode. All software was run on a 486 DX-2 66V computer (Gateway 2000) under Windows 95.

A solution of potassium ferricyanide (III) ($6x10^{-4}$ M) in potassium nitrate (1.0 M) was prepared. This was used as an electrochemical test solution having a well-known cyclic voltammagram. Solutions of $Ru(bpy)_3^{2+}$ were prepared in phosphate buffered saline (PBS, 0.15 M sodium dihydrogen phosphate with 8.5 g/L of sodium chloride). TPA assay buffer as previously described was used as a co-reactant.

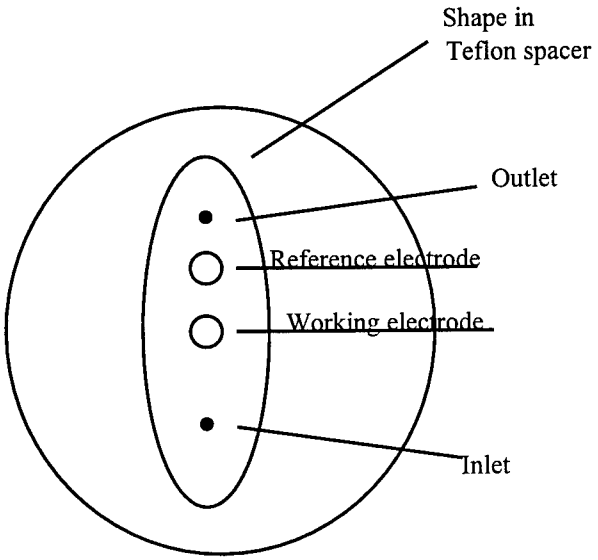

Figure 18. Diagram of the ECL flow cell illustrating the relative positions of the electrodes and the flow path.

Results

A typical cyclic voltammagram (CV) obtained using the ECL flow cell is shown in Figure 19. The CV parameters are a negative scan from + 0.80 V to -0.20 V then back to + 0.80 V at 50 mV/s. This CV compares well

with published data for this reaction (15). A cleaning cycle was applied to the working electrode each morning. This cleaning cycle consisted of 3 cyclic sweeps from 0.0 to -3.0 V to +3.0 V at 0.5 V/s. Without the cleaning cycle no visible oxidation or reduction waves were seen with the test electrochemical solution. Presumably this cleaning cycle removes any deposits on the surface of the electrode.

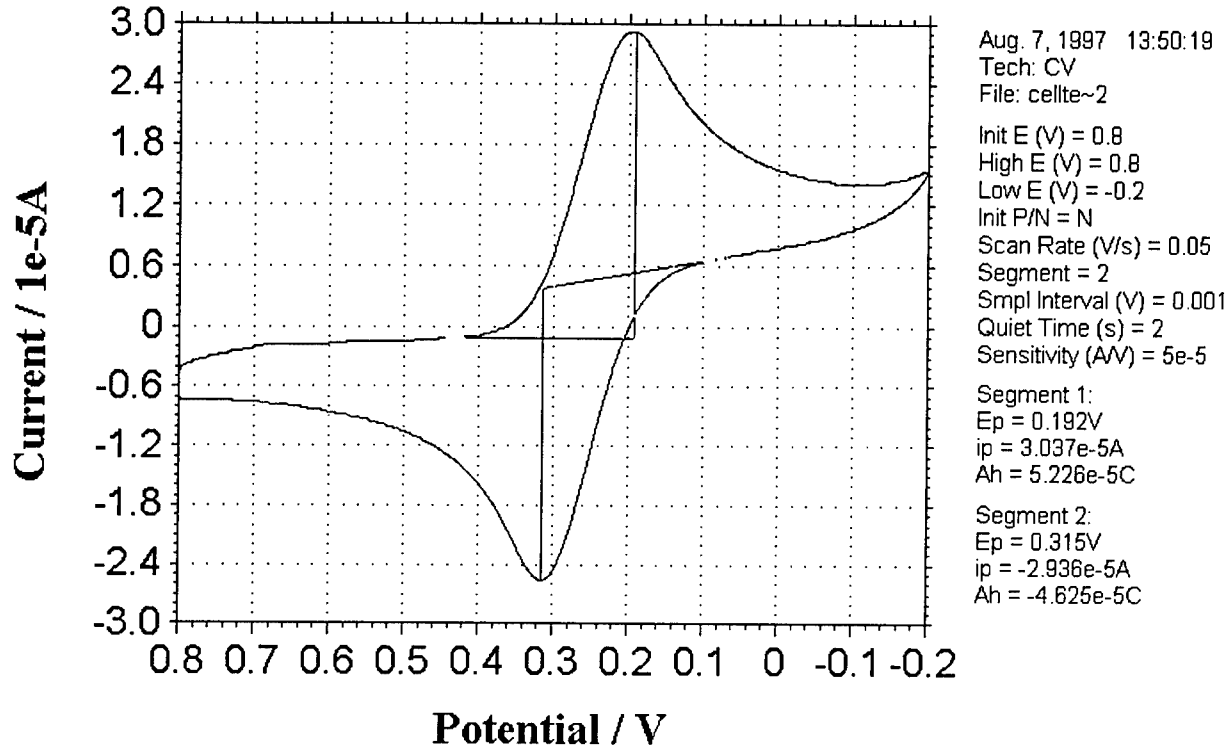

Figure 19. Typical cyclic voltammagram obtained from potassium ferricyanide (III) in the ECL flow cell.

Data Acquisition Software

The Labview program for data acquisition was written in house. Labview is a graphically orientated programming language that interfaces between the data acquisition board and the computer via drivers. LabVIEW is an acronym for Laboratory Virtual Instrument Engineering Workbench and is based on the graphical programming language G. Essentially LabVIEW turns a computer into a virtual instrument. The final program at the time of this report is given in Figure 20.

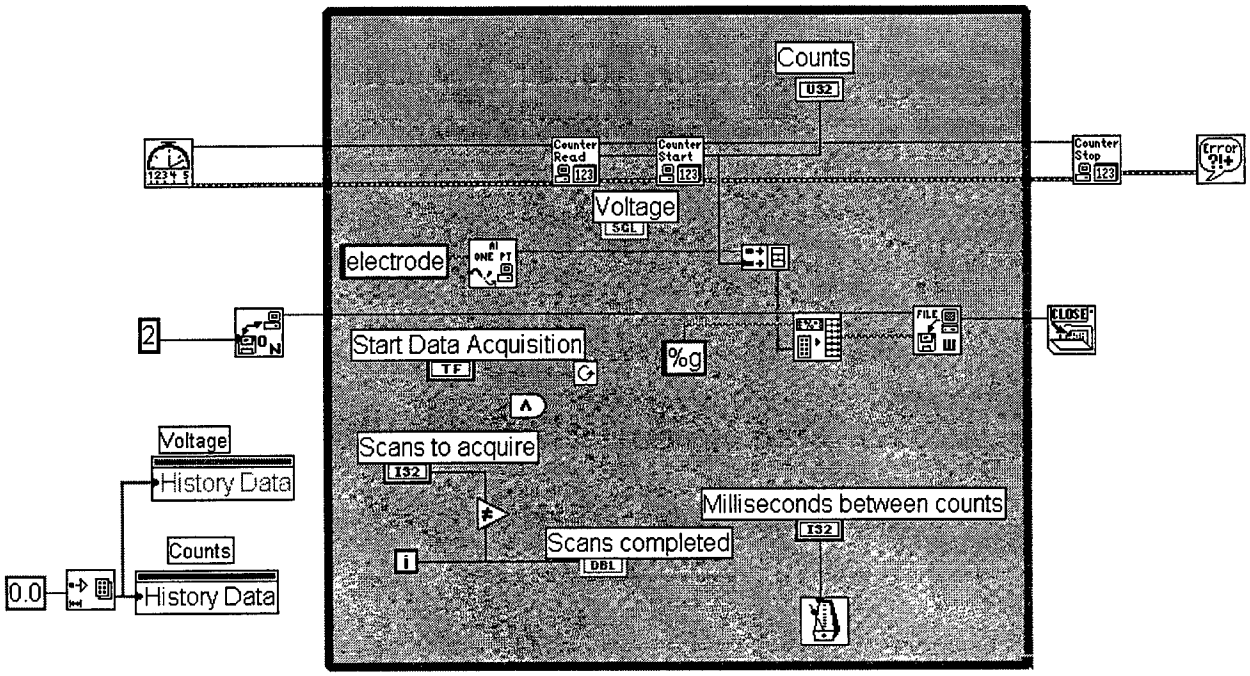

Figure 20. The data acquisition program in Labview 4.1.

This program first clears the graphical displays, opens a dialog box to prompt for a file name and initialises the counter. Once a file name has been entered the program enters the while loop. Inside the while loop it checks the iteration number of the loop against the user input number of scans to be taken. If the numbers match, the program exits the loop after completing the following cycle; reading the counter value, resetting that value to zero, reading the voltage and a wait for a user specified number of milliseconds. An off control switch is also checked for the true/false value at the same time as the iteration number is checked. Data is constantly written to disk during the acquisition process. Upon exiting the while loop the counter is stopped and the data file closed.

ECL of $Ru(bpy)_3^{2+}$:

The ECL generated by the $Ru(bpy)_3^{2+}$ /TPA solution was clearly visible, even in a room with fluorescent lights on except directly over the flow cell. A simple visual comparison of the four types of working electrode was carried out. Solution was kept flowing for 10 minutes and the working electrode maintained at a sufficiently positive voltage to generate ECL from the $Ru(bpy)_3^{2+}$ /TPA solution. No emission was seen with the silver electrode. Both the gold and glassy carbon electrodes gave a bright emission initially upon imposition of the voltage. However, the emission from both of the electrodes decreased over the 10 minute period. Cleaning of the electrode surface by wiping with a lint free tissue restored the emission. Platinum showed no visible decrease over the 10 minute period. No visible signs of emission decrease were seen with platinum over a full working day. For this reason platinum was chosen as the most suitable electrode to use in the flow through system.

A scan of emission against voltage was obtained for $Ru(bpy)_3^{2+}$ ($1x10^{-5}$ M) with TPA assay buffer over the voltage range 1 to 2 V with the voltage scanned at 0.001 V/s and emission and voltage readings taken approximately every 1 s. The average of three such scans is shown in Figure 21.

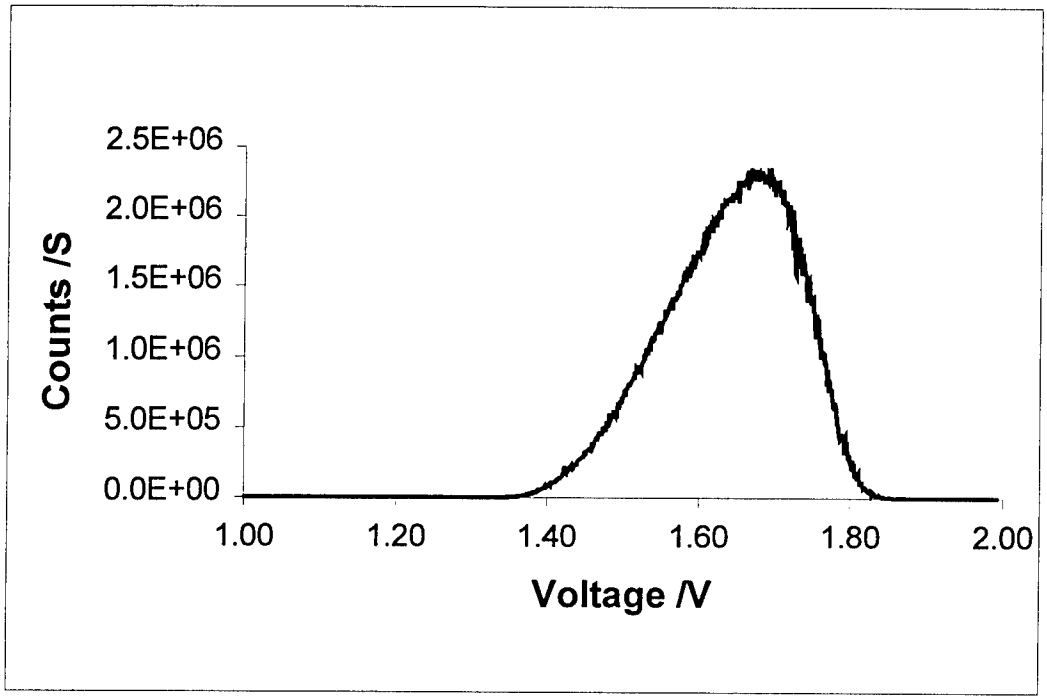

Figure 21. Scan of emission against voltage for $Ru(bpy)_3^{2+}$ /TPA.

Conclusions

This work has discovered some novel ECL reactions that may have potential for use in the detection of metal ions. In particular, cadmium shows strong ECL with some compounds. Optimisation of the static reaction conditions led to LOD values for cadmium in the low ppb range. This is below the Federal standard for cadmium in drinking water. Several other promising ECL reactions were not studied in depth due to time constraints.

A prototype flow through ECL instrument has been constructed. This instrument has undergone preliminary testing with a well known ECL compound, $Ru(bpy)_3^{2+}$. Similar results to those given in the literature have been obtained. More detailed studies and evaluation of the instrumentation with $Ru(bpy)_3^{2+}$ are currently underway will be reported at a later data.

Future Work

Some suggestions for experiments to further probe the ECL reactions discovered here are:

- Optimise the reaction conditions for other ECL reactions discovered in the screening phase.

- Screen more compounds for ECL activity.
- Characterise the ECL reactions already discovered.
- Investigate the effect of immobilisation on the ECL of the compounds investigated here.
- Investigate ECL quenching as a possible detection method.

The advantage to be gained from further study into ECL is the potential for sensitive and selective sensors using the reactions characterised by the instrument. These sensors or other ECL sensors could be used for remote automated monitoring of metal ions or possibly organic analytes. The potential for a portable, fieldable instrument, which could be use by unskilled personnel also exists.

All these potential applications require successful characterisation of ECL reactions. The experience gained in constructing an ECL instrument to monitor these reactions will be invaluable when applied to development of a fieldable instrument. Such an instrument may have applications as a detector for use with ion-chromatography or HPLC.

References

1) A.W. Knight and G.W. Greenway, Analyst (London), 1994, 119, 879.

2) J.B. Noffsinger and N.D. Danielson, J. Chromatogr., 1987, 387, 520.

3) N.D. Danielson, L. He, J.B. Noffsinger and L. Trelli, J. Pharm. Biomed. Anal., 1989, 7, 1281.

4) J.A. Holeman, and N.D. Danielson, J. Chromatogr. A, 1994, 679, 277.

5) S.N. Brune and D.R. Bobbitt, Talanta, 1991, 38, 419.

6) D.R. Skotty, W.-Y. Lee, , and T.A. Nieman, Anal. Chem., 1996, 68, 1530.

7) T.M. Downey and T.A. Nieman, Anal. Chem., 1992, 64, 261.

8) A. Knight, and G.M. Greenway, Analyst (London), 1995, 120, 2543.

9) P. Liang, R.I. Sanchez, and M.T. Martin, Anal. Chem., 1996, 68, 2426.

10) D.E. Ryan, N.D. Ghatlia, A.E. McDermott, N.J. Turro, K. Nakanishi, and K. Kustin, *J. Am. Chem. Soc.*, 1992, 114, 9659.

11) J.G. Bruno, S.B. Collard, D.J. Kuch, and J.C. Cornette, *J. Biolumin. Chemilumin.*, 1996, 11, 193.

12) J.G. Bruno and J.C. Cornette, *Microchem. J.*, 1997, 56, 305.

13) J.G. Bruno, S.B. Collard, A.R.J. Andrews, *J. Biolumin. Chemilumin.*, In Press

14) Paul Taverna, Chapter 27 This report.

15) P. T. Kissinger and W. R. Heineman, *J. Chem. Educ.*, 1983, 60, 702

INVERSTIGATION OF SAMPLING INTERFACE FOR PORTABLE MASS SPECTROMETRY AND A SURVEY OF FIELD PORTABLE ANALYTICAL EQUIPMENT

Stephan B. H. Bach
Associate Professor
Department of Earth and Physical Science

Texas University at San Antonio
6900 Loop 1604 West
San Antonio, TX 78249-0663

Final Report for:
Summer Research Program
Armstrong Laboratory

Sponsored by:
Air Force Office of Scientific Research
Bolling Air Force Base, Washington, DC

And

Armstrong Laboratory

September 1997

INVESTIGATION OF SAMPLING INTERFACES FOR PORTABLE MASS SPECTROMETRY AND A SURVEY OF FIELD PORTABLE ANALYTICAL EQUIPMENT

Stephan B.H. Bach
Assistant Professor
Chemistry Program
Division of Earth and Physical Sciences

Abstract

The major challenge in ascertaining the hazards to humans and the environment when dealing with contaminated sites is determining the types of chemicals present. This is true whether they have been disposed of improperly or are a result of a leaking storage facility. This work has seen great improvements in recent years with the advent of field portable analytical equipment. The technology which has been developed in recent years enabling the use of complex analytical instrumentation in the field has revolutionized the site assessment and site characterization processes. But each of the field portable analytical instruments has its limitations and careful consideration of each instrument's capabilities is critical to the process of gathering useful information regarding the contaminants present at a site leading to judicious remediation decisions. This project consisted of several facets from finding and evaluating field portable instrumentation (Part I) to designing and testing interfaces for sample introduction into mass spectrometers (Part II).

Investigation of Sampling Interfaces for Portable Mass Spectrometry and a Survey of Field Portable Analytical Equipment

Stephan B.H. Bach

The technology which has been developed in recent years enabling the use of complex analytical instrumentation in the field has revolutionized the site assessment and site characterization processes. But each of the field portable analytical instruments has its limitations and careful consideration of each instrument's capabilities is critical to the process of gathering useful information regarding the contaminants present at a site leading to judicious remediation decisions. This project consisted of several facets from finding and evaluating field portable instrumentation (Part I) to designing and testing interfaces for sample introduction into mass spectrometers (Part II) [1].

Part I: Field Portable Analytical Equipment

Mass Spectrometry

Three specific areas of field portable instruments where targeted; mass spectrometry, infrared spectroscopy, and X-Ray fluorescence spectroscopy. The combination of these three techniques covers a wide range of materials from volatile and semi-volatile organic compounds, to bulk liquids and solids, to metals.

There are currently three portable or transportable mass spectrometers on the market. The primary hurdle which must be addressed in taking a mass spectrometer into the field is how to maintain the vacuum. The two field portable

mass spectrometers available for demonstration in the U.S. are the Hapsite manufactured by Inficon (portable) and the SpectraTrak manufactured by Viking Instrument Corp. (transportable). The two instruments address the pumping issue in different ways and therefore have different capabilities which leads to different applications in the site assessment process. The Hapsite is a truly portable mass spectrometer weighing about 35 lbs. It addresses the pumping issue by using a NEG pump. This requires minimizing the amount of material entering the vacuum system which is accomplished by using a membrane interface for sample introduction. It is an ideal screening tool for volatile organic compounds (VOCs) either using a sniffer for real-time monitoring or using the built-in collector and gas chromatograph for separating a mixture of those compounds before mass spectrometric analysis. Inficon demonstrated the instrument at Brooks AFB on July 8th , 1997 using the test wells at Brooks AFB. The Hapsite is ideally suited for the task of rapid response to screen for VOCs in the air or from the head space of liquids or soils.

The Viking GCMS is based on an Hewlett-Packard MSD system which has been made transportable. It is essentially a fixed analytical laboratory instrument which has been ruggedized to be field transportable. Even though it has all of the capabilities of a fixed laboratory instrument it has the drawbacks of such an instrument in requiring 110 V AC power and weighing about 150 lbs. It is also equipped with a membrane interface which can be used as a sniffer or to collect a sample for GC analysis. It was demonstrated at Brooks AFB on July 9th , 1997

using only one of the "hotter" test wells because of the difficulty in moving it from site to site. The instrument required a portable generator (15 min warm up) and the instrument itself required about 15 minutes to warm up. The utility of this instrument would be vastly improved if it were able to operate using 12 V DC.

X-Ray Fluorescence

There are currently about seven portable X-Ray fluorescence spectrometers on the market with various capabilities according to the EPA's Environmental Technology Verification Program. They are the X-Met 920-MP (Metroex, Inc.), the Map Spectrum Analyzer (Scitec, Inc.), the XL Spectrum Analyzer (Niton, Corp.), the SEFA-Portable X-Ray Fluorescence Analyzer (HNU Systems, Inc.), the TN 9000, (TN Spectrac), the TN Lead Analyzer (TN Spectrace), and the X-Met 920-P and 940 (Metroex, Inc.). The Niton and Metroex portable XRFs seem to perform best in this area.

FTIR Spectroscopy

There are currently several portable FTIR spectrometers on the market that are portable and transportable manufactured by RemSpec, PetroLab, Foster-Miller, Inc., Midac, and Surface Optics Corp. The only FTIR that has so far been demonstrated for Brooks AFB was the Foster-Miller, Inc. instrument. It weighs in at about 375 lbs making it transportable because the case in which it is mounted has wheels. It is a fixed laboratory instrument which has been ruggedized to be transportable but is not useable for any type of rapid response mission. It does use the latest in fiber optic coupled ATR sampling devices. The commercially available

truly portable FTIRs for which information was received are supplied by RemSpec Corp., Surface Optics Corp., and by PetroLab Co. RemSpec makes a portable system which weighs under 50 lbs and operates on 12 V DC. The only drawback is the MCT detector which needs to be cooled to liquid nitrogen temperatures (RemSpec currently requires liquid nitrogen). This problem can be remedied by modifying the system to use a mechanical cooling device. The RemSpec is supplied with a choice of fiber optic ATR sampling devices. Surface Optics Corp. makes a full scan portable FTIR which weighs 18 lbs. The optical system consists of a barrel ellipse detector. The instrument is designed specifically for surface analysis. The IROX from Grabner Instruments (Distributed by PetroLab Co.) is designed primarily as a gasoline analyzer. It can operate using 12 V DC and weighs under 35 lbs. It uses a 5 ml sample cell to analyze liquids. Whether this instrument can be modified for general IR purposes remains to be determined.

Part II: Sampling Interfaces for Mass Spectrometry

As a general rule field analytical instrumentation requires sample preparation be kept to a minimum. One of the most powerful field portable instruments is a mass spectrometer. But the primary drawback in using mass spectrometry in the field is the preparatory work necessary before a sample can be introduced into the mass spectrometer. The preparatory work is a direct result of the analyzer of a mass spectrometer being under vacuum and that the molecules to be analyzed must be in the gas phase. Traditional sample preparation methods

involve a liquid-liquid extraction step in order to remove the organic compounds of interest from the sample.

A variety of interfaces are available to bring the analyte into the mass spectrometer and concentrate the sample. Various possible MS interfaces are listed below:

- Membrane interface - allows for direct sampling of air or the headspace above liquids or soils by using a special material which preferentially excludes nitrogen and oxygen.
- Headspace interface - allows for direct sampling of the air space above a sample. The sample can be either liquid or solid. The interface can either be heated or operated under ambient conditions. The material can either be pulled into the mass spectrometer or swept into a GC.
- "Sniffer" interface - similar to purge and trap where volatile samples are collected by pulling volatiles in through an activated carbon bed. The flow is reversed and the material is transported to the analyzer.
- Gas Chromatographic interface - use of a portable GC with a portable mass spectrometer. It might be advantageous from a portability stand point to separate the two units. In that case it would be important to determine how quickly and reliably these can be combined in the field.
- Macro Solids Probe interface - heated probe for directly introducing sample into mass spectrometer. This is a possible method for analyzing soils and other solid materials without the need for extraction. (Being developed at UTSA)

- Capillary interface - a direct inlet which creates a controlled leak into the mass spectrometer to sample volatile materials.
- Atmospheric Pressure Ionization interface - standard interface for electrospray ionization sources.
- Liquid Chromatographic interface - for compounds not amenable to GC analysis or solids probe analysis because of their thermodynamic properties.

Some of the above listed interfaces are commercially available and others would have to be developed in-house.

The investigation of various types of interfaces for sample introduction into mass spectrometers was undertaken because the portable mass spectrometers rely to varying extents on membrane interface mass spectrometry (MIMS) for accomplishing sample introduction into the ionizer. The various types of membrane materials used have a direct impact on the instrument's response characteristics. This is because the various materials being used have specific properties which determine what type of compounds they will allow across the membrane into the ionizer of the mass spectrometer. It was therefore critical to develop a test bed to verify the utility of various membrane materials for use in environmental analysis.

To address the issue of getting the sample into the mass spectrometer, we are investigating the membrane introduction technique and solid phase microextraction (SPME). The goal of the investigation is to simplify the separation of organic compounds from the sample matrix. These techniques will be evaluated using a Finnigan Magnum ion trap mass spectrometer at Brooks AFB.

Membrane Introduction Mass Spectrometry (MIMS)

MIMS has been used for the trace analysis of organic compounds from aqueous solutions [2 - 6]. Detection limits at the part-per-billion level have been measured directly from water samples with no preconcentration or derivatization. This enables the use of this technique for continuous monitoring [2]. A brief outline of the technique and its reported capabilities is given below.

Two commonly used membrane devices [2]

1) mounted in the fluid sample
2) mounted near mass spectrometer ion source

Typical Characteristics of a sheet direct insertion membrane probe [2]

1) Membrane	silicon membrane, Dow Corning silastic sheeting, medical grade
2) Membrane thickness/area	0.25 mm or 0.13 mm/30 mm^2
3) Response time	8 s
4) Operation temperature	70 °C
5) Sampling frequency	15 sample injections and standards per hour
6) Quantitative Accuracy	5 %

The first step was to obtain various membrane materials. The materials for this project were obtained from a variety of sources. The most common membrane material used is silicone rubber sheeting (Dow Corning Corp. Silisatic) obtained

from Specialty Manufacturing Inc. (0.005" thick [70P001-104-005] and 0.010" thick [70P001-104-010]. Other materials were obtained from Small Parts Inc. They include Teflon sheeting (0.005" thick), latex rubber sheeting (0.006" thick), and plastic (oriented polyester except for the 0.002" and the 0.004" thicknesses which are made of cellulose triacetate) shim stock in a variety of thicknesses (from 0.0005" to 0.004" thick).

Figure 1 shows a diagram of the membrane interface that was built for the Finnigan Magnum ion trap mass spectrometer. It was designed to fit into the 1" o.d. ultra torr connector used for the GC transfer line. It was made using 6" of a 1" (o.d.) stainless steel rod. The material is transported to the membrane via 3/16" holes which allow for flow past the membrane. The membrane is held between the Top Plate and the Top of the Interface. The Top Plate is held in place by four hex head screws. The membrane forms the vacuum seal between the mass spectrometer and the membrane interface housing. Material can then be either drawn through using a pump or pumped through to a waste container. Flow rates past the membrane are set by using a needle valve.

Membrane materials used so far have been the Teflon sheeting (0.005") and the silicone rubber sheeting (0.010"). Initial experiments with perfluorotributyl-amine showed no material crossing the Teflon sheeting and good results with the silicon rubber sheeting. It should also be noted that the background atmospheric contamination was more of a problem with the silicon rubber sheeting than with the Teflon sheeting. It seems that the Teflon sheeting simply was not allowing any

material to cross. Further investigations will be conducted in order to determine which membrane materials will work best for a given class of target compounds.

Solid Phase MicroExtraction (SPME)

SPME requires no solvent extraction or sparging apparatus to concentrate the sample. It can be used to concentrate volatile and non-volatile components in both liquid and gas samples [7 - 12]. SPME is a relatively new technique in which analytes are adsorbed on to a phase coated fused silica fiber which is immersed into a liquid sample or held above a solid sample being heated.

The SPME device consists of a fused silica fiber attached to a stainless steel plunger. The fused silica fiber is coated with one of the following commercially available films (Supleco, Bellefonte, PA):

1) carbowax - 50 μm coating for extracting surfactants
2) polyacrylate - 85 μm coating for extracting very polar analytes from polar samples
3) polydimethylsiloxane - a) 100 μm coating for low molecular weight or volatile compounds; b) 7 μm coating for larger molecular weight or semi- volatile compounds
4) polydimethylsiloxane/divinylbenzene - 65 μm for analytes such as alcohols and amines.

Sample extraction is routinely accomplished using the following steps. First, the SPME needle is passed through the sample vial septum with the fiber retracted.

Then the fiber is exposed by depressing the plunger and either immersed into the liquid sample or placed into the head space of a solid sample. The analytes are adsorbed onto the fiber in 2 to 30 minutes depending on the sample. The fiber is then retracted into the needle and removed from sample vial.

Analysis of the materials adsorbed onto the needle can now proceed using a gas chromatograph. The needle is inserted into GC injector port and the plunger is depress which inserts fiber into GC injector port. Analytes are desorbed from the fiber in heated zone of GC injector and GCMS analysis can proceed as usual. The SPME work will begin in the Fall of 1997 in a joint project between UTSA and Brooks AFB.

Other Investigations:

During the course of the summer several samples were investigated. All samples were run on a Finnigan Magnum ion trap GCMS using a Varian 3400 GC and a Tekmar LSC 2000 purge and trap. Liquid samples were purged for 11 minutes, then desorbed at 245 °C. The GC temperature profile consisted of a hold at 40 °C for five minutes, increasing the temperature to 210 °C at a rate of 6.3 °C per minute, and then a hold at 210 °C for 2 minutes. The mass spectrometer was operated in the positive ion mode, ionizer at 70 eV, mass range from 30 - 240 amu. No delay was used for the filament/multiplier. Analyses were also performed using sample headspace.

An aqueous sample with the potential for human health risk yielded some interesting results. There were two prominent peaks in the chromatogram: one

around scan 400 and the other around scan 1271 (Figure 2). The analysis of mass spectrum from scan 400 gave the following information. The base peak was observed at m/z = 45 with M-1 and M+1 peaks being prominent as well as a peak at m/z = 32. The chromatographic peak is most likely due to CHS^+, but could also be from $COOH^+$. A more informative mass spectrum was obtained from scan 1271 (Figure 3). The analysis of mass spectrum from scan 1271 yielded a base peak at m/z = 45 (100%), M-1(53 %), and M+1 (31 %) with other large peaks at m/z = 94 (92 %), 79 (51 %), 64 (15 %), and 61 (22 %). Analysis of the M+1 and M+2 peaks for m/z = 94 and 79 yielded the following assignments. The peak at m/z = 94 is most likely due to $H_3C\text{-}S\text{-}S\text{-}CH_3^+$. The peak at m/z = 79 being due to loss of CH_3 and the peak at m/z = 64 being due to the loss of the second CH_3.

Samples were also run from the test wells at Brooks AFB. The head space from the aqueous samples were initially analyzed using a portable GC with a PID detector. This gave inconclusive results as to the identities of one of the chromatographic peaks. The resulting chromatogram from the GCMS analysis is shown in Figure 4. Two peaks are prominent, one at scan 891 and the other at scan 1110. The mass spectrometric analysis of the larger chromatographic peak at scan 891 (Figure 5) yielded as expected from the portable GC analysis, trichloroethylene. The second chromatographic peak at scan 1110 was not positively identified using the portable GC. Analysis of the mass spectroscopic data from scan 1110 (Figure 6) yielded the identity of the peak as being dichloroethylene. A not unexpected result.

References

1) M.B. Wise and M.R. Guerin, Anal. Chem., 69, 26A (1997).

2) T. Kotiaho, F.R. Lauritsen, T.K. Choudhury, R.G. Cooks, G.T. Tsao, Anal. Chem., 63, 875A (1997).

3) G.J. Tsai, G.D. Austin, M.J. Syu, G.T. Tsao, M.J. Hayward, T. Kotiaho, R.G. Cooks, Anal. Chem., 63, 2460 (1991).

4) D.A. Markham, J.R. Gilbert, R.J. West, G.M. Klecka, Proceedings of the 44th ASMS Conference on Mass Spectrometry and Allied Topics, Portland, OR, 863 (1997)

5) R. Kostiainen, R. Ketola, T. Honkanen, T. Mansikka, T. Kotiaho, V. Komppa, K. Wickström, H. Vahervuori, Proceedings of the 44th ASMS Conference on Mass Spectrometry and Allied Topics, Portland, OR, 173 (1996).

6) A.J. Maden, S.B. Ficarro, M.J. Hayward, Proceedings of the 44th ASMS Conference on Mass Spectrometry and Allied Topics, Portland, OR, 169 (1996).

7) A.A. Boyd-Boland, S. Magdic, J.B. Pawliszyn, Analyst, 121, 929 (1996).

8) K. Jinno, T. Muramatsu, Y. Saito, Y. Kiso, S. Magdic, J. Pawliszyn, J.Chrom. A, 754, 137 (1996).

9) Y. Liu and M.L. Lee, Anal. Chem., 69, 190 (1997).

10)J.J. Langenfeld, S.B. Brown, D.J. Miller, Anal. Chem., 68, 144 (1996).

11)R. Eisert and K. Levsen, J. Am. Soc. Mass Spectrom., 6, 1119 (1995).

12)M. Chai, C.L. Arthur, J. Pawliszyn, R.P. Belardi, K.F. Pratt, Analyst, 118, 1501 (1993)

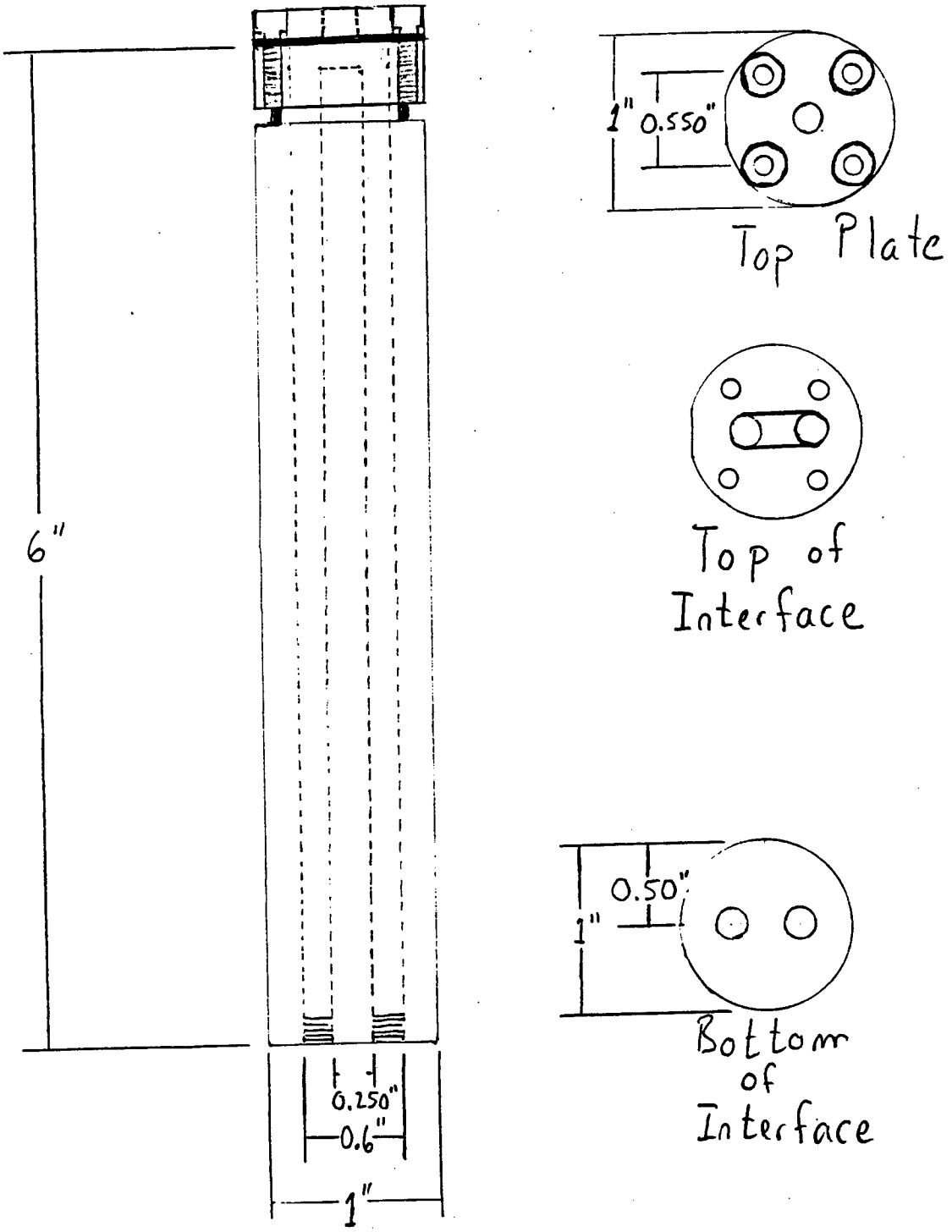

Figure 1 Membrane interface designed for Finnigan Magnum GCMS

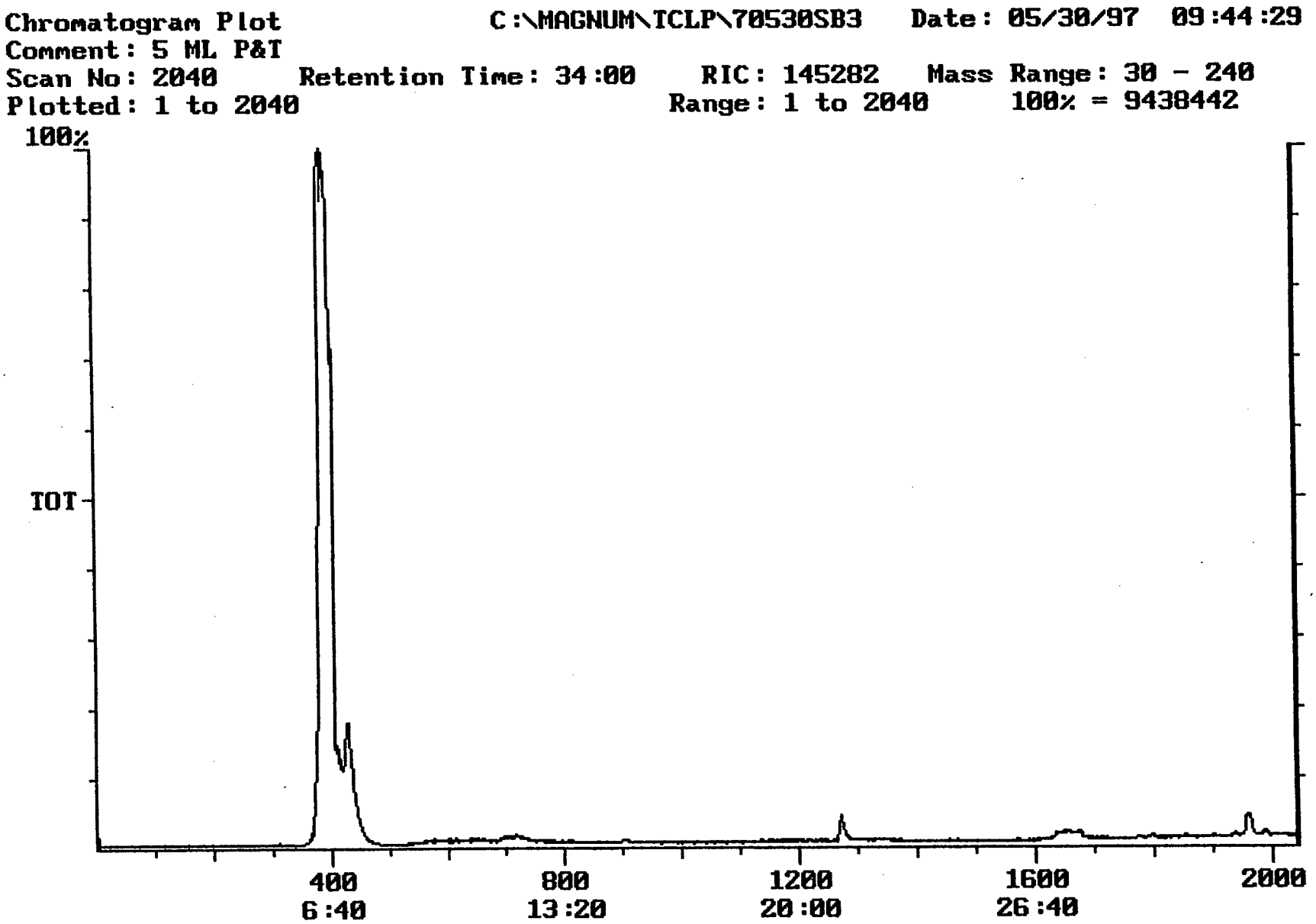

Figure 2 Chromatogram of aqueous sample, 5 ml purge and trap

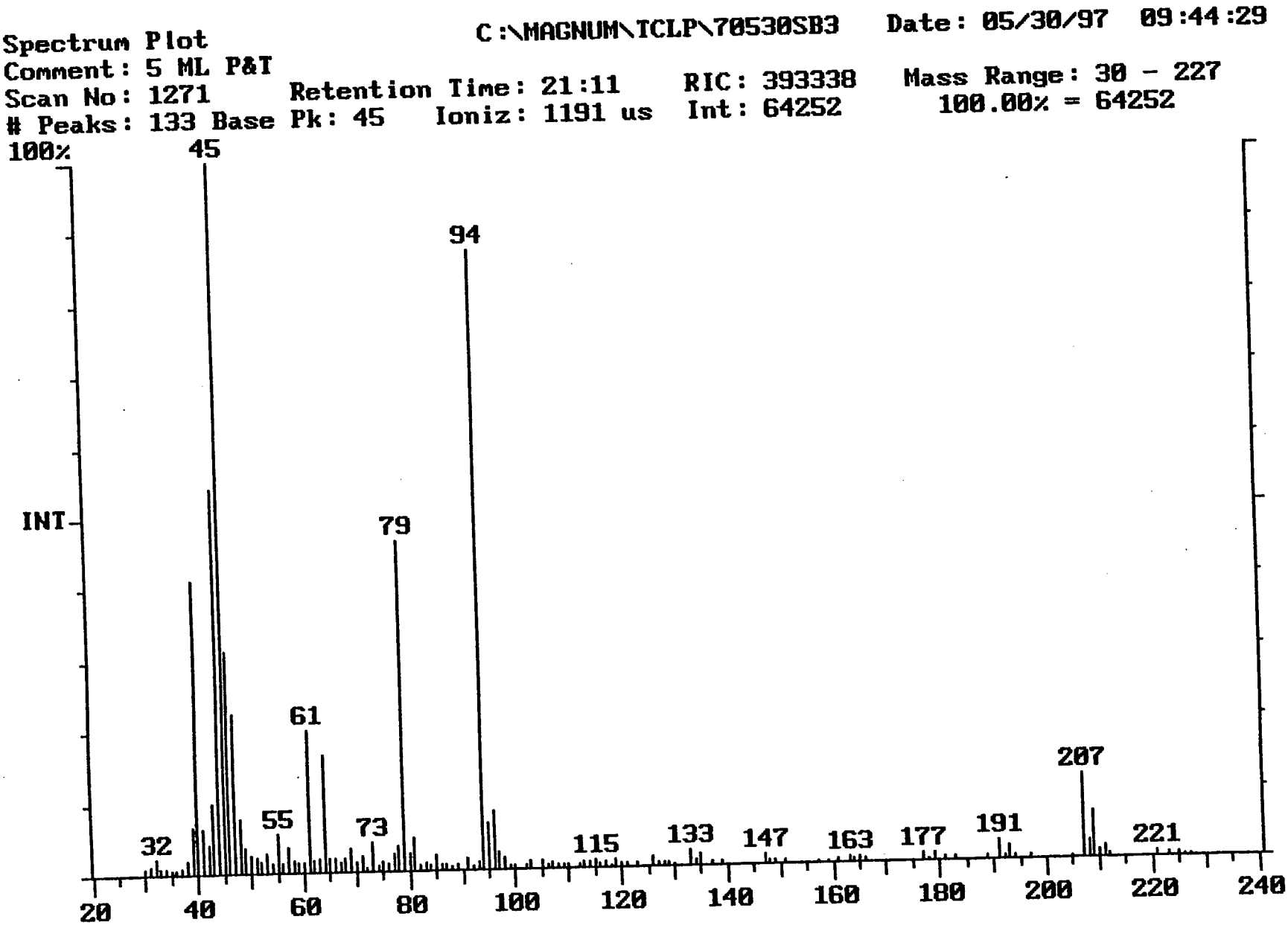

Figure 3 Mass spectrum from scan 1271 of aqueous sample

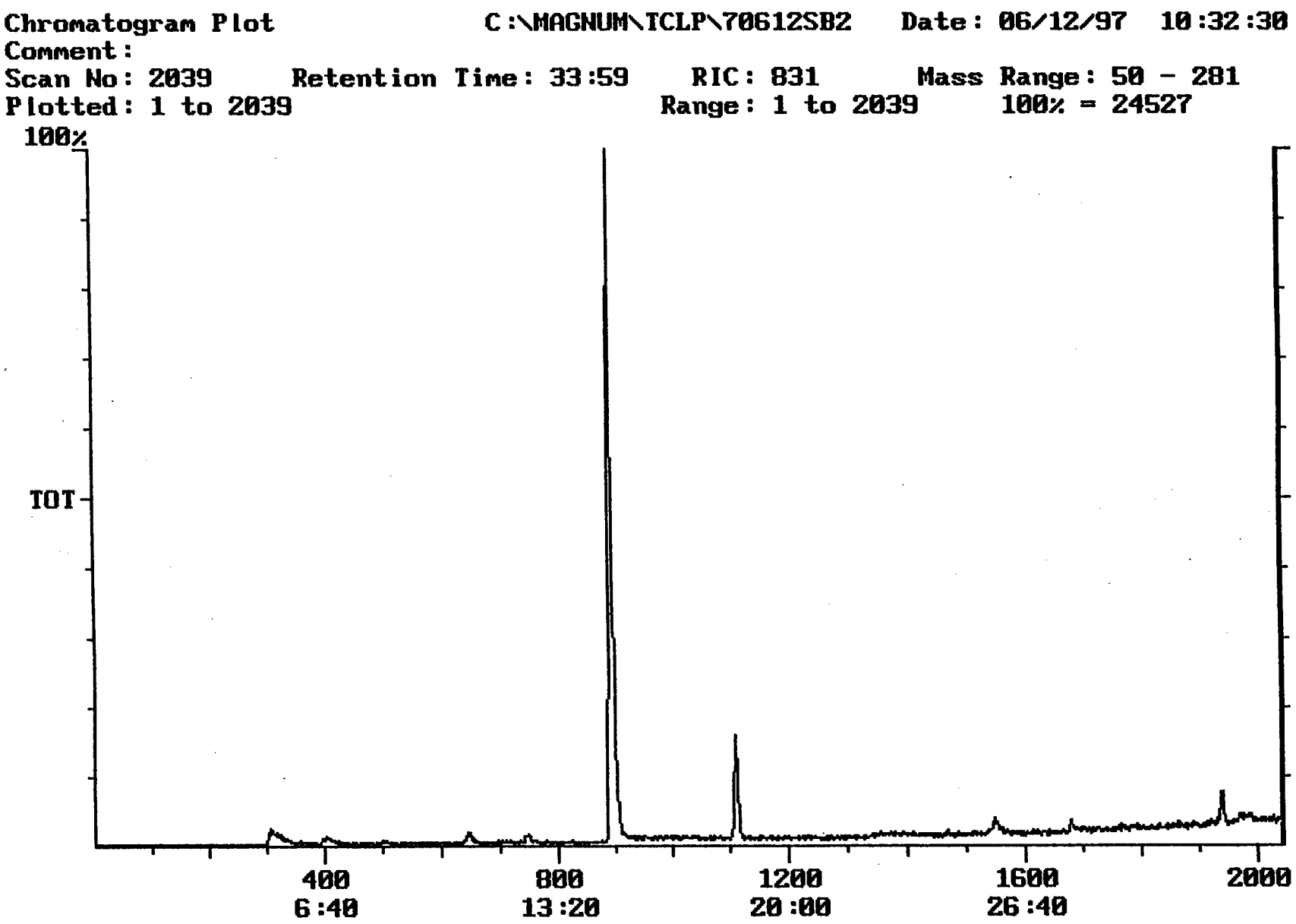

Figure 4 Chromatogram of Brooks AFB test well head space, 50 ul injection

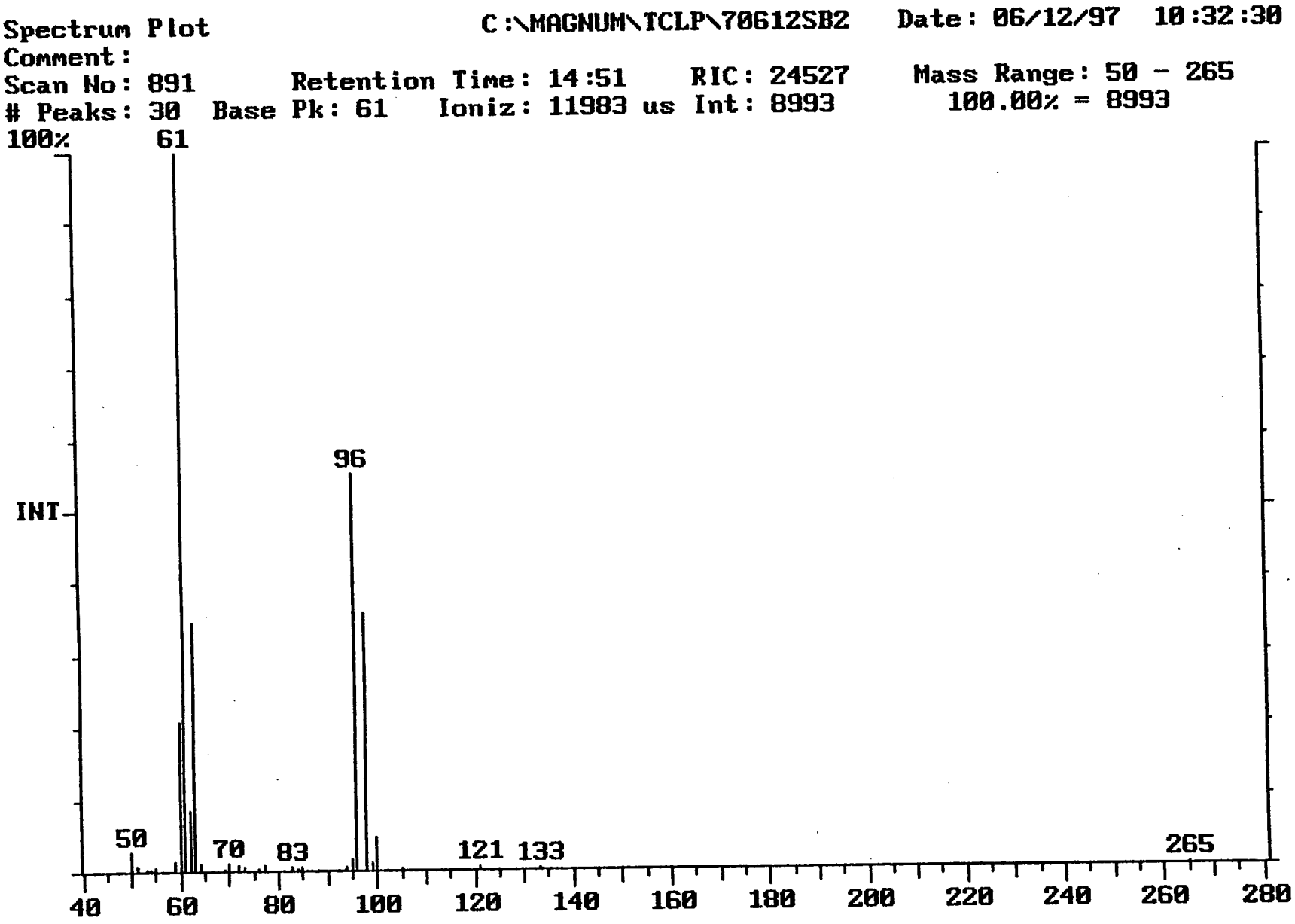

Figure 5 Mass spectrum from scan 891 of Brooks AFB sample

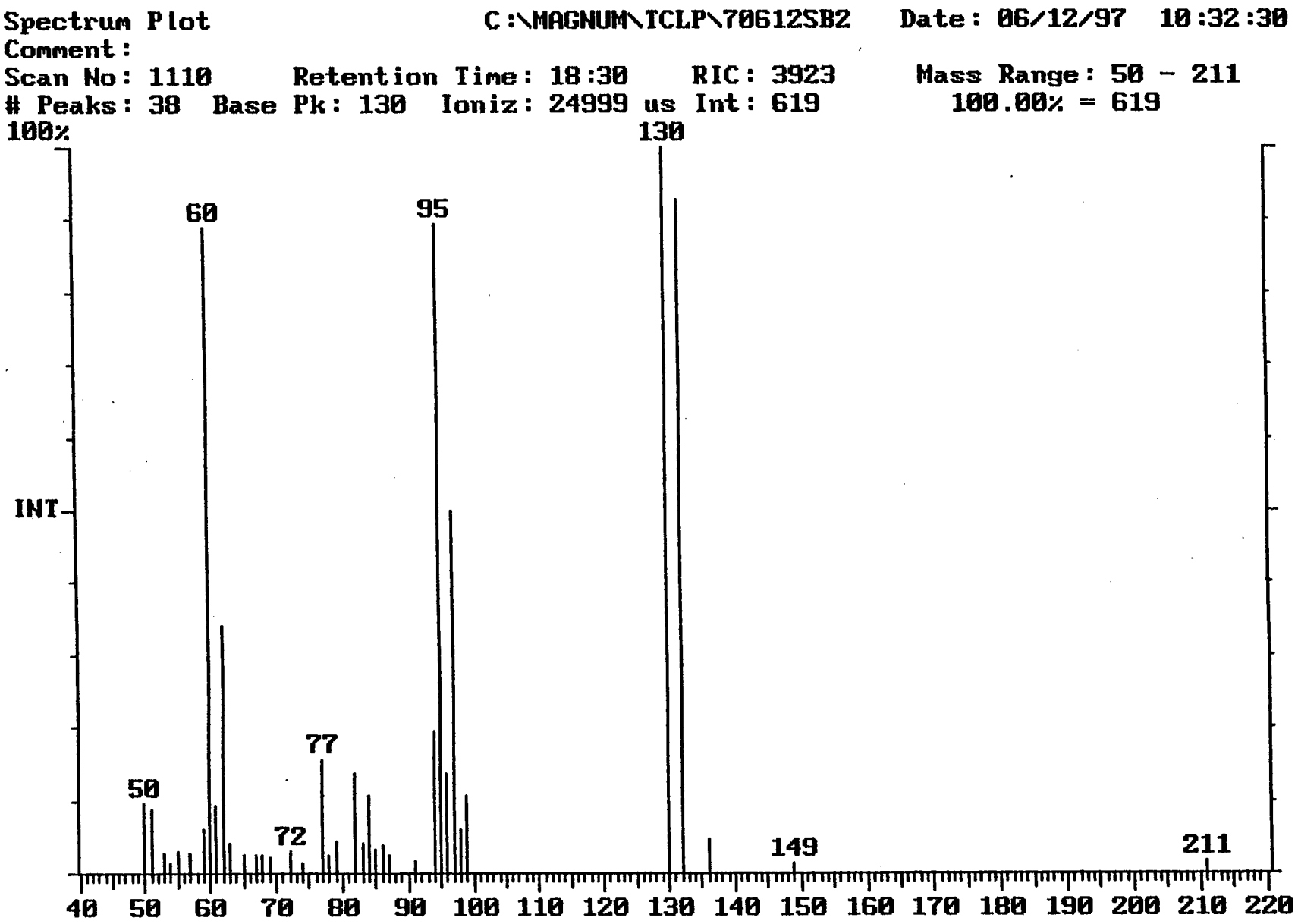

Figure 6 Mass spectrum from scan 1110 of Brooks AFB sample

ANALYSIS FOR THE ANAEROBIC METABOLITES OF TOULENE AT FIRE TRAINING AREA 23 TYNDALL AFB, FLORIDA

Marilyn Barger
Assistant Professor
Department of Civil Engineering

FAMU-FSU College of Engineering
2525 Pottsdamer St.
Tallahassee, FL 32310-6046

Final Report for:
Summer Faculty Research Program
Armstrong Laboratory

Sponsored by:
Air Force Office of Scientific Research
Bolling Air Force Base, DC

and

Armstrong Laboratory

September 1997

ANALYSIS FOR THE ANAEROBIC METABOLITES OF TOULENE AT FIRE TRAINING AREA 23 TYNDALL AIR FORCE BASE, FLORIDA

Marilyn Barger
Assistant Professor
Civil Engineering Department
FAMU-FSU College of Engineering

Abstract

Benzyl succinic acid, an anaerobic metabolite of toluene under nitrate and sulfate reducing conditions and believed to be a dead-end byproduct, was investigated as a potential indicator of natural attenuation for fuel contaminated sites. Screening for this metabolite at the decommissioned, fire-training area (FTA-23) at Tyndall Air Force Base, Panama City, Florida, did not reveal the presence of any benzyl succinic acid in the groundwater samples drawn from the existing monitoring wells. Similar metabolites, alkyl-substituted benzyl succinic acids that have been identified as products of meta- and para- xylenes and ethyl benzene were also not detected. Detection limits of the separation and analytical method used for benzyl succinic acid were determined for the groundwater from selected monitoring wells. The monitoring wells chosen for study had significantly different contaminant concentrations. The detection limit for groundwater samples that were relatively clean, was found to be near 100 nanograms benzyl succinic acid per liter, for the ether extraction, diazomethane derivatization to the methyl ester, and ultimate GC/MS detection that was used. However, the separation and analysis technique was not reliable for groundwater samples from monitoring wells at the site that were heavily contaminated with fuel components. Although ubiquitous at this particular site, no effects on the analysis could be directly attributed to the presence in the groundwater of residual surfactants from the aqueous film forming foam (AFFF) used to put out the fires.

ANALYSIS FOR THE ANAEROBIC METABOLITES OF TOULENE AT FIRE TRAINING AREA 23 TYNDALL AFB, FLORIDA

Marilyn Barger, P.E.

Introduction

Natural or intrinsic bioredmediation is an environmental protocol that requires intensive site monitoring to document that natural subsurface phenomena are degrading contaminants found to be present. There are several natural processes that may occur simultaneously or sequentially which can contribute to the degradation of the chemicals of concern. These processes can be observed by monitoring the groundwater chemical constituents in the context of the type, amount and age of the contamination as well as the local geology and hydrogeology. Unfortunately, there no single positive indicator has been identified for use with most types of subsurface contamination. Instead of a single indicator, a site-specific array of physical, biological, and chemical water quality parameters is used together with available historical site data and detailed hydrogeological and geologic information to ensure that the natural attenuation processes are occurring as predicted. Although natural attenuation can be a cost-effective technique for remediation of many sites, more effective monitoring could make it more successful and, perhaps, less expensive. One current area of effort to streamline the monitoring process, is focused on identifying stable products and possible dead-end metabolites of biological degradation. An identifiable, non-toxic and non-degradable metabolite could provide convincing evidence that the contaminant of interest is being degraded and not just being dispersed or adsorbed to the soil. An ideal indicator of natural attenuation of would have to be stoichiometrically related to the contaminant being degraded, stable and not further degradable, originate from the sole source contaminant, easily analyzed for, and not be toxic to humans or the environment.

The focus of this project was to explore and evaluate the potential usefulness of benzyl succinic acid, a stable metabolic product of toluene degradation under nitrate and sulfate reducing conditions, as one such intrinsic bioremediation indicator. Ortho-, meta-, and para-xylene, as well as ethyl benzene have also been reported to be degraded to the corresponding substituted benzyl succinic acids (2, 3, 8, 15, 17, 22, 32). This group of metabolites should be detectable with the same separation and analysis techniques. The separation and analysis

procedures for low concentrations of benzyl succinic acid reported in the literature consists of ether extraction, derivatization to the methyl ester with diazomethane, solvent exchange to methylene chloride and GC/MS analysis (2).

The described method was used to screen for benzyl succinic acid (and related alkyl substituted analogs) in the monitoring wells at FTA-23, a decommissioned fire-training site contaminated with jet fuel (primarily JP-4) on Tyndall Air Force Base. Toluene, and other water soluble fuel components have been identified in several monitoring wells at the site, that are also known to be anaerobic (dissolve oxygen concentration < 1.0 ppm) (20, 21, 22, 27, 28). However, no benzyl succinic acids or its analog metabolites were found in the groundwater samples from this site. Other known anaerobic degradation products of toluene and the BTEX compounds were qualitatively identified.

Lack of published field data and the long-term potential of benzyl succinic acids as positive indicators of natural attenuation of BTEX contamination prompted investigation of several aspects of the separation and analysis techniques to better understand the analytical limitations of the methods. Solid phase extraction was investigated as an alternative separation technique. Detection limits for the metabolites using the prescribed methods in different groundwater matrices were determined. Studies were also undertaken to determine the effects on the separation and analysis of the metabolites, if any, of the ubiquitous presence of the fluorinated surfactants that comprise AFFF (aqueous film forming foam) used to control the practice fires and found in most groundwater samples at this particular site.

Background

Natural Attenuation

Natural attenuation is a passive remediation technique now being used at a number of sites where the groundwater is contaminated with organic chemicals (1, 12, 26, 33). Primarily, natural attenuation is used for sites contaminated with petroleum products and industrial solvents that are known to undergo in-situ biodegradation. The passive nature of the natural (intrinsic) remediation lies in the fact that no active technology or natural process enhancement is applied to remove or transform the contaminants. Technically, natural attenuation is a protocol of strategic monitoring that requires an array of chemical, physical and biological indicators of the contaminant degradation in the subsurface to be followed for over time (26, 32). Both biological and abiotic processes in the subsurface may be contributing to the loss of the contaminant.

These processes include aerobic and anaerobic degradation, abiotic chemical transformations, dispersion, precipitation, ion exchange, dissolution, dilution, sorption, and volatilization (12, 18, 26).

The protocols for implementation of natural attenuation require relatively large arrays of secondary indicators, all of which serve as evidence that subsurface organic contaminants are being degraded, and collectively can provide a strong argument for natural attenuation. The specific group of physical, chemical, and biological parameters chosen to monitor at each site are based on historical records, hydrogeology, the biogeochemical properties, the contaminant to be removed, as well as the size and age of the spill. The groundwater parameters to monitor generally include several physical properties that define the geochemical properties of the system and groundwater concentrations of the contaminant and known byproducts, dissolved minerals and gases. Inorganic constituents to monitor should include the electron acceptors (oxygen, sulfate, nitrate, hydrogen, iron (III) and manganese (II)) which define the redox zones associated with the biodegradation of the plume; carbon dioxide; carbon isotope ratios; alkalinity; pH; ammonia; and hydrogen sulfide (1, 12, 13, 16, 26, 33). Despite the long list of indicators, none of these listed provide conclusive evidence of degradation of the organic contaminants.

In addition to the intensive groundwater-monitoring program, it is important to define and understand the subsurface geology and hydrogeology of the groundwater flow (26, 33). For natural attenuation to be verified, background (clean) composition of the groundwater should be documented. If groundwater composition at the site is not known prior to the contamination, up gradient groundwater may be monitored and used as a surrogate "clean" reference. Information about the resident microbial populations in the clean subsurface and groundwater is also valuable for comparisons to data collected during and after the natural attenuation processes.

Development of the sampling plan requires inclusion of temporal and spatial considerations (26, 33). Depending on the site, a number of up gradient contamination plume, and down gradient monitoring wells should be installed and sampled. Decisions about the areal extent of the monitoring program are heavily dependent on the site geology and hydrogeology, as well as the contaminant. Additionally, the possible vertical extent of the contamination must also be determined and considered when developing the groundwater monitoring protocol for a site. The dynamics of dispersion phenomena require that that the loss of the contaminant as the plume moves down gradient from the spill site be normalized to the migration of a non-

degradable constituent of the plume that is expected to travel at the same rate as the degradable components (26, 29, 33). Needless to say, modeling and prediction of natural attenuation can be seriously limited by lack of the appropriate field data.

Anaerobic Metabolites of Toluene

It is well documented that toluene (and other related alkyl benzenes) can be degraded in anaerobic conditions (5, 7, 9, 10, 11, 12, 13, 15, 17, 19, 22, 31, 32). In pure culture experiments with *pseudomonas* sp. strain T1 and K172, strain PROTOL1, *Thauera aromatica*, and *Azoarcus tolulyticus* Tol-4, anywhere from 80% to 99% of the toluene substrate provided to the microorganisms was mineralized to carbon dioxide and water or was transformed to new biomass (5, 6, 8, 11, 20, 25, 32). The remaining toluene was transformed to a mixture of benzyl succinic acid, benzyl fumeric acid, benzyl maleic acid, and/or E- and Z-phenylitaconic acid. These anaerobic metabolites appear to be dead-end by-products of toluene metabolism. Similar observations were made for disparate anaerobic bacteria derived from an aviation fuel contaminated site in Maryland under sulfate reducing conditions (8). Proposed biochemical mechanisms are illustrated in Figure 1 and suggest that the competitive pathway that results in the production of these substituted benzyl acids proceeds via the addition of succinyl-coenzyme A (succinyl-CoA) to the methyl group on benzene. The succinyl-CoA is hydrolyzed, leaving benzyl succinic acid, which looses two hydrogens to become one of the two unsaturated acids, benzyl maleic (cis) or benzyl fumaric (trans) acid (17). At this time, there is no conclusive evidence for this pathway, and at least one alternative has recently been proposed by Bellar and Spoorman (6). Meta- and para- xylene isomers degrade along the same pathway forming the corresponding alkyl-substituted benzyl succinic, benzyl maleic and benzyl fumaric or the E- and Z-phenylitaconic acid. Although the exact identification of the ultimate dead-end metabolite is uncertain at this time, there is sufficient evidence to believe that at least one of these products will not be further metabolized in the subsurface environment, and may serve as a positive indicator of toluene degradation.

Of primary concern to professionals who have the responsibility to clean up contaminated sites, is that the suggested "metabolites" remain in the groundwater and could be used as conclusive evidence that toluene and other BTEX compounds have been degraded. Benzyl succinic acid and its own metabolites have the desirable properties of natural attenuation indicators. They are not found in nature, nor are they commercially synthesized. It appears that

they do not mineralize to carbon dioxide, but are "dead-end" metabolites of toluene or a precursor to other "dead-end" metabolites. Additionally, benzyl succinic acid has a stoichiometric biochemical relationship to toluene, the contaminant being degraded. Lastly, benzyl succinic acid is not toxic. These properties of benzyl succinic acid would allow its presence in a toluene-contaminated groundwater under nitrate or sulfate reducing conditions to provide indisputable confirmation of toluene degradation.

Currently, there is little available field data documenting the presence of benzyl succinic acid or related compounds at fuel contaminated sites (22). There are several reasons for the lack of data and include the fact that the existence of these anaerobic metabolites is a relatively recent observation. Additionally, they would not be detected in the routine chemical analyses commonly performed for various organic contaminants in ground water from fuel-contaminated sites. Also, there are no commercial sources of four of the five possible anaerobic metabolites of toluene degradation and have to be synthesized and carefully characterized to obtain a pure standard. Benzyl succinic acid is commercially available. Lastly, the best analytical technique for the expected low concentrations expected, is labor intensive, and requires a large sample volume.

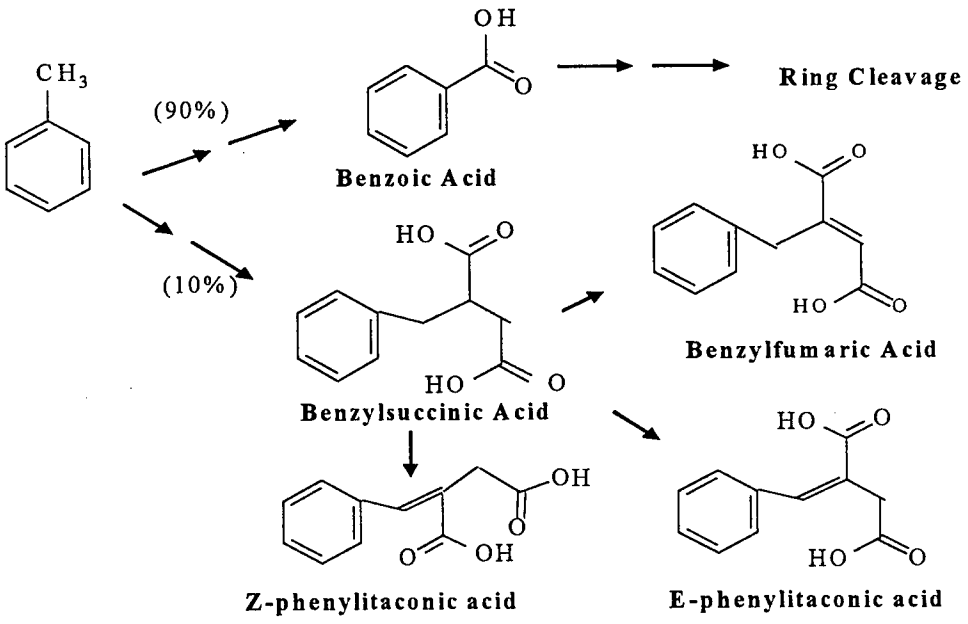

Figure 1. Anaerobic Metabolites of Toluene under Nitrate and Sulfate Reducing Conditions

FTA-23 Site Characteristics

Fire Training Area 23 at Tyndall Air Force Base is located in the central part of the Florida panhandle at 30° North latitude, a semi-tropical zone. The Air Force Base is in Bay County directly on the Gulf of Mexico. The semi-tropical climate yields 55 inches rainfall per year onto a mostly sand, gravel, and clayey sand surface soil that is very flat (maximum elevation near 30 feet above sea level), and poorly drained. The groundwater lies only 2-10 feet below the surface, and is directly connected to the nearby Gulf and inter coastal waters into which it drains. Because of the site's proximity to the open water, the groundwater is strongly influenced by tidal fluctuations, especially at high tides and surges caused by typical tropical storms. This surficial aquifer is about 100 feet deep in this area and overlies the 1100 foot thick, confined Floridian Aquifer, which is found 250 feet below sea level in this part of the state (20, 21, 22, 27, 28). The aquifer, which underlies much of the state, is primarily a karst formation of dolomite and limestone and provides significant amounts of drinking water to many communities.

Ground water in the surface aquifer flows in a southwesterly direction across the site towards Little Cedar Bayou Creek under a hydraulic gradient of 0.01 - 0.03 ft/ft. The recorded velocity ranges from 0.03 to 0.112 feet/day. The hydraulic conductivity varies over the small site with no real pattern, from values of 0.091 feet/day to 1.8 feet/day (20, 21, 22, 27, 28). Lower values are typically found closer to the discharge points.

The fire training area was decommissioned in 1992 after 11 years use. The one-half acre site is a flat and grassy open area bordered on the west by a small creek that empties into the inter coastal water less a mile north of from the site. Fires were set on a concrete pad using JP-4 jet fuel pumped about 15 feet to the fire pit by means of an underground pipe system from an above ground, contained 12,000 gallon storage tank. The fires were put with a combination of water and commercial mixtures of fluorinated surfactants know as aqueous film forming foams (AFFF). Excess runoff was directed to an oil-water separator before being discharged back to the adjacent creek, Little Cedar Bayou. Ground water contamination at the site is the result of leaks in the underground pipeline and oil-water separator, excess fuel and foam washed off from the pit itself, and miscellaneous spills (20, 21, 22, 27, 28).

Thirteen monitoring wells (12 shallow, 2-15 ft, and one deep, 37 ft) on the site are the result of several contamination assessment investigations performed under the Air Force

Installation Restoration Program prior to 1997 (20, 21, 22, 27, 28). Currently, another contaminant investigation is under way, for which four additional shallow wells were installed in July and August of 1997 (30). The shallow monitoring wells define the horizontal and vertical extent of the ground water contamination that results primarily from two areas of floating free product. One plume lies under the pipeline, the second near the pump house. Soil vapor analyses have also been used to better define the extent of the subsurface contamination.

Methodology

Sampling

All thirteen monitoring wells on the site in June 1997 were sampled for site characterization. Additionally, several wells chosen for the anaerobic metabolite studies were sampled several times during the summer months of 1997. All wells sampled were representative of the region around them. All wells were pre-bailed before collecting samples. All samples were transferred to appropriate containers, pretreated as specified in Standard Methods for the Analysis of Water and Wastewater, and temporarily stored on ice for the duration of the sampling event. Dissolved oxygen, pH, and ground water temperature were measured on site with field calibrated probes. Five milliliters of ground water was filtered immediately and added to 2 ml of Ferrozin-Herpes buffer solution for later analysis for iron (II) by reading the ultra violet absorbance at 652 nm.

Analyses

All samplings and analyses were conducted with approved QA/QC procedures and methods in compliance with Standard Methods (34). Samples drawn for anions, and total organic carbon, were stored at 4°C in the laboratory prior to analysis. The anions (including nitrate, sulfate, chloride, bromide, propionate, nitrite, bromate, carbonate, phosphate, phthalate) were run on a Dionex Ion Chromatograph using a conductivity detector. The mobile phase was isocratic sodium hydroxide. The total organic carbon analyses were run on a Shimadzu Total organic Carbon Analyzer. Surfactants were measured using the methylene blue active substance method (MBAS) Hach Method. Analysis of the above water quality parameters were collected to add to the historic data of the site and also to establish background information about the general water quality characteristics as well as to define the current redox conditions of the ground water at each well.

Hydrocarbon Analyses

A range of expected volatile components of the spent fuel were determined using a Solid Phase Micro Extraction (SPME) technique with gas chromatography (flame ionization detection) as described in detail elsewhere (22, 24) on a HP 5890 Series II chromatograph with a flame ionization detection (FID). Samples were compared to similarly extracted standard solutions containing known concentrations of benzene, toluene, ethyl benzene, 1,2-dimethyl benzene, 1,4-dimethyl benzene, 1,3,5-trimethyl benzene, 1,2,3,5-tetramethyl benzene, isopropyl benzene, n-propyl benzene, butyl benzene, and 1-methyl naphthalene. The internal standard was *d10*-ethyl benzene prepared in 2-propanol.

Anaerobic Metabolites Analyses

The procedure of Bellar, et al, was used for the analysis of the anaerobic metabolites (4, 8, 22, 23). A 1-liter sample of ground water was collected and immediately acidified to pH 2 with 6 N HCl. All samples were injected with 4-fluorobenzoic acid, which served the internal standard for the analytical method. Laboratory controls of benzyl succinic acid in distilled deionized water were also run through the entire procedure with the field samples. Duplicate 500 ml samples were extracted 3 portions (80, 40, and 40 ml) of diethyl ether. The combined extracts were concentrated in a rotary evaporator to 2-5 ml and dried with sodium sulfate. The methyl esters were prepared by adding ethereal diazomethane to the concentrated ether extract. The ether was exchanged for high purity methylene chloride for injection into the HP 5890 gas chromatograph (GC) coupled to a HP 5970 mass spectroscopy detector (MSD). Two columns were used. Early samples of the summer were run on a 20 m x 0.1 mm x 0.4 μm DB-5 column from J & W Scientific Co, Folsom, CA. After June 24, the samples were injected onto a 20 m x 0.175 mm x 0.4 μm DB-17 column, from J & W Scientific Co. The retention times and response factors were slightly different, however, both column gave good separation of the species of interest. After a 2 minute hold at 45°C, the oven was temperature was programmed to increased to 110°C at 8°C/minute, followed by a second increase to 250°C at 4°C/minute, and finished with a 5 minute hold. Anionic perfluroinated sulfonates were also detected during this analysis.

In addition to this GC/MS method for benzyl succinic acid, other analytical methods have been reported. Benzyl succinic acid can be separated and detected directly by HPLC methods, but the detection limits are considerably higher than the derivatization with GC/MS method (19).

For laboratory studies, isotope trapping of radio-labeled toluene has also been used successfully, with the radiolabled products being separated by HPLC with isotope counting detection (14)

Metabolite Detection Limits

About 5 liters of ground water was drawn from 4 of the wells at FTA-23 with different water quality for the determination of the separation and analytical method detection limits for benzyl succinic acid. Four sets of duplicate 500-ml samples of the water from each of these wells were spiked with benzyl succinic acid. The wells sampled included one up gradient well (T11-1), one well with floating free product, and 2 down gradient wells (T11-3 and MW-3), still in the contaminated groundwater zone. Additionally, laboratory control samples of increasing amounts of benzyl succinic acid in distilled, deionized water were also run for detection limits. Metabolite spikes of the well samples ranged up to 1000 nanograms/liter, or 1.0 µg/l. 4-fluorobenzoic acid was also added to all samples as the internal standard. Assuming a 10% conversion, the maximum expected concentration of benzyl succinic acid in ground water with toluene concentration of 10 micrograms/liter, would be 2.6 micrograms/liter, if it were 100% retained through the extraction and derivatization procedures. For 50% extraction/derivatization efficiency, the expected detectable concentration would be near 1.0 µg/l.

Solid Phase Extraction of Benzyl Succinic Acid

Solid phase extraction of benzyl succinic acid using Oasis HLB (Waters, Inc.) cartridges was explored as an alternative concentration technique to the ether extractions. A workable method was developed to handle the large sample volume in the 3 ml cartridges using a standard control of benzyl succinic acid in distilled water. This method also worked well when surfactant components of AFFF were added in low concentrations to the laboratory prepared benzyl succinic acid solutions to better simulate the groundwater at FTA-23. Thirty to fifty percent greater recoveries of benzyl succinic acid and 4-fluorbenzoic acid were achieved compared to the ether extraction method. Unfortunately, using the methods recommended by the manufacturer, the solid phase extractions did not work well when ground water from the site were subjected to the separation technique. Several problems arose, apparently due the complex nature of the contaminated ground water and its matrix. However, further exploration and method development for a solid phase extraction technique will most likely yield a workable method that has a higher net recovery of benzyl succinic acid than the ether extraction method.

Results

Water Quality Parameters

The results of the monitoring of ground water quality are currently being compiled with the historic ground water data in a database at FAMU-FSU College of Engineering and will be made available in digital form to Armstrong Laboratory when completed. It should be noted that all 13 wells were found to be anaerobic, with D.O. concentrations of less than 1.0 ppm. The groundwater temperature reflected ambient conditions, 25 – 29°C, and the pH ranged from 4.5 to 6.6, with most samples falling between 5 and 5.5. Visually, the many of the well samples were sudsy, indicating the presence of AFFF, and the fuel could be smelled in the most heavily contaminated wells.

Nitrite was not detected in any well and nitrate was detected in only 2 wells, MW-1 and MW-3, having 0.87 and 0.67 ppm, respectively. Relatively high concentrations (11-14 ppm) of Fe(II) were detected at the wells on the perimeter of the site, and very low concentrations (< 5 ppm) were found in most of the wells found in the contaminate plume. Elevated sulfate concentrations (> 30 ppm) were detected in 2 of the wells down gradient of the free product plumes. TOC values ranged from 0.2 to nearly 200 ppm, again with no real pattern with respect to the free product plume.

Volatile Organic Compounds

Eleven VOC's were detected by the method described above. High concentrations of all eleven compounds were found in the wells located directly in the fuel plume, AFMW-1 (> 0.5 ppm total VOC concentration) and MW-5. Significant levels of toluene (10.8 µg/l) and low, but detectable levels of the other nine compounds were found in T11-1, up gradient of the free product plume. No well, including those previously considered to be up gradient or out of range of the plume was completely free of volatile organics. Outside the free product plume area Except for the wells in the area of free product, all VOC concentrations were under 10 µg/l, and most were under 5 µg/l.

Anaerobic Metabolites and Fluorosurfactants

Benzyl succinic acid was not detected in any of the ground water samples from FTA-23. However, several other anaerobic metabolites were detected by this method, and qualitatively identified by matching mass spectra in the instrument library. Standards were not available to confirm their retention times. Table 1 gives the details of the aromatic metabolites were

observed in the different wells, including the metabolites that are thought to intermediates of anaerobic mineralization (13, 14).

Table 1. Summary of the presence of fluorinated surfactants and anaerobic metabolites identified as methyl esters of the corresponding acids from 1996 and 1997 samplings of FTA-23 monitoring wells.

Well	Surfactant	Anaerobic Metabolites
T11-1	Y*	ND**
T11-2	Y	DMBA[a], TMBA[b], BA[c]
T11-3	Y	TMBA[b], DMBA[a]
MW-1	ND	ND
MW-2	ND	ND
MW-3	Y	ND
MW-4	Y	TMBA[b]
MW-5	Y	ND
TY22-FTA	Y	ND
TY23-FTA	-	-
AFMW-1	Y	BAA[d], MBA[e]
AFMW-2	Y	TMBA[b]
DMW-1	ND	ND

Note: Y ≡ yes, detected; ND ≡ not detected; a ≡ methyl 2,4-dimethyl benzoate; b ≡ methyl 2,4,6-trimethyl benzoate; c ≡ methyl benzoate; d ≡ methyl benzyl acetate; e ≡ 4-methyl benzoate.

This table also indicates in which wells fluorinated surfactants were detected, during these analyses. Two peaks on the chromatogram have been tentatively identified as the methyl esters of perfluorinated sulfonic acid. They have retention times of 8.4 and 20.7 minutes on the DB-5 column, and 18.6 and 22.8 minutes on the DB-1701. Characteristic peaks that are indicative of the perfluorinated fragments appeared at masses 69, 119, 131, and 169. The 18.6 minute peak on the DB-1701 column has base peak of 96, indicating the methyl sulfonate group.

Detection Limits for Benzyl Succinic Acid

When no benzyl succinic acid was found in the well water from FTA-23, several questions arose. First, was benzyl succinic acid present, but just not detected? What effects does the presence of AFFF in the water have on the separation and analysis of benzyl succinic acid? Is it present at other fuel-contaminated sites? Due to limited time and the unavailability of samples from another fuel-contaminated site that was know to anaerobic, no other surveying was done. However, experiments to determine the detection limits in the ground water matrix were devised. Because the ground water quality and amount of contamination varies over the site, detection limits experiments were run on 4 different wells. T11-1, has been considered to be up

gradient from the spills, and until summer of 1997, it was relatively free of contamination, when toluene and surfactants were detected. The10 microgram/liter concentration of toluene at this site makes it a well to run. Well AFMW-1 is in the plume of free product, and has high concentrations of all VOC's analyzed for, with 50 micrograms toluene/liter. T11-3 is down gradient of the free product and does not have toluene, but other anaerobic metabolites have been detected (See Table 1).

The last was a made up laboratory control of benzyl succinic acid in distilled, deionized water spiked with CF-129 (a solution of 50% potassium alkyl carboxylate in water and butyl cellulose that is known to be a component of at least one of the AFFF formulations used at that site). The added CF-129 should give the distilled water samples some surfactant-like qualities, and may also help identify esterified surfactants seen in the ground water samples. Addition of the CF-129 did add a sudsy-like quality to the distilled water. Upon analysis of the CF-129 spiked samples, three or four peaks in the chromatograms with retention times between 42 and 45 minutes on the DB-1701 column, were attributed to the CF-129. However, peaks at these retention times were not observed in any of the ground water samples. Properties of thes four samples are summarized in Table 2.

Table 2. Characteristics of the water samples for detection limit determinations.

Sample	Toluene (µg/l)	Total VOC (µg/l)	D.O. (ppm)	Appearance
Benzyl succinic acid w/ CF-129	0	0.0	--	Slightly sudsy; colorless; clear
T11-1 (up gradient)	10	45	<0.5	Sudsy, yellowish with some suspended solids; sulfur odor; high humics?
AFMW-1 (in fuel plume)	41	500	<0.5	Sudsy, ½" free product; brownish with suspended solids
T11-3 (down gradient of fuel plume)	nd	10	<1.0	Sudsy; strong BTEX smell

The raw data of the detection limits analyses are a displayed in Figure 2. Good correlation is seen for the calibration curve of the made up distilled water sample and well samples from T11-1. Data from T11-3 yielded a poorly correlated relationship with a negative slope, indicating error in measurement or analysis, or a real inverse relationship between the

concentration of methyl benzyl succinicate in that particular well water matrix and the system response.

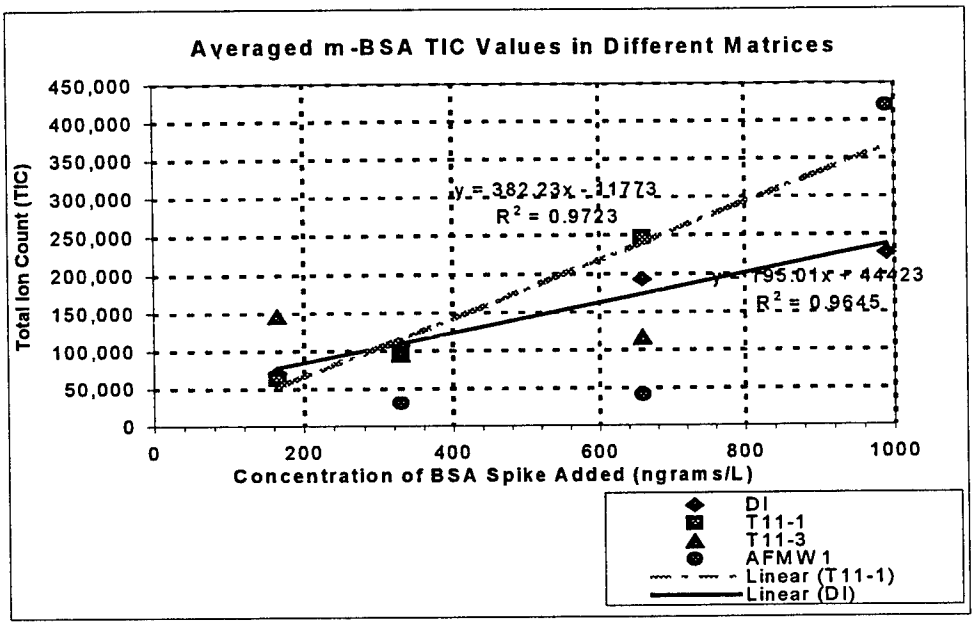

Figure 2. Raw data from benzyl succinic acid detection limit determinations in different well waters . Total ion counts are average of duplicate samples.

The standard curve for AFMW-1 had a correlation coefficient of 0.76 for a straight line fit, however, the response appears to have an exponential shape. This may indicate that the method response was not sensitive to concentration until a particular minimum value, and could be the result of matrix effects.

The detection limit of benzyl succinic acid in the well water of T11-1 would be near 20 nanograms/liter if it is read directly from the graph where the standard curve is extrapolated to the x-axis. However, no samples were run with concentrations less than 165 ng/l which had a total ion count less than 31,000 counts. Therefore, the detection limit of methyl benzyl succinate should be reevaluated using the data from all of the samples used for this set of experiments. The average of the lowest total ion counts for the four different waters is 39,000. Extrapolating where the standard curve for T11-1 intersects a horizontal line drawn at this TIC value, yields a a more reliable and conservative detection limit of 120 ng/l for the separation and analysis method used.

Caution must used in interpreting the results of this analysis technique when working with field samples whose characteristics and composition may vary greatly. How exactly the matrix of the analyte influenced the separation and analysis was not determined in this work. But evaluation of the response of the internal standard also supports the conclusion that matrix affects play an important role in this method. For the dilute solutions with the same concentration of the internal standard, the method response (total ion counts) should be the same. The response of the 4-fluorobenzoic acid in the 4 samples that were used for its standard cuve made up laboratory control was consistent. However, the response of the same concentration of 4-fluorbenzoic acid in the T11-3 samples was much more erratic and is indicative of interference from the background. Response of the internal standard is shown in Figure 3.

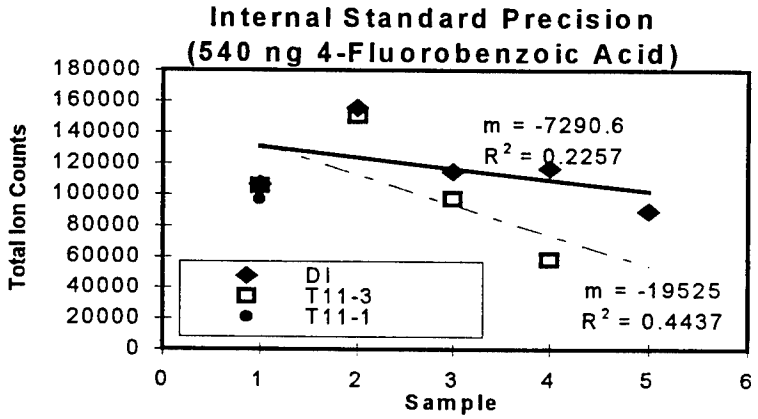

Figure 3. Precision of 4-fluorbenzoic acid internal standard in detection limits determinations.

Recommendations

There is much more work to be done to establish a good method of detection of benzyl succinic acids and its related metabolites.

1. Pursue more of these metabolites in the analysis. This implies obtaining or synthesizing some of the other dead-end metabolites for standards. They should be detected by the same methods.
2. Continue the work with the solid phase extraction separation (SPE) procedure, investigating several aspects related to working with contaminated samples including preliminary sample clean up; use of alternative solvent (to methanol) for elution from the sorbant in the cartridge; utilization of alternative SPE systems perhaps by other vendors.

3. Quantitation of the methyl benzyl succinate produced by obtaining or synthesizing standard material and subjecting them to the detection technique.
4. Optimize and quantify the ether extraction recovery of benzyl succinic acid.

Recommendations for developing a better understanding of this site with respect to the possible presence of the anaerobic metabolites.

1. Investigate the effects of AFFF on the all aspects of the water chemistry, contaminant mobility and availability.
2. Enumerate the anaerobic microorganisms of the local consortium.
3. Quantitate the contaminants and/or their byproducts, as well as the water quality of what leaves the site via the creek to better understand both the hydrogeology and ultimate fate of the contaminants.
4. Confirm the water quality anomalies noted during the summer of 1997, particularly the presence of BTEX in wells previously thought to be up gradient and clean.
5. Collect seasonal data to better characterize the site.
6. Study the influence of the tidal flow on the hydrogeology of the site.
7. Consolidate and evaluate the historic site water and soil characteristics.

Acknowledgements

The staff at Armstrong Laboratory at Tyndall Air Force Base provided technical support. Dr. Tom Stauffer was the project supervisor. Dr. Laurence Libelo provided field support. Dr. Timothy Shelley, Dr. Howard Mayfield, and Mr. Michael Henley provided laboratory support and technical guidance and assistance for all gas chromatography and GC/MS analyses and product identification. Water quality parameters (nutrients, ions, TOC, etc) were run by Ms. Eila Burr and Ms. Marlene Cantrell, both of whom regularly provide general assistance in the laboratory. Additional laboratory and field assistance was performed by Ms. Ruth Strickland.

References

1. Acton, D. W., J. F. Barker. 1991. In situ Biodegradation Potential of Aromatic Hydrocarbons in Anaerobic Groundwaters. *J. Contamin. Hydrology*, 9, 325-352.
2. Baedecker, M. J., I. M. Cozzarelli, R. P. Eganhouse, D. I. Steigel, P. C. Bennett. 1993. Crude Oil in a Shallow Sand and Gravel Aquifer-III. Biogeochemical Reactions and Mass Balance Modeling in Anoxic Groundwater. *Appl. Geochem.*, 8:569-586.
3. Beller, H. R. 1995. Anaerobic Metabolism of Toluene and Other Aromatic Compounds by Sulfate-Reducing Soil Bacteria, Ph.D. Dissertation, Stanford University.

4. Beller, H. R., W. H. Ding, M. Reinhard. 1995. Byproducts of Anaerobic Alkylbenzene Metabolism Useful as Indicators of in Situ Bioremediation. *Environ. Sci. Technol.*, 29, 2864-2870.

5. Beller, H. R., A. M. Spoormam. 1997. Anaerobic Activation of Toluene and o-xylene by Addition to Fumarate in Denitrifying Strain T. *J. Bacteriology*, 179:3, 670-676.

6. Beller, H. R., A. M. Spormann, P. K. Sharma, J. R. Cole, M. Reinhard 1996 Isolation and Characterization of a Novel Toluene-Degrading, Sulfate-Reducing Bacterium. *Appl. Environ. Micobiol.*, 62:4, 1188-1196.

7. Beller, H. R., M. Reinhard.1995. The Role of Iron in Enhancing Anaerobic Toluene Degradation in Sulfate-Reducing Enrichment Cultures. *Microb. Ecol.*, 30; 105-114.

8. Beller, H. R., M. Reinhard, D. Gbric-Galic. 1992. Metabolic By-Products of Anaerobic Toluene Degradation by Sulfate-Reducing Enrichment Cultures. *Appl. Environ. Microbiol*, 58:9, 3192-3195.

9. Biegert, T., G. Fuchs. 1995. Anaerobic Oxidation of Toluene to Benzoate by Whole Cells and by Cell Extracts of a Denitrifying Bacterium *Thauera sp. Arch. Microbiol*, 163:407-417.

10. Biegert, T., G. Fuchs, J. Heider. 1996. Evidence That Anaerobic Oxidation of Toluene is the Denitrifying Bacterium *Thauera aromatica* is Initiated by Formation of Benzylsuccinate from Toluene and Fumarate, *Eur. J. Biochem.*, 238:661-668.

11. Chee-Sanford, J. C., J. W. Rost, M. R. Fries, J. Zhou. 1996. Evidence for Acetyl Coenzyme A and Cinnamoyl Coenzyme A in the Anaerobic Toluene Mineralization Pathway in *Azoarcus tolulyticus* Tol-4. *Appl. Environ. Microbiol.*, 62:3, 964-973.

12. Clark, D., D. Ours, L. Hineline. 1997. Passive Remediation for Groundwater Impacted with Hydrocarbons. *Remediation Management*, 1, 50-54.

13. Cozzarelli, I. M., J. S. Heman, M. J. Baedecker. (1995) Fate of Microbial Metabolites of Hydrocarbons in a Coastal Plain Aquifer: The Role of Electron Acceptors. *Enviorn. Sci. Technol.* 29:2. 458-469.

14. Edwards, E. A., A. M. Edwards, D. Grbic-Galic, 1994, A Method for Detection of Aromatic Metabolites at Very Low Concentration: Application to Detection of Metabolites of Anaerobic Toluene Degradation, *Appl. Environ. Microbiol.*, 60:1, 323-327.

15. Edwards, E. A., D. Gbric-Galic. 1994. Anaerobic Degradation of Toluene and o-Xylene by a Methanogenic Consortium. *Appl. Environ. Microbiol.*, 60:1, 313-322.

16. Eganhouse, R. P., M.J. Baedecker, I. M. Cozzarelli, G, R. Aiken, K. A. Thorn, T. F. Dorsey. 1993. Crude Oil in a Shallow Sand and Gravel Aquifer-II. Organic Geochemistry. *Applied Geochemistry*, 8: 551-567.

17. Evens, P.J., W. Ling, B. Goldscmidt, E. R. Ritter, L.Y. Young. 1992. Metabolites Formed during Anaerobic Transformation of Toluene and *o*- Xylene and Their Proposed Relationship to the Initial Steps of Toluene Mineralization. *Appl. Enviorn. Microbiol.*, 58:2, 496-501.

18. Feldman, P., D. Tremblay, 1997, Natural Attention. *Environmental Protection*, May 1997.

19. Frazer, A. C., W. Ling, L.Y. Young. 1993. Substrate Induction and Metabolite Accumulation during Anaerobic Toluene Utilization by the Denitrifying Strain T1. *Appl. Environ. Microbiol.*, 59:9, 3157-3160.

20. Geraghty and Miller, Inc. 1991. Analytical Resluts report for fire Training Areas. Tyndall Air Force Base, Florida.

21. Geraghty and Miller, Inc. 1994. Draft Contamination Assessment Report for Active Fire Training Area Site FT-23. Tyndall Air Force Base, Florida.

22. Levine, A. D. September 1996. Biogeochemical Assessment of Natural Attenuation of JP-4 Contaminated Groundwater in the Presence of Fluorinated Surfactants. AFOSR Report.

23. Henley, M. V., H. T. Mayfield, T, J. Shelley. 1996. Diazomethane Derivatizaiton and GC/MS Analysis of Perfluorinated Surfactants. Unpublished procedure. Armstrong Laboratory, Tyndall Air Force Base.

24. Mayfield, H. T. 1996. Unpublished laboratory procedure. Armstrong Laboratory, Tyndall Air Force Base.

25. Migaud, M. E., J. C. Chee-Sanford, J. M. Tiedje, J. W. Frost. 1996. Benzylfumaric, Benzylmaleic, and Z-and E- Phenylitaconic Acids: Synthesis, Characterization, and Correlation with a Metabolite Generated by Azoarcus tolulyticus Tol-4 during Anaerobic Toluene Degradation. *Appl. Environ. Microbiol.* 62: 3, 974-978.

26. National Research Council. 1993. In Situ Bioremediation-When does it Work? Washington D.C., National Academy Press.

27. OHM Remediation Services Corp. 1994. Free Phase Hydrocarbon Delineation and Soil Quality Investigation of Fire Training Area 23. Tyndall Air Force Base.

28. OHM Remediation Services Corp. 1995. Pilot Test Work Plan for Insitu Bioremediation Using Microbubbles, Fire Training Area 23, Tyndall Air Force Base.

29. Rifai, H. S., C. J. Newell, R. N. Miller, S. Taffinder, M. Rounsaville. 1995. "Simulation of Natural Attenuation with Multiple Electron Acceptors, in Intrinsic Bioremediation, ed. R. E. Hinchee, J. T. Wilson, D. C. Downey. Battelle Press, Columbus, OH.

30. Rust Environment and Infrastructure. 1997. Field Sampling Plan for Site Characterization and Testing for Sites FT-16 and FT-23. Tyndall Air Force Base.

31. Schmidtt, R., H. R. Langguth, W. Puttmann, H. P. Rohns, P. Eckert, J. Schubert. 1996. Biodegradation of Aromatic Hydrocarbons under Anoxic Conditions in a Shallow Sand and Gravel Aquifer of the Lower Rhine Valley, Germany, Org. Geochem., 25:1/2, 41-50.

32. Seyfried, B., G. Glod, R. Schocher, A. Tschech. 1994. Initial Reactions in the Anaerobic Oxidation of Toluene and m-Xylene by Denitrifying Bacteria, Appl. *Environ. Microbiol.*, 60:, 11: 4047-4052.

33. Weidenmeir, T. H., D.C. Downey, J. T. Wilson, D. H. Kampbell, R. N. Miller, and J. E. Hansen. 1994. Technical Protocol for Implementing the Intrinsic Bioremediation with Long-Term Monitoring Option for a Dissolved-Phase Fuel Contamination in Ground Water. Air Force Center for Environmental Excellence, Brooks Air Force Base, San Antonio TX.

34. WEF, AWWA, APHA. 1992. Standard Methods for the Examination of Water and Wastewater, 18th Edition.

THE NET EFFECT OF A COVARIATE IN ANALYSIS OF COVARIANCE

Dulal Bhaumik
Associate Professor
Department of Mathematics and Statistics

University of South Alabama
ILB 320
Mobile, AL36688

Final Report for:
Summer Research Program
Armstrong Laboratory

Sponsored by:
Air Force Office of Scientific Research
Bolling Air Force Base, Washington, DC

And

Armstrong Laboratory

September 1997

THE NET EFFECT OF A COVARIATE IN ANALYSIS OF COVARIANCE

Dulal K Bhaumik, Pandurang M Kulkarni
Associate Professors
Department of Mathematics and Statistics
University of South Alabama

and

Joel E Michalek
Armstrong Laboratory
Brooks Air Force Base
Texas 78235-5250

Abstract

When we compare two groups or a treatment with a control, the effect of a covariate on the response variable may play an important role. When a covariate is not a demographic variable, it may have to be measured and the measurements may be expensive or complicated. In such cases, it may be wise to assess the importance or effectiveness of it with respect to the response variable. In this paper, we develop some inferential measures that can be used to assess the net effect of the covariate on the response variable. The procedures developed can be used for both fixed and random covariates. We also develop an index similar to the percent reduction index to assess the percent decrease (or increase) in the mean difference due to the covariate. We provide confidence intervals for this index.

The Net Effect of a Covariate in Analaysis of Covariance

Pandurang M. Kulkarni, Dulal K. Bhaumik, and Joel E. Michalek

1. INTRODUCTION

In biomedical experiments, it is common to have a covariate while comparing a treatment with a control. When the covariate is a demographic variable, an adjustment for this is usually made at the time of comparing two or more groups. It is possible in some experiments that the covariate might be a complicated health related measurement or it might be expensive to measure. In such cases one may have to carefully assess the effectiveness of the net effect of this covariate on the response variable. In the following example we try to clarify this idea.

Example : Air Force Health Study (AFHS) The Air Force Health Study is a 20-year prospective epidemilogical study of possible health effects from exposure to herbicides and their contaminant, 2,3,7,8-tetrachlorodibenzo-p-dioxin (dioxin) in veterans of Operation Ranch Hand, the unit responsible for spraying Agent Orange and other herbicides in Vietnam from 1962 to 1971 (for a detailed discussion see Wolfe et al (1990), Michalek et al (1996a)). A group of Air Force Veterans who served in Southeast Asia during the same period but who were not involved with spraying herbicides serve as controls. Control veterans were matched to Ranch Hand veterans on age, military occupation and race. The study compares the health, reproductive outcomes and mortality of Ranch Hand veterans, the index subjects, with control veterans. Physical examinations are administered and a measurement of dioxin in serum has been used as the index of exposure. An investigation of endocrine function included serum insulin, measured in mIU/ml. In previous studies researchers have treated the health variable (insulin) and dioxin as log-normal random variables (see Flanders et al. (1992), Michalek et al. (1996a), Kulkarni and Wang (1997)). Flanders et al. (1992) considered that the observed dioxin with measurement error had a log-normal distribution and they assumed that the true dioxin also had a log-normal distribution. Recently, a reliability study of dioxin measurments (Michalek et al.(1996b)) concluded that the reliability is very high. Therefore, in this article we will not consider the measurement error. Various aspects of this AFHS data are described in several articles (see Wolfe et al. (1990), Grubbs et al. (1995), Michalek et al. (1997)). In this article we are interested in studying the net effect of dioxin on the health (insulin) among nondiabetic veterans. Our sample contains 959 controls and 779 Ranch Hands.

Adjusting for the covariate while comparing two groups or a treatment with a control is well known and is usually referred to as the analysis of covariance (ANCOVA). However, for completeness we will discuss this in brief. Consider an experiment in which we compare a treatment group with a control group. Then, the usual model, if the two groups are matched on all the important variables, is given by

$$y_{ij} = \beta_0 + \tau\delta_{ij} + \epsilon_{ij},\ j = 1, \ldots, n_i,\ i = 1, 2, \tag{1}$$

where $\delta_{ij} = 1$ for the control group and 0 otherwise, τ represents the treatment effect, and is estimated by $\hat{\tau} = \bar{y}_1 - \bar{y}_2$, y_{ij} is the health effect of the jth individual belonging to the ith group and $\bar{y}_1$ and $\bar{y}_2$ are the first and second group means of y_{ij}'s.

Now, suppose there is a covariate x (say, a continuous variable) which has a linear relationship with y. Suppose that the two groups (treatment and control) were not matched or could not be matched before

the experiment was conducted. Since x has a relationship with y, the estimate of τ given in (1) will not be unbiased for the treatment effect unless the covariate means in the two groups are the same. Therefore, consider the usual analysis of covariance model (to adjust for the covariate),

$$y_{ij} = \beta_0 + \beta_1 x_{ij} + \tau \delta_{ij} + \epsilon \tag{2}$$

where δ_{ij} is as defined in (1), and it is assumed that x_{ij} is linearly related to y_{ij} with the same slope β_1 in both the groups (i.e. no interaction). The "adjusted" estimator of τ, adjusted for the covariate x, is given by $\hat{\tau} = (\bar{y}_1 - \bar{y}_2) - \hat{\beta}_1(\bar{x}_1 - \bar{x}_2)$. It is well known (see Cochran and Rubin (1973)) that $\hat{\tau}$ is an unbiased estimator of τ. The second term, $\hat{\beta}_1(\bar{x}_1 - \bar{x}_2)$, is the "estimate of the adjustment effect due to x". This adjustment effect, which we refer to as the "net effect" due to x, is the quantity of interest in this paper. This quantity is usually referred to as "bias".

In this article we give procedures for assessing the effectiveness of the net effect conditionally on x and unconditionally on x in terms of obtaining its standard error, confidence intervals and test statistic. If one is interested in relating y with treatment conditionally on x, then standard regression theory can be applied. However, as this aspect of the AFHS has not been considered before, we provide some results in that direction. If the covariate is random and has a genuine probability distribution, then that information should be utilized in the asssessment of the effectiveness of the net effect. Therefore, we provide the unconditional results as well.

In dental research an index $\delta = 100(\mu_1 - \mu_2)/\mu_2$, where μ_1 and μ_2 are the means of control and treatment populations, is used to indicate the percent reduction in mean DMFS (decayed, missing and filled surfaces of teeth) increment due to a new treatment relative to a standard one (see Zacherl and McPhail (1965), Dubey (1966), Wallenstein, Fleiss and Chilton (1981) and Fleiss (1986)). Dubey (1966) gave procedures for constructing confidence intervals for δ for large and small sample sizes. These results were generalized by Wallenstein et al.(1981) to include the case where μ_1 and μ_2 represent adjusted means, namely μ_1^A and μ_2^A, in an analysis of covariance. The percent reduction obtained by Wallenstein et al. (1981) indicates, for example, the percent reduction in 'the adjusted mean DFMS increment due to a new treatment' relative to 'the adjusted mean DFMS increment due to standard treatment (or control)', where the covariate is the measurement prior to the treatment.

Our goal is slightly different, in that, we are interested in the 'percent reduction (or increment) we should have achieved in $(\mu_1 - \mu_2)$ if we were to adjust for the covariate and calculate $(\mu_1^A - \mu_2^A)$'. In otherwords, we are interested in

$$\delta = 100\left[\frac{\Delta_{U-A}}{\Delta_U}\right],$$

where $\Delta_{U-A} = (\mu_1 - \mu_2) - (\mu_1^A - \mu_2^A)$ and $\Delta_U = \mu_1 - \mu_2$. If $\delta = 0$, then the covariate has no effect and therefore the unadjusted and the adjusted mean differences would be identical. When $\delta > 0$, this indicates that, due to the covariate adjustment, the adjusted mean difference, $\mu_1^A - \mu_2^A$, is a result of a $\delta\%$ decrease in the unadjusted mean difference. Similarly, $\delta < 0$ implies that, due to the covariate adjustment, the adjusted mean difference is the result of $\delta\%$ increase in the unadjusted mean difference. Notice that δ can be between $(-\infty, +\infty)$. Large absolute values of δ would indicate a serious need for adjusting for the covariate. We provide conditional confidence intervals for this index.

In Section 2, we formally define the conditional and unconditional "net effect," and study their properties in terms of their standard error, confidence intervals and test statistics. In Section 3, we derive the conditional confidence intervals for the index δ. In Section 4, we apply the results developed in Sections 2 and 3 to AFHS data.

2. INFERENCES CONCERNING THE NET EFFECT

With the notations in Model (2), consider the following assumptions.

Assumptions

(1) x_{ij} is a continuous covariate and is related linearly to the response variable, y_{ij}.
(2) There is a common slope, β_1, for the two groups.
(3) The e_{ij}'s are independent normal random variables with mean 0 and variance σ_e^2.

Further, we consider the cases that (i) the covariate is fixed, in which case all the results are derived fixing x_{ij}, and (ii) the covariate is random, $x_{ij} \sim Normal(\mu_{x_i}, \sigma_{x_i}^2)$, $j = 1, \cdots, n_i, i = 1, 2$, and x_{ij} are independent of ϵ_{ij}. In this presentation, conditional statements refer to the fixed covariate case and unconditional statements refer to the random covariate case.

Now we formally define the net effect under both fixed and random covariates.

Definition 1: Conditional net effect: The conditional net effect due to the covariate x, conditional on x, is given by $E_C = \beta_1(\bar{x}_1 - \bar{x}_2)$.
Definition 2: Unconditional net effect: The unconditional net effect due to the covariate x, is given by $E_{UC} = \beta_1(\mu_{x_1} - \mu_{x_2})$.

2.1 Estimation

Small samples

Let S_{y_1} and S_{y_2} denote the sample standard deviations of y in groups 1 and 2, respectively, and let $SS_{xx} = \sum\sum(x_{ij} - \bar{x}_i)^2$. Then, it can be shown that with either a fixed or random covariate the usual estimators $\hat{\beta}_1 = \sum\sum(y_{ij} - \bar{y}_i)(x_{ij} - \bar{x}_i)/SS_{xx}$, $S_y^2 = [(n_1 - 1)S_{y_1}^2 + (n_2 - 1)S_{y_2}]^2/(n_1 + n_2 - 2)$, and $\hat{\tau} = (\bar{y}_1 - \bar{y}_2) - \hat{\beta}_1(\bar{x}_1 - \bar{x}_2)$ are the maximum likelihood (ML) estimators of β_1 and τ. The ML estimator of E_C and its estimated standard error, conditioning on x, are given by

$$\hat{E}_C = \hat{\beta}_1(\bar{x}_1 - \bar{x}_2) \quad \text{and} \quad se(\hat{E}_C) = [(\bar{x}_1 - \bar{x}_2)^2 S_y^2/SS_{xx}]^{1/2}.$$

When the covariate is random, and if $\sigma_x^2 = \sigma_{x_i}^2$, $i = 1, 2$, it can easily be verified that $\hat{\beta}_1$ is an unbiased estimator of β_1 with $Var(\hat{\beta}_1) = \sigma_e^2/(\sigma_x^2(N - 4))$, where $N = n_1 + n_2$. The assumption of equal variances is not crucial and can be relaxed as shown in Result 3, below.

Result 1: If $\mu_{x_1} = \mu_{x_2}$, $\sigma_{x_1} = \sigma_{x_2} = \sigma_x$, then the estimated standard error of $\hat{E}_{UC}$ is given by

$$\text{se}(\hat{E}_{UC}) = \left[\frac{(N-2)S_e^2}{N-4} + S_x^2\,\hat{\beta}_1^2\right]^{1/2}\left(\frac{1}{n_1} + \frac{1}{n_2}\right)^{1/2},$$

where $S_x^2 = [(n_1 - 1)S_{x_1}^2 + (n_2 - 1)S_{x_2}]^2/(n_1 + n_2 - 2)$, where $S_{x_1}^2$ and $S_{x_2}^2$ are the sample variances of the x_{ij}'s in groups 1 and 2, and $S_e^2 = SS_{yy} - \hat{\beta}_1^2 S_{x_2}$, provided $SS_{yy} > \hat{\beta}_1^2 S_{x_2}$, otherwise $S_e^2 = 0$.

Result 2: If $\mu_{x_1} \neq \mu_{x_2}$, $\sigma_{x_1} = \sigma_{x_2} = \sigma_x$, then the estimated standard error of $\hat{E}_{UC}$ is given by

$$se(\hat{E}_{UC}) = \left[\frac{S_e^2(1+\lambda^2)}{n_1+n_2-2} + \hat{\beta}_1^2 S_x^2\right]^{1/2} \left(\frac{1}{n_1}+\frac{1}{n_2}\right)^{1/2},$$

where

$$\lambda = \frac{(\bar{x}_1 - \bar{x}_2)}{\sqrt{S_x^2(\frac{1}{n_1}+\frac{1}{n_2})}}.$$

Result 3: If $\mu_{x_1} \neq \mu_{x_2}$, $\sigma_{x_1} \neq \sigma_{x_2}$ then the estimated standard error of $\hat{E}_{UC}$ is given by

$$se(\hat{E}_{UC}) = \left[S_y^2\, U_1 + \hat{\beta}_1^2\, U_2\right]^{1/2},$$

where $U_1 = \frac{\lambda_1^2}{b(C-2)}$ and $U_2 = \frac{S_{x_1}^2}{n_1} + \frac{S_{x_2}^2}{n_2}$, with

$$\lambda_1 = (\bar{x}_1 - \bar{x}_2)^2 + \left(\frac{S_{x_1}^2}{n_1} + \frac{S_{x_2}^2}{n_2}\right) \quad , \quad b = \frac{(n_1-1)S_{x_1}^4 + (n_2-1)S_{x_2}^4}{(n_1-1)S_{x_1}^2 + (n_2-1)S_{x_2}^2}$$

and

$$C = \frac{[(n_1-1)S_{x_1}^2 + (n_2-1)S_{x_2}^2]^2}{(n_1-1)S_{x_1}^4 + (n_2-1)S_{x_2}^4}.$$

Large samples:

It can be shown (see the Appendix) that for large N, $(\hat{\beta}_1 - \beta_1)/\sqrt{Var(\hat{\beta}_1)}$ follows the standard normal distribution. Using this asymptotic distribution and the sufficient statistics it is easy to verify that $\hat{\beta}_1$ and $\bar{x}_1 - \bar{x}_2$ are asymptotically independent random normal random variables. Further, $\hat{\beta}_1(\bar{x}_1 - \bar{x}_2)$ follows an approximate normal distribution (see the Appendix) with mean $\beta_1(\mu_{x_1} - \mu_{x_2})$ and estimated standard error as obtained in the small sample cases in Results 1 or 2, depending on the distributions, conditioning on x. It is not easy to obtain a similar result for the case of Result 3. Therefore, to draw inferences about E_{UC} we only consider the conditions of Results 1 and 2.

2.2 Inference

Given x, a $(1-\alpha)\%$ CI for E_C is given by

$$\hat{E}_C \pm t_{\frac{\alpha}{2},n_1+n_2-2}\; se(\hat{E}_C),$$

where $t_{\frac{\alpha}{2},n_1+n_2-2}$ is the upper $(\frac{\alpha}{2}100)$th percentile of a central t-distribution with (n_1+n_1-2) degrees of freedom (df).

Conditionally on x, and if $x_1 \neq x_2$, a test of the hypothesis $H_0 : E_C \quad d_0$, for some d_0 is the same as that of testing $H_0 : \beta_1 = \frac{d_0}{(\bar{x}_1 - \bar{x}_2)}$ and therefore can be conducted using the usual regression techniques. Now we provide unconditional results.

Result 4: Unconditionally on the covariate x, an approximate $(1-\alpha)100\%$ C.I. for E_{UC} is given by

$$\hat{E}_{UC} \pm Z_{\frac{\alpha}{2}}\; se(\hat{E}_{UC}),$$

where $\hat{E}_{UC} = \hat{E}_C$, and se$(\hat{E}_{UC})$ is obtained from Results 1, or 2 depending on the conditions of the means and variances and $Z_{\alpha/2}$ is the upper $1-\alpha/2$ quantile of the standard normal distribution.

Result 5: Unconditionally on the covariate x, an approximate α level test of the hypothesis $H_0 : E_{UC} = 0$ rejects H_0 if

$$\left|\frac{\hat{E}_{UC}}{\text{se}(\hat{E}_{UC})}\right| > Z_{\frac{\alpha}{2}}.$$

To interpret the "net effect" due to x, we consider the two cases.

Case (i) $\hat{\beta}_1 > 0$, $(\bar{x}_1 - \bar{x}_2) > 0$ and $\hat{\beta}_1(\bar{x}_1 - \bar{x}_2) = C_1$, say. This means that an increase of C_1 units in the difference between the mean responses of Group 1 and Group 2 is attributed to the covariate x.

Case (ii) $\hat{\beta}_1 < 0$, $(\bar{x}_1 - \bar{x}_2) > 0$, and $\hat{\beta}_1(\bar{x}_1 - \bar{x}_2) = -C_2$, say. Then, a decrease of C_2 units in the difference between the mean responses of Group 1 and Group 2 is attributed to the covariate x. Similar interpretations follow for other cases.

In the next section we develop an index to measure the percent reduction in the mean response that is attributed to the covariate.

3. PERCENTAGE REDUCTION INDEX DUE TO THE COVARIATE

Using the notations of the previous sections, a point estimate of δ is obtained by

$$\hat{\delta} = 100\left[\frac{\hat{\Delta}_{U-A}}{\hat{\Delta}_U}\right] = 100\left[\frac{\hat{\beta}(\bar{x}_1 - \bar{x}_2)}{\bar{y}_1 - \bar{y}_2}\right].$$

Let $v_1 = var(\hat{\Delta}_{U-A}|x) = (\bar{x}_1 - \bar{x}_2)^2 S_y^2/SS_{xx}$, $v_2 = var(\hat{\Delta}_U|x) = S_y^2(1/n_1 + 1/n_2)$, and $g = t^2_{\frac{\alpha}{2},n_1+n_2-2}\, v_2/\hat{\Delta}_U^2$. Small values of g indicate significant differences in the unadjusted group means. The following result is an application of Fieller's theorem (see Wallenstein et al. (1982)) and the result is valid if $g < 1$.

Result 6: Conditionally on the covariate x, a $(1-\alpha)100\%$ confidence interval for δ, is given by

$$\frac{1}{1-g}\left[\hat{\delta} \pm \frac{t_{\frac{\alpha}{2}}}{\hat{\Delta}_U}((1-g)v_1 + \hat{\delta}^2 v_2)^{\frac{1}{2}}\right].$$

Unconditional confidence intervals are difficult to obtain. However, a nonstandard closed form for the density function of the random variable $V = \left[\frac{\hat{\beta}_1(\bar{x}_1 - \bar{x}_2)}{\bar{y}_1 - \bar{y}_2}\right]$ can be obtained (see the Appendix) and is given by

$$f(v) = \frac{\sqrt{2\pi}BC}{A^{\frac{3}{2}}} e^{\frac{B^2}{2A}} - \frac{2\sqrt{2\pi}BC}{A\sqrt{A}} e^{\frac{B^2}{2A}} \Phi(-\frac{B}{\sqrt{A}}) + \frac{2C}{A},$$

where $A = \frac{v^2}{\sigma^2_{x_1}} + \frac{1}{\sigma^2_{x_2}}$, $B = \frac{\mu_{x_1} v}{\sigma^2_{x_1}} + \frac{\mu_{x_2}}{\sigma^2_{x_2}}$, and $C = [2\pi\sigma_{x_1}\sigma_{x_2}]^{(-1)} exp[-0.5(\frac{\mu^2_{x_1}}{\sigma^2_{x_1}} + \frac{\mu^2_{x_2}}{\sigma^2_{x_2}})]$. The quantiles of the distribution can be obtained via numerical integration.

4. APPLICATION

Refer to the example in the introduction section of this paper. Here, as has been done in the past (see Wolf et al.(1990), Michalek et al.(1996a)), we analyze logarithmically transformed data. Normal probablity

plots of log insulin (y) and of log dioxin (x) indicated a close approximation for normal distribution for both the groups. Summary statistics for the two groups are: $\bar{y}_1 = 4.2397$, $\bar{y}_2 = 4.2509$, $S_{y_1} = 0.87725$, $S_{y_2} = 0.83295$, $\bar{x}_1 = 2.7065$, $\bar{x}_2 = 1.5223$, $S_{x_1} = 0.99407$, and $S_{x_2} = 0.56864$. Tests for the equality of the variances were conducted on both y and x. The hypothesis of equality of the variances for x was rejected ($p - value < 0.001$). As expected, the index group has considerably more variation in log dioxin measurements than the control group. We fitted the usual one-way ANCOVA model (equation (2)) with two groups and x as the covariate. The model was found significant ($p < 0.0001$) with $\hat{\beta}_1 = 0.1923$. Since the interaction was not significant (p-value=0.45), we did not include the interaction term in our model. We denote the index group by 1 and the control by 2. An estimate of the net effect of dioxin on health variable insulin is given by $0.1923(\bar{x}_1 - \bar{x}_2) = 0.1731$. Therefore, an increase of 0.1731 units in mean log insulin of index group compared to that of control is due to dioxin. A 95% conditional confidence interval for the net effect is given by 0.1731 ± 0.045. Further, to obtain the unconditional confidence interval for the net effect we use Result 4. Thus, an approximate 95% unconditional confidence interval for the net effect is given by 0.1731 ± 1.33. It is clear that once the distribution of x is taken into account the net effect fails to be significant. This is mostly attributable to the variances of x in the two groups.

The estimated percentage reduction index is given by $\hat{\delta} = -173\%$. Thus, if not for the covariate (x), the mean difference between the control and the index group would have been 173% more than what it is now. For this data there was not a significant difference between the unadjusted means (i.e. $g \not< 1$). Therefore, the confidence intervals will not be valid for the index group. In the usual treatment versus control experiments, a marked difference between the unadjusted means is usually found and the difference may be reduced (or increased) by adjusting for the covariate. In such cases, the confidence intervals for the index group can be quite helpful and will indicate if the reduction (or increment) is significant.

APPENDIX

The proofs of some of the results listed in Section 2 will be outlined here.

Unless specified otherwise, all the conditional arguements conditional on x imply that they are conditional on all of the information available on the covariate in both groups.

Variance of $\hat{\beta}_1$: Use the identity $Var(\hat{\beta}_1) \equiv E(Var(\hat{\beta}_1|x)) + Var(E(\hat{\beta}_1|x))$.

Unconditional variance of $\hat{\beta}_1(\bar{x}_1 - \bar{x}_2)$:

$$\begin{aligned} Var\ (\hat{\beta}_1(\bar{x}_1 - \bar{x}_2)) &= E\ Var\left[(\hat{\beta}_1(\bar{x}_1 - \bar{x}_2)|x\right] + Var\ E\left[\hat{\beta}_1(\bar{x}_1 - \bar{x}_2)|x\right] \\ &= \sigma_e^2 E\left[\frac{(\bar{x}_1 - \bar{x}_2)^2}{\sum\sum(x_{ij} - \bar{x}_i)^2}\right] + \beta_1^2\ Var(\bar{x}_1 - \bar{x}_2) \\ &= \sigma_e^2 U_1 + \beta_1^2 U_2, \end{aligned}$$

where U_1 and U_2 are obtained under three cases (i) $\mu_{x_1} = \mu_{x_2}$, $\sigma_{x_1} = \sigma_{x_2}$, (ii) $\mu_{x_1} \neq \mu_{x_2}$, $\sigma_{x_1} = \sigma_{x_2}$, and (iii) $\mu_{x_1} \neq \mu_{x_2}$, $\sigma_{x_1} \neq \sigma_{x_2}$.

<u>case (i)</u>: $\mu_{x_1} = \mu_{x_2}$, $\sigma_{x_1} = \sigma_{x_2} = \sigma_x$.

Note that $(\bar{x}_1 - \bar{x}_2)/\sqrt{S_x^2(\frac{1}{n_1} + \frac{1}{n_2})} \sim t_{N-2}$, where S_x^2 is the pooled variance estimate of σ_x^2. Thus,

$$\begin{aligned} U_1 &= E\left[\frac{\bar{x}_1 - \bar{x}_2}{\sqrt{\sum\sum(x_{ij} - \bar{x})^2}}\right]^2 \\ &= \frac{N-2}{N-4}\left(\frac{1}{n_1} + \frac{1}{n_2}\right) \end{aligned}$$

and $U_2 =$ var $(\bar{x}_1 - \bar{x}_2) = \sigma_x^2(\frac{1}{n_1} + \frac{1}{n_2})$.

Case (ii) $\mu_{x_1} \neq \mu_{x_2}$, $\sigma_{x_1} = \sigma_{x_2} = \sigma_x$

Here, $(\bar{x}_1 - \bar{x}_2)/\sqrt{S_x^2(\frac{1}{n_1} + \frac{1}{n_2})} \sim t_{n_1+n_2-2}(\nu)$, where $t_{n_1+n_2-2}$ (ν) is the non-central t-distribution with non-centrality parameter ν given by $\nu = \frac{\mu_1 - \mu_2}{\sqrt{\sigma_x^2(\frac{1}{n_1}+\frac{1}{n_2})}}$. Thus,

$$U_1 = \frac{(1 + \lambda_1^2)}{n_2 + n_1 - 4}\left(\frac{1}{n_1} + \frac{1}{n_2}\right),$$

and U_2 is the same as in case (i) above.

Case (iii) $\mu_{x_1} \neq \mu_{x_2}$, $\sigma_{x_1} \neq \sigma_{x_2}$

Here,

$$E\left(\frac{(\bar{x}_1 - \bar{x}_2)^2}{\sum\sum(x_{ij} - \bar{x}_o)^2}\right) = \lambda_1^2 E\left[\frac{1}{\sigma_{x_1}^2\chi_{n_1-1}^2 + \sigma_{x_2}^2\chi_{n_2-1}^2}\right].$$

Now, since $\sigma_{x_1}^2\chi_{n-1}^2 + \sigma_{x_2}^2\chi_{n_2-1}^2$ is a linear combination of independent χ^2 random variables with weights $\sigma_{x_1}^2$ and $\sigma_{x_2}^2$, it does not follow a χ^2 distribution. However a good approximation to this can be obtained by equating the first two moments of this combination to the first two moments of another χ^2 distribution of the type $b\chi_C^2$. This approximation is known to work quite well (see Johnson and Kotz (1970), Mee et al.(1987), and Kulkarni and Shah (1995)).

Let $A = a_1\chi_{b_1}^2 + a_2\chi_{b_2}^2$ and $B = b\chi_C^2$. The idea is to find b and c such that the first two moments of A match with those of B and therefore approximate the distribution of A by B. In our case, $a_1 = \sigma_{x_1}^2$, $b_1 = n_1 - 1$, $a_2 = \sigma_{x_2}^2$, $b_2 = n_2 - 1$. Thus,

$$b = \frac{\sigma_{x_1}^4(n_1 - 1) + \sigma_{x_2}^4(n_2 - 1)}{\sigma_{x_1}^2(n_1 - 1) + \sigma_{x_2}^2(n_2 - 1)}, \quad C = \frac{(\sigma_{x_1}^2(n_1 - 1) + \sigma_{x_2}^2(n_2 - 1))^2}{\sigma_{x_1}^4(n_1 - 1) + \sigma_{x_2}^4(n_2 - 1)},$$

and $\sigma_{x_1}^2\chi_{n_1-1}^2 + \sigma_{x_2}^2\chi_{n_2-1}^2 \tilde{\sim} b\chi_C^2$, with $E(\chi_C^2)^{-1}/b = (b(C-2))^{-1}$. This yields

$$U_1 = (1 + \nu_1^2)\frac{1}{b(C-2)},$$

and

$$U_2 = \beta^2\left(\frac{\sigma_{x_1}^2}{n_1} + \frac{\sigma_{x_2}^2}{n_2}\right),$$

where b and C are as defined earlier.

In the following derivations we choose $\sigma_x = \sigma_{x_1} = \sigma_{x_2}$. Other cases follow similarly.

Asymptotic distribution of $\hat{\beta}_1$: First we note that the conditional distribution of $\hat{\beta}_1$, conditional on x, is normal with mean β_1 and variance σ_e^2/SS_{xx}. Therefore, SS_{xx} provides sufficient information for obtaining the distribution of $\hat{\beta}_1$. Also, SS_{xx}/σ_x^2 has a central chi-square distribution with $N - 4$ df. Therefore,

$$f(\hat{\beta}_1) = \int_0^\infty f_1(\hat{\beta}_1/SS_{xx})f_2(SS_{xx})dSS_{xx}.$$

After some algebraic manipulations and making the transformation $T = \sqrt{N-4}(\hat{\beta}_1 - \beta_1)\sigma_x/\sigma_e$, it can be verified that T follows a central t-distribution with $N - 4$ df and therefore $(\hat{\beta}_1 - \beta_1)/\sqrt{Var(\hat{\beta}_1)}$ follows a standard normal distribution for large N.

Asymptotic distribution of $\hat{\beta}_1(\bar{x}_1 - \bar{x}_2)$: Let $u = \hat{\beta}_1$ and $v = \bar{x}_1 - \bar{x}_2$ and $z = uv$. First, note that asymptoically, u and v are independent normal random variables. Now using the moment generating function method, it can be shown that

$$M_z(t) = E(e^{tz}) = exp[t\mu_z + \frac{t^2}{2}\sigma_z^2][1 - t^2\frac{\sigma_e^2}{N-4}(\frac{1}{n_1} + \frac{1}{n_2})]^{-\frac{1}{2}},$$

where $\mu_z = \beta_1(\mu_{x_1} - \mu_{x_2})$ and $\sigma_z^2 = \beta_1^2\sigma_x^2(\frac{1}{n_1} + \frac{1}{n_2}) + \frac{(\mu_{x_1} - \mu_{x_2})^2\sigma_e^2}{\sigma_x^2(N-4)}$. Thus, if we assume that $\frac{\sigma_e^2}{N-4}(\frac{1}{n_1} + \frac{1}{n_2}) \approx 0$, then $M_z(t)$ is the moment generating function of a normal distribution.

Density of V: In order to obtain the density function we note that asymptotically the numerator and denominator of V are independent normal random variables. Therefore, the density can be obtained using the standard transformation of variables procedure.

REFERENCES

Cochran, W.G. and Rubin, D.B.(1973). Controlling bias in observational studies:a review. Sankhya A, 35; 417-446.

Dubey, S.D.(1966). On the determination of confidence intervals of an index. Biometrics, 22; 603-609.

Fleiss, J.L.(1986). The design and analysis of clinical experiments. New York: John Wiley.

Flanders, W.D., Lillian, L., Pirkle, J.L., and Caudill, S.P.(1992). Assessing the direction of casuality in cross-sectional studies. Am J Epidemiol, vol. 135, 8; 926-935.

Grubbs, W.D., Lustik, M.B., Brockman, A.S., Henderson,S.C., Burnett, F.R., Land, R.G., Osborne, D.J., Rocconi, V.K., Schrieber M.E., Williams, D.E., Wolfe, W.H., Michalek, J.E., Miner, J.C., Henricksen, G.L., and Swaby, J.A.(1995) The Air Force Health Study. An epidemiological investigation of health effects in Air Force personnel following exposure to herbicides. 1992 follow-up examination results. (NTIS accession numbers not yet available)Springfield VA:National Technical Information Service.

Johnson, N.L. and Kotz, S.(1970). Distributions in statistics. Continuous univariate distributions-2. Boston: Houghton Mifflin Company.

Kulkarni, P.M. and Shah, A.K.(1995). Testing equality of several binomial proportions to a prespecified standard. Stat Prob Ltrs, 25; 213-219.

Kulkarni, P.M. and Wang, S.(1997). Letter to the editor. Am J Epidemiol, In press.

Mee, R.W., Shah, A.K., and Lefante, J.J.(1987). Comparing k independent sample means with a known standard. J Quality Techn, 19; 75-81.

Michalek, J.E., J.E., Pirkle, J.L., Caudill, S.P., Tripathi, R.C., Needham, L.L., Patterson Jr, D.G. (1996a). Pharmacokinetics of TCDD in veterans of Operation Ranch Hand:10 year follow-up. J Toxicol Environ Health, 47; 209-220.

Michalek, J.E., Tripathi, R.C., Kulkarni, P.M., and Pirkle, J.L.(1996b). The reliability of the serum dioxin measurements in veterans of Operation Ranch Hand. J Exposure Anal Environ Epidemiol, 6; 327-338.

Wallenstein, S., Fleiss, J.L. and Chilton, N.W.(1981). Confidence intervals for percentage reduction in caries increments. J Dental Res, 61 (6); 828-830.

Wolfe, W.H., Michalek, J.E., Miner, J.C., Rahe, A., Silva, J., Thomas, W.F., Grubbs, W.D., Lustik, M.B., Karrison, T.G., Roegner, R.H., Williams, D.E.(1990). Health status of Air Force veterans occupationally exposed to herbicides in Vietnam I. Physical Health. J Am Med Assoc, 264; 1824-1831.

Zacherl, W.A. and McPhail, C.W.B.(1965). Evaluation of stannous fluoride-calcium pyrophosphate dentifrice. J Canadian Dental Assoc, 31; 174-180.

ASSESSMENT OF THE RELIABILITY OF ROUND-BASED OBSERVERS FOR THE DETECTION OF ARICRAFT

Marc L. Carter
Associate Professor
Department of Psychology

Hofstra University
128 Hofstra University
Hempstead, NY 11549

Final Report for:
Summer Research Program
Armstrong Laboratory

Sponsored by:
Air Force Office of Scientific Research
Bolling Air Force Base, Washington, DC

And

Armstrong Laboratory

August 1997

Assessment of the Reliability of Ground-Based Observers for the

Detection of Aircraft

Abstract

In situations in which ground-based lasers are propagated through the atmosphere, either for entertainment or scientific pursuits, there is the chance that aircrew may be exposed to the beam. In most cases this exposure would not be eye-hazardous, but the effects of flashblindness and veiling glare can nonetheless impair mission performance, with potentially catastrophic consequences. In most situations where such lasers are employed, ground-based observers attempt to identify aircraft that are in or near the beam path; occasionally these observers are aided by FAA radar feeds that can assist them in locating these aircraft. In this study we attempt to determine the effectiveness of observers in the detection of aircraft under a variety of conditions, including day versus night, and with and without the assistance of a radar feed. Data collected at Sandia National Labs in Albuquerque, NM, suggest several points. First, detection range is very much greater at night than in the day, probably due to the high contrast between the aircraft and night sky from aircraft lighting, and the increased visual sensitivity of the observers in scotopic viewing. Second, the assistance of a radar feed for daytime observation is important in aircraft detection, not so much to increase the range at which the aircraft is visually acquired, but to increase the likelihood that the aircraft will be detected at all. Overall, the data indicate that the use of a radar feed increases the reliability of the observers, and hence reduces the chances that aircrew will suffer laser eye exposure.

Assessment of the Reliability of Ground-Based Observers for the Detection of Aircraft

As lasers have come into widespread commercial and military application, enormous effort has been dedicated to ensuring their safe use. Much of this has aimed at assessing the biological effects of ocular exposure to laser, and at determining eye-safe levels of exposure for a variety of lasers, both battlefield and other. Laser ocular effects can vary widely, depending on the level of exposure, a function both of the type and energy of the laser, as well as the distance from the eye to the laser source (McLin & Keppler, 1997). The most serious effects are permanent eye damage, such as from lesions and consequent scotomata. But even at exposure levels below those sufficient to cause permanent damage, temporary effects can also impair performance on a variety of visual tasks. These temporary effects can range from a startle reaction or distraction from a relatively weak exposure, to glare -- scattered light veiling a scene (Pulling, Wolf, Sturgis, Vallancourt, & Dolliver, 1980; Vos, 1984) -- or flashblindness -- the loss of sensitivity which follows exposure to intense light (Brown, 1965; Thomas, 1994). Glare is only a problem during exposure to the laser, but flashblindness can last for many seconds or minutes, and although these effects are temporary, even momentary functional blindness or visual distraction can devastate, especially when the aircraft is near the ground, such as for landing or takeoff.

For some time glare and flashblindness have been of great interest to the military, increasingly as the potential for laser eye exposure has increased due to the potential use of lasers as weapons by enemies or the actual use of lasers as tools by friends. More recently, however, laser exposure to civilian aircrew has become a concern as the number of lasers employed in entertainment, advertising, and scientific applications has increased (Aviation Week & Space Tech, Sept. 26, 1994; Weiss, 1996). The potential for danger became a reality when a commercial airline pilot, upon departure from Las Vegas' McCarran International Airport, was temporarily blinded by a

casino laser, and forced to turn control of his aircraft over to the copilot (Scott, 1995). This event, having been preceded by complaints of approximately fifty similar incidents at Las Vegas from 1993 to 1995, and more than 100 other documented aircrew (both military and civilian) exposures since 1990, has prompted the FDA to temporarily prohibit laser light shows in the city of Las Vegas, and to consider a similar, nationwide moratorium (Air Line Pilot, 1996). Since that time, there have been other incidents in other locations, notably a November 1996 incident at Los Angeles International Airport (see McLin & Keppler, 1997), and an April 1997 incident off the northwest coast of Washington state (Gertz, 1997).

However, such a prohibition could be fully effective only if it also banned use of atmospherically transmitted scientific lasers, whose high-intensity, low-divergence beams remain hazardous over far greater distances than the typically low-power beams employed by commercial displays (Weiss, 1996). A representative commercial laser (say, for entertainment) can easily have a nominal ocular hazard distance (NOHD) of as little as 650 meters, whereas the laser at Apache Point Observatory in New Mexico has an NOHD of over 200 nautical miles. A summary proscription of outdoor lasers, then, would confiscate a tool of both science and commerce; there is no requirement for an outright ban if laser use can be controlled to prevent exposure of aircraft.

One popular safeguard against the dangers of outdoor lasers is the simple use of ground-based observers to monitor the airspace through which the lasers are deployed, and to control the firing of lasers when there are aircraft in or approaching the beam path. In 1996 the FDA (in concert with the FAA) promoted Laser Safety Notice No. 47, in which controls of outdoor (and indoor) lasers were proposed. In that document, the FDA recommends that a reasonable range for visual observers to reliably detect aircraft in clear air is three miles horizontal from the laser aperture, and that laser control be maintained under a trained operator. A more sophisticated and

potentially more reliable operation employs a radar feed from (typically) FAA radar located at an airport in the vicinity. Such a system, although perhaps better than simple observation, still suffers from several defects, among them the inability of FAA radar to accurately locate aircraft near the ground (where they most obviously are during takeoff and landing, perhaps the most critical portions of any flight) as well as in the "blind spot" inherent in ground-based radar systems (Weiss, 1996), and the temporal lag involved in registration of an aircraft's location on the radar display. The combination of a radar feed along with visual observation offers the best solution available: a radar operator can direct the observers to a region of airspace in which an aircraft is indicated by the radar; the visual observers then are able to very accurately determine the current location of the aircraft with respect to the beam path. Such a system is in use at Sandia Laboratories, where this study was conducted.

Under most current circumstances, however, unassisted observers are likely to be the sole safeguard against laser exposure to commercial and private aircraft, in spite of the fact that their reliability has not been assessed. Past research has generally examined the ability of observers to acquire aerial targets appearing against the relatively uniform backdrop of a daylight sky (e.g., Akerman & Kinzly, 1979; O'Neal, Armstrong, & Miller, 1988), and models of visual target acquisition have likewise, explicitly or implicitly, assumed photopic illumination (e.g., Akerman & Kinzly, 1979; Koopman, 1986). For several reasons, the results of these efforts cannot be easily generalized to many of the conditions under which outdoor lasers are deployed. Under photopic illumination, a distant aircraft at threshold contrast will likely appear as a still, dark patch, undistinguished by color or motion (Akerman & Kinzly, 1979; Koopman, 1986). On the other hand, color, motion, and temporal transients might be the most salient sources of information about the approach of a night-flying aircraft bearing an array of identification, landing, and stroboscopic

anticollision lights. This information, along with increased visual sensitivity that accompanies a decline in ambient light levels, may well allow acquisition ranges measured at night to exceed those obtained in daylight. Unfortunately, the dark-adapted eye is most susceptible to glare (Sturgis & Osgood, 1982) and nighttime performance, vulnerable to the ambient light of a city or airport, may be somewhat less reliable.

Daytime and nighttime target acquisition are likely to represent fundamentally different visual abilities, such that performance between tasks will differ substantially. The present research will therefore examine the ability of visually unaided ground-based observers to monitor airspace under photopic and scotopic conditions. Additionally, acquisition ranges will be compared between conditions in which observers work in concert with a radar operator, and those in which observers freely scan an assigned area of airspace. Results will be used to assess the efficacy of such observers as a safeguard against exposure of aircrew to atmospherically propagated lasers.

Method

Observers

Seven male and one female volunteers were recruited from among the employees of Sandia National Laboratory, and paid for their participation. The observers were screened to ensure normal color vision, and visual acuity of 20/20 or better, and ranged in age from 30 to 45 years. The observers used in this study had a variety of experience at spotting for aircraft, some having never performed the task prior to testing, and others having 30 or more hours experience.

Procedure

Data were collected at Sandia National Laboratories' LAZAP Facility, located on the Sandia Military Reservation, Albuquerque, New Mexico. The facility is the site of a high-powered, low

beam-divergence, ruby laser, used for the calibration of on-orbit DOD and DOE satellite payloads. The data were collected apart from the Facility's normal operations, and were not collected during the firing of the laser. The LAZAP Facility is located approximately 2.7 miles from the end of the runway at Albuquerque International Airport, and about 5 miles from the FAA radar tower there.

Subjects were stationed approximately 3 m above ground level, on a rooftop near the Laboratory's outdoor laser, during times at which the laser was not operational. For day observation sessions, subjects were encouraged to use appropriate sunscreen. Test sessions lasted approximately four and one-half hours, divided into one-hour shifts of data collection separated by periods of rest, with a long rest (approximately one-half hour) after two hours.

The design is chiefly a simple 2 (unaided vs. aided search) x 2 (day vs. night) factorial design. In all conditions, observers were asked to indicate when they visually acquired the target. In the free scanning (unassisted) conditions, the airspace surrounding the point of observation was divided into hemifields facing either north or south, or east or west. Throughout a single shift, observers monitored an assigned hemifield of airspace, and reported any aircraft seen within that airspace. In aided scanning conditions, observers monitored 360 degrees of airspace each shift, but were given the range, azimuth, and altitude of targets entering the monitored airspace. Daylight shifts were run largely between 10:00 AM and 4:00 PM, in order to minimize cues from glint off the aircraft or having the aircraft in line with the position of the sun; night sessions were conducted after sunset, and usually before 11 p.m.

Aircraft location information was provided by a feed from the FAA radar at the Albuquerque airport, and aircraft locations were logged by a Radar Airspace Monitoring System (RAMS) operator. The RAMS system was developed at Sandia Labs to provide laser operations with information about air traffic. It consists principally of a radar feed, the data from which are displayed

on a computer CRT, along with a representation of a low-divergence cone, which under operating conditions would be centered on the beam path. The RAMS operator is at once presented with aircraft altitude, heading, and range, along with a representation the region of space through which the beam will pass.

Data collected include the time of day at which each target appears, cloud cover and visibility at that time, the range, azimuth, and altitude of the target when the observer was notified of an aircraft in the monitored region of space, and the range, azimuth and altitude of the target when detected. If a target was undetected, its point of nearest approach to the observer was recorded. The straight-line distance from the observer (slant range) at which a target is acquired is the most immediate measure of performance, but we also consider elevation (the angle from the ground generated by the line of sight to an aircraft) and azimuth (to include variables such as mountains, the presence of the airport, and scatter from the lights of the city at night).

Results

The first cut made with respect to the data is to distinguish data collected from simple detection, versus detections aided or hampered by a variety of confounding events or conditions. For example, many detections were aided by the observers noting either glint (the sun reflecting off the skin of the aircraft), contrails from high-flying aircraft, or sound. Likewise, many detections were made more difficult (or impossible) due to the fact that a large portion of the traffic in the airspace was airport traffic, and the runway at Albuquerque International is actually at a lower altitude than the location of the observers. This means that the elevations of some aircraft that were very close to the observation location were negative, and were occluded by buildings and vegetation along that azimuth. Additionally, directly to the east of the LAZAP facility lie the Sandia Mountains, effectively making a ridge approximately 3000 feet higher than the facility, about six

miles distant. Low-flying aircraft coming from the east could not be seen until they were relatively close to the observers. On the other hand, these factors would contribute to observer performance in a real-world setting, so we also consider the data with these mitigating factors. The data are classified as hits based on the location of the aircraft at which the observer reported it, or misses, in which case the data reflect the aircraft's closest point of approach to the observer.

Daytime Observations.

The median detection range for the unassisted condition (including detections aided by contrails, glint and sound) was 8.5 miles, with a range of 0 to 60 mi; excluding contrails, glint and sound (the "clean" detections) the median was 9.6 mi (range of .3-33.5 mi). Trimmed means (2 standard deviation) were 12.72 (s = 9.24) for all detections, and 10.35 (s = 6.64) for the clean detections. Overall, of 207 aircraft recorded by the RAMS operator, 130 were detected.

For the assisted condition, overall median range was 13.43 mi with a range of 1.1-40.5 mi; meadian for the clean data was 11.87 miles, with the same range. Trimmed means were 13.9 mi (s = 6.86) and 11.7 (s = 5.1) for the raw and clean data, respectively. Of 273 aircraft recorded by the RAMS operator during these sessions, 218 were reported by the observer. Figure 1 shows the proportion of aircraft detected as a function of range, grouped into 2-mile bins (out to 24 miles--for both conditions performance of the observers at the farther ranges was apparently very good, but there were few aircraft by which to assess performance) for the cleaned data of the daytime conditions. Although irregular, the data do suggest a clear advantage for the cued (assisted) condition, at least for the longer ranges. For the closer aircraft (less than 10 miles) the unassisted observers were essentially as reliable as those getting information from the RAMS operator. Much of the irregularity in the data can be attributed to the fact that this is a field study, with no control over the arrival of aircraft into the testing area.

Figure 2 is a polar plot of median detection range (in miles) as a function of azimuth. A comparison of the data in Figures 1 and 2 clearly suggests that the advantage of the RAMS operator lies more in increasingly the likelihood that an aircraft will be seen, not that the median distance to the detected aircraft will be increased.

Nighttime Observations.

The median detection range for the unassisted condition (no distinction is made in the nighttime data for detections aided by lights, etc., since in almost every case the aircraft was detected by either the identification/anti-collision or landing lights) was 20.9 miles, with a range of 3.4 to 48 mi. The trimmed mean (2 standard deviation) was 21.94 mi (s = 10.23). Overall, of 140 aircraft recorded by the RAMS operator, 110 were detected.

For the assisted condition, median range was 19.9 mi with a range of .9-40.3 mi; the trimmed mean was 20.1 mi (s = 8.87). Of 141 aircraft recorded by the RAMS operator during these sessions, 130 were reported by the observer. Figure 3 shows the proportion of aircraft detected as a function of range, again grouped into 2-mile bins. These data suggest even more the advantage accrued by providing the observers with some information about the location of aircraft, except at the very shortest ranges.

Figure 4 is another plot of median detection range as a function of azimuth, but for the nighttime conditions. Some directions suggest that there is an advantage for the assisted conditions in that the cued medians appear significantly larger than the uncued; however, some caution in arriving at this conclusion is warranted since in fact these medians represent relatively few (less than 10) observations. The safe conclusion is that again, the advantage with a RAMS operator or other such source of information lies in an increased likelihood of detection, not an increased range.

Discussion

The chief aim of this project is to assess whether or not ground-based observers gain an advantage for detecting aircraft when they are assisted by information from another source, such as from a radar feed. Additionally, we were interested making some assessment of the general reliability of the observers to acquire aircraft entering into a monitored region of airspace. The issue is most relevant currently for policy decisions about the protocols for the use of ground based lasers, whether for scientific or entertainment purposes.

To the first question, the answer should be an equivocal "yes." Having information about the direction and altitude of an aircraft does in fact increase the probability that the aircraft will be spotted, and the observer will then be in a good position to determine whether or not the aircraft is likely to enter the beam path of the laser. Especially for medium ranges, this advantage can be considerable, and is perhaps more pronounced at night, when presumably most outdoor laser activity would be concentrated.

The caveat here, however, lies in the fact that the added information provided in the assisted conditions did not markedly or reliably increase the *range* at which the aircraft were spotted. This is rather surprising, since we did expect that in the case that an observer was provided with information about where to look, the chances that the observer would see the aircraft would have increased. In fact, it did, as long as the aircraft *was already "visible."* By that I mean that given that the contrast and spatial resolution are adequate, having information about where the aircraft is does increase the likelihood that it will be seen. But the limitations of contrast and spatial resolution in fact are apparently what determines the range at which the aircraft will be detected, not whether or not the observer knows that it is there.

It is difficult to accurately assess these factors, especially in the current study, since no direct

measurement was made with respect to different types (sizes) of aircraft, neither was session-by-session data collected on atmospheric haze (which would markedly affect contrast), or detection-by-detection position of the sun. However, the results of this study can be contrasted with the predictions of Akerman and Kinzly's (1979) VIDEM model, and the data from their accompanying field study. Although conditions in their study were much more closely controlled (they had considerable information about the azimuth and altitutude of the target aircraft), their observers were reliable (50%) at a mean slant range of only a little over 5 km (3.1 mi). One reason that their data may be so different from these lies in the fact that the aircraft were approached at relatively low altitudes (elevations), were almost surely smaller than the typical airliner found around Albuquerque International Airport, and approached the observers with a relatively low aspect angle (nearly head-on). Each of these factors would contribute to a smaller angular subtense for Akerman and Kinzly's observers to spot, and could have produced the relatively short ranges found in that study. This also suggests that the simple detectability of the aircraft (in terms of angular subtense, modified, of course, by contrast) is of greater import than information from the RAMS feed.

The approach of aircraft at night, however, presents a clearer picture. The presence of the lights on the aircraft, especially the landing lights, almost surely allowed the detection of the aircraft at suprisingly long ranges, almost regardless of angular subtense. In fact, the curvature of the earth (hence the decrease in the elevation of the aircraft at normal cruising altitudes) was probably the limiting factor in simple detections. Trees, mountains, city lights, and other obscuring factors also limit the performance of the observers, but these factors that would have to be considered in each particular instance wherein the use of observers is contemplated. The anticollision lights, often flashing, coupled with the movement of the aircraft against the sky provided sufficient information for reliable detection at ranges frequently in excess of 30 miles. Aircraft safety at night would be

considerably greater than during the day, but since almost all commercial lasers employed in entertainment are not used during the daylight hours, this would be less helpful than we would like.

One or two other points bear mention. This is a field study, and as such, many of the no doubt important factors cannot easily be controlled for. In the case of this project, the presence of the airport and its traffic patterns, city lights, the mountains to the east, and even the particular buildings at the Sandia site will no doubt contribute to some of the irregularity and idiosyncracy of these data. For these reasons we should avoid making particular conclusions. Additionally, in this study we relied on only one observer, whereas the current FAA and FDA guidelines mandate two. No doubt having two observers would increase the likelihood that aircraft, if detectible, would be detected, and the advantage conferred by the RAMS information would be lessened.

Nonetheless, there is sufficient reason to conclude that the safety of aircraft flying into or around airspace in which lasers are fired is increased by the presence of advance information for the ground-based observers, inasmuch as their safety depends on being seen by the laser operators.

References

Akerman III A, & Kinzly RE. (1979). Predicting aircraft detectability. *Human Factors*, 21, 277-291.

Brown JL. (1965). Flashblindness. *American Journal of Ophthalmology, 60*, 505-520.

Gertz, Bill. (1997, June 11). Laser investigation nearing completion. *The Washington Times*, p. A.

Hood DC, & Finkelstein MA. (1986). Sensitivity to light. In Boff, KR, Kaufman, L, & Thomas, JP (Eds.), *Handbook of Perception and human performance.* New York: Wiley.

Editors. (1996). FAA, FDA put hold on outdoor lasers, but only at Las Vegas. Air Line Pilot, 65, 40-41.

McLin, Jr., LN & Keppler, KS. (1997). Examination of laser levels associated with flight hazards. International Laser Safety Conference Proceedings, *3*, pp 447-456. Orlando, FL: Laser Institute of America.

O'Neal, MR, Armstrong, HG, & Miller, RE. (1988). Further investigation of contrast sensitivity and visual acuity in pilot detection of aircraft. Harry G. Armstrong Aerospace Medical Research Laboratory, Wright-Patterson AFB, OH: 1988; AAMRL-TR-88002.

Pulling, NH, Wolf, E, Vaillancourt, DR, & Dolliver, JJ (1980). Headlight glare resistance and driver age. *Human Factors, 22*, 103-112.

Olzak LA, Thomas JP. Seeing spatial patterns. In Boff, KR, Kaufman, L, & Thomas, JP (Eds.), *Handbook of Perception and human performance.* New York: Wiley.

Scott WB. (1995). Southwest pilot injured by laser. *Aviation Week & Space Technology*, Nov 20, 1995.

Sturgis, SP, & Osgood, DJ (1982). Effects of glare and background luminance on visual

acuity and contrast sensitivity: Implications of driver night vision testing. *Human Factors*, 24, 347-360.

Thomas SR. (1994). Review of personnel susceptibility to lasers: Simulation in SIMNET-D for CTAS-2.0. Occupational and Environmental Health Directorate, Optical Radiation Division, Brooks AFB, TX: 1994; AL/OEO-TR-1994-0060.

Vos JJ. (1984). Disability glare--a state-of-the-art report. *C.I.E Journal*, 3, 39-53.

Weiss SA. (1996). Aviation officials look warily at scientific lasers. *Photonics Spectra*, May.

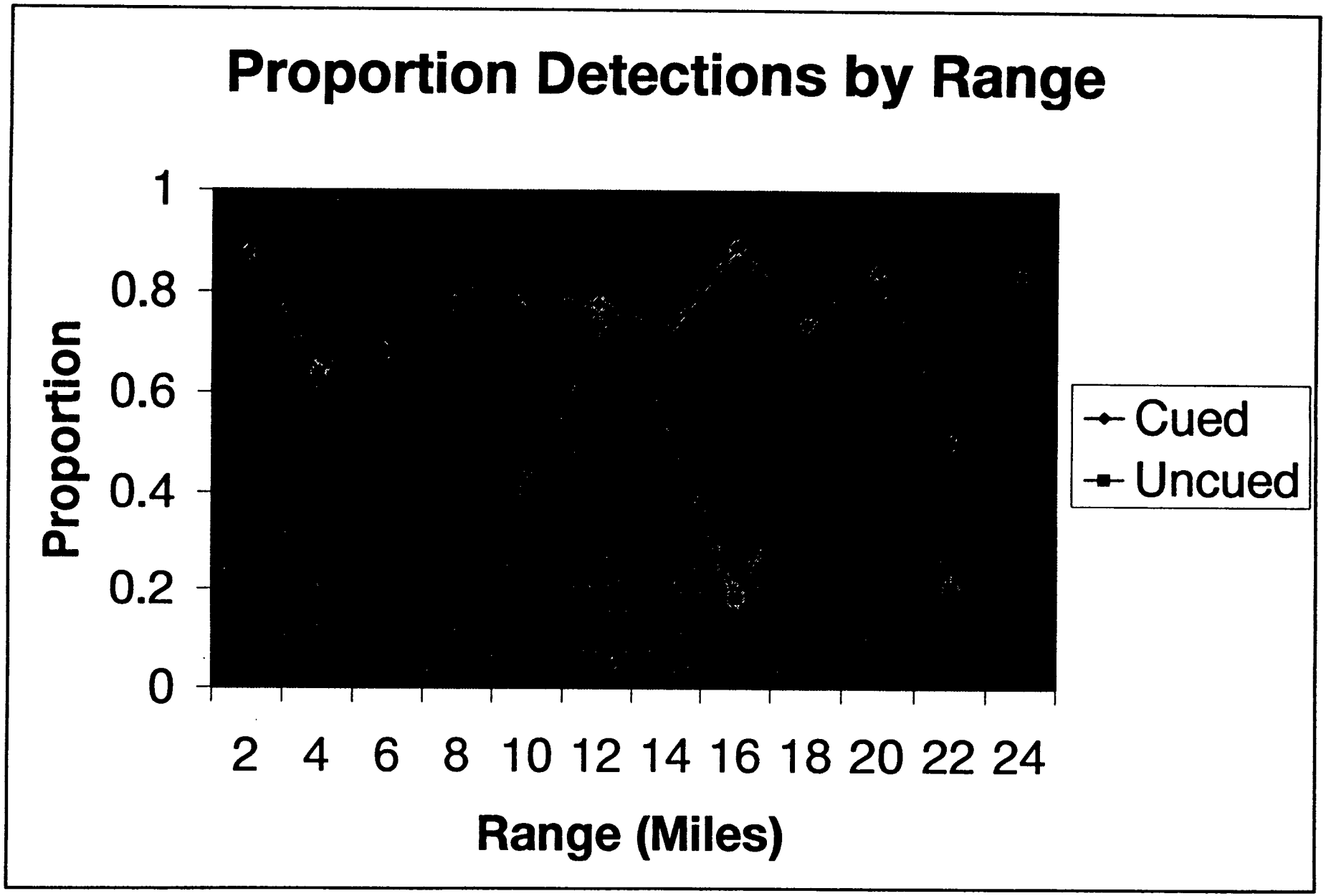
Proportion Detections by Range
Proportion
1
0.8
0.6
0.4
0.2
0
2 4 6 8 10 12 14 16 18 20 22 24
Range (Miles)
Cued
Uncued

Day: Median Range by Azimuth

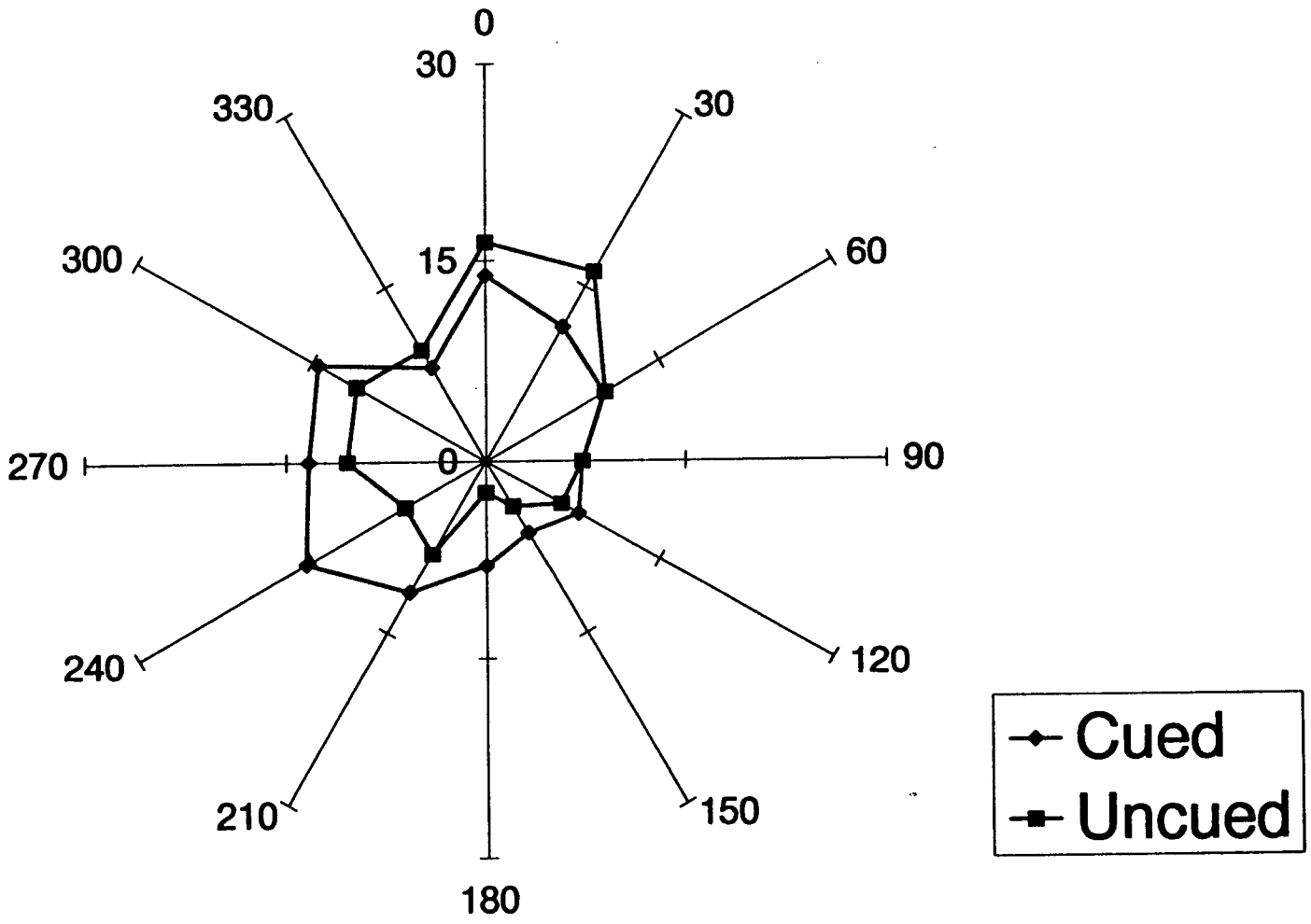

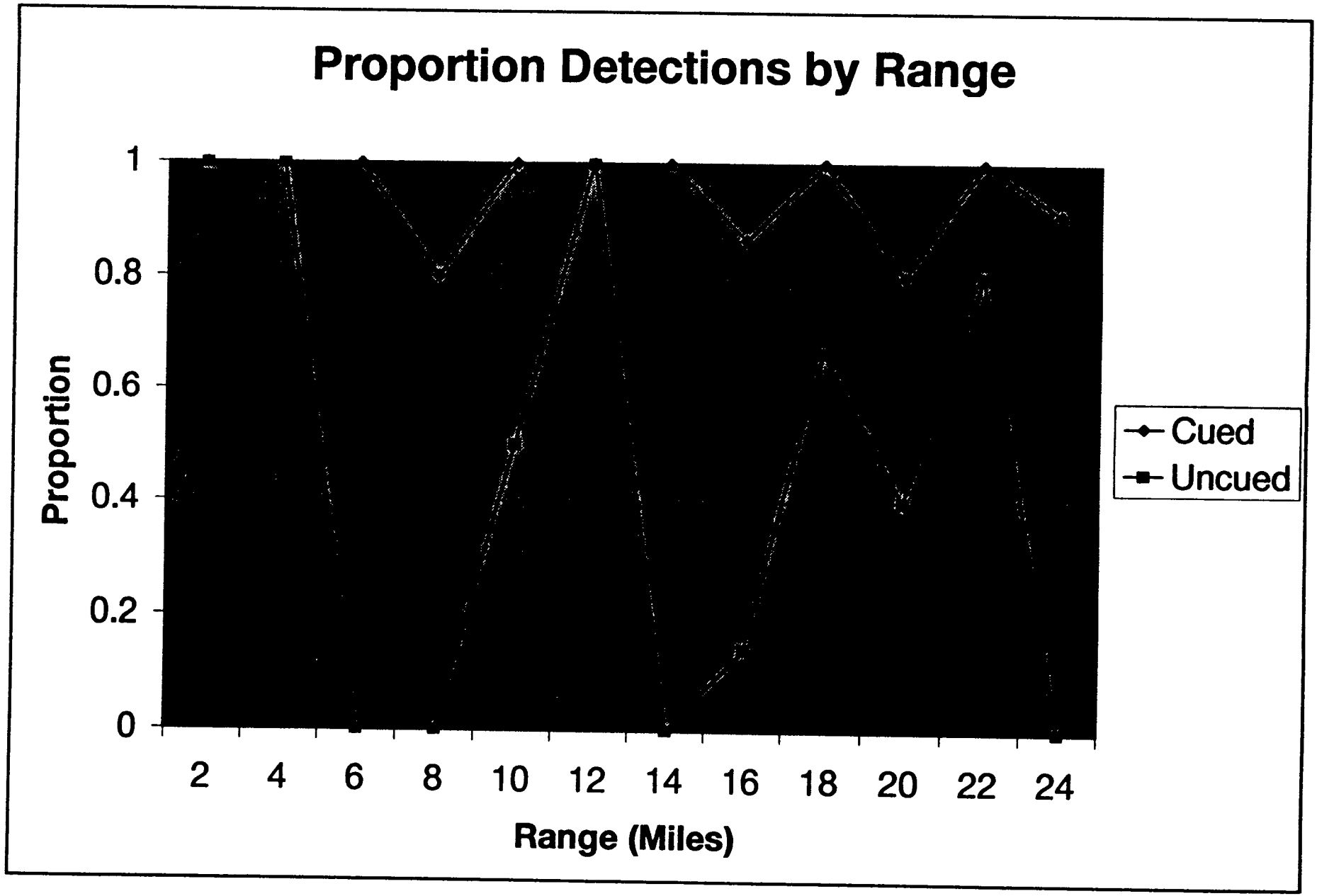
Proportion Detections by Range
Proportion
1
0.8
0.6
0.4
0.2
0
2
4
6
8
10
12
14
16
18
20
22
24
Range (Miles)
Cued
Uncued

Night: Median Range by Azimuth

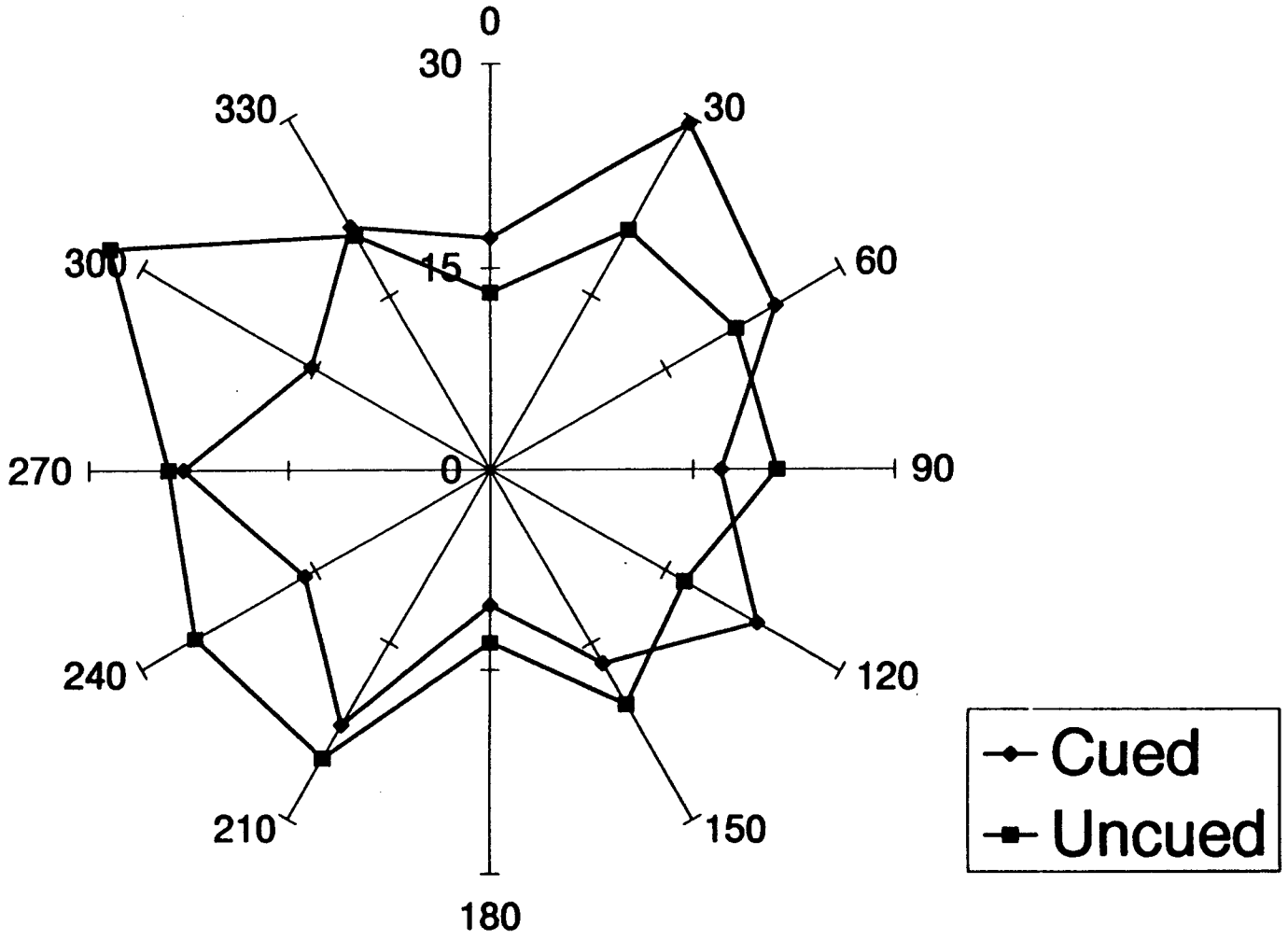

DEVELOPING A RELATIONAL DATABASE FOR NATURAL ATTENUATION FIELD DATA

Huseyin M. Cekirge
Associate Research Scholar
Geophysical Fluid Dynamics Institute

Florida State University
Keen Building
Tallahassee, FL 32306

Final Report for:
Summer Research Program
Armstrong Laboratory

Sponsored by:
Air Force Office of Scientific Research
Bolling Air Force Base, Washington, DC

And

Armstrong Laboratory

August 1997

DEVELOPING A RELATIONAL DATABASE FOR NATURAL ATTENUATION FIELD DATA

H. M. Cekirge
Associate Research Scholar
Geophysical Fluid Dynamics Institute
Florida State University
Tallahassee, FL 32306

Abstract

A relational database has been developed to aid interpretation of the results obtained from the test release of a model weathered jet fuel. In an ongoing natural attenuation study conducted at Columbus AFB, a hydrocarbon mixture was emplaced in a well characterized and highly instrumented heterogeneous aquifer. Data is collected at the site through an existing network of more than 300 multilevel sampling wells. This provides a sampling network of more than 6000 sampling points. Water samples at each sampling point can be analyzed for pH, temperature, dissolved hydrocarbons; bromide; electron acceptors including dissolved oxygen, nitrate, nitrite, sulfate, carbon dioxide, dissolved hydrogen, methane, ferrous iron; and stable carbon isotopes. Data from the field and laboratory measurements are placed into several databases. The data are then subsequently analyzed in order to gain insight into the evolution of the geochemical and biochemical processes that contribute to the natural attenuation of hydrocarbons. This research endeavor resulted in the development of a Microsoft ACCESS7 database that will access the various databases, thereby permitting efficient interpretation of the experimental results.

DEVELOPING A RELATIONAL DATABASE FOR NATURAL ATTENUATION FIELD DATA

H. M. Cekirge

Introduction

Natural attenuation is rapidly becoming the most commonly used method for remediation of groundwater contaminated with hydrocarbon fuels and solvents. In natural attenuation, subsurface physical, chemical and biological processes act to decrease groundwater contaminant concentrations down-gradient from a contaminant source. While there is extensive empirical evidence for natural attenuation, the mechanisms and rates of these processes are not well characterized.

In order to better understand the processes involved in natural attenuation, the Environics Directorate of Armstrong Laboratory is conducting a study at Columbus AFB, MS. A simulated jet fuel spill containing Decane (75.5%), Naphthalene (6.2%), p-Xylene (6.1%), Ethylbenzene (6.0%), Toluene (6.2%), Benzene (0.05%), and 2 Kg of Potassium Bromide as a conservative tracer was mixed with 30 m^3 of local aquifer material to create a 16 % residual phase mixture. In November 1995, the mixture was emplaced below the water table in the aquifer. Over 300 multi-level sampling wells, representing more than 6000 discrete sampling locations, are located downgradient from the source. Groundwater, driven by natural hydraulic gradients, percolates through the source and forms a plume containing the hydrocarbons and bromide tracer. The size and composition of the plume is monitored periodically by collection and analysis of water samples from the sampling wells. Careful analysis of the field data is allowing an understanding of the geochemical and biochemical processes that contribute to natural attenuation.

Scientists at the Environics Directorate have identified a number of chemical parameters that must be measured in order to provide information about the natural attenuation process. At most of the Columbus AFB sampling locations, more than a dozen parameters are measured. The results of the measurements are collected into a number of databases for processing. The huge volume of data, coupled with the fragmented nature of these databases, makes it difficult to integrate all the data to give a unified view of the natural attenuation processes. This research endeavor undertook the development of a

relational database that would allow Environics scientists an efficient way to access, query, and manipulate the data contained in the individual databases.

Structure of the Database

I - Source of the Database

An existing network of more than 300 multilevel sampling wells representing 6000+ sampling points is available for groundwater sampling. Additionally, new wells are being installed as needed. Groundwater and aquifer solids were sampled prior to source emplacement to measure background conditions in the aquifer. Since source emplacement, samples have been collected approximately quarter-annually. Dissolved oxygen, pH, and temperature measurements are taken in the field. Groundwater is taken to laboratories and analyzed for dissolved hydrocarbons; bromide; electron acceptors including nitrate, nitrite and sulfate; and microbial degradation reaction products including carbon dioxide, dissolved hydrogen, methane, ferrous iron; and stable carbon isotopes. Aquifer solids are analyzed for aerobic microbial population and degradation activity; anaerobic microbial activity and bulk and iron mineralogy. Results from these measurements, as well as field sampling notes, are maintained in a variety of database forms.

II - Path to the Database

The following files were prepared as Microsoft EXCEL7 files from the data contained in various database files. These files are :

1 - The WELLMAP file presents x, y and z coordinates of location of the samples, see Table 1.
2 - The TIMER file is the record file which consists of recording time of each sample, see Table 2.

Table 1. The structure of the WELLMAP file.

Index	Well	Level	X(m)	Y(m)	Z(m)
1	M001	1	4.6	-1.07	54.03
2	M001	2	4.6	-1.07	54.28
3	M001	3	4.6	-1.07	54.54
4	M001	4	4.6	-1.07	54.79
5	M001	5	4.6	-1.07	55.05
6	M001	6	4.6	-1.07	55.3
7	M001	7	4.6	-1.07	55.55

Table 2. The structure of the TIMER file.

Index	Snapshot	Well	Date	Time	FBNumber	Order	Comments
1	-2	D018	24-Aug-95		1	1	
2	-2	M011	24-Aug-95		1	1	
3	-2	M013	24-Aug-95		1	1	
4	-2	M014	24-Aug-95		1	1	
5	-2	M017	24-Aug-95		1	1	
6	-2	M018	24-Aug-95		1	1	
7	-2	M019	24-Aug-95		1	1	
8	-2	M020	24-Aug-95		1	1	
9	-2	M021	24-Aug-95		1	1	
10	-2	M024	24-Aug-95		1	1	

3 - The ORGANIC file consists of benzene, toluene, ethylbenzene, m&p xylene, o-xylene, decane, o-dichloro benzene and naphthalene data for samples, see Table 3.

4 - The ANIONS file consists of fluoride, acetate, propionate, formate, bromate, chloride, nitrite, bromide, nitrate, carbonate, sulfate, phthalate and phosphate data for samples, see Table 4.

5 - The CARBON file consists of values for DIC, del 13C (DIC), CH4 and the standard variances of these data, see Table 5.

6 - The BROMIDE file consists of low level bromide data for samples, see Table 6.

Table 3. The structure of the ORGANIC file.

Index	Snapshot	Order	Date	Time	Well	Level	Benzene (ppb)	Toluene (ppb)	Ethyl benzene (ppb)	m&p Xylene (ppb)	o-Xylene (ppb)	Decane (ppb)	o-Dichloro Benzene (ppb)	Naphthalene (ppb)	Run Number	Laboratory	Comments
1	0	1			M017	1	11	0	0	0		0		0		TAFB	
2	0	1			M017	2	11	0	0	0		0		0		TAFB	
3	0	1			M017	9	0	14	7	7		0		1		TAFB	
4	0	1			M017	10	0	14	7	7		0		1		TAFB	
5	0	1			M017	18	9	11	3	3		0		0		TAFB	
6	0	1			M017	19	9	11	3	3		0		0		TAFB	
7	0	1			M019	1	5	0	0	0		0		0		TAFB	
8	0	1			M019	8	0	0	0	25		1		0		TAFB	
9	0	1			M019	9	0	0	0	25		1		0		TAFB	

Table 4. The structure of the ANIONS file.

Index	Snapshot	Order	Date	Time	Well	Level	Fluoride (ppm)	Acetate (ppm)	Propionate (ppm)	Formate (ppm)	Bromate (ppm)	Chloride (ppm)	Nitrite (ppm)	Bromide (ppm) >1 ppm	Nitrate (ppm)	Carbonate (ppm)	Sulfate (ppm)	Phthalate (ppm)	Phosphate (ppm)	Comments
1	0	1	12/08/95		M017	1						7.89	0.00	0.00	7.02		0.66			
2	0	1	12/08/95		M017	2						7.89	0.00	0.00	7.02		0.66			
3	0	1	12/08/95		M017	9						7.07	0.00	0.00	5.68		0.95			
4	0	1	12/08/95		M017	10						7.07	0.00	0.00	5.68		0.95			
5	0	1	12/08/95		M017	18						6.68	0.00	0.00	4.27		1.23			
6	0	1	12/08/95		M017	19						6.68	0.00	0.00	4.27		1.23			

Table 5. The structure of the CARBON file

Index	Snapshot	Order	Date	Time	Well	Level	DIC (mMol/l)	sig DIC (mMol/l)	del 13C (DIC) per MIL	sig del 13C (DIC) per mil	CH4 (µM)	sig CH4 (µM)	d13C (CH4)	sig d13C (CH4)	Comments
1	-2	1	Aug-95		M011	1	1.184	0.005	-19.26	0.078					
2	-2	1	Aug-95		M011	2	1.184	0.005	-19.26	0.078					
3	-2	1	Aug-95		M011	8	1.25	0.021	-19.067	0.069					
4	-2	1	Aug-95		M011	9	1.25	0.021	-19.067	0.069					
5	-2	1	Aug-95		M011	14	1.203	0.027	-19.522	0.3					
6	-2	1	Aug-95		M011	16	1.203	0.027	-19.522	0.3					

Table 6. The structure of the BROMIDE file

Index	Snapshot	Order	Date	Time	Well	Level	Z (m)	Bromide (ppm) < 1 ppm	Laboratory	Comments
1	0	1	12/8/95		M017	1		0.56	TAFB	
2	0	1	12/8/95		M017	2		0.56	TAFB	
3	0	1	12/8/95		M017	9		0.13	TAFB	
4	0	1	12/8/95		M017	10		0.13	TAFB	
5	0	1	12/8/95		M017	18		0.28	TAFB	
6	0	1	12/8/95		M017	19		0.28	TAFB	
7	0	1	12/8/95		M019	1		0.05	TAFB	
8	0	1	12/8/95		M019	17		0.46	TAFB	
9	0	1	12/8/95		M019	18		0.46	TAFB	
10	0	1	12/8/95		M024	1		0.32	TAFB	

7 - The FIELD file consists of pH, temperature and dissolved oxygen data for samples, see Table 7.

8 - The IRON file consists of ferrous iron (Fe^{2+}) data for samples, see Table 8.

Table 7. The structure of the FIELD file.

Index	Snapshot	Order	Date	Time	Well	Level	pH	Temperature (C)	DO (mg/l)	Comments
1	-2	1			M011	1	5.120	26.400	2.200	
2	-2	1			M011	2	5.120	26.400	2.200	
3	-2	1			M011	8	5.280	26.300	2.300	
4	-2	1			M011	9	5.280	26.300	2.300	
5	-2	1			M011	14	5.420	25.500	0.800	
6	-2	1			M011	16	5.420	25.500	0.800	
7	-2	1			M013	1	5.080	26.100	1.700	
8	-2	1			M013	2	5.080	26.100	1.700	
9	-2	1			M013	8	5.170	26.000	2.800	

Table 8. The structure of the IRON file.

Index	Snapshot	Order	Date	Time	Well	Level	Fe2 (mg/l)	Comments
1	-2	1			M011	1	0.018	
2	-2	1			M011	2	0.018	
3	-2	1			M011	8	0.015	
4	-2	1			M011	9	0.015	
5	-2	1			M011	14	0.373	
6	-2	1			M011	16	0.373	
7	-2	1			M013	1	0.018	
8	-2	1			M013	2	0.018	
9	-2	1			M013	8	0.009	

9 - The HYDROGEN file consists of hydrogen data for samples, see Table 9.

Table 9. The structure of the HYDROGEN file.

Index	Snapshot	Date	Time	Well	Level	Hydrogen (nM/l)	Comments
1	1	1/17/96		M038	2	nd	
2	1	1/17/96		M038	9	nd	
3	1	1/17/96		M038	15	nd	
4	1	1/17/96		M038	19	nd	
5	1	1/17/96		M040	1	nd	
6	1	1/17/96		M040	8	0.01	
7	1	1/17/96		M043	1	3.2	
8	1	1/17/96		M043	13	nd	

Tables 1-9 present the recommended file format for the relational database. This file format is completely compatible with other databases or spreadsheets.

The data files were imported into the Microsoft ACCESS7 database system. An example of an ACCESS7 listing of the data tables developed for this project is shown in Figure 1. At this point, all data tables could be accessed using relational database functions. Numerous queries were executed on the data tables to ensure that every data entry in the tables had a WELLMAP location and TIMER date/time associated with it. A listing of the queries developed to provide quality control for the data tables is shown in Figure 2. Examples of the use of these queries is given in Figures 3 & 4. A query to compare entries in the ANIONS data table to the TIMER table is shown in Figure 3. In Figure 4, the ANIONS data table is checked against the WELLMAP table. Results from the queries prove whether or not each entry in the ANIONS table has a location and sampling time entry contained in WELLMAP and TIMER. Corrective actions to resolve all data inconsistencies were performed before proceeding. This phase of the project, data validation, proved to be the most time consuming portion of the project.

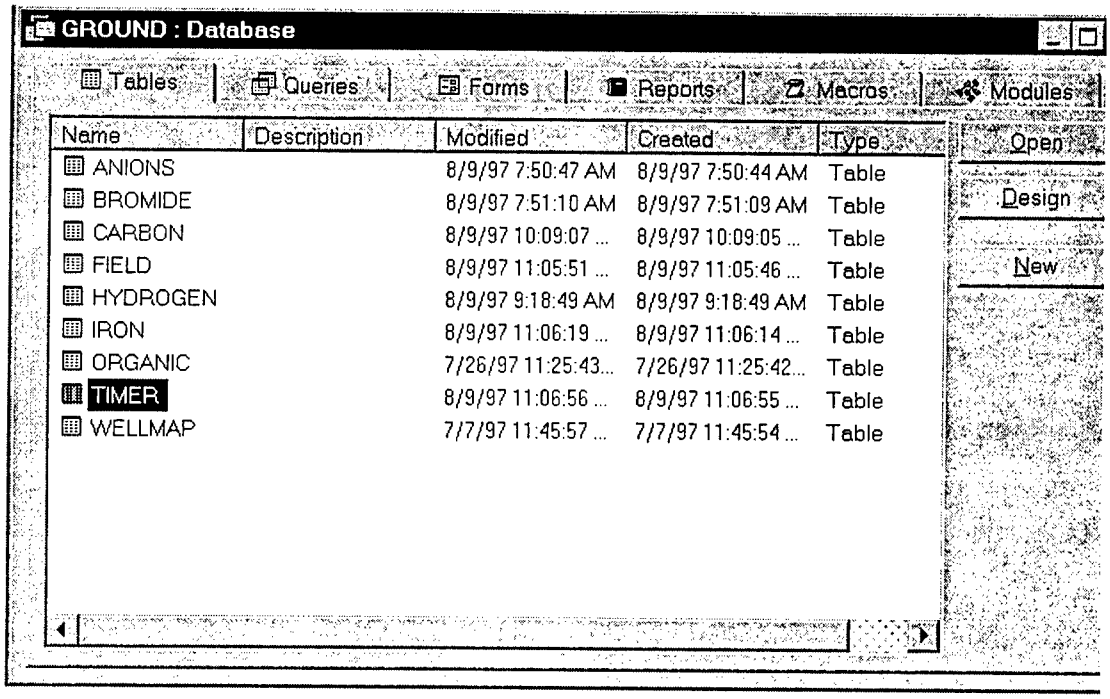

Figure 1. A MICROSOFT ACCESS7 database listing of data tables developed for this project.

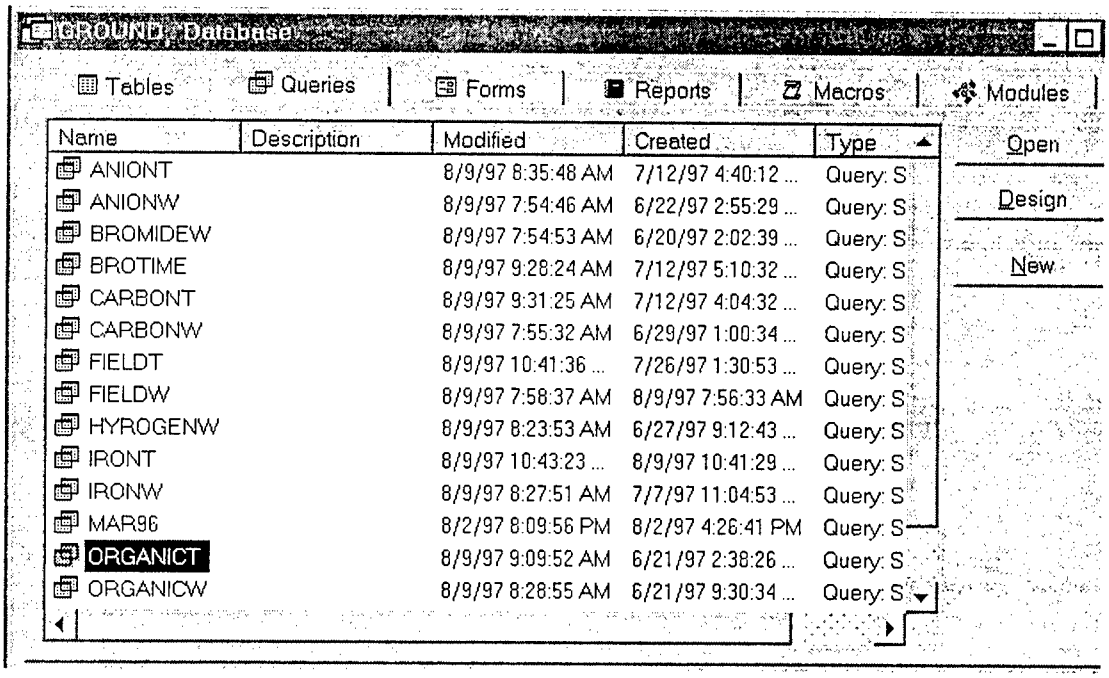

Figure 2. The list of queries developed to provide consistency and quality control of data entries in the MICROSOFT ACCESS7 database.

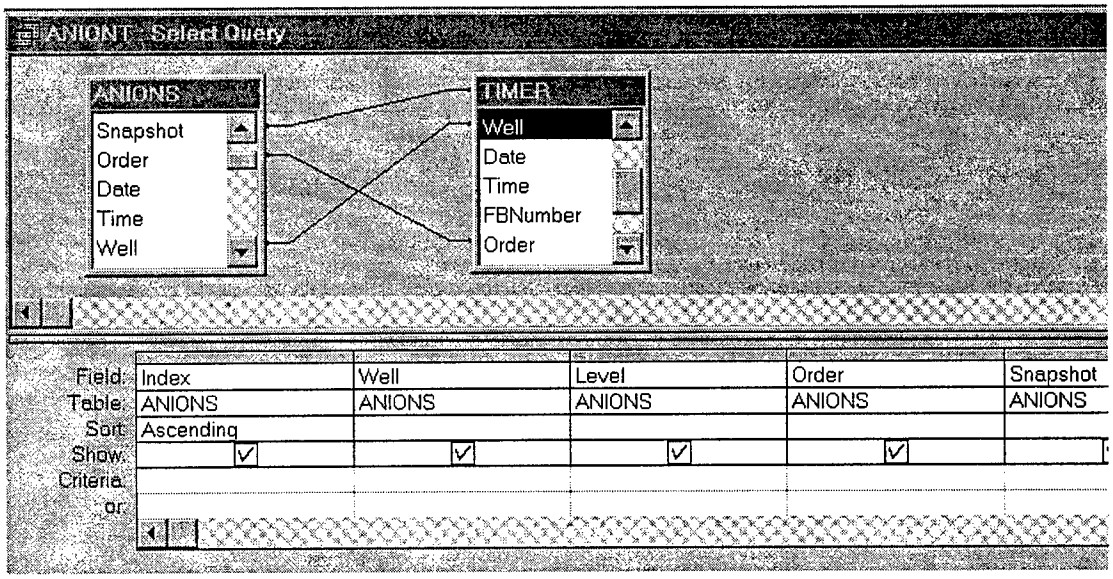

Figure 3. The design of the query for checking time records of the data in the ANIONS file.

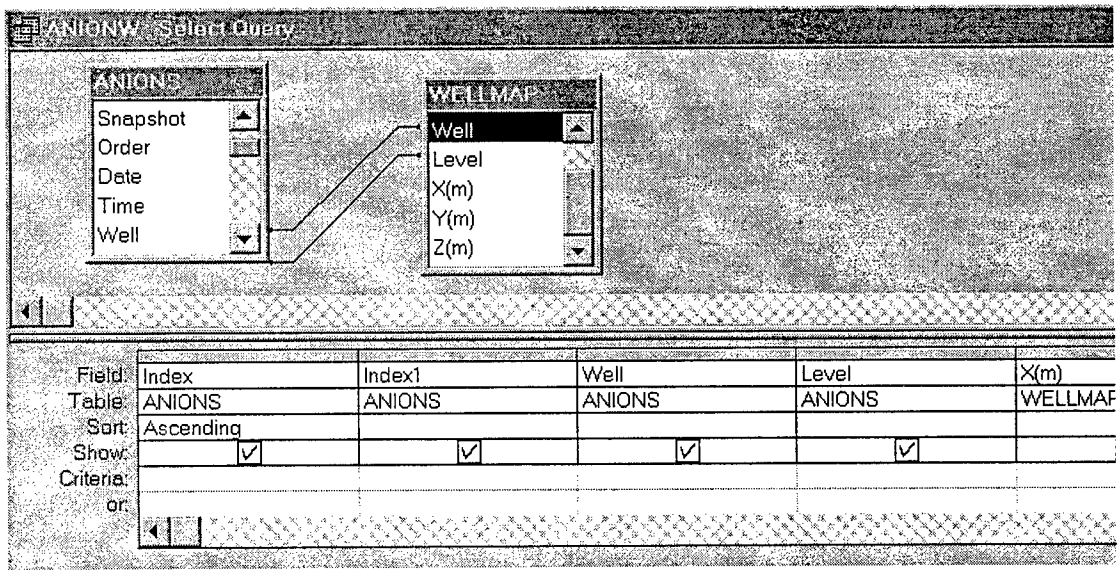

Figure 4. The design of the query for checking the location record of the data in the ANIONS file.

III - Target of the Database

Once the data tables contained in the Microsoft ACCESS7 relational database had been thoroughly checked for completeness, the data were ready for query development. Queries are database functions enabling one to organize and filter data. A query functions as a sieve into which the data is placed. Any data not meeting the selection criteria pass through the sieve. The relational database takes the retained data, processes it into tables or reports, and readies the data for export to other graphical, statistical or numerical software packages. A query can be used as a powerful data processing tool to help one visualize plume behavior.

Figure 5 shows the construction of a query that accesses the IRON and the FIELD data tables. The query selects all samples for which both IRON and FIELD data exist and then attaches the appropriate sampling time and location to each entry in the output table. The results of this query are presented in Table 10. The results shown here are in Microsoft EXCEL7 format; however they could be exported in any format to accommodate the needs of other users.

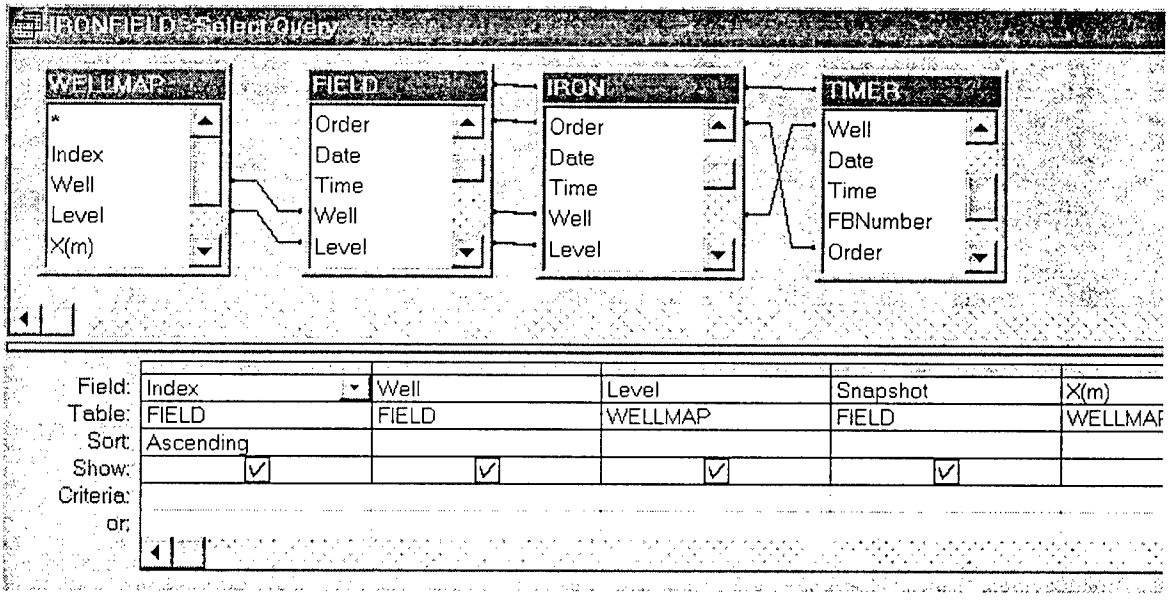

Figure 5. The design of the query which merges the WELLMAP, FIELD, IRON and TIMER files.

Table 10. Output table as the result of merging the WELLMAP, FIELD, IRON and TIMER files in the database.

Index	Well	Level	Snapshot	X(m)	Y(m)	Z(m)	Date	Fe2 (mg/l)	pH	Temperature (C)	DO (mg/l)
1	M011	1	-2	0.11	5.8	55.67	8/24/95	0.018	5.120	26.400	2.200
2	M011	2	-2	0.11	5.8	55.92	8/24/95	0.018	5.120	26.400	2.200
3	M011	8	-2	0.11	5.8	57.45	8/24/95	0.015	5.280	26.300	2.300
4	M011	9	-2	0.11	5.8	57.7	8/24/95	0.015	5.280	26.300	2.300
5	M011	14	-2	0.11	5.8	58.97	8/24/95	0.373	5.420	25.500	0.800
6	M011	16	-2	0.11	5.8	59.48	8/24/95	0.373	5.420	25.500	0.800
7	M013	1	-2	5.76	3.82	55.83	8/24/95	0.018	5.080	26.100	1.700
8	M013	2	-2	5.76	3.82	56.08	8/24/95	0.018	5.080	26.100	1.700
9	M013	8	-2	5.76	3.82	57.61	8/24/95	0.009	5.170	26.000	2.800
10	M013	9	-2	5.76	3.82	57.86	8/24/95	0.009	5.170	26.000	2.800
11	M013	14	-2	5.76	3.82	59.13	8/24/95	0.006	5.160	26.400	2.700
12	M014	1	-2	9.55	2.49	54.48	8/24/95	0.026	5.220	27.500	2.800

Conclusions

This project resulted in the development of a working relational database that uses Microsoft ACCESS7 software. The database provides an important tool for processing laboratory and field data generated by the Natural Attenuation Study conducted at Columbus AFB. Queries generated during this project have already helped aid visualization of the natural attenuation processes, and allow Environics scientists to more effectively plan future sampling missions. The increased accessibility of the data, coupled with the data query capabilities of ACCESS7, make this an invaluable tool for efficiently processing data from the natural attenuation study.

INVESTIGATION OF TWO STATISTICAL ISSUES IN BUILDING A CLASSIFICATION SYSTEM

Cheng Cheng
Assistant Professor
Department of Mathematical Sciences

The Johns Hopkins University
Baltimore, Maryland, 21218

Final Report for:
Summer Faculty Research Program
Armstrong Laboratory

Sponsored by:
Air Force Office of Scientific Research
Bolling Air Force Base, DC

and

Armstrong Laboratory

August 1997

INVESTIGATION OF TWO STATISTICAL ISSUES IN BUILDING A CLASSIFICATION SYSTEM

Cheng Cheng
Assistant Professor
Department of Mathematical Sciences
Johns Hopkins University

Abstract

This research investigates two statistical issues of relevance to current approaches in building a personnel classification system within the Air Force. The first issue is the effect of the non-random selection of the accessions sample on the least square estimates of the regression models used in predicting job performance. The second issue is the effect of the reliability (unreliability) of the predictors (ASVAB subtest scores) on the regression weights estimates. Several carefully designed simulation experiments were performed. The results show: (1) estimation based on the nonrandomly selected samples does not produce systematically biased regression weights estimates (although the estimates have inflated standard deviations primarily due to reduced sample size); (2) estimation based on not perfectly reliable predictors produces biased estimates of the regression weights. Certain "remedy" procedures were proposed and were evaluated by simulation studies as well.

INVESTIGATION OF TWO STATISTICAL ISSUES IN BUILDING A CLASSIFICATION SYSTEM

Cheng Cheng

1. Introduction

Current approaches to building a classification system require the construction of regression models to predict the applicants' performance (represented by predicted technical school grades) on the basis of accessions data. Ree (1997, personal and group discussions) raised two issues about the reliability of the least square estimation of regression weights (coefficients).

1. Non-random sampling. In building the regression model for a job (family), values of the criterion variable are available only for the accessions assigned to the job (family). Thus, the available data represent only the portion of the population who are (presumably) above the selection standard of that particular job. This truncation by the selection standard implies that the regression weights are estimated based on a biased sample. Thus *intuitively*, the regression model so estimated represents the relationship between the criterion and the predictors (ASVAB subtest scores) only for those who are selected into that job, and hence is biased in representing the relationship between the criterion and the predictors for all the applicants.

This problem can be stated formally as a non-response problem in multiple linear regression. Let $[X_{11},...,X_{1p},Y_1]$, ..., $[X_{n1},...,X_{np},Y_{n1}]$, ..., $[X_{N1},...,X_{Np},Y_{N1}]$ be the data and let

$$Y_i = b_0 + b_1 X_{i1} + ... b_p X_{ip} + \varepsilon_i, \quad i = 1,2,...,n,...,N$$

be the regression model. However, the Y-values are available for only the first n sample points selected by a truncation in the predictors given by

$$a_1 X_{i1} + ... + a_p X_{ip} \geq s, \quad i = 1,2,...,n$$

(such as a composite) where $a_1,...,a_p$ and s are known numbers; and $Y_{n+1},...,Y_N$ are not observed (nonresponse). It is suspected that the least square estimation based on the first n sample points only produces coefficient estimates containing systematic deviations (bias) from the corresponding true values.

2. Unreliable predictors. The predictors used in the models are often considered as surrogates of some latent construct: the ASVAB test scores are surrogates of "true intelligence, abilities, knowledge," etc. The interest is of course in the relationship between the criterion and the latent variables which, quite often, are not observed or too difficult to observe.

Formally, if, for example, X_{i1} is the surrogate of "math knowledge" of the ith individual in the sense that X_{i1} is "math knowledge" measured with error:

$$X_{i1} = [\text{"math knowledge"}]_i + \text{error}_i,$$

where the error is independent of $[\text{"math knowledge"}]_i$. Then the *reliability* of X_{i1} is defined as the variance of the $[\text{"math knowledge"}]_i$ divided by the variance of X_{i1}. It can be shown theoretically (see e.g. Fuller, 1987) that when the reliability is not 100% (which is equivalent to the error_i not being constantly zero), the least square estimate of the regression weights based on those observed predictors is biased toward zero for the regression coefficients on the latent variables, i.e. the real underlying relationship; see also the simulation study in Section 4.

With these two problems in mind, one can think of four possible situations in the actual process of building a regression model.

(a) Perfect reliability and no truncation on predictors => unbiased regression modeling

(b) Perfect reliability and truncation on predictors => suspected biased weight estimates

(c) Imperfect reliability and no truncation on predictors => biased weight estimates

(d) Imperfect reliability and truncation on predictors => biased weight estimates

In each regression modeling task, one can think about which case may be pertinent.

Investigations of these issues by simulation studies, together with some remedies, are given in the subsequent sections.

2. Simulation Study of the Non-random Sampling Issue.

A simulation study was designed to investigate the issue of whether or not the least square estimates of regression weights have systematic bias from the corresponding population values when the estimation is based only on the selected (biased) subsample.

The following 10-predictor model was used in this study.

(1) $$Y_i = 40 + X_{i1} + 2X_{i2} + X_{i3} + X_{i4} + \varepsilon_i, \quad i = 1,2,\ldots,N,$$

where the coefficients on $X_5, \ldots, X_{10}$ are all zero, giving the population (true) values of the regression weights as 40 (intercept), 1, 2, 1, 1, 0, 0, 0, 0, 0, 0 respectively. The total sample size N was set to 1,000. The ε_i's are independent normal variates with mean 0 and standard deviation 9.75. The predictors were generated according to the model

(2) $$X_{ik} = G_i + \theta_{ik}, \quad k = 1,\ldots,10, \; i = 1,2,\ldots,N,$$

where G_i's are independent normal variates with mean 50 and standard deviation 2.22; θ_{ik}'s are independent normal variates with mean 0 and standard deviation 9.75, and are independent of G_i's and ε_i's. (Hence each X_{ik} has mean 50 and standard deviation 10.)

The subsample selection is determined by $X_{i1} + 2X_{i2} + X_{i3} + X_{i8} \geq 300$. This represents a rather stringent selection because 300 corresponds to roughly the 96.25% percentile of $X_{i1} + 2X_{i2} + X_{i3} + X_{i8}$; hence only the top 3.75% is selected into the subsample.

Notational remark. Hereafter, symbols with a tilde (~) denote statistics/estimates based on the selected subsample; symbols with a hat (^) denote the statistics based on the full sample; symbols with a bar on top denote quantities averaged over simulation runs.

One thousand simulation runs are performed. Throughout the sequel, the subscript s denotes the sth simulation. Each simulation run (s = 1,2,...,1000) consisted of the following steps:

(i) Generate G_i's;

(ii) Generate X_{ik}'s according to equation (2), giving the 1000×10 predictor matrix X_s. Generate the Y_i's according to model (1), giving the 1000×1 criterion variable vector $\vec{Y}_s$.

(iii) Fit by least square the regression model (1) based on the full data set $(X_s, \vec{Y}_s)$, obtaining the regression weights estimates vector (0 subscript stands for the intercept) $\hat{b}_s = (\hat{b}_{s,0}, \hat{b}_{s,1}, \hat{b}_{s,2}, \ldots, \hat{b}_{s,10})$. Compute the residual standard deviation $\hat{\sigma}_s$; compute the "observed" standard deviation of each $\hat{b}_{s,k}$ (k=0,1,2,...,10) according to the usual formula $\hat{SD}_{s,k} = \hat{\sigma}_s \sqrt{C_{kk}}$, where C_{kk} is the kth diagonal element of $(X_s' X_s)^{-1}$. Compute the multiple correlation coefficient (validity) $\hat{R}_s^2$.

(iv) Select the subsample according to the selection criterion and the corresponding Y values, forming the subsample $(\tilde{X}_s, \tilde{Y}_s)$.

(v) Fit by least square the regression model (1) based on the subsample $(\tilde{X}_s, \tilde{Y}_s)$, obtaining the regression weights estimates vector $\tilde{b}_s = (\tilde{b}_{s,0}, \tilde{b}_{s,1}, \tilde{b}_{s,2}, \ldots, \tilde{b}_{s,10})$. Compute the residual standard deviation $\tilde{\sigma}_s$; compute the "observed" standard deviation of each $\tilde{b}_{s,k}$ according to the usual formula $\tilde{SD}_{s,k} = \tilde{\sigma}_s \sqrt{\tilde{C}_{kk}}$, where $\tilde{C}_{kk}$ is the kth diagonal element of $(\tilde{X}_s' \tilde{X}_s)^{-1}$. Compute the multiple correlation coefficient (validity) $\tilde{R}_s^2$.

After 1000 simulations, the following statistics are computed for the estimates based on full and selected subsample respectively.

1. Mean of the regression weights estimates:

$$\bar{\hat{b}}_k = \frac{1}{1000} \sum_{s=1}^{1000} \hat{b}_{s,k} \quad k = 0,1,\ldots,10 \quad (\textit{full sample})$$

$$\bar{\tilde{b}}_k = \frac{1}{1000} \sum_{s=1}^{1000} \tilde{b}_{s,k} \quad k = 0,1,\ldots,10 \quad (\textit{subsample})$$

2. Mean "observed" standard deviation of the weights estimates:

$$\bar{\hat{S}}D_k = \frac{1}{1000}\sum_{s=1}^{1000}\hat{S}D_{s,k} \quad k = 0,1,\ldots,10 \quad (\textit{full sample})$$

$$\bar{\tilde{S}}D_k = \frac{1}{1000}\sum_{s=1}^{1000}\tilde{S}D_{s,k} \quad k = 0,1,\ldots,10 \quad (\textit{subsample})$$

3. "Actual" standard deviation of the weights estimates across 1000 simulations:

$$\hat{S}D_k = \sqrt{\frac{1}{999}\sum_{s=1}^{1000}(\hat{b}_{s,k} - \bar{\hat{b}}_k)^2}, \quad k = 0,1,\ldots,10 \quad (\textit{full sample})$$

$$\tilde{S}D_k = \sqrt{\frac{1}{999}\sum_{s=1}^{1000}(\tilde{b}_{s,k} - \bar{\tilde{b}}_k)^2}, \quad k = 0,1,\ldots,10 \quad (\textit{subsample})$$

4. P-values of the t statistics describing the deviation of the estimates based on the subsample from the population values, $(\tilde{S}D_k)^{-1}\left|\bar{\tilde{b}}_k - b_{0,k}\right|$, where $b_{0,k}$ is the corresponding population value. These P-values will show statistical significance if there is systematic bias in the estimates based on the subsample.

5. Mean R^2 values: $\bar{\hat{R}}^2 = \frac{1}{1000}\sum_{s=1}^{1000}\hat{R}_s^2$ (full sample); $\bar{\tilde{R}}^2 = \frac{1}{1000}\sum_{s=1}^{1000}\tilde{R}_s^2$ (subsample).

The results are tabulated in Table 2.1. In the table $b_{0,k}$ is the population value of the regression weights, and $p.T$ is the P-values described above.

Table 2.1

		Estimation based on full data set			Estimation based on subsample			
k	$b_{0,k}$	$\bar{\hat{b}}_k$	$\bar{\hat{S}}D_k$	$\hat{S}D_k$	$\bar{\tilde{b}}_k$	$\bar{\tilde{S}}D_k$	$\tilde{S}D_k$	$p.T$
0	40	40.119	4.091	4.007	40.116	64.065	66.998	.99
1	1	1.000	0.031	0.032	0.989	0.267	0.276	.97
2	2	2.001	0.031	0.031	2.002	0.417	0.435	.99
3	1	1.000	0.031	0.032	0.999	0.268	0.278	.99
4	1	1.001	0.031	0.031	1.012	0.196	0.205	.95
5	0	-0.002	0.031	0.032	0.004	0.195	0.202	.98
6	0	0.001	0.031	0.031	0.004	0.195	0.206	.98
7	0	0.000	0.031	0.032	-0.007	0.195	0.200	.97
8	0	-0.001	0.031	0.031	0.002	0.195	0.288	.99
9	0	-0.001	0.031	0.032	-0.011	0.195	0.199	.95
10	0	-0.002	0.031	0.032	0.003	0.194	0.204	.99

$\bar{\hat{R}}^2 = 0.893$ $\qquad$ $\bar{\tilde{R}}^2 = 0.799$

A different truncation scenario, $106 \le X_1 + X_2 < 110$, is also simulated. On average about 9.4% of the sample points satisfy this selection criterion. The results are given in Table 2.2.

Table 2.2

		Estimation based on full data set			Estimation based on subsample			
k	$b_{0,k}$	$\bar{\hat{b}}_k$	$\bar{\hat{S}}D_k$	$\hat{S}D_k$	$\bar{\tilde{b}}_k$	$\bar{\tilde{S}}D_k$	$\tilde{S}D_k$	$p.T$
0	40	40.054	4.089	4.198	38.230	100.41	100.25	.99
1	1	1.001	0.031	0.031	1.106	0.926	0.930	.99
2	2	2.001	0.031	0.032	2.002	0.108	0.111	.99
3	1	1.000	0.031	0.031	1.005	0.108	0.109	.96
4	1	0.998	0.031	0.031	1.000	0.108	0.106	.99
5	0	0.000	0.031	0.031	0.000	0.108	0.111	.99
6	0	0.000	0.031	0.031	0.013	0.927	0.929	.99
7	0	0.000	0.031	0.032	0.002	0.108	0.107	.99
8	0	-0.001	0.031	0.033	0.001	0.108	0.107	.99
9	0	-0.001	0.031	0.032	-0.006	0.108	0.109	.96
10	0	0.001	0.031	0.031	0.001	0.108	0.110	.99
		$\bar{\hat{R}}^2 = 0.894$			$\bar{\tilde{R}}^2 = 0.890$			

Summary. (a) The P-values clearly show NO significant statistical evidence (based on 1000 simulation runs) that the regression weights estimates based on the selected subsample are systematically biased for the population values. (b) The standard deviations of the estimates based on the selected subsample are profoundly larger than those of the estimates based on the full sample. This is primarily caused by the greatly reduced sample size for the subsample due to stringent selection. The increase in the standard deviation of the estimates could be a concern in practice when the size of the selected subsample is small. (c) There tends to be a slight reduction in the R^2 value for the fitted regression models based on the selected subsample.

3. An Estimation Procedure Based on Data Imputation.

A natural question at this point is whether there is some method to remedy the inflation of the standard deviation of the regression weights estimates and the reduction in the validity value R^2, when only a selected subsample has observed Y (criterion) values. A procedure based on data imputation for this purpose is described in this section.

The proposed estimation procedure is described through an illustrative example. Suppose a sample of size 20 is given as follows.

X_1	X_2	Y
50	62	86
56	53	83
66	47	95
40	65	78
58	52	87
51	54	77
60	63	91
53	51	
33	58	
47	54	
50	44	
56	46	
53	42	
52	36	
55	46	
27	43	
49	45	
41	52	
44	44	
65	36	

The Y values are available only for the first 7 cases for which $X_1 + 2X_2 > 155$.

The estimation procedure goes as follows.

(i) Estimate the regression weights and compute desired statistics based on the subsample where Y values are available:

Coefficients estimates and significance:

variable	estimate	sd	T	p.T
intercept	11.718	26.641	0.44	0.34
X1	0.902	0.232	3.88	0.01
X2	0.433	0.288	1.51	0.10

Multiple R-square = 0.816
residual standard deviation = 3.446

(ii) Impute the unobserved Y values based on the model fitted in step (i) by

$$\tilde{Y}_i = 11.718 + 0.902X_{i1} + 0.433X_{i2} + E_i, \qquad i = 7,8,\ldots,20,$$

where E_i's are independent normal random variates with mean 0 and standard deviation 3.446 which is the residual standard deviation from (i). These E_i's can be generated by the RANOR function in SAS. The sample with imputed Y values now looks like

X_1	X_2	Y or $\tilde{Y}$
50	62	86
56	53	83
66	47	95
40	65	78
58	52	87
51	54	77
60	63	91
53	51	82.964
33	58	67.375
47	54	78.531
50	44	78.785
56	46	89.137
53	42	77.166
52	36	79.185
55	46	79.096
27	43	59.204
49	45	81.294
41	52	74.114
44	44	68.909
65	36	82.700

(iii) From now on, base the entire analysis on the above full sample (in which some of the Y values are imputed). Repetition of the computations in step (i) gives

Coefficients estimates and significance:

variable	estimate	sd	T	p.T
intercept	22.309	6.305	3.54	0.00
X1	0.802	0.074	10.79	0.00
X2	0.345	0.088	3.93	0.00

Multiple R-square = 0.876
residual standard deviation = 3.099

Noticeably, the standard deviations of the regression weights estimates have been reduced, and the multiple R-square is increased slightly.

This estimation procedure was evaluated by a simulation study with the setup exactly the same as that given in Section 2. The subsample selection criterion is $X_{i1} + 2X_{i2} + X_{i3} + X_{i8} \geq 300$. In each simulation run, the regression weights were estimated based on the imputed sample according to the above procedure. The statistics listed in Section 2 were calculated at the end of 1000 simulation runs. The results are given in Table 3.1.

In the table $\bar{\hat{S}}D_k$ is the mean "observed" standard deviation of the estimates (cf. Item 2. in Section 2); $\hat{S}D_k$ is the "actual" standard deviation of the estimates (cf. Item 3. Section 2).

Table 3.1

Estimation based on full sample with imputation

k	$b_{0,k}$	$\bar{\hat{b}}_k$	$\bar{\hat{S}}D_k$	$\hat{S}D_k$
0	40	40.119	4.021	67.179
1	1	1.000	0.031	0.277
2	2	2.001	0.031	0.435
3	1	1.000	0.031	0.281
4	1	1.001	0.031	0.207
5	0	-0.002	0.031	0.203
6	0	0.001	0.031	0.208
7	0	0.000	0.031	0.202
8	0	-0.001	0.031	0.290
9	0	-0.001	0.031	0.203
10	0	-0.002	0.031	0.207

$$\bar{\hat{R}}^2 = 0.893$$

Comparing $\hat{S}D_k$ with $\tilde{S}D_k$ in Table 2.1, there is hardly any change in the "actual" standard deviation across 1000 simulation runs. However, comparing $\bar{\hat{S}}D_k$ with $\bar{\tilde{S}}D_k$ in Table 2.1 clearly shows that the mean "observed" standard deviation of the estimates are brought back to the level where they should be. The latter has an implication to the

significance tests of the regression weights: using the proposed procedure, the estimates of truly non-zero weights will be more likely to be statistically significant than the estimates based on the subsample only; and at the same time the estimates of truly zero weights will stay as insignificant as before.

Remark. The above data imputation procedure is based on the assumption that the same linear relationship between the criterion variable and the predictors holds across the population. This is also the basic assumption for multiple range restriction. The possible relationship between the proposed procedure and range restriction is an interesting open problem.

4. Simulation Study of the Unreliable Predictor Issue.

This simulation study was conducted based on the following model of unreliable predictors: The model has 10 predictors, and the true underlying regression equation is given by

(3) $$Y_i = 40 + T_{i1} + 2T_{i2} + T_{i3} + T_{i4} + \varepsilon_i, \qquad i = 1,2,..,N.$$

Here the T's are the underlying (latent) predictors, and the weights on $T_5,...,T_{10}$ are zero; hence the true regression weights are 40 (intercept), 1, 2, 1, 1, 0, 0, 0, 0, 0, 0, the same as those in Section 2. ε_i's are independent normal variates with zero mean and standard deviation 9.75. The sample size N=1000. It is assumed that the T's have the same structure as the X predictors defined in (2), i.e.

(4) $$T_{ik} = G_i + \theta_{ik},\ k = 1,...,10,\ i = 1,2,...,N,$$

where G_i's are independent normal variates with mean 50 and standard deviation 2.22; θ_{ik}'s are independent normal variates with mean 0 and standard deviation 9.75, and are independent of G_i's and ε_i's. The observed predictors $X_{ik}, k = 1,...,10, i = 1,...,N$ are defined as the latent predictors plus normal random error:

(5) $$X_{ik} = T_{ik} + \tau_{ik},\ k = 1,...,10,\ i = 1,2,...,N,$$

where τ_{ik}'s are independent zero-mean normal random variates, and are independent of all the other random variables involved in the model. The reliability of the observed predictors X_{ik} is defined as the ratio of the variance of T's to the variance of X's:

$$r_{ik} = \frac{Var(T_{ik})}{Var(X_{ik})} = \frac{Var(T_{ik})}{Var(T_{ik}) + Var(\tau_{ik})}. \tag{6}$$

The situation simulated here assumes that the reliability values r_{ik}'s are available (either known or can be accurately estimated). Hence the variance of τ_{ik} is determined by r_{ik} as $Var(\tau_{ik}) = [(1 - r_{ik}) / r_{ik}]Var(T_{ik})$, where $Var(T_{ik})$ can be calculated from equation (4).

The simulation study also considered the situation in which Y values are available only in a subsample, and the reliability of the observed X predictors are different for the subsample with observed Y's and the subsample without observed Y's. Because it has been demonstrated in Section 2 that non-random selection of the subsample dose not introduce any significant systematic bias in the regression weights estimates, to keep things simple, in this simulation study the subsample is determined by the first 150 sample points (i.e. for $i = 1,2,...,150$).

One thousand simulation runs were performed. The sth run (s=1,2,...,1000) consisted of the following steps:

(i) Generate G_i's, and generate T_{ik}'s according to equation (4).

(ii) Generate the Y_i's for the first 150 sample points (i=1,2,...,150) according to model (3), giving the subsample Y vector $\tilde{Y}_s$.

(iii) Generate X_{ik}'s according to equation (5), giving the 1000×10 observed predictor matrix X_s; then discard T_{ik}'s.

(iv) Based on the data (X_s, $\tilde{Y}_s$), estimate the regression weights using the imputation procedure described in Section 3, obtaining the weights estimates $\hat{b}_s = (\hat{b}_{s,0}, \hat{b}_{s,1}, \hat{b}_{s,2}, ..., \hat{b}_{s,10})$. Compute the multiple correlation coefficient (validity) $\hat{R}_s^2$.

Essentially the same statistics as in Section 2 were gathered. The simulation results are given in Table 4.1. In the table Δ_k is the relative error $(\bar{\hat{b}}_k - b_{0,k})/b_{0,k}$; see Section 2 for notation and definition of the other statistics.

Table 4.1

k	$b_{0,k}$	predictor reliability for the subsample with Y	predictor reliability for the subsample w/o Y	$\bar{\hat{b}}_k$	$\hat{SD}_k$	$p.T$	Δ_k
0	40			134.778	20.601	0.00	2.369
1	1	0.6	0.8	0.606	0.144	0.01	-0.394
2	2	0.5	0.8	1.001	0.132	0.00	-0.500
3	1	0.7	0.7	0.716	0.154	0.07	-0.284
4	1	0.7	0.65	0.704	0.150	0.05	-0.296
5	0	0.5	0.6	0.021	0.124	0.87	
6	0	0.5	0.6	0.006	0.125	0.96	
7	0	0.5	0.4	0.012	0.130	0.92	
8	0	0.5	0.6	0.012	0.128	0.92	
9	0	0.5	0.6	0.010	0.126	0.93	
10	0	0.5	0.6	0.014	0.128	0.92	

$\bar{\hat{R}}^2 = 0.483$

Summary. (a) When the predictors are not 100% reliable, the least square estimates of the regression weights are systematically biased toward zero from the corresponding underlying population values; this is clearly demonstrated by the mean values of the estimates and the significant P-values in Table 4.1. (b) There is also degrading of the R^2 value: Had the observed X predictors been 100% reliable (hence they coincide with the T 's), the average R^2 would have been about 0.89 as shown in Table 2.1. Whereas the average R^2 in Table 4.1 is only 0.48.

5. Bias Correction in Presence of Heterogeneous Reliability.

A remedy procedure to correct the bias in the regression weights estimates in the presence of unreliable predictors is given in this section. This procedure is described through an example.

Consider again the example used in Section 3. Suppose now that the predictors a not 100% reliable: for the first 7 points where Y values are available, the reliability of

X_1 is 0.7, the reliability of X_2 is 0.6; for the next 13 data points where Y is not observed, the reliability of X_1 is 0.8, the reliability of X_2 is 0.9.

The proposed procedure goes as follows:

(i) Perform the steps (i) and (ii) described in Section 3 to obtain the imputed sample. Compute the mean of all the variables in the imputed sample. The data now look like the following (with comments on reliability):

	X_1	X_2	Y	predictor reliability
	50	62	86	
	56	53	83	0.7 for X_1
	66	47	95	0.6 for X_2
	40	65	78	
	58	52	87	
	51	54	77	
	60	63	91	
	53	51	82.964	
	33	58	67.375	0.8 for X_1
	47	54	78.531	0.9 for X_2
	50	44	78.785	
	56	46	89.137	
	53	42	77.166	
	52	36	79.185	
	55	46	79.096	
	27	43	59.204	
	49	45	81.294	
	41	52	74.114	
	44	44	68.909	
	65	36	82.700	
mean	50.3	49.65	79.773	

(ii) Center the variables: subtract the corresponding mean from each column, obtaining the centered data. Put the columns of the centered predictors into a matrix, X^*; call the column (vector) of centered Y's Y^*.

	X_1 centered	X_2 centered	Y^* (Y centered)
	-0.3	12.35	6.227
	5.7	3.35	3.227
X_1^*	15.7	-2.65	15.227
	-10.3	15.35	-1.773
	7.7	2.35	7.227
	0.7	4.35	-2.773
	9.7	13.35	11.227
	2.7	1.35	3.191
	-17.3	8.35	-12.398
	-3.3	4.35	-1.242
	-0.3	-5.65	-0.988
	5.7	-3.65	9.364
	2.7	-7.65	-2.607
	1.7	-13.65	-0.588
X_2^*	4.7	-3.65	-0.677
	-23.3	-6.65	-20.569
	-1.3	-4.65	1.521
	-9.3	2.35	-5.659
	-6.3	-5.65	-10.864
	14.7	-13.65	2.927

(iii) Partition the matrix X^* row-wise into X_1^* and X_2^* (see above illustration):

$$X^* = \begin{bmatrix} X_1^* \\ X_2^* \end{bmatrix}$$

where X_1^* corresponds to the subsample having observed Y values; X_2^* corresponds to the subsample having imputed Y values.

(iv) Compute $\Sigma_{XX}^{(1)} = X_1^{*T} X_1^*$, $\Sigma_{XX}^{(2)} = X_2^{*T} X_2^*$ (the superscript T denotes transpose), obtaining the two matrices

$$\Sigma_{XX}^{(1)} = \begin{bmatrix} 539.030 & -33.685 \\ -33.685 & 609.058 \end{bmatrix}, \qquad \Sigma_{XX}^{(2)} = \begin{bmatrix} 1260.17 & -261.215 \\ -261.215 & 683.493 \end{bmatrix}.$$

(v) Adjust for reliability: multiply the diagonal elements of $\Sigma_{XX}^{(1)}$ and $\Sigma_{XX}^{(2)}$ by the respective reliabilities of X_1 and X_2 in the corresponding subsamples to obtain

$$C_{XX}^{(1)} = \begin{bmatrix} 0.7 \times 539.030 & -33.685 \\ -33.685 & 0.6 \times 609.058 \end{bmatrix} = \begin{bmatrix} 377.321 & -33.685 \\ -33.685 & 365.435 \end{bmatrix},$$

$$C_{XX}^{(2)} = \begin{bmatrix} 0.8 \times 1260.17 & -26.215 \\ -26.215 & 0.9 \times 683.493 \end{bmatrix} = \begin{bmatrix} 1008.136 & -26.215 \\ -26.215 & 615.144 \end{bmatrix}.$$

(vi) Set

$$C = C_{XX}^{(1)} + C_{XX}^{(2)} = \begin{bmatrix} 377.321 & -33.685 \\ -33.685 & 365.435 \end{bmatrix} + \begin{bmatrix} 1008.136 & -26.215 \\ -26.215 & 615.144 \end{bmatrix} = \begin{bmatrix} 1385.457 & -59.9 \\ -59.9 & 980.579 \end{bmatrix},$$

and set $$\Sigma_{YX} = X^{*T} Y^* = \begin{bmatrix} 1347.500 \\ 209.999 \end{bmatrix}.$$

(vii) The slopes are estimated by

$$\begin{bmatrix} \hat{b}_1 \\ \hat{b}_2 \end{bmatrix} = C^{-1}\Sigma_{YX} = \begin{bmatrix} 0.984 \\ 0.274 \end{bmatrix},$$

where C^{-1} is the inverse of the matrix C obtained in step (vi). The intercept is estimated by $\hat{b}_0 = \bar{y} - \hat{b}_1\bar{x}_1 - \hat{b}_2\bar{x}_2 = 79.773 - 0.984 \times 50.3 - 0.274 \times 49.65 = 16.674$.

(viii) It is not very clear at this point how the predicted Y values and the R-square value should be calculated based on the bias-corrected regression weights estimates obtained in the previous step. One simple possibility is to use the usual formulas: $\hat{Y} = \hat{b}_0 + X\hat{b} = 16.674 + X\hat{b}$, where $\hat{b} = [\hat{b}_1, \hat{b}_2]^T = [0.984, 0.274]^T$, and $R^2 = [corr(Y, \hat{Y})]^2$, with *corr* standing for correlation. Doing so on the example gives $R^2 = 0.861$.

The above estimation procedure is evaluated by a simulation study. The setup is exactly the same as that in Section 4, and the same statistics are computed. The results are given in Tables 5.1 and 5.2.

Table 5.1

k	$b_{0,k}$	predictor reliability for the subsample with Y	predictor reliability for the subsample w/o Y	$\bar{\hat{b}}_k$	$\hat{SD}_k$	$p.T$	Δ_k
0	40			74.787	34.085	0.31	0.870
1	1	0.6	0.8	0.789	0.194	0.28	-0.211
2	2	0.5	0.8	1.362	0.186	0.00	-0.319
3	1	0.7	0.7	1.018	0.225	0.93	0.018
4	1	0.7	0.65	1.071	0.233	0.76	0.071
5	0	0.5	0.6	0.023	0.220	0.91	
6	0	0.5	0.6	-0.002	0.223	0.99	
7	0	0.5	0.4	0.019	0.327	0.95	
8	0	0.5	0.6	0.007	0.227	0.98	
9	0	0.5	0.6	0.004	0.222	0.98	
10	0	0.5	0.6	0.011	0.228	0.96	
					$\bar{\hat{R}}^2 = 0.479$		

Table 5.2

k	$b_{0,k}$	predictor reliability for the subsample with Y	predictor reliability for the subsample w/o Y	$\bar{\hat{b}}_k$	$\hat{SD}_k$	$p.T$	Δ_k
0	40			36.212	38.441	0.92	-0.095
1	1	0.6	0.6	1.051	0.245	0.95	0.051
2	2	0.5	0.5	2.019	0.274	0.94	0.010
3	1	0.7	0.7	1.020	0.236	0.93	0.020
4	1	0.7	0.7	1.020	0.236	0.93	0.020
5	0	0.5	0.5	0.003	0.270	0.99	
6	0	0.5	0.5	0.001	0.277	0.99	
7	0	0.5	0.5	0.011	0.292	0.97	
8	0	0.5	0.5	-0.007	0.271	0.98	
9	0	0.5	0.5	0.001	0.273	0.99	
10	0	0.5	0.5	-0.007	0.266	0.98	
					$\bar{\hat{R}}^2 = 0.527$		

Comparing with Table 4.1, Tables 5.1 and 5.2 clearly show the effect of the proposed adjustment procedure for heterogeneous unreliability in the observed predictors. The regression weights estimates based on the proposed procedure become much closer to the underlying population values, and the P-values are no longer significant for most of the estimates, indicating the reduction of systematic bias in the estimates.

Though not presented here, cases with other configurations of the reliabilities are also simulated. The proposed method has the following pattern: it performs the best if the predictor reliabilities in the subsample having observed Y values are the same as those in the subsample without observed Y values; it performs moderately well if the predictor reliabilities in the subsample having observed Y values are lower than those in the subsample without observed Y values; it performs very poorly if the predictor reliabilities in the subsample having observed Y values are greater than those in the subsample without observed Y values.

6. Concluding Remarks

The results from the carefully designed simulation experiments clearly show (1) for normally distributed model errors, least square estimates based on non-randomly selected subsamples are not biased, but there is an inflation in their standard errors; (2) if

the observed predictors are not 100% reliable, then the least square estimates of the underlying regression weights are biased toward zero.

The proposed data imputation based estimation procedure seems to work well in the situations simulated, where the R-square value is fairly high. An open issue is the performance of this procedure when the model errors have relatively high variance, so that the R-square value is fairly low. The proposed bias correction procedure in the presence of unreliable predictors seems to work in the cases presented in Section 5. There are at least three issues remaining open for this procedure: (a) How should the predicted Y-values and the R-square be computed based on the bias-corrected regression weights estimates, for these estimates are now regarded as coefficients on the latent T variables, not the coefficients on the observed X variables; (b) Why does the procedure break down when the observed predictors in the subsample without observed Y values have lower reliability? (c) Will it make any difference to adjust for unreliability prior to imputation? Clearly both of the proposed procedures require further investigation and refinement.

More issues remain open with regard to the implications of the findings to the construction of a classification system. (a) what is the end effect on MPP? (b) Would the regression weights estimates for different job families become essentially the same (hence losing differential ability for job families) after the adjustment for predictor unreliability? Even if this turns out to be the case, what would be the implications to the ASVAB subtests and the job family formation? (c) What are the implications to construction of composites and the cut-off scores?

Refinement of the proposed estimation procedures, together with investigations of the above issues, constitutes future research efforts.

References

Fuller, W.A. (1987). *Measurement Error Models*. John Wiley & Sons, New York.

Acknowledgments

Thanks are due Ms. Melody Darby, Dr. Malcolm Ree, Mr. James Earles, Dr. Patrick Kyllonen, and Dr. Richard Roberts, for inspiring discussions and for careful readings of this report. Special thanks go to Dr. William Alley for insightful discussions on the research problems. The Human Resources Directorate of the Armstrong Laboratories provided an enjoyable research environment.

USE OF AIR SYNTHETIC FORCES FOR GCI TRAINING EXERCISES

Gerald P. Chubb
Associate Professor
Department of Aerospace Engineering

The Ohio State University
164 W. 19th Avenue
Columbus, OH 43210-1110

Final Report for:
Summer Research Program
Armstrong Laboratory

Sponsored by:
Air Force Office of Scientific Research
Bolling Air Force Base, Washington, DC

And

Armstrong Laboratory

September 1997

USE OF AIR SYNTHETIC FORCES FOR GCI TRAINING EXERCISES

Gerald P. Chubb
Associate Professor
Department of Aerospace Engineering, Applied Mechanics, and Aviation
The Ohio State University

Abstract

Air Synthetic Forces (AirSF) provide a model or air combat pilot decisions, actions, and communication that can be fed to ModSAF, which then simulates aircraft performance in a Distributed Interactive Simulation (DIS) of combat operations. In training Modular Control Equipment (MCE) operators in the performance of Ground Controlled Intercept (GCI) procedures, it would be useful to have synthetic target images that behaved like "real" pilots. AirSF has the potential for providing a computer-based surrogate for pseudo-pilots currently used in large-scale training exercises or MCE simulations.

Pseudo pilots typically are airmen who try to emulate pilot actions using the built-in MCE simulation capabilities. They often are not well-versed in MCE console operations and do not know what pilots do about air combat operations. So these pseudo pilots are not always good surrogates for actual pilots, and it was hoped that AirSF models might actually out-perform the pseudo pilots in training exercises.

The present study examined what MCE operators are expected to do and reviewed the available AirSF documentation to determine what the software could do (and how well it acted like real pilots might). However, those questions cannot be answered from the documents reviewed. Empirical testing of AirSF will be needed in order to answer the question: Can AirSF do better than (and therefore replace) pseudo pilots in training MCE operators in GCI operations?

The principal focus of activity in this effort was examining training needs of the 607th Air Control Squadron (ACS) at Luke Air Force Base (AFB) and how the facilities at the Armstrong Laboratories' Aircrew Training Division might help meet some of the identified needs for improvement. Two additional exercises were included: 1) development of a seminar on software requirements engineering and software configuration control, and 2) preparation of an IDEF0 model of the Instructional System Development (ISD) process.

1.0 Mission Statement

The Armstrong Laboratory's Aircrew Training Division has the task of validating the Synthetic Theater of War (STOW) use of Airborne Synthetic Forces (AirSF). The AirSF element of STOW is possibly reusable in other training environments, such as Ground Control Intercept (GCI) or Weapons Direction (WD) training in the Modular Control Equipment (MCE) used in the Theater Air Control System (TACS), operated by the 607th ACS. The principal questions are: a) what functions can AirSF perform to enhance such training, and 2) how well can AirSF perform those functions? To answer these questions, one must first understand MCE use, the need for operator training, and the measures that might be used to determine whether training (or performance) is effective. One must also understand what AirSF can and cannot do, and how that might help or hinder training of MCE operators.

1.1 Mission Context

The MCE consists of an Operations Module (OM) with four Operator Console Units (OCUs) and associated equipment (power, environmental control, communications gear, and radar(s)). A single OM can be used for selected functions, but two OMs are needed for an operational Control and Reporting Element (CRE), the lowest / most remote component in the hierarchy or network of command and control system elements. Two or more CREs will report to a Control and Reporting Center (CRC), which can consist of 4 OMs and associated support equipment. The CRCs then report to the Air Operations Center (AOC) associated with the TACS Headquarters.

The MCE may assist the Airborne Warning and Control System (AWACS) or replace it when not flying. There are three basic functions which must be performed: air surveillance, weapons direction, and overall battle management. In the minimal configuration, a Mission Crew Commander (MCC) will supervise two Weapons Directors (WDs). In the CRE, there will be a MCC and 3 WDs in one OM, and in the other OM there will be an Air Surveillance Officer (ASO) / Air Surveillance Technician (AST) supervisor, 2 ASOs or ASTs, and an Interface Control Technician (ICT) who manages the data link hookups. In the CRC, the MCC will supervise two Senior Directors (SDs) who in turn will oversee a WD and either an ASO or AST, supported by the one ICT for the CRC – a total operating crew of six, not counting the MCC and the ICT.

1.2 Missions

There are a number of missions that the MCE might support: air-to-air engagements (both offensive and defensive counter air), air-to-ground (both Close Air Support (CAS) and battle field or deep interdiction), intelligence and electronic combat (as well as Suppression of Enemy Air Defenses (SEAD)), logistics support, search and rescue, maritime interdiction and mine laying, and refueling exercises, which support the weapons delivery and other missions. AFM 3-1 describes Air Force missions, but that document was not accessible and has therefore not been reviewed. Combined strike operations and joint strike missions are becoming more common and typically require coordinated mission planning by the participating units.

1. 3 Basic Concept of Operation

The basic job of command and control (whether AWACS or MCE) is to prevent enemy strikes on own assets while assuring destruction of enemy capabilities and will to fight. The fundamental strategy for achieving mission success is to maintain air superiority and positive control of the airspace. Positive control of the airspace requires that all of one's own assets are identified and tracked. That way enemy aircraft can be identified, intercepted, and neutralized before inflicting damage.

1.4 The Problem

Present training is handicapped by the lack of an adequate mission simulation facility which can flexibly impose realistic, combat-like loads and event pacing on operators so they can rehearse procedures under levels of stress approximating those of combat operations. Moreover, to simulate those conditions, particular attention must be given to allowing the operators to practice and become proficient in voice communication, not just console operation. Realistic emulation of combat operations requires that whoever participates as a pseudo-pilot sounds like they know what they are doing, instead of sounding like they are there just to press buttons. Moreover, event timing and pacing are critical to successful emulation of combat operations. When actions are taken they must result in reasonable outcomes in reasonable time frames.

The MCE does have a built-in simulation capability. However, it takes extensive programming to set up hypothetical radar returns of enemy aircraft. Static depictions of those aircraft do not allow maneuvering and therefore present unrealistic threats. Dynamic representations are possible, but they require a "pseudo pilot" to monitor the air battle and then enter commands that implement only pre-defined aircraft maneuvers.

While these dynamics are more realistic than static radar tracks, there are two major deficiencies: 1) the operators must be proficient in console commands (and even then the maneuvers may not be executed in a "timely" fashion), and 2) all maneuvers must be pre-programmed, so the simulated enemy may not be able to react realistically to reasonable changes in friendly force combat tactics variations. Also, console operators acting like pilots do not have the same mental models of combat that actual pilots have and use when constructing radio communication messages about the scenario (requests for information and descriptions of the situation and / or action intentions).

2.0 Approach

The general approach in the present study was to begin with a mission task analysis in order to identify and then define measures of effectiveness and performance which could serve jointly to support verification and validation (Fuld, 1997) of the AirSF models. Similar data are needed to assess transfer of training effectiveness for any subsequent incorporation of AirSF models into a training simulation, locally or via Distributed Interactive Simulation (DIS). The mission task analysis requires access to data and tools to do the work.

The AirSF model documentation was examined to determine what the developers did and to make a preliminary assessment of how well they did it, relative to our understanding of what needed to be there for MCE training applications. Initially, the plan was to have copies of the software up and running for the evaluation this summer. However, development slipped and the code was not delivered in time to install it and perform any empirical testing. All assessments of this code had to be done from its documentation, which proved to lag significantly the implementation of the code itself.

2.1 Task Analysis Data and Methods

Several kinds of operational data were available, and more than one tool was used to do the mission / task analysis. While this study is incomplete, it is a reasonable start toward what will be needed to specify the requirements for a better mission simulator.

2.1.1 Available Systems and Operations Data

Three sets of documents were available for review of MCE operations: 1) hardcopy manuals on MCE switch actions, 2) Litton Data Systems' Computer Based Instructional Training System (CBITS) diskettes, and 3) two Hughes Training, Inc. CD ROMs on selected MCE operations. Access was also provided to several Subject Matter Experts (SMEs) on the MCE and AWACS WD operations. Access was also provided to an actual OM at Luke Air Force Base (AFB), AZ. It was not possible to review this entire database. Only selective review was accomplished.

2.1.2 Tools Used

The overall concept of operation was described using the Structured Analysis and Design Technique (SADT, Marca and McGowan, 1989), based on the introduction to the MCE (HTI: SG-809) and interviews with SMEs. Data collection from SMEs began by using "Designers' Edge", a front-end analysis tool for Instructional Systems Development (ISD) marketed by Allen Communications in Salt Lake, UT (Allen, 1994). Klein Associates' Applied Cognitive Task Analysis (ACTA) was also reviewed and templates were developed to use in applying this methodology (Militello and Hutton, in press) to obtain SME inputs about selected tasks. However, lack of time and availability to SMEs prevented application and trial of these templates.

ETAP (Reigeluth and Merrill, 1984) was examined, along with the AL/HRCC PARI method (Hall, et al., 1995). PARI is an acronym for Precursor, Action, Result, Interpretation. While originally developed for analyzing the problem solving that occurs in troubleshooting malfunctions (particularly in electronic equipment), AL/HRCC has adapted PARI to perform an analysis of AWACS WD tasks. The analysis performed here borrowed mostly from Designers' Edge, as well as work done by AL/ CFTO in the AESOP facility (e.g. Klinger, et al., 1993). Other documents which would have proven useful but were not available during the period of summer research include Eddy (1989 and 1990) and Eddy and Shingledecker (1988).

2.2 Evaluation of AirSF

AirSF is an application of the SOAR architecture (Laird, et al., 1986) to modeling pilot performance in air combat operations. SOAR is an acronym for State, Operator, And Result; the software that implements this approach to modeling human cognition or problem solving activities is now called Soar. We use these two versions (SOAR and Soar) to refer to the architecture and the model software respectively The Navy funded the development of Soar models of (flying) the F-14 and MiG-29 for use in STOW. The only documentation available for review was on-line via the World Wide Web at Uniform Resource Locator (URL) address: http://ai.eecs.umich.edu/ifor/. Selected materials were downloaded, printed, and reviewed. These included glossaries of terms, conceptual descriptions of Soar architecture for AirSF, and a limited amount of actual code.

3.0 Results

The following summarizes the results of the study effort, both in terms of the MCE modeling that was done, the review of selected AirSF documentation, and the identification of MCE training requirements. The detail provided here is limited by the page restriction. More complete documentation of the SADT model of MCE operations was provided to AL/HRAD, along with the documentation of interviews with SMEs using the Designer's Edge templates, as modified for this data collection effort. The completed Needs Analysis Report generated by Designer's Edge was also separately provided. AL/HRAD also was given the hardcopy SADT model of ISD and the PowerPoint briefing materials that treat software requirements engineering and software configuration management.

3.1 MCE Modeling

The A0 diagram of the preliminary SADT model developed for the MCE is shown in Figure 1, but without the accompanying glossary and node text. Each of the functions shown in this diagram were further decomposed to the next level, based on available documentation, without input from the SME interviews. Selected nodes on those decompositions were then developed to one additional level of detail, based upon specific additional inputs that were obtained from SMEs.

The logic of operation and actual switch actions were not described. Two possible extensions of this work will be required in order to get the templates needed for data analysis of operator activities in simulation exercises: 1) the switch action sequence(s) for implementing control actions, and 2) the verbal communication scripts for pilot-controller interchanges (as many "typical" cases as possible).

Figure 1. Top-Level SADT Diagram of MCE Functions.

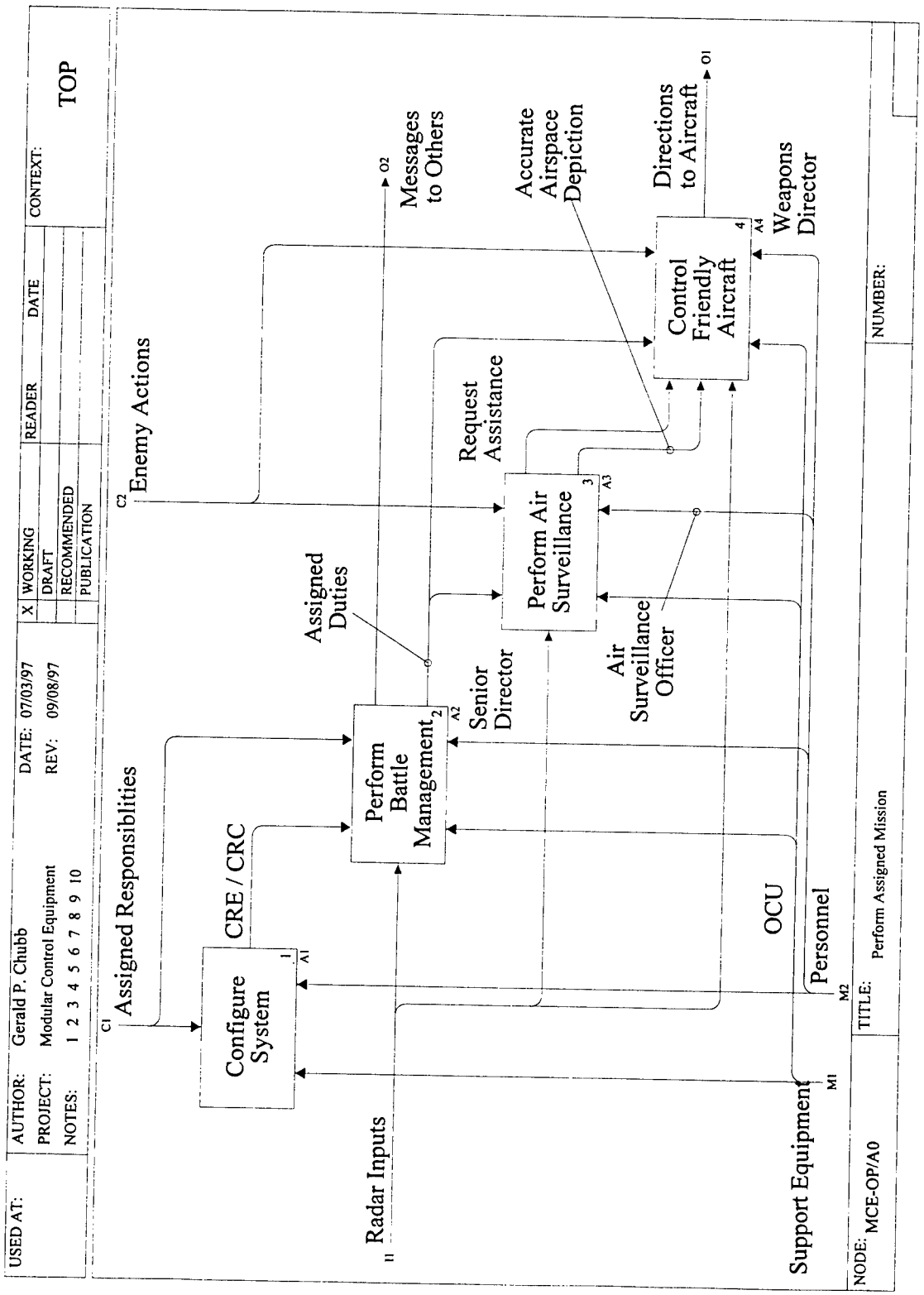

3.1.1 Measures of Effectiveness

Measures of Effectiveness (MoEs) refer to ways in which system outcomes might be determined and assessed. This is distinct from Measures of Performance (MoPs) where the focus is on individual and crew actions rather than system / mission outcomes. Hopefully, better crew performance (improved MoPs) will be reflected in better MoEs. However, perfect correlation rarely occurs. MoEs may be somewhat insensitive to changes in MoPs, and in most cases, the MoE is only partially determined by the MoP. Outcomes are determined by more than just what the MCE operators do: the pilots and their weapons have a role in determining the outcome too! A perfect intercept and ideal weapons flight can still be followed by a "dud" – a warhead that fails to activate. While "rare," such events degrade the correlation between MoPs and MoEs.

MoEs can be positive or negative indications of mission success. Enemy kills would be a positive indicator. Assets lost (like own force aircraft) would be a negative indicator. Some MoEs are combinations of others. For example, kill rates might be expressed as a ratio of two set of loss frequencies – Red versus Blue (e.g., 2 to 1 or 10 to 1). Table 1 lists some proposed MoEs.

Table 1. MoEs for Modular Control Equipment (MCE) Operation.

Measure	Indication
1. Range at First Lock-on	More is better
2. Number of Beyond Visual Range (BVR) Kills	More is better
3. Number of Within-Visual Range (WVR) Kills	More is better
4. Number of Enemy Air-to-Air Missile Launches	Less is better
5. Enemy Aircraft Shortest Range to Target	More is better
6. Number of Enemy Air-to-Ground Weapons Releases	Less is better
7. Number of Friendly Aircraft Killed	Less is better
8. Number of Missed Intercepts	Less is better
9. Number of Missed Attacks	Less is better
10. Other Friendly "Losses" (e.g out of fuel)	Less is better

3.1.2 Measures of Performance

The MoPs are of two kinds: 1) those which apply to a single individual, and 2) those which apply to a group of individuals. A group of individuals may be a team or even a set of teams: the MCE crew, the Air Surveillance team, or the Weapons Direction team, etc. Like MoEs, these measures can be positive or negative indicators and some MoPs may be composed from more elementary indicators.

Air Surveillance MoPs include: 1) number of yellow (unknown indications), 2) yellow duration statistics (average duration and standard deviation), and 3) number of misidentifications (if any: and by type). It is important to identify who the adversary is if the pilot is to employ effective combat tactics. Electronic Identification (EID) capabilities exist for some but not all radars, and while effective, EID is not perfect.

Weapons Director MoPs include: 1) number of redirects, 2) average duration of voice communication, 3) time between significant radar indication changes and information calls to pilot(s), and 4) average delay in responding to information requests. Quality of voice communication is important also, but more difficult to measure. It consists of: a) using the right (i.e., "best") terminology, b) being brief but complete, and c) giving good information when and as needed. Common MoPs: 1) duration of switch action sequences, 2) number of switch action errors, and 3) time taken for corrective action(s). Table 2 identifies possible MoPs for MCE operation.

Table 2. Possible MoPs for Modular Control Equipment (MCE) Operation.

Measure	Indication
1. No. of "Unknowns" (yellow)	Less is better
2. Duration of Yellow (Average and standard deviation)	Less is better
3. Number of Aircraft Misidentified	Less is better
4. Number of Redirects	Less is better
5. Time Between Event and Call	Less is better
6. Delays Answering Requests	Less is better
7. Quality of Communication	More is better
8. Speed of Switch Action	More is better
9. Accuracy of Switch Action (or No. of Errors)	More is better (i.e., less errors better)
10. Time for Corrections	Less is better

3.2 SOAR Documentation Review

The initial glossaries for SOAR demonstrated a lack of understanding about certain elements of air combat. Later glossaries included material from Air Combat Command (ACC) and provide evidence that the lack of understanding was being corrected. However, it also made clear the fact that the documentation might not reflect the actual capabilities of the code, since not all of the documentation available on-line was of the same vintage. The code (when accessible) shows the date of the last change, and in at least one case, the change was not a even week old.

However, in the comments on Soar code for weapons elaborations, a statement was made that only 2D reasoning is being attempted, not 3D, although it was recognized that many of the problems that have to be solved are really 3D problems. Consequently, AirSF may not solve correctly many important problems pilots must address. In any particular application of AirSF, it will be important to discern whether these limitations are important or irrelevant. In using AirSF to represent some kinds of opposing forces activities, the 2D representation and other limitations may be entirely acceptable. In other applications, its use might lead to invalid results.

Another interesting comment was discovered in the discussion of default symbolic values: "These productions elaborate the state with a number of constants that the agent reasons with... all the parameters of the system are in one place ... This is good from a software-engineering point of view, but from Soar's point of view it involves keeping around a lot of declarative structure during reasoning." It is recognized that this mis-represents human cognitive processing capabilities and limitations, however reasonable it is from a modeling implementation perspective. Solving the problem is essentially left for further research.

The default values mentioned include the following: 1) default time values, 2) maneuver values, 3) bogey elaboration values, 4) values for flying in section, 5) values for interpreting contact information, 6) values for sorting groups, 7) miscellaneous values, 8) delay values, 9) missile information, 10) radar information, 11) vehicle information, and 12) section maneuvering and formation information. An agent in Soar typically (not universally) corresponds to some flight vehicle (alternately, a controlling agent or some player on the ground: e.g. Forward Air Controller (FAC)).

Default time values include: 1) how long an agent will wait before deciding a bogey is not reacting to it, 2) how long the agent will chase a bogey that is bugging out, 3) how long the agent will consider communicated information to be valid, 4) how long the agent will wait for its partner to respond to a position request, 5) how long the agent will wait for its partner to confirm a position request, 6) how long the agent will wait to dispose of a message that it does not know how to process, 7) how long the agent will wait to fire after locking its radar on a target, 8) how long the agent will wait to decide a missile is stupid after the missile's time-of-flight has almost reached zero, 9) how long the agent will give the radar a chance to switch modes after the button is pressed, 10) how long a bogey's heading must stay constant to be interpreted as not turning, 11) how long the agent will wait after

merging with a bogey before deciding that the merge is done, and 12) how long the agent will wait for acknowledgment before repeating a message.

Maneuver values include: 1) maximum speed the agent believes its plane can fly (for bug-out), 2) maximum altitude the agent believes its plane can fly, 3) lowest desired-speed the output routines will ever allow to be set, 4) slow speed for the outbound (search) portion of a racetrack , 5) fast speed for the inbound portion of the racetrack, 6) range at which the agent may decide to do a blow-through, 7) the speed to use for a blow through, 8) the altitude to use for a bug-out, 8) amount of altitude to change (and the flight path angle to use) during a change-piece-of-sky, 9) the flight path angle to use when changing altitude, 10) the default flight path angle to use when changing altitude during an intercept, 11) the flight path angle to use when beaming, 12) the amount to turn during an F-Pole (post-missile launch defensive) maneuver, 13) the size of the heading cut (past the bogey reciprocal heading) when the agent is far away from its desired lateral separation with a bogey, 14) the size of the heading cut for medium distance from desired lateral separation, 15) the size of a heading cut for small distance from the desired lateral separation, 16) the size of a cut (past collision course) to take when a target is very high, 17) maximum value for a small heading change, 18) range below which the agent will no longer evade missiles, 19) the time the agent will remain in beam when it is far away from a bogey, 20) the time the agent will remain in beam when it is not far from a bogey, and 21) the range used to determine whether the agent is far away from a bogey.

Radar values only include: 1) maximum target aspect for which the agent believes the bogey may see it on radar, and 2) the maximum amount of angle-off that the agent believes it can have to keep the bogey safely on its radar.

Bogey elaboration values include: 1) maximum target aspect for which the agent will interpret the bogey as pointing at it, 2) the minimum target aspect for which the agent will interpret the bogey as pointing at it, 3) the maximum target aspect for which the agent will interpret the bogey as bugging out, 4) the maximum range for the agent to chase a bogey, 5) the minimum closing velocity for the agent to keep chasing a bogey, 6) the range of the target-aspect for the agent to interpret the bogey as being in the beam, 7) the target aspect at which the agent will interpret the bogey as being close to the beam, 8) the minimum angle-off to interpret a bogey as being "at 6 o'clock", 9) the minimum angle-off to interpret a bogey as being at "12 o'clock", 10) the extra range outside of the bogey's longest range that the agent considers "safe", 11) the maximum range at which the agent may interpret the bogey as heading for a merge, and 12) the maximum range at which the agent will interpret a merge with a bogey.

Values for flying in section include: 1) how much faster the agent should go when its partner's target aspect is too big, 2) how much slower the agent should go when its partner's target aspect is too small, 3) how much faster the agent should go when its partner is far away, 4) how much the agent should adjust its speed by when turning, to keep close to its partner, 5) the size of the cut (off its partner's heading) the agent should make to get to its desired lateral separation, and 6) the minimum roll for which the agent will interpret its partner as doing a hard turn.

Values for interpreting contact information include: 1) the maximum speed with which the agent will assume an old contact can move relative to the agent, and 2) ranges in which an agent will confirm a position request.

Values for sorting groups include: 1) the distance past an agent's maximum missile range at which it will sort a group, 2) angle to determine whether to sort by azimuth or by range (sort by azimuth if group-sub-bearing is greater than this value), and 3) if group members have an altitude difference bigger than some specified amount, then sort by altitude.

Miscellaneous includes: 1) the maximum range for which a waypoint is assumed to be achieved, and 2) visual range from ground to air (used by ground based agents to spot flying targets).

Delays (artificial time lapses introduced to make the agent appear more realistic) include: 1) a delay between achieving a new contact and checking the commit criteria, 2) time to wait after issuing the takeoff command to the simulator, so the simulation synchronizes properly, 3) time between when the agent simulates asking the E2C for identification of a contact and when the agent simulates a response by the E2C, 4) time between when the agent

simulates a response by the E2C and when the agent simulates "comprehending" the response, and 5) time the agent will wait between noticing a potential immediate threat and actually recording the threat.

Missile information includes: 1) unclassified numbers "made up" to give the right qualitative behavior, 2) real name (e.g. alamo, etc.), 3) alias (e.g., phoenix – where the phoenix values serve as a surrogate for the unknown alamo data), 4) type (e.g. aa-10), 5) range (medium in this case), 6) guidance (radar for this case), 7) launch-to-eject time, and 8) launch acceptability region (lar) information: a) slant range low & high values, b) target aspect (45 degrees), and c) steering circle (5 degrees).

Radar information includes: 1) similarly unclassified values that give the right qualitative behavior, 2) name (e.g. track-while-scan (tws)), 3) type (tws-auto), 4) range (160000 meters), 5) beam (pulse-doppler), and 6) notch (28 meters (m) / sec).

Vehicle information includes: 1) name (e.g. Tomcat), 2) type (F-14), 3) radar (APG-71), 4) radar warning receiver (ALR-67), and 5) weapon(s) (e.g. AIM-54, AIM-7, and AIM-9).

Section maneuvering and formation information includes: 1) default values for section turns: a) type of turn (max-small, max-medium, max-big-turn), b) maximum difference allowable between section members to be considered in formation, and c) turn rate (small, medium, and large), and 2) formation, especially for defensive combat spread: a) type (combat-spread), b) sub-type (defensive), c) lateral range: (i) medium (900 meters), (ii) mean (1300 m), (iii) max (1600 m), and (iv) too far (6000 m), d) lateral separation: (i) min (900 m), (ii) mean (1300 m), (iii) max (1600 m), and (iv) too far (5000 m), e) vertical separation: (i) min (200 m), (ii) mean (400m), (iii) max (600 m), and f) target aspect: (i) min (80 degrees, (ii) mean (90 degrees), and (iii) max (100 degrees).

Also, many references to aspects of the code were incomplete or inaccessible, making a complete evaluation impossible. As a result of not having access to all sites and running into links that resulted in data not being found, it is difficult to determine exactly what the code can do, much less how well it might actually do whatever it does. For example, the node for "Current State" was not found, the node for descriptions of timing considerations was not found, and the operator: "suggest-proposal" was not found.

Much of the documentation of the Top Problem Space (PS) is done with a frame template. The Operators frame has the following elements: overview, proposal, application, reconsider, and code files. For example, for the Operator/Goal: plan-mission, the Operator Overview is: "Plan the current mission, including refueling." The Operator Proposal is: "If the mission has not been planned or aborted." The Operator Application lists five suboperators: change-mission-brief, compute-time-to-leave, plan-attack, plan-fuel, and route. The Operator Reconsider is: "Once the mission is either planned or aborted." The Code files are: plan-mission, plan-mission/load.soar, and plan-mission/elaborations.soar. Unfortunately, in many cases, the frame is blank except for the reference to a code file. The Soar code is itself the only documentation actually available in that case. Unless the code is extensively commented (and most of it is not) or you know how to decode the Soar syntax, this will not reveal much about what Soar does or how it does it.

The diagram accompanying the description of blue fighter - red bogey geometry included reference to a heading where the angle indicated was actually the complement of the named angle, not the angle itself. It was measured counter-clockwise from North instead of clockwise. So accuracy checks of Soar code and results need to be made to be sure implementation was done correctly. Also, in several places, the documentation made reference to the fact that some of the numbers being used were simply made up or that the real values were classified. Consequently, using the AirSF for real problems requires going back and putting in the appropriate numbers, which may then make AirSF capable of only being run in a secure facility which has the appropriate provisions for running classified code.

It does appear that some attention is being given to mimicking the verbal communication as well as the control of the aircraft, both of which are significant in creating realistic interactions with MCE operators. An assessment of that is provided later in Section 3.2.7 The list of aircraft included in the simulation is not consistent from one list to another, so it is again difficult to determine just what has been included. While documentation indicates speeds are

all True Air Speed (TAS), it also notes that some will change "when we have the new dynamics in" but there is no mention of when that may occur.

The entry page for Soar/IFOR Documentation has a number of links that cannot be opened, one of which is ModSAF. All of the "primary source documentation" links are operative and were explored: 1) Requirements for Automated FWA (fixed wing aircraft) Behaviors, 2) Domain Description Documents (DDD), 3) Functional Assumptions, 4) Tac-Air Soar Implementation Documentation, 5) Interface Documentation, and 6) Documentation Search, which provides a search engine into this set of data to look for specific information.

3.2.1 Requirements for Automated FWA Behaviors

This material is essentially an outline based on a Table of Contents for BMH documentation of Automated Force Behaviors. The outline entries are coded to indicate: 1) behaviors not in Soar/IFOR (and not likely to be added), 2) those not in Soar/IFOR but expected to be additions at some later time, and 3) behaviors that are in Soar/IFOR, for which a documentation link is provided. Numerous undefined acronyms are used in this outline.

Behaviors not likely to be included in Soar/IFOR include: 1) sun angle, contrast, shadows, and time of day; 2) ground cover (foliage, desert, snow), topography, and terrain features; 3) radar / IR/ TV / Visual significance; 4) intelligence data utilization, 5) consideration of enemy order of battle / threat / situation planning; 6) selected aspects of joint service operations; 7) SID, SMO, or EMCON departures, post-takeoff checks / procedures during climbout, and emergencies / malfunctions (like radio out) procedures; 8) visual communication; 9) TACAN / GPS rendezvous and underrun maneuver; 10) security, combat, and ACM checks enroute; 11) weather related procedures: turbulence and thunderstorm avoidance, as well as icing protection systems operation; 12) communication / coordination during refueling operations; 13) Return to Base (RTB) communications; 14) selected aspects of navigation; 15) recovery / approach and landing procedures. Neither pre-flight nor post-flight activities are included, but selected aspects of mission re-planning are incorporated into mission execution.

The RoE considerations are far from complete. They are too simplistic to be even a good skeletal structure. Infra-red countermeasures apparently will be ignored. Environmental considerations at merge are not treated (e.g. cloud cover and visibility). Selected aspects of bug-out will not be covered. Reporting leakers is not included. In air-to-ground operations, shared behaviors like communication and coordination of the strike crew are not covered, nor are the low level navigation procedures (radar scope interpretation, dead reckoning, INS / GPS procedures, etc.). Low altitude tactical lookout and threat countermeasures are ignored, except for terminal threat maneuvering (reactions to Anti-Aircraft Artillery (AAA), Surface-to-Air Missiles (SAMs), and Airborne Interceptor (AI) attacks). Apparently CAS maneuvering and performing a RABFAC (unexplained acronym) attack will not be treated either. Night operations are not specifically covered, nor are defense suppression tactics (presumably because they are left to SEAD aircraft, like the Wild Weasel or its contemporary equivalent).

There seems to be some uncertainty on the part of BMH or Soar developers about relating basic maneuvers (aerobatics, unusual attitudes, stalls, and spins) to combat operations. It is therefore not clear how far one could push the Soar models into adverse operating regimes. It is presumed that their consideration of combat tactics would implicitly include consideration of relevant maneuvering, especially for what the Navy calls Close-In Combat (CIC), but that assumption should be validated by checking or running the code.

3.2.2 Domain Description Documents (DDD)

This set of documentation is supposed to describe what has been garnered from SMEs. The intent of this material was to provide "information about the doctrine, tactics, and procedures independent of any specific implementation." A dozen topics are covered: 1) command groups (Navy sections and divisions), 2) communications, 3) controllers (E-2C, DASC, etc.), 4) formations, 5) geometry, 6) missions (A-A, A-G, and support), 7) level of risk, 8) classifying threats, 9) ordnance, 10) aircraft, 11) scenarios, and 12) tactics.

This material also includes links to other data, such as glossaries, the TacAir-Soar Goal / Operator Hierarchy, and the root of the Soar / ModSAF documentation. However, a number of links come back with a message "Not

Found," so it is not always clear that the information is really there until you try to access it, other branches "timed out" giving an error message that the site (containing the information) could not be opened.

3.2.3 Functional Assumptions

This document was "to provide complete traceability of the design decisions within the TacAir-Soar code." Since the assertion is made that "these functional assumptions will ideally be removed completely," little attention was given to this section. It was supposed to shrink as the DDD was expanded. It was also noted that: "FWA will only commit to an intercept if they have identified the bogey group as containing bandits (this is not correct, but this is how we do it for now)."

3.2.4 Tac-Air Soar Implementation Documentation

This section probably best describes what AirSF does. It has links to actual code, although not every indicated link actually gets to the code. In some cases, access was denied. However, when the code is available, it usually indicates when the section was created and when it was last updated, so you can get some idea of its currency. There are embedded comments, which help interpret what is there and how it is implemented, but without knowing Soar syntax, interpreting what the code actually does is not possible. Guessing is about all one can do.

The "general knowledge" link actually takes you back to the DDD, and the "general overview" link simply takes you back to the overview of TacAir-Soar agent architecture. That page has multiple entries, all but one of which are non-functional. The next two links are the debriefing facility (which is "Not Found") and the "programming conventions" (which returns a "server error" message), so the link to "our data structure documentation" is the next link on this opening page that actually works. It leads to a page with four links: 1) missions, 2) command groups, 3) formation, and 4) supernode: goal / operator hierarchy. The Operator / Goal: Top-PS is apparently the entry point for all processing. A discussion of some of its features is treated in section 3.2.6.

3.2.5 Interface Documentation

This section was meant to document the Soar / ModSAF interface and is broken down into three sections: 1) input link, 2) output link, and 3) right-hand side functions. The latter are general-purpose functions, like trigonometric and arctangent calculations, degrees to radian conversion, string processing, rounding, etc.

3.2.6 Top PS

Since Soar is a problem solver, it works within a specified problem space. The formal definition of a problem space includes the goal (desired state), the present (or current) state (which is the initial state at t=0), and the operators that can change states. The top problem space simply sets the overall boundaries for "execute the mission" and initializes what are essentially global variables. Solving the problem of executing a mission will require solving other subordinate problems, with their associated problem spaces. Before starting a mission, Soar creates agents (pilot/vehicle) for both own ship forces and opposing forces, each with its own identity (e.g. F-14, F-15, MiG-29, etc.) and call sign. An elaboration can amplify the definition of states, operators, agents, etc. in Soar.

CAS missions are handled a bit differently than others. Most missions are under control of some group (e.g. AWACS), but the FAC in a CAS missions does not really control the mission in the sense that a WD does for OCA/DCA. Soar recognizes this distinction. The typical, standard, "nine-line brief" is also incorporated into Soar for CAS. Targets can include air, tower, road, armor, bunker, command-post, artillery, and convoy. It appears that Bomb Damage Assessment (BDA) is either high or low depending on criteria applied to miss distance. New targets are treated as "available missions" and replanning a mission is included in Soar to handle cases like this. Special instructions (SPINS) for CAS are considered.

SPINS categories include: Control points, communication plan, frequency color codes (color and frequency), and daily code words. Control points include: entry-exit points, holding points, contact points, and initial points.

Communication plans include: agency, call-sign, circuit, color, and frequency. Daily code words have the following list of associated attributes: date, continue, cancel, change, and abort.

In examining the 22 pages of "states," there are 33 variables at the first level, one of which is a category called "input-link." The input-link values include ten sub-categories. Within these, a heading rate of change is identified but no roll rate nor any acceleration / deceleration appears in the list. These are typically included in most representations of vehicle dynamics, so it is not clear why Soar does not include these values for internal reference. The category "output-link" has 19 variables, all but four of which start with "desired" as a qualifier. Certain variables identified at one level also appear again at another level, such as RoE and waypoints. For waypoints, the order and kind of information included differs between the two lists. Without a better understanding of Soar syntax and processing, it is not clear why this was done.

Aircraft maneuvers appear to be controlled as step inputs. However, reference is made to plans to change the dynamics, so it is not clear how this is being done in any particular implementation. It needs to be checked. Some defensive as well as offensive maneuvering is considered, but neither seems very complete. Package elaborations indicate turn rates falling into the following categories: small, moderately-hard, medium, pretty-hard, and big hard. No other control inputs (pitch, yaw, flaps, throttle, etc.) were found, perhaps because not all of the code was reviewed. There is no check on whether the steering circle was achieved before firing; it is assumed that it was if the angle off is within the appropriate amount. Again, this ignores the 3D flight vector control problem and focuses on only simplified 2D dynamics.

Mission types include: strategic-attack, SEAD, and escorts (for either or both). Formations include: v, line abreast, and trail. Aircraft records are kept on position (latitude and longitude) as well as BRASH: bearing, range, altitude, speed, and heading. Bearings and ranges are presumed to be with respect to some bullseye.

US aircraft covered appear to include: 1) A-10 and OA-10, 2) A-6, 3) E-2C and -3C, 4) F-14D, 5) F-15 C & E, 6) F-16C, 7) FA-18, and 8) KC-10 & -135. The AC-130 was included but its site was not accessible. Soviet aircraft include: 1) MiG 21F, -23, -23M, -25P, and -29, 2) S-3, 3) Su- 17, -22U, -25, and -27, and 4) F-1E (sic). However, the documentation implies consideration has been given to incorporating many other vehicles. Data for those listed include: 1) fuel: minimum landing, joker margin, combat margin, total capacity, cruising consumption, and fuel transfer rate; 2) maneuvers: max-speed (max thrust when new dynamics are incorporated), attack speed, lowest desirable (just above stall), fast race track speed, slow grid search speed, intercept speed, and max. altitude; 3) missiles: optimal minimum range missile (mrm) range, and optimal mrm aspect,; and 4) transit parameters: turn rate, radar mode (e.g. scan rate), min. speed, normal speed, max. speed, most efficient speed. Values are metric though, so they are not easily interpreted (in terms of knots, etc.). Reasonableness of the values provided was not assessed.

In some cases, additional data are provided for specific aircraft. Often (not always) a generic "name" is associated with the designation, e.g. "Hawkeye" for the E-2C, "Tomcat" for the F-14D, and "Eagle" for the F-15C. The type of radar used by a platform may also be included (only the APG-71 is mentioned, and it is shown for the E-2C, F-14D, F-15C/E, F-16C). Fighters may include a radar warning receiver (RWR, the ALR-67 is the only system mentioned) and specific weapons load (AIM-54, AIM-7, and AIM-9 for the F-14D). The OA-10 has no radar or RWR, but carries (only) the AIM-9. The F-15C / E and F-16C are given an AIM-120 instead of the AIM-54. Surprisingly, the FA-18 is given neither radar, RWR, nor AIMs. Avionics and missile load are not specified for the MiG-21F, MiG-23M, or MiG-25P but are for the MiG-23 Flogger: slot-back radar, SPO-15 RWR, and AA-2, AA-8, AA-10, and AA-11 missiles. The MiG-29 Fulcrum is given the same equipage, except it does not have the AA-2. The Su-17 Fitter (and Su-22E Fitter-E) has no radar, RWR, or missiles associated with its data table, but the Su-25 Frogfoot is given an AA-8 (only). The Su-27 "Fulcrum" (sic) is given the AA-8, AA-10, and AA-11. This suggests that avionics capabilities and limitations are not well-treated in these models (or that additional data is provided elsewhere, and we saw no evidence of that).

The Soar code that appears to load the vehicle data is actually set up into categories of Air Force, Navy / Marine, Op For (Opposing – basically Soviet equipped – Forces), UK, and Other aircraft. GCI and controller are included separately in this same list of "vehicles." The list includes some entries for Air Force aircraft not found in

the aircraft data tables: EC-130E, F-117, RC-135, MC-130 EH/NP, U-2R and the MH-53J and MH-60G helicopters, presumably vehicles which may be added later. Navy aircraft in this list but not in the data tables included: AV-8B, EA-6B, EP-3E, ES-3A, F-14B, and four helicopters. Two versions of the FA-18 were also recognized: C and D, which were not distinguished in the data tables. The Soviet aircraft listing did not differentiate the models of the MiG 21 or -23 as the data tables did, and the Su-22 and -27 were missing from the list. The F-1 and BTR-60PU were included, but the latter was not in the data tables. These mismatches make it somewhat difficult to determine just what the code really does and does not do.

An attack plan includes: attack-geometry, attack-entry, attack-delivery, attack-altitude, and ordnance. Weapons loads are maximums, not what might realistically be carried. Timing includes consideration of wingman, if there. Target attributes include its priority, size, and whether it is stationary. Some preliminary thinking about cloud cover problems has been done, but apparently has not yet been completely implemented. Ordnance is either programmed or low-level-release. Some consideration is also given to terrain, but it is not clear how terrain elevation is treated (other than simply to consider target elevation versus aircraft altitude). Entry types include: level, pop-up, and standoff-pgm – with many different entry and delivery ranges considered (but all appear to be pairs of fixed values). Attack geometry appears to consider possible threats, but how that is done is not clear (it appears binary: there or not; and the consequence of the answer is not apparent). Ordnance selection explicitly includes HARM, Maverick, and weapons bay. It also implicitly includes other categories of ordnance (see section 3.2.7 that follows). While Maverick is mentioned in ordnance elaborations, it was not included here in ordnance selection or in the verbal communications list.

The amount of emphasis on bingo and joker fuel estimates suggests possible over-kill. It is not completely clear how all of the implied planning is actually implemented in the pilot's cognitive processing. The planning may simply be there to set up the problem space appropriately, but the actual sampling of one's fuel level probably would not be as frequent or as detailed as it appears to be in this representation. Again, that may be a misinterpretation based upon not understanding well how to interpret the Soar source code. Only one burn rate (cruising) appeared to be considered, and it appears to be a constant. Tank capacity and refueling are considered. Calculations of burn are done leg-by-leg for the planned route of flight. At a minimum, some consideration of climb, acceleration, deceleration, etc. would help improve these calculations, but it is more important to first determine how they are used before deciding whether they even need improvement.

A 4-ship formation appears to be as large as things get, but there may be strike packages with three 4-ship formations. However, up to 4 ships are counted in each of up to four groups of bogies. Participants are identified by two alphabetic characters as: a flight lead (fl), first wingman (fw), a second lead (sl), and the second wingman (sw). Once the targets have been detected and assigned, emphasis is placed on maneuvering into the lar (0-40 degrees aspect, ideally 15-25, and in-range). Two key concepts are: 1) keeping lateral separation at about the same value as aircraft altitude to allow adequate turning room, and 2) estimating lateral separation as approximately 100 x range x aspect angle -- a general "rule of thumb." Provisions are made for reforming the group if a member is "lost" – for whatever reason. An F-Pole maneuver is typically implemented as a defensive move after missile launch. While most of the logic is geared at own-ship, and provisions are made for inter-ship communication, it is not entirely clear how group maneuvers and tactics are executed.

Commit criteria are specified in terms of: 1) position limits (latitude / longitude high and low values), 2) bearings (high-low), 3) angles off(high-low), 4) aspect angle (high-low), and 5) range (no-earlier-than and no-later-than). Comments in the Soar code indicate that the lower range bound is not really applicable: always commit, but by now you certainly should have done so, and if not, do so! Altitude was not in this list. The evaluation results in either a YES or a NO as to whether the commit criteria were achieved.

There is also some code which assures the model trudges on even if things went sour. The mission will be restarted at some prior point to see if recovery can be accomplished. Restarts can occur from launch (the beginning), a point, a route, or from the detection point of some generated error message. One type of error that is checked is deviation from a point or route. The implications of this procedure are not entirely clear. It forces a continuation where a halt might be better. If only used during debugging sessions, it would presumably not have any impact on run-time operation of the model. If used during run-time of the model, processing can continue, and

it is not clear what kind of spurious effects such restarts might then inject into companion simulations (like ModSAF to which AirSF interfaces). Again, the logic of this has to be worked through in greater detail than was possible here.

There are some "known" bad (or at least questionable) assumptions built into the model (e.g. in radar elaborations). In treating the decisions associated with determining whether we think the bad guy has us locked up, it was assumed that the bad guy's radar capabilities were the same as ours. Other assumptions could have been made that would be a bit more realistic, but what impact that would have is not clear until some comparative analysis is done.

3.2.7 Verbal Communication

"The vocalization elaborations allow the radio messages generated by an agent to be played on the computer's loud speaker." There are some caveats about what data files are needed to do so, and where they must be placed. Unfortunately, the radio message list seems somewhat limited. It consists of: 1) call signs (mine / others'), 2) qualitative compass directions (n, nne, ne, ene, etc.), 3) numbers (any), digits (0-9), hours (0-23), minutes and seconds (0-59), 4) angles (thousands), 5) heading (1-360 or 0-359 not specified), 6) range (unit not specified: slant or ground: in kilometers, statute miles, or nautical miles), 7) hostility (red or white), 8) colors (blue, red, white, violet, silver, orange, black, green, yellow, or indigo), 9) latitude or longitude, 10) waypoint name, 11) 9-line brief symbol for relative heading (left, right, none, or not applicable), 12) vehicle (type), 13) target description (tanks, bunker, or vehicle type), 14) marker type (laser, beacon, wp-rocket), 15) mission code words (fixed set of 8), 16) attack geometry (90-10, split, direct-to-target, or trail), 17) entry type (level or pop-up) and delivery (only laydown indicated), 18) qualitative altitude-range (low-level, medium-level, or high-level), 19) ordnance type (smoke bomb, MK-82, MK-84, GBU-10, GBU-15, Exocet, HARM, BLU-73B, BLU-87 AB, ISCB-1, Rockeye, CBU-87B, DAACM, MK-82-Regp, MK-83-Regp, or MK-84-Regp), 20) distance (in meters), 21) letter (A-Z) and their phonetic representation, 22) relative direction (right / left), 23) military time in hours and minutes (e.g., 1425), 24) formation type (line-abreast, combat-spread, cruise, bearing, parade, fighting-wing, trail, wall, box, offset-box, or vic), 25) formation sub-type (defensive, offensive, short, or long), and 26) CAS-remarks (none, expect-multiple-runs, and heavy-small-arms-fire-request-multiple-runs-for-30-minute-loiter).

Other message strings could be incorporated like CAS-remarks. It appears that many unique messages could be generated by combining terms that are already in this lexicon, but the mechanics for doing that were not immediately clear, so the limitations imposed are unknown. This is an area that needs further examination in reviewing Soar code capabilities: top-ps/vocalize-elaborations.soar.

3.2.8 SRI's CommandTalk

In a follow-on to STOW, Soar will be linked with SRI's CommandTalk in order to enhance its verbal communication capabilities. Command talk documentation is available on the web at the following URL:

http://www.ai.sri.com/~elesaf/commandtalk.html

The web page at that site explains that, "CommandTalk is implemented within the DASLING (Distributed-Agent Spoken Language Interfaces based on Nuance and Gemini) framework for spoken-language interface applications. DASLING combines the Nuance speech recognizer (a commercially available system based on SRI-developed technology) with SRI's Gemini natural-language understanding system, using SRI's Open-Agent Architecture."

The site has three brief overview documents: 1) The CommandTalk web brochure (an overview of the interface for the Marines' Leathernet System), 2) The CommandTalk Grammar Browser Versions for AirSF, ArmySF, MCSF, and NavySF versions of CommandTalk), and 3) ModSAF Agent Layer Language (21 pages). The CommandTalk Grammar Browser for AirSF consists of: 1) a 13 page description of categories of words and phrases (applied with different rules to create varied expressions), 2) a 28 page list of vocabulary (much of which are minor variants: like plural vs. singular forms, synonyms, etc.), and 3) a 3 page browser help sheet. The Grammar Categories of words and phrases provides a list with two links: 1) rules that use a category, and 2) ways the category

can be expressed (how the category is defined). This is a voluminous set of materials, and not immediately intelligible without further instruction. The browser help sheet provides an introductory set of instructions, illustrating that any phrase requires constructions using one or more pointers, sometimes to other rules as well as to specific word categories. For example, the digits zero through 99 can be phrased at least three different ways: saying a digit, saying a "teen", or saying some decade and a nonzero digit, but there is a rule for any digit: it consists of either the non-zero digits or the number zero.

"Every voice command that AirSF CommandTalk can understand can be constructed by expanding the definition of one of the top-level categories shown on the grammar browser home page. If there is more than one top-level category shown there, it means that the system expects different commands in different situations." The User's Manual provides further explanation.

Two GNU-compressed postscript documents (most easily handled by a UNIX machine) are also downloadable: 1) CommandTalk: A Spoken-Language Interface for Battlefield Simulations, and 2) CommandTalk 2.0 Language Description. The first document is a nine page article with three references. It explains that Nuance has been modified to make it more sensitive as a speech recognizer (16 versus 8 bits). Also, the full power of Gemini is not exploited in this application, because the vocabulary can be constrained. A Contextual Interpreter (CI) takes the Natural Language (NL) logical forms (limited to what is in the uttered statement) and converts them into ModSAF commands (by adding context (situation) dependent information, often from ModSAF itself). This may take some interaction (a series of queries) to interpret the utterance properly in the current context of a ModSAF scenario, drawing on the following kinds of resolvers or CI agents: noun phrase, predicate phrase, temporal, or vagueness, each of which are explained in this paper. CommandTalk will run on Sun SPARC or OS workstations and SGI MIPS/IRIX platforms, and CommandTalk is available at no cost to Government users, under restricted rights, and may be licensed by contractors for use on government projects.

The CommandTalk 2.0 Language Description is a 34 page manual that describes the language that can be processed, but not necessarily converted into ModSAF commands, since some may be understood but not yet convertible. This manual helps understand the power and flexibility of the language, illustrating how it works and explaining the conventions used in their language description. Provisions are made for a wide body of varied expressions, all of which might mean the same thing. For example cancel that = delete that = undo that, where that = last command or some point, line, or unit. Provisions are also made for allowing the speaker to append one simple command with other simple commands to get compound commands (e.g. climb to and maintain FL "x" on heading "xxx").

In any case, checks are made to be sure the interpretation "makes sense" and if not, a message is issued indicating the command was not understood. Section 2.0 of the manual describes Action Commands, rules for subphrases peculiar to these action commands, and ways of modifying and conjoining them. Because most of this was developed for the Marine Corps, the commands are largely driven by the need to control ground forces in combat. Air combat would require developing a different vocabulary and rule set, but the methodology appears sufficient for doing that. There are already several relevant commands: FLY to ... , from ... (some point or line); LINK (rendezvous) with ... (at: ...); and weapons status = (hold tight free); plus others that could be modified.

Modifying actions can come before or after a command, e.g. "on my order" ... or "when" (condition / time), etc. Also, commands can be issued to the simulation system, not just to the simulated entities or agents. This facility aids in setting up scenarios or making modifications to them. It can also be useful in looking at the results of scenario execution. It provides a voice-driven instructor / operator station interface. Also, this facility allows the user to ask for something that is not conditionally dependent on the current contents of the display screen (which is a limitation of menu driven systems: something has to be there to select from in order to change the display).

A number of different units are already captured in the vocabulary and phrase sets. These include some air assets (none Air Force), and many more ground assets. The vocabulary and rule set also is well-developed for describing locations on the ground (points, lines, coordinates) and times. Basic numbers, the phonetic alphabet, limited (six) color names, selected (seven) bird names, and the eight cardinal directions are all incorporated in the vocabulary. Rules exist to use these in specifying distances, orientations, and scales. The "nine-line" brief used by

FACs is already encoded. So, the ability to support CAS and interdiction missions should be quite easy to accomplish (e.g. communications between FACs and pilots).

The ModSAF Agent Layer Language (MALL) is not limited to communicating with a ModSAF simulation, but that is its primary purpose. "This document presumes a significant background knowledge of ModSAF's Persistent Object (PO) database." Also, "Messages in the Open Agent Architecture are implemented as strings which encode Prolog terms." Prolog is a programming language designed specifically for implementations of predicate logic statements, often encountered in applications of artificial intelligence. A brief explanation of Prolog term syntax is provided for the reader. In dialogues with ModSAF, two kinds of command modes exist: 1) setup mode that affect future actions, and 2) simulation mode, which has an immediate impact on on-going activities. Apparently, there is provision for changing the rules of engagement for a particular simulated unit, at least in terms of firing: free, tight, or hold. CommandTalk expects that its MALL will grow to provide: 1) more comprehensive coverage of persistent object types for query, creation, and modification functions; 2) "more complete use of symbolic constants when appropriate;" and 3) new messages for dealing with multiple ModSAFs and several concurrently running databases of POs.

For those not familiar with Army map designations (Universal Transverse Mercator: UTMs), they are represented by five arguments in MALL: 1) zone number (2 digits), 2) zone letter (single uppercase alphabetic character), 3) map sheet (two uppercase letters), 4) Easting (5 digit number), and 5) Northing (another 5 integers). A point on the earth denoted by latitude and longitude can be expressed in equivalent UTMs. The F-16 navigates by latitude and longitude but can bomb by UTM coordinates (e.g., for CAS missions). Another unexplained concept found here is h-hour: typically some "stop" point in a planned activity, where everything pauses unless some stipulated condition has been met (e.g., authorization to execute the planned activity). It can be used to assure that everyone gets to some initial position before starting the execution of a coordinated mission or maneuver, which is carefully timed from h-hour.

3.3 Designer's Edge and Training Needs Analyses

Designer's Edge training needs analysis templates for Expert Analysis, Focus Groups, Audience Analysis, and Organizational Analysis were modified and tailored to support the data collection effort. The Common Errors form was useful "as is." The Expert Analysis form was essentially a structured interview, conducted one-on-one with two different SMEs. The Focus Group form was used with two SMEs, both at the same time, one of whom had participated in the Expert Analysis interview prior to the Focus Group discussion. Capt. Bryza also participated in answering questions posed on the Organization Goals survey, but it was not possible to interview others in the 607th ACS as originally planned.

Data gleaned from the SME exchanges were used to develop a set of needs, goals, and learning objectives, using Designer's Edge. These were then incorporated into a Needs Analysis Report, a standard Designer's Edge output product that reformats the data and prompts the addition of supplemental, supporting text. This proved to be an excellent tool for documenting the front end analysis required by the ISD methodology (Meister, 1985). A Mission Statement Report was also prepared, outlining the recommended schedules for three follow-on activities, described below in section 4.0.

3.3.1 Simulation Deficiencies

While the MCE has its own built-in simulation capabilities, these are not satisfactory for several reasons. First, it takes a large effort to design, implement, and then exercise any credible scenario script. Second, the exercise of the scenario script requires using personnel to act as pseudo-pilots who: a) do not understand what pilots do or how they do it, and b) do not understand how to operate the MCE console proficiently. As a consequence, the pacing of events is destroyed even if the scenario was perfectly credible. However, it is impossible to implement a credible script, because that would require anticipating perfectly what every one might do for the entire duration of the mission, which – even if possible – would imply no spontaneity at all on the part of anyone.

What the Instructor WDs want is a rich, flexible simulation environment that they can "control" – such that a more experienced WD student can be challenged by unexpected activities (initiated by the instructor), increasing workload stress when appropriate to do so. This means the simulation should incorporate reasonably intelligent artificial agents as enemy bogeys. It also implies that own-force aircraft should be able to respond intelligently to re-direction, without pseudo-pilot intervention. That means being able to initiate and respond to voice communication when and as appropriate. The ability to re-start and re-play segments of a scenario would be important, and the difficult part is to determine what portions of the scenario should be identical versus comparable (but varied) from the prior execution.

3.3.2 Specific Training Needs

Currently, a number of activities which occur in theaters of operation are not required in garrison. While some changes in current practice may be sufficient to compensate for lack of experience gained in garrison, and simple training remedies can be proposed for certain other identified training needs, there is a legitimate need for developing a better simulation of theater operations: one that properly prepares people for the type and tempo of operations they will encounter overseas.

In garrison, there is no need to deal with the complexities of daily combat operations. Practicing the daily set-up activities is important but not done currently. Some degree of simulating activities associated with the destruction of classified materials would help people get used to what is required, but this could be over-done with little real benefit. The set-up activities include: 1) using the HAVE QUICK radios (which are not normally used in garrison but are available), as well as using other secure communication facilities, 2) loading a large Air Tasking Order (ATO) daily, 3) reprogramming radio communication and datalink capabilities, 4) using code words and researching call signs, and 5) handling large scale operations, including multiple LFEs. Building the simulation should include building the ATO datasets that correspond to the scenario, thus giving units the opportunity to practice load and verification procedures as an inherent part of the simulated exercise.

Part of the requirement for better simulation comes from the need to accomplish two things: 1) getting all six crew members actively engaged in an exercise, and 2) imposing realistic levels of workload. Present simulations are best suited to individualized training, and while that is necessary, it is not sufficient. There are at least two levels of operator training needed: 1) familiarity with how to operate the equipment console, and 2) being able to adapt and apply that knowledge to the specific combat situation being handled. "Switchology" is what is presently emphasized in existing training, and adaptation / application is what is needed to better prepare for theater operations. In garrison, there is no opportunity to get experience working with LFEs: they simply do not occur because they require multiple aircraft opposing multiple aircraft. LFEs must be simulated if they are to be learned.

Because garrison operations do not involve LFE, there is no real incentive to operate as a full combat team. Most OM training is with a smaller set of crew members, so coordination and teamwork are different than would be experienced in theater operations. Simulating LFE would require assembling the full combat team, and the imposed load level would require the kind of collaboration and cooperation that are needed in theater operations. This experience would give crews the confidence they want to have prior to deployment (knowing they could "keep up" with the pace of combat and not fall behind). On one wants to do a bad job, but unless they have some experience doing what is expected, crews are understandably anxious about whether they can do the job well or not.

4.0 Recommendations

The development of an improved simulation for MCE operator training should adopt a system engineering approach. A concept of operation and operational requirements need to be formulated that adequately reflect the users' requirements (i.e., what the 607th ACS wants to have). This ought to be formally reviewed and approved by the 607th CC (ACS Commander) and DO (Director of Operations) after both MCCs have reviewed the document for content accuracy.

Based on the Operational Requirements Document (ORD), the basic functional requirements must be identified and then documented a formal specification: the Functional Requirements Document (FRD). Once the functions have been identified and related to one another, the preliminary and detailed designs should lead to the documentation of the technical requirements: what must be done and how well in order to provide the desired simulation and training capabilities. This Technical Requirements Document (TRD) will identify quantitatively what has to be done to meet the FRD, which in turn meets the ORD. This allows complete traceability of the requirements from user needs to functions and from functions to actual capabilities (hardware and software items) that provide the capability to meet requirements. This assures that nothing was inadvertently left out and that everyone agrees on exactly how the requirements will be met (and where: in hardware and software).

Once the requirements are defined at this level of detail, tradeoffs analysis can be performed. These will examine the various approaches to meeting those requirements, determine the advantages and disadvantages of those approaches, and select the approach that is regarded as best. It is already clear that a number of existing products could be interfaced to provide the capability needed. Presently, the problem is that these proposed solutions are being pursued before the requirements are properly defined. That can lead to surprises later, when the demonstrated capabilities are discovered to be less than what is needed, because the requirements were not identified apriori as recommended here.

Two kinds of analysis are still required that were not done during the present study. First, identify the "switchology" necessary and sufficient to carry out all of the operator actions that will need to be exercised during training scenarios: what sequence of FOG (finger-on-glass) and other switch actions (FS and VS) have to be implemented (and which can safely be ignored)? Second, what is the complete vocabulary, syntax, and grammar for operator communication with pilots (and conversely: pilots with operators)? This will be needed both for data analysis during training and for enhancing CommandTalk and Soar in the AirSF modeling.

Finally, someone needs to prepare the training materials which will be needed to use the simulation that is developed and to provide instruction in the other areas where needs were identified that simulation will not by itself address: handling of classified, datalinking to AWACS (and or other sites), and improving self-esteem – an attitudinal training problem.

Preliminary schedules for these threes activities are as follows:

A. Simulator Development

Oct. 1997 Finish Defining 607th ACS' Training Requirements
Nov. 1997 Define Concept of Operation for Mission Simulator
Dec. 1997 Define Operation Requirements Document for Mission Simulator
Jan. 1998 Define Functional Specification for New Mission Simulator
Feb.-Mar. 1998 Define Technical Requirements for Implementing Simulator Functional Specifications
Apr. 1998 Perform Tradeoff Analysis of Simulation Options: Build New or Modify Existing Package
May - July 1998 Design Simulation
July - August 1998 Develop Simulation
September 1998 Test Simulation and Training Materials

B. Training Development

Oct. 1997 Complete Common Error Analysis and Audience Analysis
Nov.-Dec. 1997 Develop Course Map for Training Materials
Jan.-Feb. 1998 Develop Storyboards for Content of Course Map
Mar.-April 1998 Develop Mission Scenario Scripts
May - June 1998 Develop Lesson Storyboards
July-August 1998 Develop Training Materials
September 1998 Test Training Materials with Simulator Testing

C. Data Analysis System Development
Oct.-Dec. 1977 Identify ACC / ACS Measures of Effectiveness
Oct.-Dec. 1977 Identify ACC Measures of Performance
Jan.-Mar. 1977 Identify Vocabulary and Phrase Construction Rules for Pilot-Controller Communication
Jan.-Mar. 1977 Develop Switch Action Models and Action Logic Diagrams
Apr.-June 1977 Develop Software Design for Capturing Voice Communication and OCU Switch Activities.
July-Aug. 1977 Develop Code for Implementing Data Capture / Data Reduction
September 1977 Perform Data Analysis of Test Results & Identify Model & Software Deficiencies

REFERENCES

Allen, R. J. (1994), "Who Had Better Be on First: Getting Optimum Results from Multimedia Training," in J. Keyes, editor, The McGraw-Hill Multimedia Handbook, McGraw-Hill, Inc., New York, NY.

Eddy, D. R. (1989), Selected Team Performance Measures in a C3 Environment – An Annotated Bibliography, Technical Report USAFSAM-TR-87-25, USAF School of Aerospace Medicine, Brooks Air Force Base, TX.

Eddy, D. R. (1990), "Performance-Based in Individual and Team Complex Decision Making," Proceedings of the Seventh Annual Workshop on Command and Control Decision Aiding, Air Force Institute of Technology (AFIT), Wright-Patterson Air Force Base, OH.

Eddy, D. R. and C. A. Shingledecker (1988), Synthesis of Performance Measures for the C3GW, Interim Report on Research and Development, CDRL 14, Contract F33615-87-D-0601, Sustained Performance Branch, Brooks Air Force Base, TX.

Fuld, Robert B. (1997), "V & V: What's the Difference?" Ergonomics in Design, July, 28-33.

Hall, Ellen P., Sherrie P. Gott, and Robert A. Pokorny (1995), A Procedural Guide to Cognitive Task Analysis: The PARI Methodology, AL/HR-TR-1995-0108, Human Resources Directorate, Manpower and Personnel Research Division, Brooks Air Force Base, TX.

Klinger, David W., Stephen J. Andriole, Laura G. Militello, Leonard Adelman, Gary Klein, and Marie F. Gomes (1993), Designing for Performance: A Cognitive Systems Engineering Approach to Modifying an AWACS Human Computer Interface, AL/CF-TR-1993-0093, Crew Systems Directorate, Human Engineering Division, Wright-Patterson Air Force Base, OH.

Laird, John, Paul Rosenbloom, and Alan Newell (1986), Universal Subgoaling and Chunking: The Automatic Generation and Learning of Goal Hierarchies, Kluwer Academic Press, Boston, MA.

Marca, David and Clement McGowan (1989), Structured Analysis and Design Technique (SADT), McGraw Hill Book Company, New York, NY.

Meister, David (1985), "Instructional Systems Development," in Behavioral Analysis Techniques and Measurement Methods, Wiley, New York, NY.

Militello, Laura, and R. Hutton (in press), "Applied Cognitive Task Analysis (ACTA): A Practitioner's Tool Kit for Understanding Cognitive Task Demands," Ergonomics: Special Issue on Task Analysis.

SUITABILITY OF ASCIDIANS AS TRACE METAL BIOSENSORS-BIOMONITORS IN MARINE ENVIRONMENTS: AN ASSESSMENT

Sneed B. Collard
Professor
Biology Department

University of West Florida
11000 University Parkway
Pensacola, FL 32514

Final Report for:
Summer Research Faculty Program
Armstrong Laboratory

Sponsored by:
Air Force Office of Scientific Research
Bolling Air Force Base, DC

and

Armstrong Laboratory

August 1997

SUITABILITY OF ASCIDIANS AS TRACE METAL BIOSENSORS-BIOMONITORS IN MARINE ENVIRONMENTS: AN ASSESSMENT

Sneed B. Collard
Professor
Biology Department
University of West Florida

Abstract

Ascidian tunicates are filter-feeding benthic invertebrates known to concentrate a wide variety of trace metals of no known biological function in their blood and tissues. An investigation was initiated to determine whether wild populations of these organisms could reliably be used to monitor trace metal enrichment in marine ecosystems. Research was conducted in St. Andrew Sound, a shallow marine lagoon bounded by Tyndall Air Force Base, Florida. The present report summarizes habitat preferences, seasonal distributions and the relative abundance of dominant ascidian taxa in the lagoon. Many of the 21 species collected have some potential use as trace metal biomonitors. However, only *Styela plicata* and *Molgula occidentalis* are present in abundance year-round, occupy all major habitats, and are easily maintained in laboratory conditions. Significant intra- and inter-colony phenotypic variation in *Didemnum*, *Diplosoma*, and *Distaplia* species resulted in equivocal identification at the species level, and the geographic and/or seasonal distributions of *Trididemnum*, *Clavelina*, *Eudistoma*, *Aplidium*, *Ecteinascidia* and *Botryllus* species were limited, or restricted to uncommon habitats in the lagoon. Taxonomic uncertainties and low survivability of didemnid and polycitorid colonies in laboratory conditions suggest that use of these taxa in metals accumulation/toxicity bioassays, or in environmental assessments, is impractical.

SUITABILITY OF ASCIDIANS AS TRACE METAL BIOSENSORS-BIOMONITORS IN MARINE ENVIRONMENTS: AN ASSESSMENT

Sneed B. Collard

Introduction

Ascidian tunicates ("sea squirts") are numerically abundant, ecologically important members of filter-feeding guilds in marine epibenthic communities from shallow subtidal to abyssal depths. Many ascidians have wide biogeographic distributions, and a number of continental shelf species occur circumglobally within broad, temperature-defined faunal provinces (e.g., boreal, warm temperate, tropical seas). These sedentary tunicates colonize surfaces comprised of unconsolidated sediments, biogenous deposits, wood, metals, plastics, glass, seagrasses, mangroves, and the tests, shells, and exoskeletons of other marine invertebrates, including non-conspecific sea squirts. Hundreds of individuals or colonies may occupy a given square meter of substrate. In high salinity embayments (e.g., deepwater ports) sea squirts are conspicuous members of fouling communities that may completely cover subtidal portions of man-made structures such as piers, pilings, seawalls and ship's hulls.

With few exceptions, sea squirts obtain food by pumping large volumes of water through an elaborate branchial basket within which organisms and particulates as small as 0.1 μm are retained on a continuously moving sheet of mucus produced by an endostyle. Plankters and particulates too large for processing are detected by circlets of tactile tentacles located beneath the branchial (incurrent) siphon, and these are ejected by means of a rapid contraction of the siphonal muscles. Substances entering the branchial basket are trapped in mucus and moved by cilia into the gut. Filtered water passes through stigmata in the branchial basket, where it is forcibly expelled from solitary individuals or colonies through a muscular atrial siphon or, in some colonial forms, a common cloacal opening. Gametes, embryos, larvae and fecal pellets are ejected into the water column by this stream of excurrent water {1}.

Members of all ascidian orders extract some iron or vanadium from seawater and/or their bioseston and plankton forage. However, only the phlebobranchs are known to accumulate Fe and V in their blood and tissues at high concentrations (10^6-10^7 that of ambient seawater) {2}. The sites and mechanism(s) of Fe and V capture, sequestration and at least in the case of vanadium, detoxification,

remain unknown. Iron and vanadium have uncertain biological function(s), but putatively participate in the polymerization of cellulose-like polysaccharides (α-*L*- glycans), which form the structural matrix of the tunic of some (e.g., *Styela plicata*), but not all ascidians. In contrast to the phlebobranchs, some aplousobranch ascidians (*Didemnum* spp., *Tridemnum* spp.) accumulate strontium at higher than ambient concentrations {3}. This metal is believed to be incorporated into the stellate spicules characteristic of most of the didemnid genera {4}. Other metals, including Ag, Al, As, Ba, Cd, Ce, Co, Cr, Cs, Cu, Eu, Ga, Ge, La, Mn, Mo, Nb, Ni, Pb, Ru, Se, Ta, Tc, Th, Ti, W, Zn and Zr have been found in ascidians at levels above, or much above, average ambient seawater concentrations {5}. A majority of these elements (e.g., Ag, Ba, Cd, Ni, Pb, W) have no known metabolic function, and many are toxic to marine organisms at low concentrations.

Because they are common in most in marine benthic habitats where salinities exceed ~20-25 psu and accumulate trace metals in significantly greater concentrations than normally found in seawater, ascidians were considered to be good potential candidates for utilization as *in situ* trace metal sensors (see Table 1). The initial phase of assessing this potential — the species problem, is discussed in the present report. Aspects of the ecology of ascidians in St. Andrew Sound are discussed in {6}.

Table 1. Desirable characteristics of biological sensors possessed by ascidian tunicates {e.g., 7}.

All species:
Are sedentary as adults
Filter large volumes of water and retain small particulates
Many species:
Accumulate and tolerate a wide variety of trace metals
Live long enough to permit analysis of different age groups
Are large enough to provide adequate amounts of tissue for analysis
Are numerically abundant and widely distributed
Have a high concentration factor for certain metals — preconcentrations are not necessary
Accumulate metals in proportion to their concentration in sea water
Are easily collected from shallow water habitats
Are hardy enough to survive and reproduce under laboratory conditions

Methods

Field and laboratory investigations of ascidians were conducted during 1995-1996 and June-August 1997 in St. Andrew Sound, a shallow, relatively pristine marine lagoon on the Gulf of Mexico coast of the Florida Panhandle {8}. Systematic, morphological and reproductive studies were based on 152 multi-species collections from eastern portions of St. Andrew Sound. Most collections were photographed immediately after capture using Kodak Vericolor III/ISO 166 color print film with Minolta, Nikon, Pentax or Cannon 35 mm SLR cameras equipped with polarizing filters.

Sound-wide field surveys of ascidians were conducted at irregular intervals during each season and following episodic climatic and biological events (e.g., hurricanes, heavy rains, toxic algal blooms) while wading or snorkeling. A trynet was used to collect *Molgula occidentalis* from deep, turbid water. Collections were made in monospecific and mixed-species seagrass meadows (*Thalassia testudinum* and *Halodule wrightii*), and from unvegetated mud, sand and shell hash sediments. Except for the genera *Didemnum* and *Molgula*, ascidians were also collected from nylon, cotton and polypropylene ropes, lattice-like aluminum grids, plate glass, and sheets of galvanized metal suspended from a dock supported by weathered, creosoted pilings in water 1-3 m deep. Artificial substrates were deployed from this dock to facilitate observations of recruitment and successional sequlae at a single location in the Sound where environmental variation in plankton, temperature, salinity, turbidity and dissolved oxygen between closely spaced collection sites (artificial substrates and pilings) was presumed to be minimal. Observations of ascidians on artificial substrates were recorded at intervals of 2-10 days. Colonial *Aplidium* spp. were collected from pilings standing in moderately hydrocarbon-contaminated water at a boathouse located ca. 60 m northeast of the dock. *Aplidium* spp. occurred only on these pilings, and were the largest tunicates (up to 11.8 kg wet weight) collected during the multi-year study.

Collections were returned to the laboratory in seawater and narcotized for 2-6 hours in ethyl 3-aminobenzoate methanesulfonic acid ("MS 222"). Other narcotizing agents (e.g., menthol crystals, potassium chloride, magnesium sulfate, ethanol) had no significant narcotizing effect, and MS 222, gave only partially satisfactory results. Following narcotization and (some) photographs of partially relaxed specimens, collections representing >1000 individual colonies were labeled and preserved in 10%

formalin-seawater for 24-48 hours. After removal of the fixative in water over a 24 hour period, thick (~0.1-1.0 mm) sections of preserved specimens were made with a razor blade. Thick sections were required to permit the anatomy of individual zooids to be viewed in their entirety. Using standard methods, sections were cleared in glycerol, stained with Harris hematoxylin, or dehydrated without staining in EtOH, and cleared in xylene or methyl benzoate. More than 400 permanent slides were made with stained and unstained sections mounted in Permount. More than 200 glycerol-cleared sections were retained in vials. Remainders of partially sectioned colonies were archived in 70% ethanol, as were additional intact colonies collected at the same time and location. Representative subsamples from all collections were sent to the U.S. National Museum, Smithsonian Institution.

Sections mounted in glycerol or Permount were examined using a Wild dissecting microscope equipped with a fiber-optic light source, and a Nikon EFD-3 phase contrast microscope at magnifications of 100-400 X. Photomicrographs of zooids and colony structures were made of images viewed through the microscope and captured on a computer monitor. Images were frozen onscreen, labeled, and printed with a Mitsubishi color video printer through a 586 Micron Millenia computer. The microscopic examination and photographic documentation of each section of a colony required up to 20 hours.

Results and Discussion

Three orders, six families, 11 genera and 21 species of ascidian tunicates were collected in St. Andrew Sound during 1995-1997 (Table 2). Of these, *Styela plicata*, *Molgula occidentalis*, *Didemnum* spp., *Diplosoma* spp. and *Distaplia* spp. were consistently the most abundant and widely distributed taxa observed. With exceptions noted below, the stolidiferans *S. plicata* (Styelidae) and *M. occidentalis* (Molgulidae), exhibited relatively little gross phenotypic variation, and information intended to be useful in assessing their suitability as trace metals monitors is discussed. Brief discussion is also given to non-trivial taxonomic uncertainties encountered during attempts to confirm the specific identities of *Didemnum* spp. and *Diplosoma* spp. (Didemnidae), and of *Distaplia* spp. (Polycitoridae). Detailed descriptions of the natural history and ecology of all species collected in the lagoon (see Table 2) are described elsewhere {1, 6}.

Table 2. Ascidian tunicates collected in St. Andrew Sound, Florida: 1995-1997.

Aplousobranchia

Didemnidae: *Didemnum conchyliatum* [= *D. candidum*]; *D. duplicatum* [= *D. vanderhorsti*];
Didemnum sp.
Diplosoma macdonaldi; *D. glandulosum*; *Diplosoma* sp.
Tridemnum savignyi

Polycitoridae: *Clavelina gigantea*; *C. oblonga*
Distaplia bermudensis; *Distaplia* sp. A; *Distaplia* sp. B
Eudistoma capsulatum

Polyclinidae: *Aplidium constellatum* [= *Amaroucium* spp.]; *Aplidium bermudae*
Aplidium sp.
Eudistoma olivaceum

Phlebobranchia

Perophoridae: *Ecteinascidia turbinata*?

Stolidobranchia

Styelidae: *Botryllus planus*; *B. schlosseri*
Styela plicata

Molgulidae: *Molgula occidentalis*

Species Accounts

1. *Molgula occidentalis*

Molgula occidentalis is a large solitary ascidian whose range in the Atlantic Ocean extends from south of Cape Hatteras to Brazil. It has also been recorded on the coast of California, perhaps as a result of accidental transport by ships. In the author's view, California records of *M. occidentalis* may be incorrect. Published descriptions strongly suggest that California collections represent an undescribed species of *Molgula*. *M. occidentalis* reaches its maximum abundance in the nearshore shelf waters of the Atlantic and Gulf of Mexico coasts of Florida, and it is the most abundant and widely distributed tunicate in subtidal benthic habitats of St. Andrew Sound. The species occurs year-round, in discontinuous patches containing hundreds to many thousands of single or pseudocolonial individuals in asymmetrical

clumps of two to more than ten animals. Collections from shallow water sediments commonly contained 200-300 *M. occidentalis* per square meter.

M. occidentalis live on the surface of, or partially buried in, relatively flat sediments. Many of the animals are anchored to the seafloor or to each other in pseudocolonies, by fine, thread-like filaments resembling the byssal threads of mussels. Sediment particles (primarily quartz sand), diatom frustules and other materials are attached to the surface of the thin, but tough leathery tunic by elastic filaments. After the removal of sand by gentle scrubbing with a wire brush, specimens are seen to have a translucent tan, brown or gray test through which the visceral mass and heart are visible. Details of filament production (production stimuli, cell types, chemical composition) and adhesion mechanisms are unknown and deserve further investigation. *M. occidentalis* tunic filaments appear to have the following possible functions: (1) attaching sand and other particles to the tunic (a) for structural support, and/or (b) to deter predators, and/or (c) to discourage fouling organisms; (2) attaching conspecifics to increase mass and resistance to displacement from favorable environents by currents; (3) to reduce gamete wastage and increase the probability of successful outcrossing. Interestingly, the only invertebrate fouling organisms found on *M. occidentalis* in St. Andrew Sound were other ascidians. *Styela plicata* and *M. occidentalis* commonly co-occurred in clumps, and small colonies of *Diplosoma macdonaldi* were occassionally found on upper portions of the tunic.

Most *M. occidentalis* found on the surface of hard-packed sand bottoms are unattached by filaments, and are moved about by the action of tidal currents. In soft mud or silt habitats most individuals are buried, with only their siphons protruding above the sediment-water interface. Mud habitats are often hypoxic or anoxic at the sediment surface, and the tunics of *M. occidentalis* in these reducing habitats are stained black. With some exceptions, *M. occidentalis* do not form pseudocolonies in hypoxic or anoxic habitats.

Both surface-dwelling and buried *M. occidentalis* are commonly found in seagrass habitats, where they remain during winter months when emergent leaves are not present. In shallow water (~0.2-1.0 m) the species appears to be equally abundant in seagrass meadows and in unvegetated areas.

Numbers of individuals tend to increase with depth. The species is rarely found on surface irregularities (e.g., oysters), vertical surfaces (e.g., pilings), or on substrates suspended in the water column.

Based on size alone, two distinct populations of *M. occidentalis* occur in St. Andrew Sound. The "normal" morphotype, while variable in color (light grey, beige, brown, black), attains a size of > 60 mm in diameter, and was abundant at all locations surveyed. *M. occidentalis* of this size are considered to be unusually large in other areas within their range. A "small", (10-15 mm) black morph was found only in the turbid, shallow water of a stunted *Thalassia testudinum* bed approximately 200 m west of the dock where artificial substrates were deployed. "Normal" morphs did not occupy the restricted area of the "small" morph's population. The population was located in summer 1993 and disappeared, for unknown reasons, in mid-summer 1996. Specimens of both "normal" and "small" morphs were identified as *M. occidentalis* by L. Cole (U.S.N.M.). Gross internal anatomical features of both *M. occidentalis* morphs were indistinguishable to the author, and no explanation is suggested for the occurrence of two size classes in the lagoon. "Blood" used in electrochemiluminescence experiments {9} was obtained from "normal" *M. occidentalis*.

Mass mortalities of shallow-water (<1-2 m) *M. occidentalis* often occur following large pulses of fresh water from heavy rains and stormwater runoff. The species apparently can not tolerate extended exposures to salinities less than ca. 30 psu, suggesting that this ascidian is stenohaline, but broadly eurytopic with respect to its temperature and dissolved oxygen tolerances. As suggested by its abundance in nearshore coastal waters, *M. occidentalis* may be, as is its cooler water ecological equivalent, *M. manhattensis*, tolerant to a variety of anthropic pollutants {10}. To the author's knowledge, *M. occidentalis* has not been examined for the presence of trace metals, but its large size, year-round abundance, broad Atlantic Ocean distribution, and observed physiological tolerance limits in a variety of benthic habitat types suggest that the species is a good candidate for use in coastal water trace metal monitoring programs.

2. *Styela plicata*

Styela plicata is the largest and most abundant year-round ascidian found on midwater artificial substrates (e.g., ropes, pilings, crab trap floats), and the second most abundant ascidian on natural

substrates in St. Andrew Sound. *S. plicata* is a common species of cool and warm temperate waters world-wide, occuring from the lower intertidal zone to depths of at least 100 m. Both *Molgula* occidentalis and *S. plicata* occur singly or form pseudocolonies. Unlike *M. occidentalis*, which is with rare exceptions found only on flat benthic sediments, *S. plicata* individuals and pseudocolonies readily colonize flat and irregular (e.g., oyster reef) benthic and midwater substrates and, for example, the shells of both live and empty scallop shells (*Argopecten irradians*), pen shells (*Atrina* spp.), and barnacles (*Balanus eburneus*). As noted, *S. plicata* co-occurs with, and is frequently found attached to *Molgula occidentalis*.

Aggregations of *S. plicata* on midwater substrates are often comprised of hundreds or thousands of individuals of various size and age groups. The number of individuals colonizing these habitats is limited only by the space available for recruitment and the weight of the aggregated population. *S. plicata* larvae are able to colonize most substrates and, with one exception, space does not seem to limit the size of aggregations: *S. plicata* larvae do not settle on midwater or benthic colonial ascidians or sponges, presumably because of antifouling chemicals or structures possessed by these animals. During optimal conditions (early spring through late fall in St. Andrew Sound), the weight of midwater aggregates may exceed 50 kg, and recruitment and growth continue until groups of attached individuals tear away from suspended ropes and pilings and fall to the sea floor. Many sloughed off individuals survive this abrupt change of habitat.

S. plicata aggregations are found on all midwater substrates in the lagoon, where they have no known predators, but their distribution on benthic sediments is patchy and unpredictable. Long-term observations suggest three partial explanations for this seemingly chaotic distribution. First, sea urchins, *Lytechinus variegatus*, one of the most abundant epibenthic invertebrates in the Sound, cover themselves with shells, algae, seagrass leaves and, very commonly, *Styela plicata,* during the day. Daytime excursions of *L. variegatus* are limited, but some movement occurs, particularly during crepuscular periods. When night falls, urchins release their assorted camouflage— including *S. plicata*, and become active foragers. It seems likely that *S. plicata* propagules are dispersed, as well as introduced to new areas of the lagoon by sea urchins.

Second, although *S. plicata* can survive exposure to the atmosphere at extreme temperatures (as evidenced by their survival on pilings and suspended ropes), they are not abundant in shallow water areas that are rarely exposed even during spring tides. The gastropod *Melongena corona* is the dominant epibenthic macroinvertebrate inhabiting shallow water areas where *S. plicata* is uncommon, and one of the few species known to prey on this ascidian. The author observed and videotaped *M. corona* detect, approach, attack and consume *S. plicata* in the field and in experimental conditions. *M. corona* is an opportunistic scavenger-predator (particularly on the saltmarsh periwinkle, *Littoraria irrorata*) whose distribution is restricted to very shallow water. The distributional overlap between *S. plicata* and its only observed predator is minimal, and *M. corona* does not climb pilings where *S. plicata* reaches its maximum abundance. Third, unlike *M. occidentalis*, *S. plicata* is not found in patchy hypoxic or silt-mud areas of the lagoon, and its distribution on the bottom generally corresponds to the distribution of consolidated sands, hard substrates and seagrass meadows.

Whereas the tunic of *Molgula occidentalis* is thin, leathery and encrusted with sediments, the tunic of *Styela plicata* is soft, massive (most of the mass and volume of the animal), aspiculate, and not encrusted with sand. Abrasive sand particles may offer *M. occidentalis* some protection from predators, and bulk may serve a similar function in *S. plicata*. The tunic of *S. plicata* is not indigestible by vertebrates — the species is used for human consumption in Japan and elsewhere. Bulk alone may not be the most important predator avoidance "strategy" employed by *S. plicata*, however. In the field, one of the most noticeable characteristics of the species is that its tunic is often almost completely covered with epibionts except during cold, winter months. While *S. plicata* tolerates short periods of exposure to air temperatures of 0°C, and survive water temperatures as low as 5-10°C for at least a week, many of their epibionts die, or slough off at these temperatures. Common epibionts include bryozoans, barnacles, algae, the nest-building mussel, *Musculus lateralis*, and perhaps most importantly, colonial ascidians (*Diplosoma* spp. and *Eudistoma capsulatum*), which themselves have few known predators. The envelopment of *S. plicata* by other organisms may be a selective advantage for the ascidian, and it is speculated that settlement cues to encourage the settlement of other invertebrates may be produced by the host ascidian.

Most authors report the lifespan of *S. plicata* to be less than a year, with sexual reproduction occurring at different times and for different durations, depending on location (which may be a function of photoperiod, food availability or water temperature). *S. plicata* in St. Andrew Sound live for two years or more, and reproduce sexually throughout the year in water temperatures below approximately 28-30°C.

Individual *S. plicata* filter about 70 L of water per day {1}, from which they trap and consume protozoans, some small metazoans and a wide variety of phytoplankton species, including toxic dinoflagellates. These ascidians have been reported to accumulate the following trace metals at above ambient seawater concentrations: Ba, Cd, Ce, Co, Cu, Fe, Mn, Nb, Pb, Sr, Ta and Zn. In addition, experiments conducted in our laboratory confirmed that *S. plicata* could survive indefinitely in water enriched with 1.0 ppm Cr(VI). Because of its broad geographic distribution and wide physiological tolerance limits, *S. plicata* exhibits characteristics of useful biological sensor and monitor of trace metals (Table 1).

Family Didemnidae

An extensive descriptive literature treats didemnid ascidians, which are among the most speciose and widely distributed of the aplousobranch families. Authors caution that phenotypic variability in the various genera (e.g., *Didemnum, Diplosoma, Tridemnum*) makes them extremely difficult to identify with confidence. Didemnid specialists also note that the unusual and varied reproductive modes exhibited by different zooids within a single colony may differ; that reproduction between colonies in the same location at the same time may differ; and that different colonies in the same or different geographic areas may have, for example, different colors, growth patterns or spicule densities. Recent claims that spicule morphology could be used to distinguish species were found to be unwarranted by the author. Within-colony spicule populations varied in both size and shape in all didemnid colonies examined. The chemical composition of spicules may or may not prove to be of some taxonomic value, as suggested by our finding of strontium in *D. conchyliatum* spicules. The number, position, and structure of ovaries, testes, embryos, buds, and/or larvae must often be determined in order to identify many of the didemnid genera and species. Some (or all) of these recognition characteristics may be wanting in colony(ies) at any given time or location {11}. Clearly,

some of the formally described didemnid species" are problematic, and it is likely, in St. Andrew Sound and elsewhere, that "good" species remain unrecognized and undescribed, while others are ecotypes, ecophenotypes or polymorphic forms of typologically described species whose morphological variation has not been adequately documented.

Comparisons of ascidians from St. Andrew Sound with specimens borrowed from U.S. National Museum collections for verification purposes were not helpful in a majority of cases. Anatomical features of voucher and St. Andrew Sound colonies identified as the same species were found, when examined carefully, to be substantively different. It was concluded that either the author's identifications of problematic specimens were incorrect, or that some of the USNM specimens had been misidentified (or were unidentifiable), by the experts whose names appeared on the specimen labels. In the author's opinion, several non-mutually exclusive factors resulted in taxonomic uncertainties with respect to species determinations. First, undescribed (i.e., "new") species were collected in St. Andrew Sound; second, undescribed ecotypes or ecophenotypes of described species were collected; and third, published descriptions of a majority of didemnid tunicates are vague and line drawings of species are often uninformative. Much is left to the imagination, and the temptation to "force" a specimen into an artificial key or description was compelling, but resisted. It may be concluded that determinations of the specific identities of didemnid ascidians is more an art form than a science at present, and is likely to remain so in the foreseeable future.

Didemnum conchyliatum (until recently, placed with *D. candidum* of European waters), *Didemnum duplicatum* (referred to by some authors as *D. vanderhorsti*), *Diplosoma macdonaldi*, and *Diplosoma glandulosum* were identified as common inhabitants of St. Andrew Sound. Many *Didemnum* and *Diplosoma* colonies were unidentifiable at the species level for reasons already discussed.

3. Didemnum conchyliatum [= *Didemnum candidum*]

The colonial ascidian *Didemnum conchyliatum* grows only on the leaves of *Thalassia testudinum* in St. Andrew Sound, although the species grows on a variety of substrates (sponges, corals, gorgonians, etc.) elsewhere within its broad geographic range, which extends from New Hampshire to southern Brazil, and includes Bermuda, the West Indies and the Gulf of Mexico. The color, shape, size, texture,

substrate, habitat, spicule density and zooid size and morphology of this common ascidian are highly variable. The species recently been split into the New World *Didemnum conchyliatum* and Old World/Asian *D. candidum*. The author has no opinion on whether the recognition of two species that are morphologically so similar is justified.

On *Thalassia* the appearance of *D. conchyliatum* is that of thickly applied smooth, grainy or somewhat ropey chalk white to grey latex paint. Tan-brown colors are not uncommon, but thought to result from accumulations of fecal pellets in quiet water areas. Young colonies appear as oval spots less than 0.5 mm in diameter on one side of a single leaf, while older specimens (consisting of a variable number of propagules) may "glue" up to 50 or more leaves together in an asymmetrical mass. After larval settlement on the lower portion of a live *Thalassia* leaf, colony growth occurs in all directions: to the base of the leaf; toward the distal (oldest) living part of the leaf; and around the leaf, completely investing it. Colony growth may be inhibited by intense light, and *D. conchyliatum* is seldom found above about half the distance from the base to the tip of leaves, and is not found on senescent or dead portions of leaves colonized with epiphytes. When multiple leaves are involved it is impossible to distinguish the number of colonies contributing to the contiguous mass.

During the *Thalassia testudinum* growing season (~ April through October), water in St. Andrew Sound becomes extremely turbid with dense phytoplankton populations (Secchi depths <1 m). Low light levels restrict the growth and bathymetric distribution of *Thalassia*, and therefore *D. conchyliatum*, to relatively warm seasons, and to depths that rarely exceed one meter, respectively. *D. conchyliatum* is abundant in areas of the Sound influenced by moderate tidal currents, and colonies are uncommon, small and temporally ephemeral in quiet water areas.

D. conchyliatum has been relatively abundant in St. Andrew Sound since 1993. For unknown reasons, however, this species, and *D. duplicatum*, disappeared from seagrass meadows between sampling periods in mid-April and early June 1997. Neither toxic algal blooms nor extreme temperature-salinity changes occurred during the spring, and neither seagrasses nor other ascidian taxa appeared to decrease in abundance. While the recruitment of solitary ascidians (*Styela* and *Molgula*) into the Sound from upstream embayments (e.g., St. Joseph Bay) and from the Gulf of Mexico is considered to be

uncommon, propagules of seagrass-associated colonial species, including *Didemnum* spp. and *Diplosoma* spp., were frequently observed attached to broken-off, floating leaves of *Thalassia* and *Halodule* at St. Joe and Mexico Beaches. Thus, recruitment into St. Andrew Sound via floating seagrass leaves may be relatively continuous from upstream locations, and it is expected that populations of these didemnids will become reestablished in the lagoon when conditions favorable to their survival return.

Gross examination of *D. conchyliatum* reveals a series of elongated slits in the tunic surface. These are common cloacal apertures, and each one is occupied by an unidentified species of symbiotic amphipod. Six-lobed branchial siphons slightly protrude from the surface of the colony in *in situ* relaxed specimens, but these are strongly retracted in aquarium-held, heavily narcotized specimens, and remain so regardless of the method of fixation used. It is assumed that zooids retract due to the contraction of branchial siphon muscles as well as the so-called *appendix fixateur*, which may be very short, or elongate on different zooids of a single colony. The morphology of zooids so contracted renders their morphology (e.g., number of stigmata, folds, papillae and blood vessels, shape and position of the atrial aperture) very difficult to discern.

The white (or gray) color of *D. conchyliatum* is caused by very dense concentrations of stellate spicules which lie just beneath the outer tunic, and surround all portions of the zooids. Dense spicule populations greatly complicated the task of determining zooid structure, and attempts to clear colonies of these crystals with EDTA and EGTA so severely distorted zooids that they were unrecognizable. Beneath the gut loop, a relatively spicule-free region of the colony extends to the surface of *Thalassia*, to which the entire colony is firmly attached. Spicules are constructed within cells of the lateral thoracic organs. These cells migrate into the tunic, undergo apoptosis and deposit the young spicules which continue to grow by non-cell-mediated chemical deposition of calcium and strontium carbonate. Spicules may (as would ground glass) provide didemnids protection from predators.

Spicules may have another function as a result of co-evolution with its substrate-hosts, many of which (e.g., corals) contain zooxanthellae or other symbiotic algae. As noted, *D. conchyliatum* lives on the surface of *Thalassia testudinum* blades in St. Andrew Sound. These seagrasses require sufficient light (~15% of downwelling solar radiation) to photosynthesize. It was expected that seagrass leaves

covered by *D. conchyliatum* would be apochloritic, or a faded green color when the tunicate was removed. Surprisingly, when *D. conchyliatum* was stripped away, the portion of the leaf that it covered was a bright, emerald green. Although spicules of *D. conchyliatum* appear white while embedded in the common tunica of the colony, they appear as water clear crystals when viewed with a light microscope. Given the glass-like appearance of spicules and the apparent photosynthetic activity of leaves covered by the colony, it is speculated that spicules may absorb and/or transmit light through the colony to the leaf surface at wavelengths and intensities sufficient to support photosynthesis. If experimental evidence (now lacking) supports this notion, it would follow that the leaf may gain protection from herbivores and shading by epiphytes by the didemnid.

The systematic confusion associated with *Didemnum* species militates against its usefulness as a biological indicator of trace metals enrichment. However, the genus is fairly easily recognized, and its distribution is very broad in all but polar seas. *D. conchyliatum* has not, to the author's knowledge, been analyzed for trace metals accumulations (other than Sr), and deserves investigative attention.

4. *Didemnum duplicatum* [= *D. vanderhorsti*]

This species closely resembles *D. conchyliatum* in appearance, morphology, and distribution. However, it occurs on the seagrass, *Halodule wrightii*, rather than *Thalassia testudinum*. Identification of the species in St. Andrew Sound was tentative, and for that reason, will not be further discussed.

5. *Diplosoma macdonaldi*

Diplosoma macdonaldi, an aspiculate didemnid, was the most common colonial tunicate in St. Andrew Sound, except during the coldest winter months. The species was most commonly found on midwater substrates, where colonies entirely covered ropes, barnacles and the large ascidian, *Styela plicata*. *D. macdonaldi* occurs world-wide in temperate and warm water ocean areas. The species has often been reported to form relatively small, thin, flat colonies (0.2-2 cm across), but in the Sound, this species formed massive colonies well over 2 m long. On pilings and ropes, folds and pendulous extensions of *D. macdonaldi* colonies assumed the appearance of heavy brown, blue-black or gray curtains. Colonies of this ascidian were seldom found on benthic substrates or on seagrass blades, shells or other hard substrates. Several very small colonies were found growing on *Molgula occidentalis*;

they were not found, however, on benthic *S. plicata*. *D. macdonaldi* does not, as far as could be determined, overgrow other colonial ascidians.

On midwater ropes, *D. macdonaldi* and *Eudistoma capsulatum* colonies merged with no standoff zone. These obvious competitors for space appeared to grow at about the same rapid rate (on ropes, as much as 5 cm per day), to reproduce asexually at about the same time of year, and to be equally resistant to predation and overgrowth by epibionts. However, *D. macdonaldi* was several orders of magnitude more abundant than *E. capsulatum*. Parsimonious explanations for this observation are that *D. macdonaldi* is longer-lived than its competitor, or is better able to accommodate levels of environmental variation characteristic of the lagoon. Either of these two speculative possibilities would result in an increase in space available for colonization by *D. macdonaldi*, and less space for settlement of larval *E. capsulatum*.

To the author's knowledge, *D. macdonaldi* has not been analyzed for its ability to accumulate trace metals. Because the biology of the species is well known, and it has a cosmopolitan distribution, *Diplosoma macdonaldi* warrants investigation.

6. *Diplosoma glandulosum*

The identification of *D. glandulosum* was tentative. Except for its rough texture and dark black color, the species is very similar anatomically to *D. macdonaldi*. *D. glandulosum* was collected only in hydrocarbon-contaminated water on boathouse pilings, where *D. macdonaldi* did not occur.

Family Polycitoridae

Many of the problems encountered with respect to identifying didemnids also occurred with the polycitorid genus *Distaplia*, a widely distributed, speciose, phenotypically plastic taxon, containing an unknown, but possibly significant number of undescribed species. The anatomical features of two "species" of *Distaplia* collected in St. Andrew Sound were incongruent with published descriptions of other members of the genus. These specimens are considered to represent either geographical races, subspecies, or, more likely, new species. Specimens of these ascidians were identified as *D. bermudensis* by Smithsonian Institution curators.

7. *Distaplia bermudensis*

Published accounts of *D. bermudensis* note that its major anatomical features (i.e., siphons, atrial languet, branchial basket, presence of parastigmatic vessels, brood pouch, gonads) conform to descriptions of the genus as a whole. The species is distinguished by the often bright (but variable) color of its colonies, and by its relative "robustness" compared to other species. In St. Andrew Sound, the vast majority of *D. bermudensis* colonies were red to orange in color, and the remainder were purple-black. The two color morphs co-occurred and were often found in direct physical contact on pilings and other artificial substrates year-round, reaching their maximum abundance during mid-spring through mid-summer. Several colonies were comprised of both red-orange and blue-black regions that were uniform within regions; mosaic color distributions were never observed. Brick red specimens similar to those from Apalachee Bay were believed to represent an undescribed species of Distaplia {10}. *D. bermudensis* were never found in benthic (i.e., bottom) habitats in the Sound, although it is reported to live in of epibenthic habitats elsewhere within its range, from Bermuda, and North Carolina through the West Indies and the Gulf of Mexico.

D. bermudensis is a massive species, and the red morph is easily recognized in the field. Because of its apparent hardiness and ability successfully to colonize a variety of substrates, several attempts were made to maintain colonies both in laboratory conditions and in aquaria placed outdoors in light conditions similar to those where they were collected (light levels were recorded using a Licor underwater irradiance meter). Regardless of the frequency with which water was replaced, with and without aeration, these colonies died within 24-48 hours. Two observations are of interest here. First, the color exhibited by *D. bermudensis* colonies is generally attributed to various species of symbiotic algae and/or cyanophytes distributed throughout the gelatinous tunica. Massive numbers of photosynthetic symbiotes were confirmed by the author, and an experiment was conducted to investigate the possibility that *D. bermudensis* might require photosynthate produced by these symbiotes in a manner similar to that of hermatypic corals and some other invertebrates (e.g., *Tridacna*). Colonies placed in dark, but aerated aquaria disintegrated with 12-28 hours. Whereas the absence of light could not be established as the cause of rapid colony disintegration, experiments on the effects of light and algal-ascidian

symbioses deserve further, more sophisticated investigation. The second observation of interest is that zooids remained alive and active following disintegration of the tunic matrix. Zooids were easily dissociated from the colony by gentle pressure. Given that colony disintegration also occurs in nature, viable zooids may be able to settle on nearby substrates to develop new colonies — a novel, and undescribed method of colony regeneration and range extension. Cellular apoptosis and tunic disintegration are, in the author's opinion, different processes.

Both iron and vanadium have been reported to occur in *D. bermudensis* at concentrations significantly higher than ambient seawater levels. Taxonomic considerations notwithstanding, *Distaplia* spp. are considered good candidates for use as trace metals monitors.

Conclusions

Results of systematic and ecological work suggest that the remarkable phenotypic variation found in those colonial ascidians whose specific identity is not confounded by taxonomic uncertainties may be related to temporal and spatial changes in lagoonal habitat characteristics. Phenotypic variation in colony architecture and zooid morphology within and between colonies precluded the unequivocal identification of species in a significant number of cases. The magnitude of variation in many, but not all of the colonial aplousobranch species examined in St. Andrew Sound militates against their use as biological indicators by other than expert tunicate systematists. Problems of species and population recognition in these species requires the use of both classical and molecular systematic techniques. In contrast, the stolidiferan species, *Molgula occidentalis*, and *Styela plicata*, are recognized with little difficulty, and exhibit characteristics of suitable trace metal biosensors/indicators.

Literature Cited

1 Collard, S.B. 1993. Styela plicata and Molgula occidentalis (Urochordata: Ascidiacea: Stolidifera) in St. Andrew Sound, Florida. Final Rept. AFOSR 19:1-20.

2 Michibata, H. 1984. Ascidians and trace metal elements. Heredity 38:18-23.

3 Ratliff, J. 1997. Accumulation of strontium and calcium by *Didemnum conchyliatum*. Final Rept. AFOSR 29:1-20

4 Monniot, C., F. Monniot and P. Laboute. 1991. Coral reef ascidians of New Caledonia. Inst. Francais Res. Sci., Coll. Faune Trop. 30, 247 p.

5 Michibata, H. et al. 1986. The accumulation and distribution of vanadium, iron and manganese in some solitary ascidians. Biol. Bull. 171:672-681.

6 Collard, S.B. Some aspects of the natural history of ascidian tunicates in St. Andrew Sound, Florida. In prep.

7 Cossa, D. 1989. A review of the use of Mytilus spp. As quantitative indicators of cadmium and mercury contamination on coastal waters. Oceanol. Acta 12(4):417-432.

8 Collard, S.B. 1992. Characterization of seagrass meadows in St. Andrew (Crooked Island) Sound, northern Gulf of Mexico. Final Rept. AFOSR 9:1-19.

9 Bruno, J.B. et al. 191996. Electrochemiluminescence from tunicate, tunichrome-metal complexes and other biological samples. J. Biolumin. Chemilumin. 11:1-14.

10 Van Name, W.G. 1945. The North and South American ascidians. Bull. Am. Mus. Nat. Hist. 84, 476 p. 11 Branham, J.M. 1958. An ecological survey of the ascidians of Alligator Harbor, Florida, and the adjacent Gulf of Mexico. M.D. Thesis, Fla. St. Univ., 71 p.

Selected References

Ballan-Dufrancais, C., A.Y. Jeantet and M. Truchet. 1995. La formation des spicules de Didemnidae (Ascidiacea). Can. J. Zool. 73:1647-1656.

Berrill, N.J. 1950. The Tunicata with an account of the British species. The Ray Soc., London, 354 p.

Goodbody, I. 1974. The physiology of ascidians. Adv. Mar. Biol. 12:1-149.

Millar, R.H. 1971. The biology of ascidians. Adv. Mar. Biol. 9:1-100.

Monniot, C., F. Monniot and P. Laboute. 1991. Coral reef ascidians of New Caledonia. Orstom, Paris, Coll. Faune Tropic. 30, 142 p.

Plough, H.H. 1978. Sea squirts of the Atlantic continental shelf from Maine to Texas. Johns Hopkins Univ. Press, Baltimore, 118 p.

Romanov, V.N. 1989. Fauna of USSR. Tunicates. 1(1):1-224.

RAT ULTRASOUND VOCALIZATION DEVELOPMENT AND NEUROCHEMISTRY IN STRESS-SENSITIVE BRAIN REGIONS

Catherine A. Cornwell
Associate Professor
Department of Psychology

Syracuse University
471 Huntington Hall
Syracuse, NY 13244

Final Report for:
Summer Research Program
Armstrong Laboratory

Sponsored by:
Air Force Office of Scientific Research
Bolling Air Force Base, Washington, DC

And

Armstrong Laboratory

September 1997

RAT ULTRASOUND VOCALIZATION DEVELOPMENT AND NEUROCHEMISTRY IN STRESS-SENSITIVE BRAIN REGIONS

Catherine A.Cornwell
Associate Professor
Department of Psychology
Syracuse University

Abstract

Three experiments tested the hypothesis that an individual rat's propensity to emit ultrasounds is related to other biobehavioral measures of stress. In the first experiment, the number of isolation-induced ultrasounds emitted by male rat pups 10 days old was positively correlated with hippocampal concentrations of the serotonergic metabolite 5-hydroxyindole acetic acid, and negatively correlated with frontal cortex concentrations of the dopaminergic metabolite 3,4-dihydroxyphenyl acetic acid. In the second experiment, vocalizations of female rats were longer when their odor preferences were tested in a situation where only unfamiliar odors were present, than in a situation where familiar nests odors were present. In the third experiment, two weeks of restraint stress immediately after weaning reduced body weight gain and thymus weight in male and female rats, and also reduced thymus to body weight ratios in females. However, restraint did not induce significant differences between control and restraint groups in vocalization parameters. Whether these parameters correlate with brain monoamine measures will be determined when assays now in progress are completed. The results to date support the hypothesis that ultrasonic vocalizations by rat pups are related to other biobehavioral indicators of stress.

RAT ULTRASOUND VOCALIZATION DEVELOPMENT AND NEUROCHEMISTRY IN STRESS-SENSITIVE BRAIN REGIONS

Catherine A. Cornwell

Rats and other rodents emit ultrasonic vocalizations under various conditions that are consistent with a stress interpretation. For example, infant rats vocalize when separated from parents and siblings (Allin & Banks, 1972; Noirot, 1972) and adult rats vocalize during acoustic startle (Kaltwasser, 1990), in response to shock and to stimuli previously paired with shock (Frysztak & Neafsy, 1991; Goldstein, Rasmusson, Buney & Roth, 1996) and in response to airpuffs directed at the head or neck regions (Knapp & Pohorecky, 1995). Pharmacological studies are also consistent with the idea that these emissions reflect stress since anxiolytic and anxiogenic drugs respectively decrease and increase such calls (see Insel and Winslow, 1991, for a review).

These findings have led to the suggestion that ultrasound vocalizations constitute an animal model for stress-induced anxiety and depression. Such states are typically long lasting conditions in humans and an animal model in which the relevant behavior differed chronically between individuals would be useful. In addition, these psychological states induce chronic biological abnormalities that are measurable in the absence of acute pharmacological manipulations (Anisman & Zucharko, 1982; Gilad, 1987) and such changes should be evident in an appropriate animal model. To date, research on ultrasound vocalizations has not addressed these issues. Therefore, the present experiments examined whether individual differences in rats' ultrasound emissions persist from infancy into the postweaning juvenile period, and whether ultrasound occurrence at either developmental stage covaries with established biobehavioral measures of stress.

Experiment 1: Rat Pup Ultrasound Vocalization and Brain Monoamine Function.

The first experiment determined whether there are correlations between isolation-induced ultrasonic vocalizations (UVs) in rat pups 10 days old and neurochemical indices of stress. Concentrations of monoamines (MAs) and their metabolites were evaluated in the frontal cortex (FC) and hippocampus (HP) because of previous evidence that psychological stress (social stress

or restraint stress) alters MA function in these regions (Cornwell-Jones, Decker, Gianulli, Wright & McGaugh, 1990; Cornwell, Chang, Cole, Fukada, Gianulli, Rathbone, McFarlane & McGaugh, 1996; Mendelson & McEwen, 91; Watanabe, Sakai, McEwen & Mendelson, 1992). There is general agreement (cf. DeSouza & Van Loon, 1986) that stress decreases brain norepinephrine (NE) concentrations and increases both 5-hydoxyindole acetic acid (5-HIAA) and serotonin (5-HT) turnover. We therefore predicted that NE concentrations and rates of UV emission wouldcorrelate negatively, and that 5-HIAA concentrations and serotonin turnover rates would correlate positively with UV emission parameters.

Materials and methods

Forty Sprague-Dawley rats from six litters born in the laboratory were used in this experiment. Time-impregnated dams were purchased from Charles River Laboratories, Portage MI. Within 24 h of birth, litters were culled to 10 pups of 5 males and 5 females, with the exception of one litter, in which 2 males were missexed as females. At the time of culling, each animal was toe-clipped for individual identification. Litters were housed with dams in clear plastic cages containing Sanichip shavings in a Bioclean enclosure. Shavings were added, but not changed, until litters were weaned on postnatal day 21. The Bioclean enclosure was on a reversed 14/10 h reversed light/dark cycle with lights on at 19:00 h and lights off at 09:00 hr (mean lux values inside the cages: 0.43-0.84 lx with lights off, 16-20 lx with lights on). Food and water were freely available.

TABLE 1

Assignment of Pups to Experiment 1 by Litter

Litter	# Males	# Females
1	2	2
2	1	1
3	2	2
4	2	2
5	1	1
6	2	2
Total	10	10

On postnatal Day 10 (Day 0=day of birth),1-2 pups of each sex were randomly selected from each litter as indicated on Table 1, for a total of 10 males and 10 females. Remaining littermates were used in Experiments 2 and 3. Litters with dams were transported in the home cages from the vivarium to the testing room in light-tight boxes. Pup UV's were recorded in a system consisting of a sound attenuation chamber with a S25 Bat Detector suspended 4 inches above the floor. The bat detector output was run through a 250kHZ, 8 channel, selectable A/D board (Data Translation #2831-G) and then to a 386 IBM PC computer Clone with Bernoulli 90M removable hard drive. Data were acquired through Global Lab software and stored on 90 megabyte Bernoulli disks.

At the beginning of the test session, individual pups were removed from their home cages and placed on a room temperature ($37^{\circ}C \pm 2^{\circ}C$) petri dish that was located in the center of the sound attenuation chamber directly below the bat detector microphone. UV recording began immediately and continued for 6 minutes. Six UV parameters were measured per pup: number of vocalizations, length of vocalizations, percent of test vocalizing, total intensity per test, intensity per millisecond of vocalization and intensity per vocalization.

After testing, pups were weighed and prepared for neurochemical examination by decapitation. Brains were dissected on an ice-cooled saline-rinsed glass plate according to the method of Glowinski and Iversen (1966). The hippcampus and frontal cortex were removed and tissue from one hemisphere was stored at $-70^{\circ}C$ until it was assayed for monoamines and their metabolites (Cornwell-Jones, Velasquez, Wright & McGaugh, 1988; Kim, Campanelli, & Khanna, 1983). High performance liquid chromatography (HPLC) was used to measure regional concentrations of NE, epinephrine (E), 5-HT, 5-HIAA, dopamine (DA), and the dopaminergic metabolite 3,4-dihydroxyphenyl acetic acid (DOPAC).

Student "t" tests were used to compare data from males and females, since sex influenced UV emissions in a previous experiment (Miller, Cobb, Baker, Curtis, Williams and Murphy, 1997). Correlation coefficients were calculated between the number of vocalizations emitted and brain chemical concentrations using the Statistica software program.

Results

Values for UV parameters are shown in Table 3. There were no significant differences between males and females on any of the parameters measured. There were also no significant sex differences in the neurochemical concentrations values shown in Table 4.

TABLE 3

UV Production by Rats Tested and Dissected on Postnatal Day 10

	# UVs	Mean Intensity/ ms	Mean Noise Level	% Time Vocalizing	Mean Signal Length	Mean Intensity per Call	Signal:Noise Ratio
mean	593.45	68.28	16.61	17.845	100.118	251.761	15.3095
sd	259.5978	48.74418	0.892011	10.210457	33.43283	138.6021	8.56719476
sem	58.04	10.9	0.199	2.28	7.47	30.99	15.91

TABLE 4

Brain Monoamine Concentrations and Body Weights for Rat Pups Tested and Dissected on Postal Day 10.

Units: body weight=grams, chemicals=ng/g wet weight tissue.

		HIPPOCAMPUS			FRONTAL CORTEX				
	Body Wt	NE	5HIAA	5HT	NE	DOPAC	DA	5HIAA	5HT
mean	21.205	36.31432	210.7328	183.9047	43.57583	45.36419	206.6158	90.57505	122.6649
sd	2.950731	17.53061	47.14046	48.69524	16.45888	14.96795	135.1818	47.34755	38.14336
sem	4.74	5.547662	14.91787	15.40989	5.208505	4.736692	42.77904	14.9834	12.07068

There were no significant correlations between the number of vocalizations emitted by females and any chemical measured in either brain area. For males, there was a significant positive correlation between vocalization number and hippocampal 5-HIAA values, [$r(6)=.78627$, $p<.05$, Fig. 1] and a significant negative correlation between vocalization number and frontal cortex DOPAC values [$r(4)=-.8269$, $p<05$), Fig. 2].

Fig. 1:_ Relationship Between Hippocampal 5-HIAA and Male Pups' UV Numbers

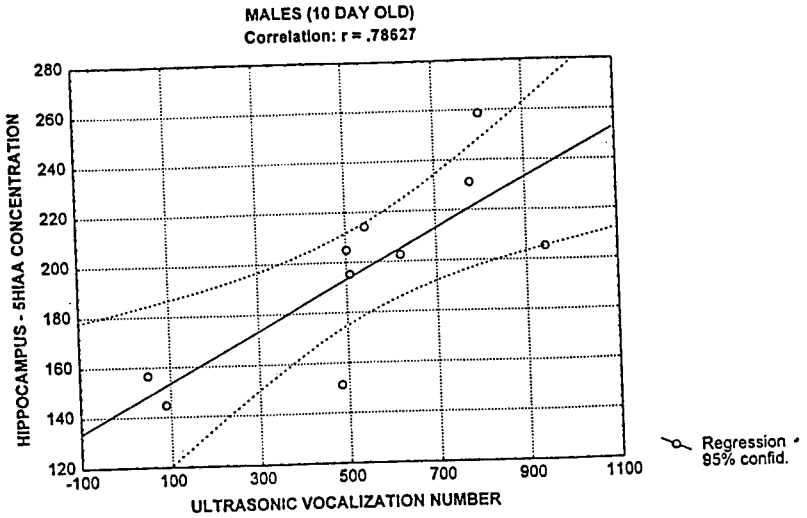

Fig. 2. Relationship between Frontal Cortex DOPAC and Male Pups' UV Numbers

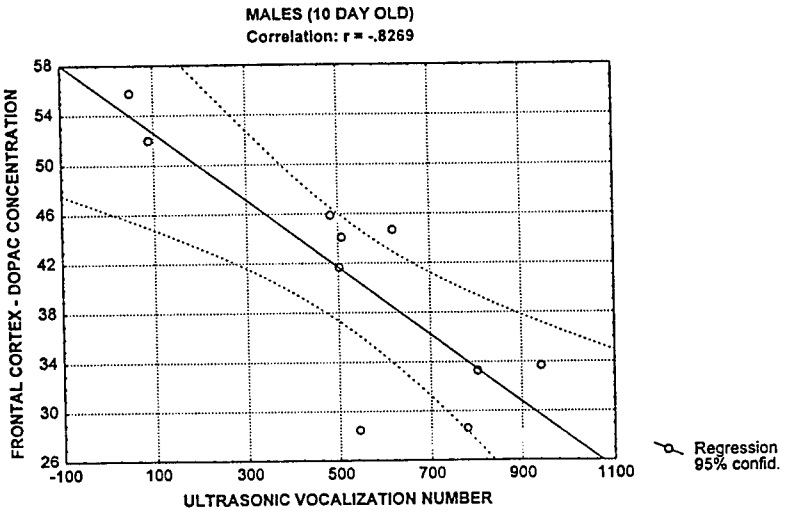

Experiment 2: Olfactory Cues and Rat Pup Ultrasound Vocalizations.

The second experiment examined whether UV rates are related to rat pups' general responsiveness to environmental stimuli, or if they are preferentially elicited by aversive stimuli. Rat pups avoid unfamiliar odors and are attracted by familiar ones (cf. Cornwell-Jones and Sobrian, 1977). These preference patterns are consistent with the idea that strange odors elicit anxiety and familiar odors reduce it. We therefore predicted that higher UV parameter values would be elicited by strange odors than by familiar ones.

Materials and Methods

Subjects were 22 male and 18 female littermates of the animals used in Experiment 1. On postnatal day 10, all of the rats were given UV tests as in Experiment 1. The next day, pups were given a 6 min olfactory preference test between the odors of either soiled Sanichip shavings from their own nests and clean Sanichips or between unfamiliar cedar shavings and clean Sanichips.

Preference tests were given in an apparatus measuring 20x26x8 cm placed inside a UV chamber. The apparatus is a Plexiglas frame with a screen floor that rests upon an odor tray that is divided into two outer right triangles separated by a central V-shaped "neutral zone" (Cornwell et. al., 1996). One of the outer sections contained either soiled shavings from the pup's nest or clean cedar shavings, and the other compartment contained an equal volume of clean Sanichip shavings. At the beginning of a session, the pup was placed in the center of the screen floor and the time spent over each odor was monitored with a stopwatch while UVs were being recorded.

Preferences scores were computed by subtracting the time spent over the fresh Sanichip shavings from the time spent over the comparison odors. Group means were compared with zero, the score expected if the animals exhibited no choice between odors, using t-tests for the significance of the difference between an observed and hypothetical mean (Dixon and Massy, 1969). Sex and odor effects on preference scores, the number of UVs, % time vocalizing and mean intensity per call were evaluated by ANOVA's. Correlation coefficients were calculated for preference scores vs. these UV parameters to test the prediction that high preference scores would be associated with low UV scores. Alpha values for multiple "t"tests were adjusted to an overall level of $p=.05$ using the Bonferoni method.

Results

Values for UV parameters are shown in Table 5. There were no significant UV parameter value vs. preference scorecorrelations on either odor choice. Odor preference scores were significantly influenced by the odor choice [$F(1,36)=20.467$, $p<.001$, Newman-Keuls], but not by sex [$F(1,36)=2.062$. $p>.05$]. Both males and females preferred nest to sanichip odor [$t(11)=6.09$, $t(7)=9.44$, $p<.01$, males and females respectively, Fig.3] but showed no preference between cedar and Sanichip odor.

TABLE 5

UV PRODUCTION BY RAT PUPS TESTED IN THE

OLFACTORY CHOICE SITUATION ON POSTNATAL DAY 11

		# UVs	Mean Intensity/ ms	Mean Noise Level	% Time Vocalizing	Mean Signal Length	Mean Intensity per Call	Signal:Noise Ratio
Nest vs. Sanichips								
	mean	85	29.63333	25.60833	2.56	61.65333	116.3175	4.52
Males	sd	105.3979	7.345788	0.427377	3.8220675	40.288	60.32137	2.30476581
	sem	30.46001	2.122933	0.123512	1.1045775	11.64323	17.43288	0.66607732
	mean	81.25	27.6375	25.4625	1.49625	44.1025	111.82	4.37625
Females	sd	120.1627	3.820223	0.277424	2.3620326	25.52323	53.35389	2.0490551
	sem	42.53759	1.352359	0.098208	0.8361596	9.035222	18.88728	0.7253655
Cedar vs. Sanichips								
	mean	113.9	38.71	25.49	5.797	110.339	174.993	6.845
Males	sd	143.26	25.75498	0.321282	8.8695986	76.8966	121.4633	4.74274007
	sem	45.27017	8.138572	0.101525	2.8027931	24.29933	38.3824	1.49870586
	mean	80.9	28.42	25.48	2.285	72.69	118.877	4.654
Females	sd	75.30007	3.819482	0.24404	2.4791004	49.80566	50.48793	1.95116603
	sem	23.79482	1.206956	0.077117	0.7833957	15.73859	15.95418	0.61656847

Fig. 3

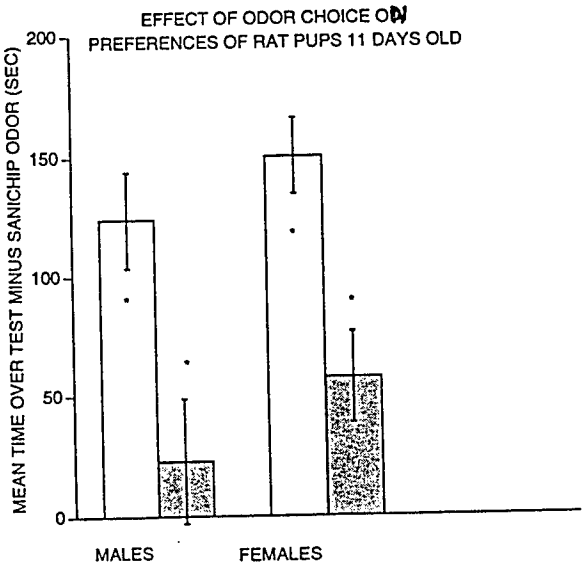

Figure 3: Preferences of rats pups for nest shavings (clear bars) or cedar chips (tinted bars) vs. sanichip odor. N-10 pups pups//histogram. Asterisks inside histograms indicate means are signiificantly different from zero (p<.05, t-test). Asterisks outside histograms indicate adjacdent means are significantly different from each other (p<.05, Newman-Keuls).

Neither UV # or mean % time vocalizing was significantly influenced by the odor choice. However, there was a significant effect of odor choice on the vocalization length [$F(1,36)=5.374$, $p<.05$}. As shown in Figure 4, females emitted significantly longer vocalizations when the comparison odor was cedar, than when it was nest.

Fig. 4

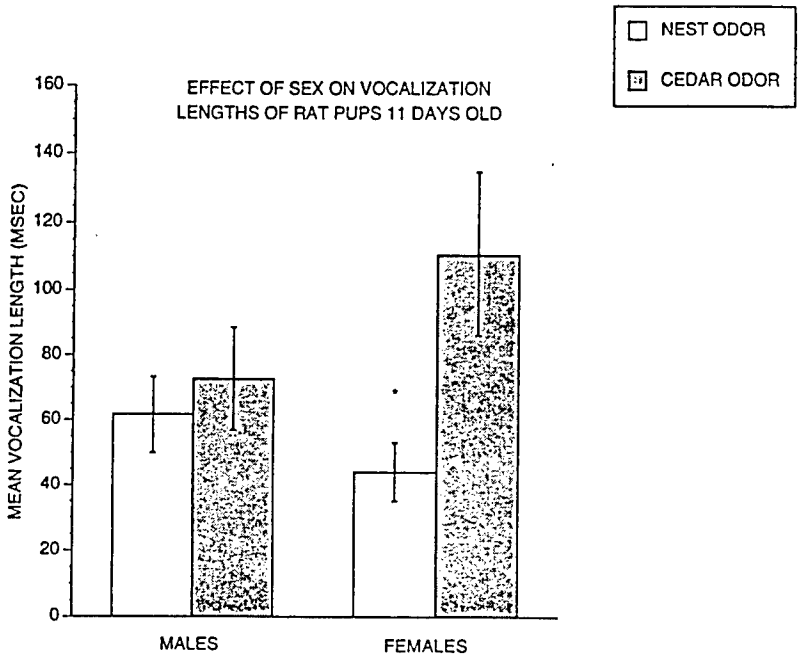

Figure 4. Female vocalizations were longer when only unfamiliar odors were present in the testing situation.

Experiment 3: Restraint Effects on Ultrasound Vocalization Development and on Biological Markers of Stress.

The third experiment examined whether infant UV levels predict postweaning levels for individual juvenile rats, whether postweaning stress alters UV development, and whether high values of juvenile UV parameters correlate with peripheral and central biological indices of stress. Acoustic startle was used to elicit juvenile UVs (Kaltwasser, 1990), since isolation does not induce UVs in rats after weaning (Okon, 1971).

Repeated daily restraint was used as a stressor because involuntary immobilization can be a source of psychological stress in various ethologically important situations ranging from

confinement in a bed because of illness to confinement to a cockpit seat while piloting a fighter airplane. Chronic restraint induces peripheral biological indicators of stress including reductions in body weight gain, and increases in adrenal to body weight ratios (Watanabe, Gould, Daniels, Cameron & McEwen, 1992; Watanabe, Gould, Cameron, Daniels and McEwen, 1992). Centrally, prolonged restraint stress decreases 5-HT binding sites in the hippocampus (Watanabe, Saiai, McEwen & Mendelson, 1992) and NE terminals in the frontal cortex (Sakaguchi & Nakamura, 1990) .

Materials and Methods

Subjects were the same rats used in Experiment 2. Animals from each litter were assigned to postweaning restraint or control conditions as indicated on Table 2, for intended totals of 10 males and 10 females in each condition. Two males that were missexed at birth as females were assigned to the restraint condition, so that restraint groups consisted of 8 females and 12 males. Animals were assigned so that infant UV values for the control and restraint groups were similar. The rats were weaned on postnatal day 21 and housed in same-sex, same-condition groups of 2-3 rats. Unstressed controls remained in their cages except for daily weighing.

TABLE 2

Assignment of Pups to Experiment 3 by Litter

	Controls		Restrained	
Litter	# Males	# Females	# Males	# Females
1	2	2	1	1
2	2	2	4	0
3	1	1	2	2
4	2	2	1	1
5	2	2	2	2
6	1	1	2	2
Total	10	10	10	10

. Restraint stress procedures were adapted from those of Watanabe, Gould & McEwen (1992) and Gruen Wenberg, Elahi & Friedhoff (1995). Stress was applied by placing animals in a

Plexiglas cylinder (Unifab Corporation) 5" long and 2" in diameter with holes on one end for the tail, and in the bottom for excrement. Experimental animals were weighed, placed in the restrainer and returned to their home cages for 6 hours per day (10 -16 h) for 14 days, ending on postnatal day 35.

On postnatal day 36, animals were given a thirty minute test of acoustic startle and simultaneous recording of UV's. A 5 in adaptation period preceded the first startle trial. Each trial consisted of a 40 msec burst of 120 dB white noise followed by a return to the background noise level of 50 dB for the 30 sec intertrial interval (ITI). The startle response was measured for 250 msec from the onset of the stimulus. Following 20 startle trials there was a 5 min post-exposure period. UV's were recorded continually using a bat detector as described in Experiment 1.

Following testing, animals were decapitated and their brains dissected as in Experiment 1. In order to verify the peripheral effects of restraint stress, the adrenal and thymus glands were taken, since restraint has been shown to increase adrenal to body weight ratios (Watanabe, Gould, Cameron, 1992), and the stress of social subordination reduces thymus weight (Blanchard, Spencer,Weiss, Blanchard and McEwen, (1995). The effects of sex and restraint were analyzed for UV numbers, % time vocalizing and mean vocalization length and biological parameters by ANOVA's. Correlation coefficients were calculated for each pair of infant vs. juvenile number of UVs. Correlation coefficients between the number of juvenile UVs and brain chemicals will be calculated when the assays now in progress are completed..

Results

As shown in Figure 5, daily body weight gain was significantly influenced by sex, and treatment group [$F(1,36=12.33$ and 31.192, $p<.001$] as well as by age [$F(15,36)=1466.19$, $p<.001$]. There were no significant differences between groups at weaning, but males gained weight more rapidly than females, and restrained rats of both sexes gained less weight than same-sex controls. As shown in Figure 6, final body weights were significantly influenced by sex and treatment group [$F(1,36)=39.46$ and 69.53, $p<.001$]. Females weighed less than males in the same treatment group, and restrained rats weighed less than controls ($p<.01$, Newman-Keuls).

Fig. 5

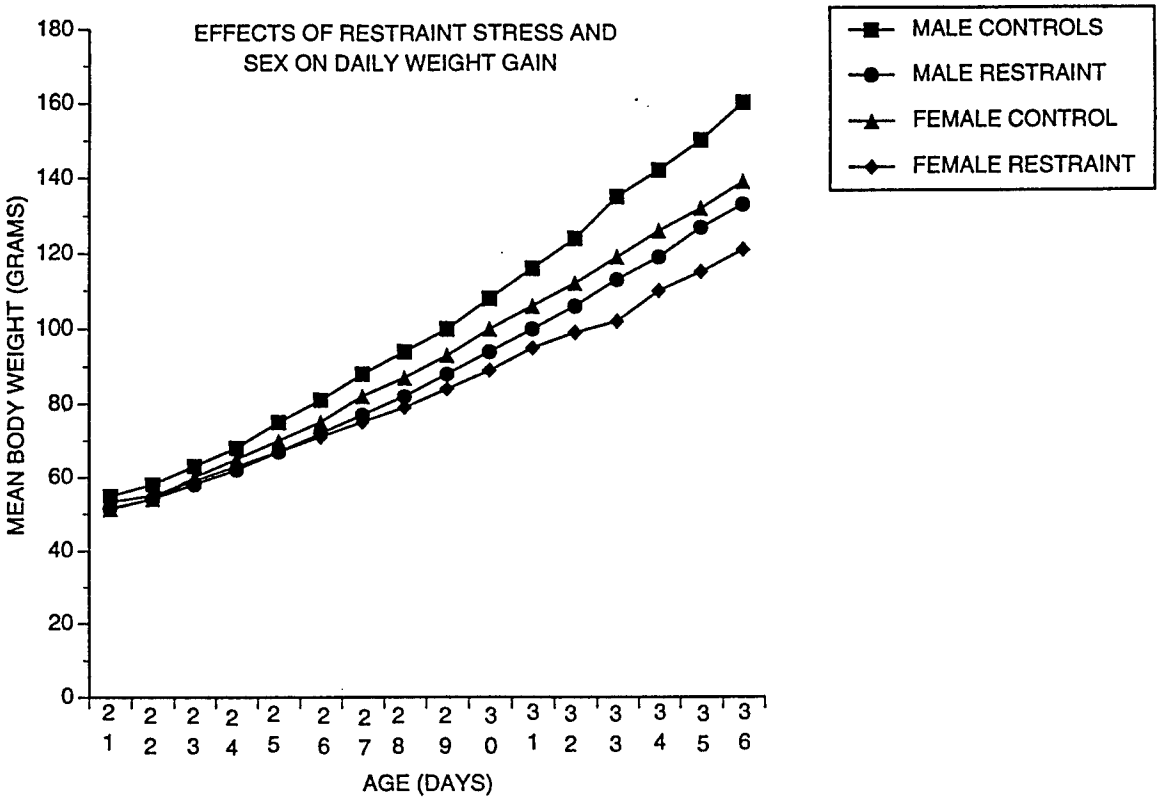

Figure 5. Males gained weight more rapidly than females, and restrained rats of both sexes gained less weight than same-sex controls. N=8-12 rats per group.

Fig. 6 Effects of Sex and Restraint on Final Body Weight.

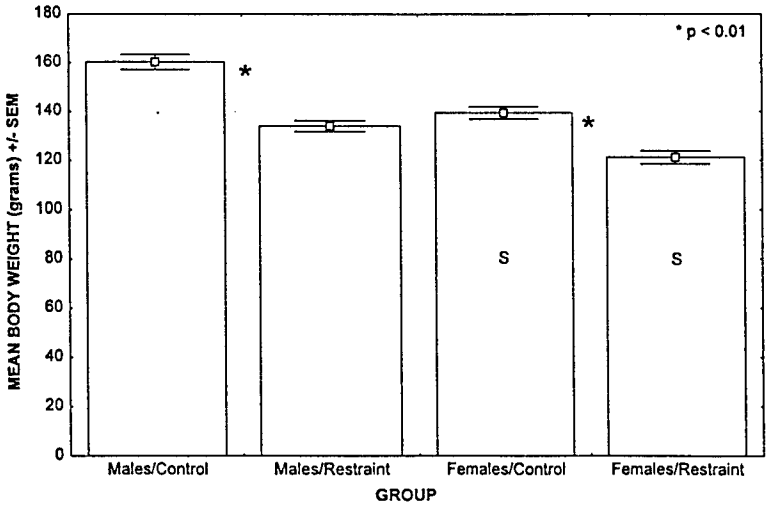

As shown in Figures 7A and B, thymus weight and the ratio of thymus to body weight were significantly influenced by treatment ([F1,26) =28.70 and 8.973, p<.01]. Thymus weights were lower in restrained rats than controls for both sexes (p<.01, Newman-Keuls), and thymus/body weight ratios were lower in restrained than control females (p<.05). Adrenal weight and its ratio to body weight was not influenced significantly by either variable.

Fig 7A Effects of Restraint on Thymus Weight.

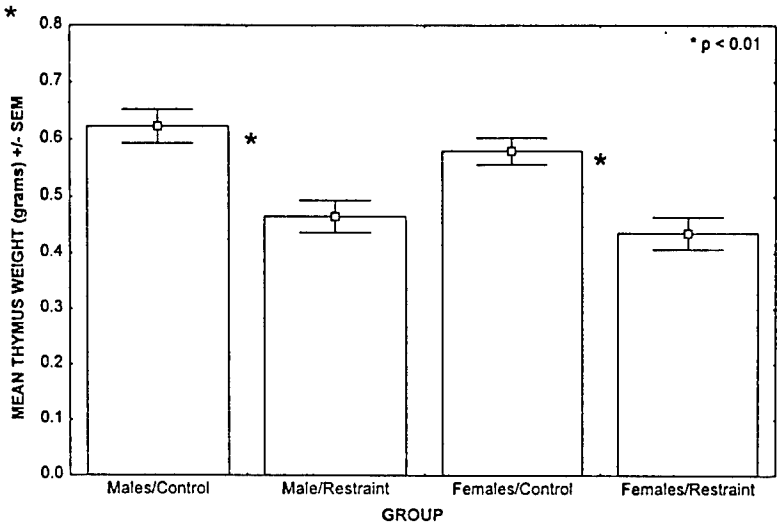

Fig. 7B. Effects of Sex and Restraint on Thymus to Body Weight Ratios

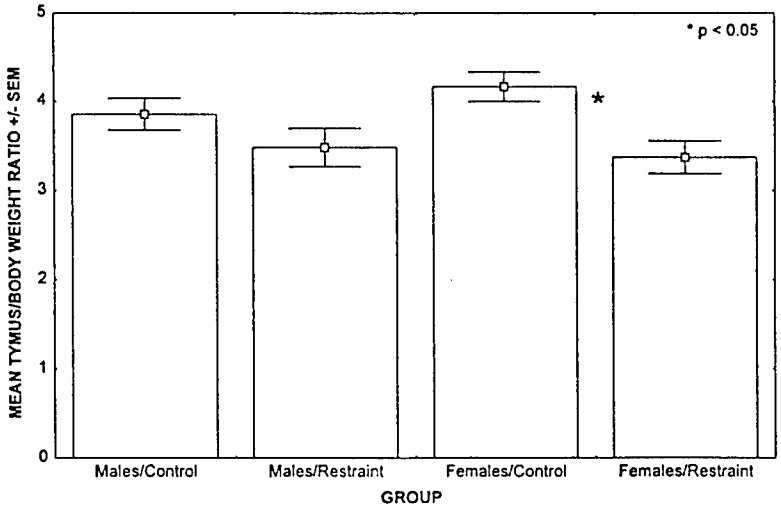

Values for UV parameters are shown on Table 6 on page 17. There were no significant correlations between infant and juvenile UV number, % time vocalizing or vocalization length. However, repeated measures analysis of variance indicated significant age effects on each of these variables [$F(1,38)=75.41$, 17.88 and 11.62, $p<.01$]. As shown in Figs. 8A, B and C, for both sexes, UV number and % time vocalizing decreased with age, while signal length increased ($p<.01$, Newman-Keuls). Correlations between juvenile chemical values and these UV parameters will be calculated when ongoing assays are completed.

Fig. 8A. Key: Open bars=infants

Shaded bars=juveniles

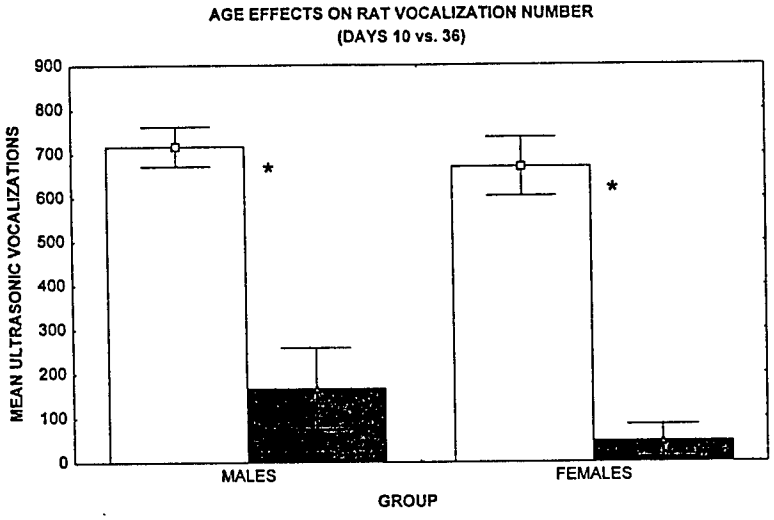

Fig. 8B.

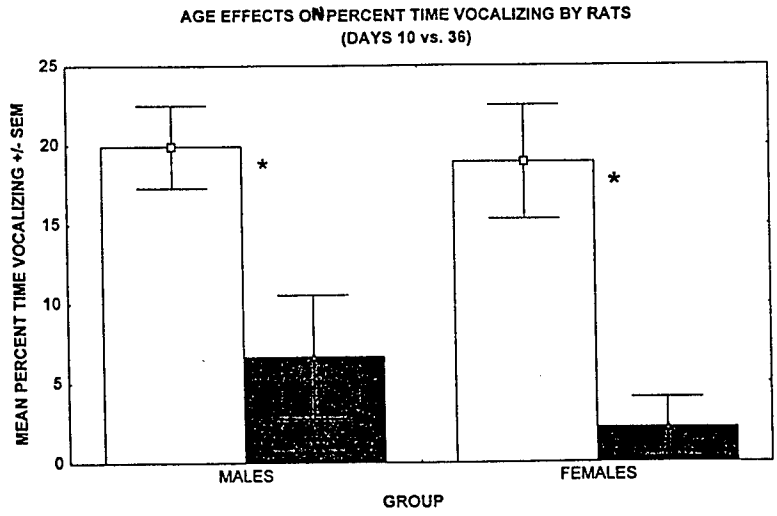

Fig. 8C

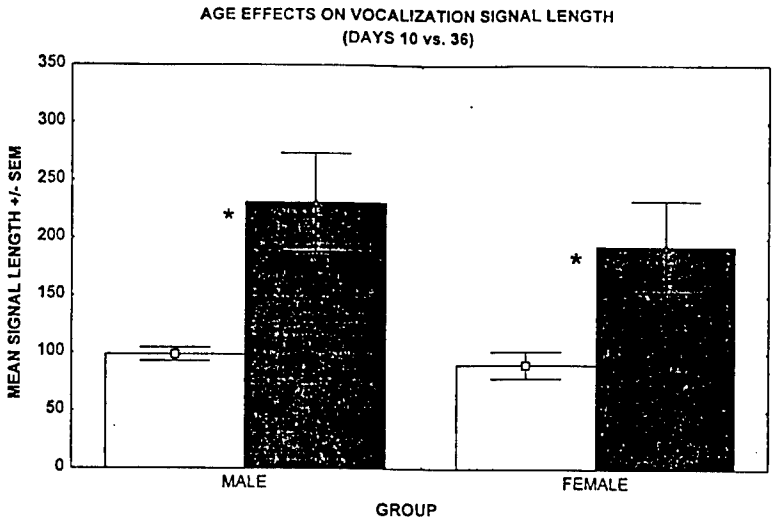

Summary

The data from these experiments support the idea that rat pup UV production is related to other measures of stress. In male pups, UV number was positively correlated with hippocampal 5-HIAA concentrations which have been previously associated with stress (cf. DeSouza & Van Loon, 1986). The number of male pup vocalizations also correlated with DOPAC, in the frontal cortex. Since DOPAC is a metabolite of the inhibitory neurotransmitter DA, it may be the case that stress allows pups to emit UV by releasing related centers in the frontal cortex from dopaminergic inhibition. In addition, the finding that unfamiliar odors induced longer vocalizations from female pups than they emitted to familiar odors, is consistent with the interpretation that anxiety-producing situations promoted some aspects of UV emission.

These data do not provide evidence for characteristic individual differences in UV emission that persist over time. Juvenile and infant parameters did not correlate significantly with each other. However, juvenile emission rates were very low, and possible did not provide an adequate sample on which to base a conclusion. Given that nearly half of the juvenile controls did not vocalize, it seems appropriate to double the sample size in future experiments that investigate UV's at this age. Finally, the increase with age in vocalization length suggests that rats 36 days of age are beginning to make the transition to adult-like vocalizations.

*Restraint began at Postnatal Day 21

TABLE 6

UV PRODUCTION BY RATS TESTED ON POSTNATAL DAYS 10 AND 36

		# UVs	Mn Intensity/ms	Mn Noise Level	% Time Vocalizing	Mn Signal Length	Mn Call Intensity	Signal:Noise Ratio
	mean	744.2	77.53	16.87	21.704	100.457	256.509	15.187
Male Controls	sd	230.758074	45.1540339	0.797287067	9.942084736	26.61734107	118.2514356	6.898036838
	sem	73.0247071	14.28925124	0.252306034	3.146229347	8.423209199	37.42134036	2.18292305
	mean	693.75	69.10833333	16.93333333	20.49666667	103.4875	238.97	14.34916667
*Male Restraint	sd	201.36675	41.2421774	1.21680157	8.259395018	20.79438697	105.461883	6.631125584
	sem	58.1984828	11.91970445	0.351676754	2.387108387	6.009938431	30.480313	1.916510284
DAY 10 UV'S								
	mean	644	60.1	16.45	15.879	82.87	246.632	14.907
Female Controls	sd	289.235775	40.16100928	0.80311892	10.01257704	26.12099879	107.4102071	6.313088784
	sem	91.5303084	12.70918015	0.254151557	3.168537037	8.266138858	33.99057188	1.997812906
	mean	702.25	59.05	16.2125	17.95	91.9575	213.84875	14.55
*Female Restraint	sd	293.238445	33.45794802	0.987692115	8.316347069	25.80485323	122.1123213	5.799709352
	sem	103.617825	11.82259647	0.349007815	2.93863854	9.118322695	43.14923014	2.049367262
	mean	288.6	48.97142857	11.97142857	12.12857143	265.0814286	187.5157143	16.29428571
Male Controls	sd	599.919476	70.67278388	2.638632402	21.03467806	194.5826996	92.29060712	8.260893529
	sem	189.847935	26.76999389	0.99948197	7.967681082	73.70556803	34.9585633	3.129126337
	mean	71	15.54285714	11.45714286	2.084285714	213.1128571	183.0142857	17.90857143
Male Restraint	sd	193.088581	9.555950527	4.412050598	4.471628552	145.8095305	46.38920559	9.985563627
	sem	55.8059482	3.90038797	1.800836979	1.825154511	59.51409409	18.93436963	4.075740256
DAY 36 UV'S								
	mean	78.2	13.06666667	8.916666667	2.72	203.4216667	150.255	17.30166667
Female Controls	sd	210.37258	12.30051489	2.923981304	6.160042208	121.7293275	31.92736115	3.417475189
	sem	66.5736011	5.020618324	1.193461757	2.514302942	49.6854398	13.03157598	1.394887832
	mean	10.2857143	16.4	15.8	0.445	162.38	155.895	10.925
Female Restraint	sd	25.4932297	7.353910524	8.202438662	0.601040764	95.99681661	23.89313814	4.108290399
	sem	8.06747776	5.215539379	5.817332384	0.426270045	68.08284866	16.94548804	2.913681134

Literature Cited

Allin, J.T., & Banks, E.M. Functional aspects of ultrasound production by infant albino rats (Rattus norvegicus). Animal Behaviour, 20, 175-185 (1972).

Anisman, H., & Zucharko, R.M. Depression: the predisposing influence of stress. Behavioral Brain Science, 5, 89-137 (1982).

Blanchard, D.C., Spencer, R.L., Weiss, S.M., Blanchard, R.J., McEwen, B., & Sakai, R. R. Visible burrow system as a model of chronic social stress: behavioral and neuroendocrine correlates. Psychoneuroendocrinology, 20, 117-134 (1995).

Cornwell, C.A., Chang, J.W., Cole, B., Fukada, Y., Gianulli, T., Rathbone, E.A., McFarlane, H., & McGaugh, J.M. DSP-4 treatment influences olfactory preferences of developing rats. Brain Research, 711, 26-33 (1996).

Cornwell-Jones, C.A., Decker, M.W., Gianulli, T., Wright, E.L., & McGaugh, J.M. Norepinephrine depletion reduces the effects of social and olfactory experience. Brain Research Bulletin, 25, 643-649 (1990).

Cornwell-Jones, C.A., & Sobrian, S.K. Development of odor-guided behavior in Wistar and Sprague-Dawley rat pups. Physiology & Behavior, 19, 685-688 (1977).

Cornwell-Jones, C.A., Velasquez, P., Wright, E.L., & McGaugh, J.L. Early experience influences adult retention of aversively motivated tasks in normal, but not DSP4-treated rats. Developmental Psychobiology, 21, 177-185 (1988).

DeSouza, E.B., & Van Loon, G.R. Brain serotonin and catecholamine responses to repeated stress in rats. Brain Research, 367, 222-227 (1986).

Frysztak, R. J. & Neafsy, E.J. The effect of medial frontal cortex lesions on respiration, "freezing," and ultrasonic vocalizations during conditioned emotional responses in rats. Cerebral Cortex, 1, 418-425 (1991).

Gilad, G.M. The stress-induced response of the septo-hippocampal cholinergic system: a vectorial outcome of psychoneuroendocrinological interactions. Psychoneuroendocrinology, 12, 167-184 (1987).

Glowinski, J., & Iversen, L.L. Regional studies of catecholamines in the rat brain: I. The disposition of [^{3}H] norepinephrine, [^{3}H] dopamine and [3H] DOPA in various regions of the brain. Journal of Neurochemistry, 13, 655-669 (1966).

Goldstein, L.E., Rasmusson, A.M., Buney, B.S. & Roth, R. H. Role of the amygdala in the coordination of behavioral, neuroendocrine, and prefrontal cortical monoamine responses to psychological stress in the rat. Journal of Neuroscience, 16, 4787-4798 (1996).

Gruen, R.J., Wenberg, K., Elahi, R. & Friedhoff, A.J. Alterations in GABA-A receptor binding in the prefrontal cortex following exposure to chronic stress. Brain Research, 684, 112-114 (1995).

Insel, T.R., & Winslow, J.T. Rat pup ultrasonic vocalizations: An ethologically relevant behaviour responsive to anxiolytics. In: Animal models in psychopharmacology, eds. B. Olivier, J. Mos, & J.L. Slangen. Basel: Birkhauser Verlag (1991).

Kaltwasser, M.T. Startle-inducing acoustic stimuli evoke ultrasonic vocalization in the rat. Physiology & Behavior, 48, 13-17 (1990).

Kim, C., Campanelli, C., & Khanna, J.M. Determination of picogram levels of brain catecholamines and indoles by a simplified chromatographic electrochemical detection method. Journal of Chromatography, 282, 151-159 (1983).

Knapp, D.J. & Pohorecky, L.A. An air-puff stimulus method for elicitation of ultrasonic vocalizations in rats. Journal of Neuroscience Methods, 62, 1-5 (1995).

Lowry, O.H., Rosebrough, N.J., Farr, A.L. & Randall, R.J. Protein measurement with the folin phenol reagent. Journal of Biological Chemistry, 193, 265-275 (1951).

Mendelson, S.D., & McEwen, B.S. Autoradiographic analyses of the effects of restraint-induced stress on 5-HT1A, 5-HT1C and 5-HT2 receptors in the dorsal hippocampus of male and female rats. Neuroendocrinology, 54, 454-461 (1991).

Miller, S.A., Cobb, B.L., Baker, S.C., Curtis, J.M., Williams, M.R., & and Murphy, M.R. The use of ultrasonic vocalizations as an assessment tool for teratology and toxicology. Presented at and abstract published in the Proceedings of the annual meeting of the International Behavioral Neuroscience Society, San Diego, (1997).

Noirot, E. Ultrasounds and maternal behavior in small rodents. Developmental Psychobiology, 5, 371-387 (1972).

Okon, E.E. The temperature relations of vocalization in infant golden hamsters and Wistar rats. Journal of Zoology, 164, 227-237 (1971).

Watanabe, Y., Gould, E., Cameron, H.A., Daniels, D.C., & McEwen, B.S. Phenytoin prevents stress- and corticosterone-induced atrophy of CA3 pyramidal neurons. Hippocampus, 2, 431-435 (1992).

EFFECT OF IRON CORROSION INHIBITORS ON RESUCTIVE DEGRADATION OF CHLORINATED SOLVENTS

Baolin Deng
Associate Professor
Department of Mineral and Environmental Engineering

New Mexico Tech
296 MSEC
Socorro, NM 87801

Final Report for:
Summer Research Program
Armstrong Laboratory

Sponsored by:
Air Force Office of Scientific Research
Bolling Air Force Base, Washington, DC

And

Armstrong Laboratory

September 1997

EFFECT OF IRON CORROSION INHIBITORS ON REDUCTIVE DEGRADATION OF CHLORINATED SOLVENTS

Baolin Deng
Assistant Professor
Department of Mineral and Environmental Engineering
New Mexico Tech

Abstract

A laboratory study has been performed to examine the inhibition effects of 14 organic and inorganic chemicals (including various amino acids, phosphate, sulfate, borate, molybdate, and silicate) on anaerobic iron corrosion and trichloroethylene (TCE) degradation. Anaerobic iron corrosion is characterized by measuring hydrogen production, and TCE degradation was evaluated by the formation of the reduction products, ethylene and ethane. Some compounds such as cysteine dramatically decrease the rate of hydrogen production and also the rate of TCE reduction. Other chemicals such as histidine may not inhibit hydrogen production but still decrease the rate of TCE degradation. Such information may provide valuable insights into the relationship between anaerobic iron corrosion and chlorinated solvent reduction. An improved understanding of corrosion inhibition will help us to improve and refine metallic iron-based remediation technologies.

EFFECT OF IRON CORROSION INHIBITORS ON REDUCTIVE DEGRADATION OF CHLORINATED SOLVENTS

Baolin Deng

Introduction

Remediation of contaminated groundwater is a challenge. As indicated by a National Research Council study (NRC, 1994), the prevailing method currently used to restore groundwater in the United States is pump-and-treat systems, which is, however, unable to restore most complex contamination sites, including majority of Superfund sites. One of the alternatives for pump-and-treat systems is to construct an in-situ reactive barrier that treats contaminated water as it passes through the barrier. Metallic iron has been identified as an effective barrier material for the degradation of chlorinated solvents such as trichloroethylene (TCE) and perchloroethylene (PCE). Field studies have shown that when a groundwater plume contaminated with TCE and PCE passed through a reactive iron wall, their concentrations were reduced by more than 90% (O'Hannesin and Giliham, 1992). Full-scale application of this technology in several contamination sites so far has successfully eliminated the spread of contamination plumes.

The reactive iron barrier technology is based on the following chemical process:

$$Fe^{\circ} + RX + H_3O^{+} = Fe^{2+} + RH + 2X^{-} + H_2O \qquad (a)$$

in which chlorinated solvents dissolved in water are reduced, forming non-toxic hydrocarbons and chloride as products. This reductive dechlorination reaction, however, is just one of the several reactions occurring in the presence of metallic iron. The metallic iron can react with water itself and react with dissolved oxygen according to the following reaction stoichiometries:

$$Fe^{\circ} + 2H_2O = Fe^{2+} + H_2 + 2OH^{-} \qquad (b)$$

$$2Fe^{\circ} + O_2 + 2H_2O = Fe^{2+} + 4OH^{-} \qquad (c)$$

If all these three reactions are in parallel, it would be beneficial to block the reactions of

metallic iron with water and oxygen (Reactions b and c), while promoting the reaction with chlorinated compounds (Reaction a). However, if the dechlorination reaction depends on the iron corrosion reactions (b) and (c), then blocking these two may retard the dechlorination process.

The objective of this study is to explore whether the iron corrosion under anaerobic environment can be inhibited, and if inhibition occurs, how will it affect the chlorinated solvent degradation.

Experimental Section

Chemicals. Deionized Milli-Q water (18 megaohm-cm resistivity and < 1 mg/l total organic carbon, Millipore Corp.) was used in all experiments. Imidazole, adenine, and various amino acids (including methionine, phenylalanine, tryptophan, cysteine, histidine, and glutamic acid) were from Sigma Chemical and had at least 98% purity. Potassium phosphate (dibasic), potassium sulfate, sodium silicate, aluminum sulfate, sodium borate, sodium molybdate, and triethanolamine were obtained from Fisher Scientific.

The metallic iron was from Sigma, a powdered material produced by pentacarbonyl iron reduction by hydrogen. The iron had a purity > 97%, an average size of 4.5 - 5.2 μm and a bulk density of 4.4 g/cm^3,as reported by the supplier. The carbon content of the iron is 0.83% (w/w) as measured on a Leco WR-112 carbon analyzer, and the N_2-BET specific surface area is 0.47 m^2/g as measured using Micrometrics FlowSorb 2300. The iron sample was used without pretreatment.

Corrosion Inhibition Experiments. The effect of various chemicals on the rates of iron corrosion in the absence of chlorinated solvents was tested in 60 ml bottles. We started by weighing 1.000 g iron into each bottle and preparing solutions containing 5.0×10^{-3} M triethanolamine (as a buffer to control pH at 7.5) and 1.00×10^{-3} M potential inhibitor. The solution was purged for 10 minutes with N_2 and capped before taking into a glove box containing pure N_2. Then 30.00 ml solution was added under the N_2 atmosphere into the iron-containing bottle and crimp-sealed. These reaction bottles with half suspension and

half headspace were mixed on a rotor drum at 8 RPM and were controlled at constant temperature of 20.0 °C by an incubator. The corrosion in the presence of various chemicals was evaluated by headspace hydrogen analysis after 70 hours of reaction.

TCE Degradation Experiments. Trichloroethylene degradation by metallic iron in the presence of various inhibitors was also examined in a headspace system. Each 160 ml bottle contains 3.00g iron, 100.00 ml solution (with triethanolamine, inhibitor, and TCE), and 60 ml headspace. Similar to the corrosion inhibition experiment just described, unaerobic condition was maintained by pure N_2 and the reaction bottles were mixed by a rotor drum and maintained at 20 °C. The reaction progress was monitored as a function of time by headspace analysis for hydrogen, TCE, and TCE reduction products.

Analysis. Hydrogen was analyzed on a gas chromatograph with vapor phase injection. A Shimadzu GC-8AIT, equipped with thermal conductivity detector and molecular sieve columns, was used. Nitrogen was used as a carrier gas for both columns at a flow rate of 22.8 ml/min each and the oven temperature was set at 60.0 °C. The current was 100 mA and the attenuation was 1.

TCE and its degradation products (hydrocarbons) were analyzed by a dual-column sequence-reversal technique employing flame ionization detection (Campbell et al. 1996). 250 µl headspace samples were injected onto a Hewlett-Packard 5890 GC equipped with a 1% SP-I 000 on Carbopack B (60/80 mesh, 8 ft X 1/8 in stainless steel) column, which was connected in series to a Carboxen 1000 (60/80 mesh, 4 ft x 1/8 in stainless steel) column. Injection port temperature was 200 °C. Carrier gas was He at 30 ml/min. A column switching valve was rotated at 1 min into the run. Oven temperature program was 60 °C for I min, ramp 18 °C/min to 210 °C, and hold for 3 min. The separations from the two GC columns are superimposed on the same chromatogram. This method allowed for low-level detection of parent compounds, intermediates and products.

Results and Discussion

Iron Corrosion Inhibition. Inhibition or enhancement of various organic and inorganic compounds on iron corrosion was examined at pH 7.5 (buffered by 5.0 mM triethanolamine). These are preliminary experiments in which H_2 production is measured only at 70 hours of reaction, rather than as a function of time. The experiments are however performed with duplicates. The structures of organic compounds are shown in Table 1. The amount of hydrogen produced in the presence of these organic compounds are listed in Table 2. In the controls which contain only iron and 5.0 mM triethanolamine, H_2 concentrations are in the range from 1721 to 4737 ppm, with an average of 2750 ppm. In comparison, H_2 production in the presence of imidazole, histidine, and methionine are very close to the control, indicating that these three compounds do not significantly alter iron corrosion rate. Phenylalanine, tryptophan, and glutamic acid clearly show inhibition effect to iron corrosion, as indicated by less than 50% of H_2 production comparing to the control. Adenine and cysteine are the two compounds that demonstrate the most dramatic inhibition effect on iron corrosion. Within the experimental time period, H_2 production is only around 3% (for adenine) and 2% (for cysteine) of the H_2 production in the control.

Some amino acids (e.g. histidine and methionine) do not inhibit iron corrosion while others (e.g. phenylalanine, tryptophan, and glutamic acid) inhibit the corrosion. This indicates that the amino acid functional group is not solely responsible for the inhibition effect. Other reactive moieties in the amino acids must be involved. Cysteine strongly inhibits iron corrosion comparing to other amino acids, suggesting that the -SH group in cysteine is very effective to block iron corrosion. The -S- group (as in methionine), however, could not significantly prevent iron corrosion. The significant inhibition effect of adenine likely results from the $-NH_2$ group attached to the ring structure, since the nitrogen fused in the aromatic ring (as in imidazole and histidine) does not have a strong effect on iron corrosion.

As shown by Table 3, among the six tested inorganic compounds (including sodium silicate, sodium molybdenate, sodium borate, potassium phosphate, potassium sulfate,

and aluminum sulfate), H_2 production in the presence of sodium silicate and sodium molybdenate are very close to those of the control, suggesting that silicate and molybdenate do not significantly affect iron corrosion. Borate and phosphate apparently inhibit iron corrosion, as indicated by approximately 50% decrease in H_2 production in the presence of these two compounds.

Different from other tested inorganic and also organic compounds, potassium sulfate and aluminum sulfate do not inhibit, but rather enhance iron corrosion. The H_2 concentration in the presence of 1.0 mM potassium sulfate is 4217 ppm, which is almost four times of the H_2 production of the control. In the presence of aluminum sulfate, even more hydrogen, that is 39 times of that of the control, is generated. The enhanced rate of iron corrosion is unique, which must be resulted from the presence of sulfate. The higher sulfate concentration ($[SO_4^{2-}]$ = 3.0 mM) in aluminum sulfate system may partially explain the high H_2 production comparing to the system with potassium sulfate ($[SO_4^{2-}]$ = 1.0 mM).

Effect of Iron Corrosion Inhibitors on TCE Degradation. Trichloroethylene reduction by metallic iron was examined in the presence of each of the following compounds: cysteine, sodium silicate, sodium borate, histidine, and potassium phosphate. The reaction system contains 100 ml suspension and 60 ml headspace. The results are shown in Figures 1-3. Hydrogen production as shown in Fig.1 is measured by GC-TCD as a function of time, and is represented by the concentration in the headspace (ppm). It is expected that hydrogen partition dominantly into the vapor phase, so the hydrogen in the headspace will account for the most of the total hydrogen produced. The H_2 concentrations should indicate the magnitude of iron corrosion in various systems. TCE degradation is demonstrated by the production of various degradation intermediates and products including acetylene, ethylene, ethane, and C_3-C_6 hydrocarbons. Since high initial amount of TCE (23.5 μmole/160ml bottle) is used, the TCE degraded is less than 10% of the total in the experimental time period. Thus the production of ethylene and ethane, rather than the TCE concentration, is used to evaluate the relative reaction rates. Ethylene and ethane

produced as a function of time, in the unit of nanomole per 160 ml bottle, is shown by Fig.2 and Fig. 3 respectively.

In the blank control with only triethanolamine (5.00 mM) and TCE, no hydrogen and TCE degradation products are observed. In the absence of corrosion inhibitors but with TCE, triethanolamine buffer, and iron, significant amount of H_2 is produced along with significant ethylene and ethane production. When one of the corrosion inhibitors is added into the system, the hydrogen production is decreased with the effect of cysteine > > phosphate > histidine ~ borate > silicate (Fig.1). The inhibitors similarly influence TCE degradation as indicated by the decreased ethylene and ethane production (Fig.2 and 3). Cysteine totally blocks the TCE degradation. Phosphate, borate, histidine, and silicate decrease ethylene and ethane production by about 50 - 70%.

Summary

This preliminary study has clearly shown that iron corrosion can totally be blocked by some chemicals such as cysteine and adenine at 1.0 mM concentration level. Other compounds, including phenylalanine, tryptophan, glutamic acid, sodium borate, and potassium phosphate, can partially inhibit iron corrosion. Sulfate is however unique, which enhances the rate of iron corrosion. The iron corrosion inhibitors can also decrease rate of TCE degradation. It is possible that H_2 generation through iron corrosion and TCE reduction occur at the same set of reactive sites, thus when a chemical such as cysteine effectively competes for these active sites, both H_2 production and TCE reduction are blocked. It is also possible that H_2 production or the related corrosion process is a pre-requisite for TCE degradation. Further research is needed in order to clearly establish the relationship between H_2-generating iron corrosion and chlorinated solvent reduction.

References

National Research Council, *Alternatives for Groundwater Water Cleanup*, National Academy Press, Washington, D. C. 1994.

O'Hannesin, S. F. and R. W. Gillham, (1992) "A permeable reaction wall for in situ degradation of halogenated organic compounds", In: *Proceedings from 45th Canadian Geotechnical Society Conference,* Toronto, Ontario October 25-28, 1992.

Campbell, T.J. and Burris, D.R. Analysis of chlorinated ethene reduction products in vapor/water phase systems by dual-column, single-detector gas chromatography. Intern. J. Environ. Chem.

Table 1. Structures of Organic Compounds Examined in This Study

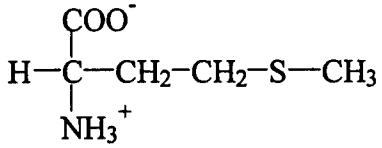

Methionine

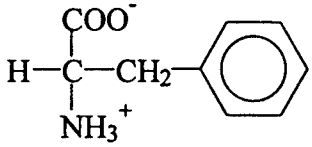

Phenylalanine

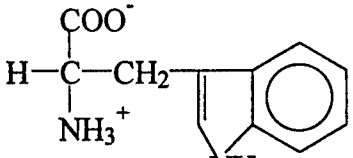

Tryptophan

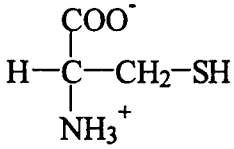

Cysteine

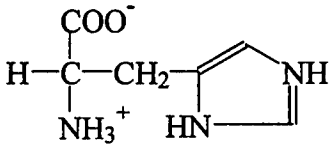

Histidine

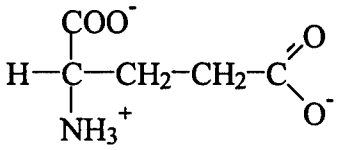

Glutamic Acid

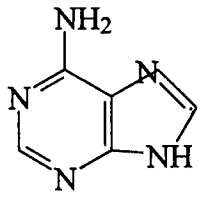

Adenine

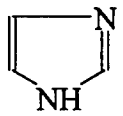

Imidazole

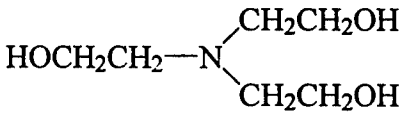

Triethanolamine

Table 2. Hydrogen Production in the Presence of Various Organic Compounds Under Anaerobic Conditions (pH 7.5 buffered by 5.0 mM Triethanolamine, 1.0 mM Organic Compound).

Inhibitor	Hydrogen Production (ppm)	Average (ppm)
Control (with Triethanolamine)	1721	
	4737	
	1801	2753
Imidazole	2697	
	1266	1981
Histidine	1689	
	1796	1742.5
Methionine	1523	
	1166	1344.5
Phenylalanine	911	
	779	845
Tryptophan	434	
	937	685.5
Glutamic acid	81	
	646	363.5
Adenine	88	
	86	87
Cysteine	63	
	52	57.5

Table 3. Hydrogen Production in the Presence of Various Inorganic Compounds Under Anaerobic Conditions (pH 7.5 buffered by 5.0 mM Triethanolamine, 1.0 mM Inorganic Compound).

Inhibitor	Hydrogen Production (ppm)	Average (ppm)
Control (with Triethanolamine)	1066 1350	1208
Na_2SiO_3	2234 860	1547
Na_2MoO_4	1006 754	880
$Na_2B_4O_7$	182 626	404
K_2HPO_4	575 358	466.5
K_2SO_4	4139 4295	4217
$Al_2(SO_4)_3$	51923 42753	47338

Figure 1. Hydrogen Production in Systems with TCE

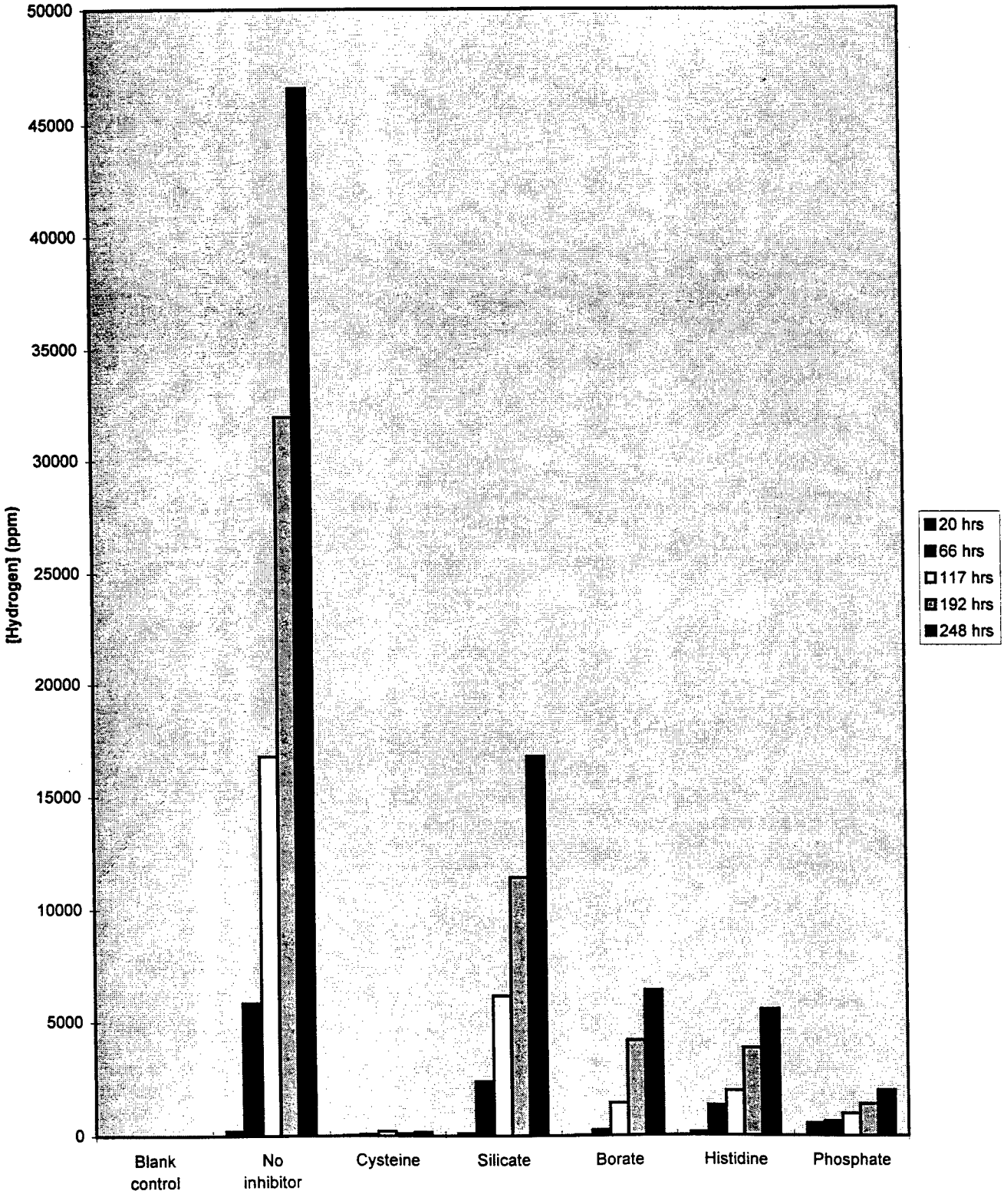

Figure 2. Ethylene Production From TCE Degradation

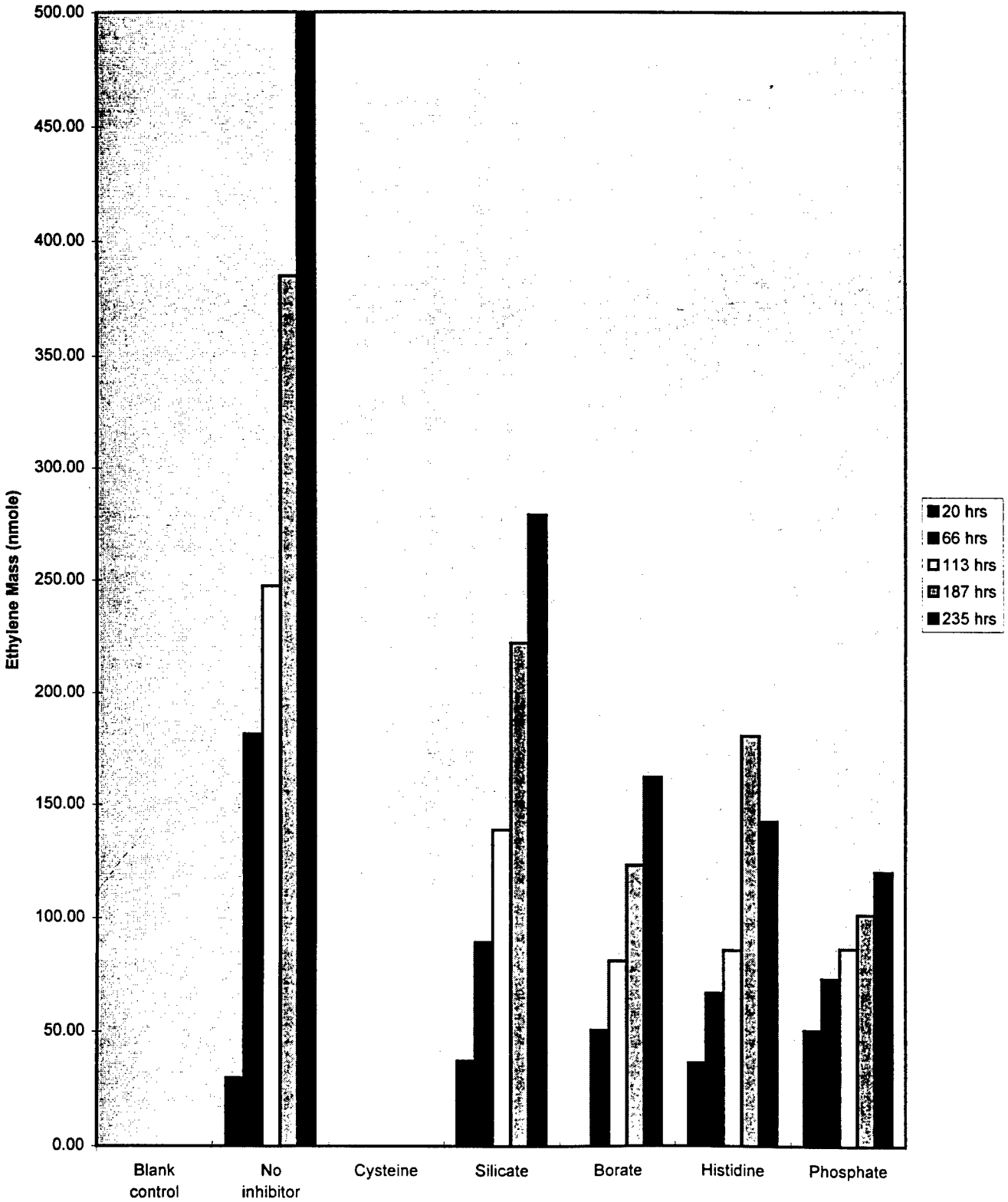

Figure 3. Ethane Production From TCE Degradation

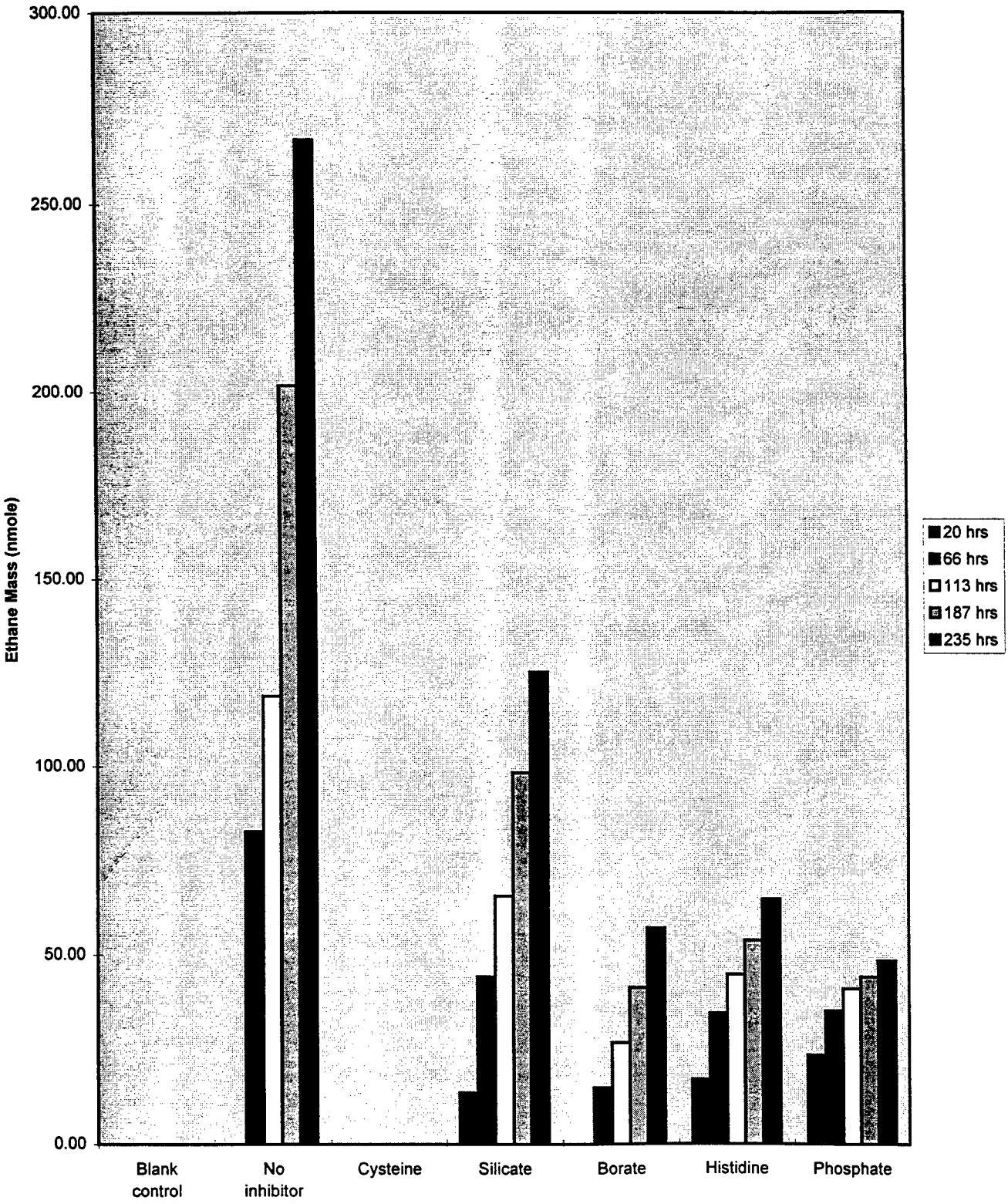

COPULATORY RESPONSE, FERTILIZING POTENTIAL, AND SEX RATIO OF OFFSPRINGS SIRED BY MALE RATS EXOSED IN UTERO TO AN ULTRAWIDEBAND ELECTROMAGNETIC FIELD OR LEAD ACETATE DURING DAYS 3 TO 18 OF GESTATION

Michael P. Dooley, MS, PhD
Assistant Professor
Department of Physiology

Iowa State University
College of Veterinary Medicine
2032 Veterinary Medicine
Ames, IA 50011-1250

Final Report for:
Summer Research Program
Armstrong Laboratory

Sponsored by:
Air Force Office of Scientific Research
Bolling Air Force Base, Washington, DC

And

Armstrong Laboratory

September 1997

COPULATORY RESPONSE, FERTILIZING POTENTIAL, AND SEX RATIO OF OFFSPRINGS SIRED BY MALE RATS EXPOSED *IN UTERO* TO AN ULTRAWIDEBAND ELECTROMAGNETIC FIELD OR LEAD ACETATE DURING DAYS 3 TO 18 OF GESTATION

Michael P. Dooley, MS, PhD
Affiliate Assistant Professor of Physiology
College of Veterinary Medicine
Iowa State University

Abstract

To evaluate whether Ultrawideband (UWB) exposures have the potential to affect developmental processes, studies were initiated using a rat model at Brooks AFB. The UWB source used for that study (Cobb **et al.**,1996) was a microwave transmitter that was capable of generating electromagnetic pulses ranging from near DC to several GHz, but had, as a primary component, microwave pulses in the MHz range. Mated females were obtained from a commercial vendor (Charles River, Inc.). On arrival, post-mating day 3, females were randomly assigned to UWB-exposure, sham-exposure, or a lead-treatment group. Treatments were administered to rats during days 3 to 18 of pregnancy and included the UWB exposures using a parallel-plate transmission line, sham-exposure, or administration of lead acetate (2 mg/ml) via the drinking water provided to the dams as a positive control (Cobb **et al.**,1996). Females were monitored for pregnancy, birth and survival of offspring, and sex distribution of the pups born. Offsprings born to control and treated groups were evaluated for evidence of neurological impairment using behavioral tests (Cobb **et al.** 1996). All behavioral testing was completed for these rats by post-partum day 62. From these pups (Cobb **et al.**, 1996), 12 male rats, 2 litter mates from each of 2 litters for each treatment group, were retained for evaluation of reproductive capability at sexual maturity and to evaluate whether prenatal exposure to the prescribed conditions exerted latent reproductive toxicity in the exposed feti. For this purpose, male rats born to females from sham-exposed, UWB-exposed, and lead-treated groups were caged individually and then paired with estrous female rats beginning on post-partum day 132. A total of 98 pairings with estrous females were made and 43/98 (44%) resulted in mating. Data analysis data revealed a trend ($P < 0.1$) for an effect of treatment on the number of male-female pairings to result in mating, however no effect of treatment was found for the proportion of fertile matings, viability and development of embryos, survival to term, and sex-ratios of offspring born to males that were exposed *in utero* to the UWB field.

COPULATORY RESPONSE, FERTILIZING POTENTIAL, AND SEX RATIO OF OFFSPRINGS SIRED BY MALE RATS EXPOSED *IN UTERO* TO AN ULTRAWIDEBAND ELECTROMAGNETIC FIELD OR LEAD ACETATE DURING DAYS 3 TO 18 OF GESTATION

Michael P. Dooley, MS, PhD

Introduction

Exposure to electromagnetic radiation is inherent to life within industrialized societies. In recent years, increasing numbers and types of radiowave and microwave transmitters have been developed and others are being developed with the potential for use in military and/or civilian applications. These systems produce relatively unique forms of electromagnetic field exposure, including electromagnetic pulses at high frequencies, with rapid risetime, and in the case of Ultrawideband (UWB) systems, result in the simultaneous emission of electromagnetic pulses over a broad frequency spectrum.

Although microwave radiation effects on biological systems have been clearly demonstrated for exposures that cause heating of cells and tissues, there has not been consensus regarding cell or animal models to identify thermal and athermal effects. Such biological models are needed to provide an experimental basis to confirm or refute the numerous associations which appear to exist between certain forms of electromagnetic radiation and cellular responses observed *in vitro* and/or in human disease states.

Maintenance of reproductive functions is essential to the continued survival of the species. Thus, factors affecting reproductive processes which have the potential to exert profound effects in either artificial or natural biological systems need to be identified. Over the past 15 years, the Reproductive Assessment by Continuous Breeding (RACB) model has been used to identify chemical toxicants affecting reproductive processes. Initial studies using the RACB paradigm relied heavily on the mouse as the animal model (Gulati, **et al.**,1991). In recent years, such studies have increasingly relied on rats, as this animal model may more correctly identify those human reproductive toxicants that are chemical in nature (Chapin and Sloane, 1997). Unfortunately, this type of breeding study is expensive to perform and should only be used for the testing of agents for which a dose-response relationship can be identified. At this time, the RACB model cannot be applied and effectively used for the evaluation of electromagnetic field effects because electromagnetic field responses to athermal exposures do not evidence a dose-response relationship.

As a result of studies performed in our laboratories at Iowa State University, we have proposed (Dooley, **et al.**,1994; Lamont **et al.**,1994) that mammalian embryos

at the preimplantation stages offers an animal model system in which the cellular effects of exposure to electromagnetic fields can be determined. Further, we have developed a non-toxic assay to complement the morphological evaluation of early embryonic development. Because the continued viability and development of embryonic cells are essential to the survival of the species, they may provide a sensitive and biologically relevant indicator to assess for detrimental consequences of electromagnetic field exposure, particularly for those forms of electromagnetic radiation that are generated as a result of human activity.

Such systems are needed in view of the fact that several epidemiological surveys have detected statistically significant associations between biological effects and residential and/or occupational exposures to electromagnetic fields ranging from extremely-low-frequency fields (<300 Hz), particularly those at 50 and 60 Hz, to high frequency radiation in the kHz to MHz range. The bioeffects which have been linked to exposure to electromagnetic radiation include an increased incidence of cancer in children, reduced fertility in humans, alteration of behavioral responses in rats and humans, developmental abnormalities in chickens, mice, and rats, and a reduced rate of development in fish and mammalian embryos (Frey, 1993; Zusman et al.,1990).

This study was performed to obtain preliminary evidence as to whether daily exposures of female rats to an UWB electromagnetic field on post-mating days 3 to 18 affected the development of male embryos and feti born to exposed females. Males used for this study were obtained from a prior study (Cobb **et al.** 1996) for which offspring had been exposed *in utero* to a UWB electromagnetic field and were evaluated for signs of abnormal or delayed development and then subjected to behavioral tests (ultrasonic stress vocalizations, locomotor responses, and Morris-maze activity). As part of that study, dams were provided lead acetate (2 mg/ml) in their drinking water as a positive control for the behavioral functions that were to be evaluated. Assessment of reproductive function was determined in these males during adulthood.

Specific objectives of this phase of the study were to use these males to evaluate whether treatment of male rat embryos during the late preimplantation stages and feti during most of the post-implantation period affected male reproductive capacity and behavior at sexual maturity. For this purpose, a total of 12 males, 2 males per dam and 2 dams per treatment group, were retained for matings beginning on post-natal day 132. Males were paired with the female overnight and mating was confirmed on the following morning based on the presence of spermatozoa in fluids obtained by lavage of the female's vagina. Pregnancy was then confirmed for each mated female by the recovery of viable embryos at the expected stage(s) of development on post-mating day 3 or the birth of live offspring at term.

Materials and Methods

Animals

Sprague-Dawley-derived male and female rats obtained through Charles River, Inc., were used for this study.

A total of 12 male rats (> 300 g, > 132 days of age) and 45 virgin female rats (> 200 g, > 100 days of age) were available for use in this study. Males were caged individually and provided food and water **ad libitum**. Female rats were caged in pairs and provided food and water as for the males. All rats were housed in plastic cages, kept in the same room, and maintained at 23 °C (range 21 - 27 °C during the study) and were provided a 14-hour light / 10-hour dark illumination cycle.

Males for this study were born to dams that were exposed to either: 1) UWB irradiation; 2) sham irradiation; or 3) as a positive control, lead acetate solution (2 mg/ml) which was continuously available in the drinking water supplied to the female. Offspring were examined for ontogeny of development (weights, coat appearance, tooth-eruption, eye-opening, air-righting) and subjected to testing with various performance measures (ultrasonic stress vocalizations, locomotor, Morris-maze activity), see Cobb et al, 1996.

Mating and Assignment to Treatment

Female rats were selected for pairing with a male based on vaginal cytology indicative of proestrus or estrus. Female rats were then placed with the designated male rat and left in the male's cage during the dark phase of the illumination cycle (14 hours' light; 10 hours' dark). Pairings were sequentially allocated to males such that each would be exposed to a comparable number of sexually receptive females during the study period. This portion of the study was "blinded", such that the individual responsible for the pairing rats and recovery and evaluation of embryos did not know the treatment to which the males had been exposed *in utero*. Mating was confirmed on the morning following pairing (day 0) by the presence of spermatozoa in the vaginal smear (Dooley, 1988). Those females for which spermatozoa or spermatozoal remnants could be identified within at least 10 microscopic fields (400x magnification) of the vaginal smear were considered to be pregnant. Unmated females were monitored and then paired when a vaginal smear consistent with proestrus or estrus was obtained. Females were paired with another male, or that same male depending on the sequence of male use, in successive cycles until mating occurred. Most females were euthanized on day 3 to confirm that fertilization had occurred, to determine the fertilization rate for the oocytes released during the pairing, that normally developing embryos were present in the oviducts, and to confirm the viability of embryos. For each treatment group,

several females were allowed to maintain the pregnancy to term to confirm that the embryos produced by these matings were capable of implantation and survival to term. Preliminary data related to the sex-ratio of offsprings born to UWB-treated rats was obtained.

UWB Exposure during *in utero* development

A Kentech microwave transmitter was used to generate microwave pulses at multiple frequencies in the MHz range. The pulse characteristics were as follows:

Peak E-field intensity = 55 kV/m
Pulse risetime = 300 ps
Pulse width = 1.8 ns
Pulse rate = 1000 pps.

The output of the Kentech source was controlled using a commercial pulse generator (Hewlett-Packard Model 8112A). The settings for the pulse controller used for these studies were as follows:

MODE = Norm
CTRL = Off
PER = 1.00 ms (1000 Hz)
DEL = 65.0 ns
WID = 100 μs
DBL = 200 μs
DTY = 50%.

During each and every animal exposure, the output of the Kentech source could be continuously monitored by the detection of an E-field signal generated between the parallel transmission plates of the exposure system. An oscilloscope amplified and displayed an image of the waveform that was considered to be representative of the E-field generated by the exposure system. Thus, this display was used to verify that the Kentech system was functional, to monitor the output as recorded from the parallel plates, and, with the aid of a Polaroid camera, to provide for photographic documentation of the waveform for the signal generated during the daily exposures provided to UWB-treated rats. Additionally, this oscilloscopic display confirmed the absence of an E-field during the exposures to the sham-treated rats.

Each UWB or sham animal exposure was performed within an anechoic chamber. Over the course of this study, chamber temperature was regulated at 24 $\pm$ 0.2 °C during each UWB and/or sham exposure. Independent measures of surface or core body temperatures of rats were not obtained. However, preliminary studies

indicated that heating of the animals did not occur. To expose rats, animals were transferred to the UWB exposure facility from animal housing facilities located in an adjacent building. Rats were transferred in an enclosed cage, equipped with a lid containing a filter to minimize exposure to potential airborne contaminants. Immediately prior to UWB exposure or sham treatment, the rat was placed in a Plexiglas restraint. The rear restraint plate was taped to ensure that the rat remained in same orientation during the exposure period. The animal was then transferred to the anechoic chamber for treatment. UWB-exposed and sham-treated rats were lightly restrained within this Plexiglas holder for periods in excess of 2, but not for more than 10 minutes. Rats were positioned within the microwave exposure chamber such that the cranial portion of each rat was closest to the microwave source (k-orientation). The Plexiglas restraint was then positioned on a Styrofoam support and taped to the support such that the rat would be positioned between the parallel plates of the transmitter and within the central portion of the E-field that was generated by the Ultrawideband exposure system.

Once each rat was positioned within the transmission facility, the door to the anechoic chamber was closed and each animal was provided a 2-minute exposure that was regulated using a computer that had been programmed to control the application of the UWB field or a sham procedure in which the experimental conditions were identical except no UWB pulses were applied. At the end of each exposure, the female rat was removed from the restrainer, replaced within the transport cage, and then returned to the facility housing the rat colony. Thus, dams were exposed daily for this 2-minute period to either the UWB or sham-treatment for 16 days, beginning on post-mating day 3. Exposures were provided to female rats, such that it could be anticipated that preimplantation stage embryos present within the oviducts and uterine horns would be exposed during their 4^{th} and subsequent cellular cycles (8-cell, 16-cell, etc.), during the peri-implantation period, throughout organogenesis, and for most of the period of sexual differentiation (events occurring during the post-implantation period). Pups born alive were evaluated for clinical signs reflecting normal development and for behavioral responses including vocalization tests and locomotor behavior (Cobb **et al.**,1996). All locomotor and related behavioral testing was completed by day 62. Rats were then maintained without further testing until used for the evaluation of reproductive capacity beginning on day 132.

Experimental Endpoints

The following endpoints were recorded for each pairing of a male with an estrous female rat:

Date of pairing.
Presence of spermatozoa in the post-pairing vaginal smear.

The following endpoints were recorded for each mated female rat:

Number, developmental stage, and viability of embryos recovered on day 3.

Or

Date of parturition

Number of offspring born at term.
Viability of offspring born at term.
Sex of offspring.

Statistical Analyses

Chi-square analysis of ratios was used to compare the proportion of male-female pairings to result in mating for the lead-exposed, UWB-exposed, and sham-treated male rats and the proportion of mated females that were pregnant, as determined by the presence of normal embryos within the reproductive tracts on post-mating day 3 or by the birth of live offsprings at term. For those females that were allowed to go to term, the number of pups born alive for each rat and the proportion of male and female offspring born to these rats were compared using Chi-square analysis of ratios in order to determine the effects of treatment applied to a male during *in utero* development on the endpoints to be analyzed. Analyses of variance (ANOVA) were used to compare the litter size and gestation interval for sham-treated, lead-exposed, and UWB-exposed rats. Statistical significance was preestablished at $P \leq 0.05$ for all planned comparisons.

Results

For these males, male-female pairings were performed such that a total of 43 female rats were mated and either euthanized on post-mating day 3 to evaluate the status of early embryonic development and rate of fertilization, or allowed to go to term to confirm the birth of live offsprings and sex ratio of offspring sired by sham-exposed, lead-treated, and UWB-exposed male rats. All of the male-female pairings were performed as rapidly as possible based on the estrous cyclicity of the females which were available for use in this study. All matings were completed within a 2-month period and inspection of the pairing records (data not shown) revealed that for the 12 males used in this study, no male had mated more than 3 times in any given 7-day period and none had mated more than 4 times within any given 14-day period. A total of 98 male-female pairings were necessary to obtain the 43 pairings which resulted in mating. Of these, 20 female rats (47%) were mated by sham-treated males, 14 (33%) were mated by lead-exposed males, and 9 (21%) by the UWB-exposed males (see data in Table 1).

The treatments applied to the dams which fostered these males, the identification number assigned to each male offspring used, the number of pairings performed, the number of matings detected, and the number of fertile matings are summarized in Table 1.

Although the number of male-female pairings was comparable for the 3 treatments, there was a trend for an effect of treatment ($P < 0.1$, Table 2) on the proportion of male-female pairings to result in mating. Much of the observed variation was due to the low frequency for copulation for 2 of the UWB-exposed males (Nos. 7 and 8) derived from dam No. 6. For these 2 males, only 2 of 19 pairings with females presumed to be in estrus resulted in mating (refer to data shown in Table 1). The proportion of pairings to result in copulation ranged from 1/9 (11 %) for 1 lead-exposed male and 2 of the UWB-exposed males, to 8/9 (89 %) for the sham-exposed male designated No. 2. All but one of the males produced a fertile mating during this study. The one male that failed to produce a pregnancy (No. 8) was from the UWB-exposure group. This male copulated only once in the 9 times for which the male was paired with an estrous female and no embryos or oocytes were recovered from that female when the oviducts and uterine horns were flushed to collect embryos on post-mating day 3. The other litter mate to this male also copulated with only 1 of the 9 estrous females presented, however, that mating was fertile.

Table 1. No. of male-female pairings, matings, and fertile matings obtained for male rats from sham-exposed dams and for males born to dams that were treated with lead acetate or exposed to an UWB electromagnetic field during days 3 to 18 of pregnancy.

Treatment Group	Dam No.	Male No. (Offspring ID)	No. Pairings	No. Matings	No. Fertile Matings (%)
Sham-exposed	1	1 (ID = 5)	7	5	4 (80)
		2 (ID = 7)	9	8	7 (88)
	3	5 (ID = 21)	10	5	3 (60)
		6 (ID = 23)	8	2	1 (50)
Lead-treated	2	3 (ID = 13)	9	1	1 (100)
		4 (ID = 15)	8	4	4 (100)
	5	9 (ID = 37)	8	3	3 (100)
		10 (ID = 39)	8	6	5 (83)
UWB-exposed	6	7 (ID =45)	9	1	1 (100)
		8 (ID = 47)	9	1	0 (0)
	8	11 (ID = 29)	7	4	4 (100)
		12 (ID = 31)	6	3	3 (100)

No. Pairings: Number of pairings for a given male with female rats presumed to be in proestrus or estrus.

No. Matings: Number of females for which a sperm-positive vaginal smear was obtained on the morning after pairing with the male.

No. Fertile Matings: Number of females with a sperm-positive vaginal smear for which one or more viable embryos were recovered on post-mating day 3 or which produced one or more live offspring at term.

Regardless of the treatment group from which the male was obtained, most of the initial pairings of males with females judged to be in proestrus or estrus, based on the cytological characteristics of the vaginal smear, resulted in mating during the first pairing (23/43; 53%, data not shown in Tables). However, consistent with the data shown for mating frequency, see Table 2, the first pairing data for these 43 females revealed that 10/14 (71%) of the pairings with sham-exposed males resulted in copulation during the female's first pairing with a male, but only 8/17 (47%) of the initial pairings of females with lead-exposed males, and 5/12 (42%) of the initial pairings of females with UWB-exposed males resulted in a mating during the first exposure of the female to a mature male.

Table 2. Proportion of male-female pairings for which matings occurred for male rats from sham-exposed dams and for males born to dams treated with lead acetate or exposed to an UWB electromagnetic field during days 3 to 18 of pregnancy.

Treatment Group	Mated		Non-Mated	
	No. Rats	(%)	No. Rats	(%)
Sham-exposed	20	(59)	14	(41)
Lead-treated	14	(42)	19	(58)
UWB-exposed	9	(29)	22	(71)

Mating was confirmed by the presence of spermatozoa in the vaginal smear obtained on the morning after pairing with the male.

The proportion of pairings with female rats presumed to be in proestrus or estrus that resulted in mating was not different among groups, but there was a trend ($P < 0.1$) for an effect of the treatment to which the males were exposed during days 3 to 18 of pregnancy to influence the likelihood of a mating when the male was placed with a sexually receptive female.

Table 3. Proportion of fertile matings for male rats from sham-exposed dams or for males from dams treated with lead acetate or exposed to an UWB electromagnetic field during days 3 to 18 of pregnancy.

Treatment Group	Pregnant		Non-Pregnant	
	No. Rats	(%)	No. Rats	(%)
Sham-exposed	15	(75)	5	(25)
Lead-treated	13	(93)	1	(7)
UWB-exposed	8	(89)	1	(11)

For female rats euthanized on post-mating day 3, a fertile mating was considered to have occurred if one or more morphologically normal embryos at the 8-cell stage were recovered. For rats allowed to go to term, a fertile mating was considered to have occurred if one or more live offspring were born at term.

The proportion of fertile matings for sham-exposed male rats was not different ($P > 0.1$) than for males born to dams that were treated with lead acetate or UWB-exposed during days 3 to 18 of pregnancy.

Table 3 summarizes the data for fertile matings among control and treated rats. The proportion of matings which were fertile was not affected by treatment ($P > 0.1$) and ranged from 75% for the sham-exposed males to 93 % for the male offspring from dams that were exposed to lead during days 3 to 18 of gestation.

Data obtained for oocyte and embryo recovery on post-mating day 3 are shown in Table 4. The ratios of unfertilized oocytes/degenerate embryos, retarded embryos, and normal embryos which resulted from pairings with males which were treated during *in utero* development were not affected by treatment ($P > 0.1$).

The number of oocytes and/or embryos recovered, ranged from 0 to 16 (mean $\pm$ SD = 9.2 $\pm$ 5.2) for the 15 females mated with sham-exposed males, 0 to 15 (mean $\pm$ SD = 11.7 $\pm$ 4.7) for the 9 females mated with lead-exposed males, and from 0 to 17 (mean $\pm$ SD = 9.7 $\pm$ 7.3) for the 6 females mated with UWB-exposed males (data not shown in Tables). No embryos or oocytes were recovered from 2 of the females which copulated with sham-exposed male rats,

Table 4. **Number of oocytes and/or embryos recovered on post-mating day 3 from female rats paired with male rats born from sham-exposed dams or for matings performed with males born to dams treated with lead acetate or exposed to an UWB electromagnetic field during days 3 to 18 of pregnancy.**

Treatment Group	No. Females	Total No. Embryos Recovered	Stage of Embryonic Development					
			Degenerate / Unfertilized		Retarded		Normal	
			No.	(%)	No.	(%)	No.	(%)
Sham-exposed	15	138	44	(32)	4	(3)	90	(65)
Lead-treated	9	105	21	(20)	14	(13)	70	(67)
UWB-exposed	6	58	11	(19)	5	(9)	42	(72)

Degenerate / Unfertilized = Abnormal embryos and fragmented oocytes.

Retarded = Viable embryos that were morphologically normal, but at the 2-, 3-, or 4-cell stage of development at the time of recovery.

Normal = Viable embryos that were morphologically normal at the time of recovery and were comprised of ≥ 5 blastomeres.

The proportion of normal embryos that resulted from matings with males born to sham-exposed rats was not different ($P > 0.1$) than for those from matings with males born to dams that were lead-treated or UWB-exposed during days 3 to 18 of pregnancy.

1 of the 9 females which copulated with lead-exposed male rats, or from 1 of the 6 females which copulated with UWB-exposed male rats. For the remaining females, only degenerate embryos or unfertilized oocytes were detected in 2 of the females which were mated with sham-exposed males. All of the other females had one or more morphologically normal embryos at the time of recovery. The proportions of normal embryos in females judged to be pregnant ranged from 20 to 100% for the sham-exposure group, from 23 to 93% for the lead-exposure group, and from 52 to 100% for the UWB-exposure group.

All of the females that were allowed to go to term produced litters. The litter size was not affected by treatment ($P > 0.1$, Table 5) and ranged from 10 to 17 pups. All of the pups born to these females ($n = 13$) were born alive.

Table 5. Mean litter size at term for females mated to male rats born to sham-exposed dams and for males from dams treated with lead acetate or exposed to an UWB electromagnetic field during days 3 to 18 of pregnancy.

Treatment Group	Litter Size		
	Mean	(± SD)	Range
Sham-exposed	14.2	(1.3)	13 - 17
Lead-treated	14.0	(2.5)	10 - 16
UWB-exposed	13.7	(0.6)	13 - 14

Data are mean (± SD) for sham-exposed ($n = 5$), lead-treated ($n = 5$) and UWB-exposed male rats ($n = 3$).

The mean litter size of dams mated with males born to sham-exposed rats was not different ($P > 0.1$) than for dams mated with males born to females that were lead-treated or UWB-exposed during pregnancy.

The sex-ratios of offspring born to sham-exposed, lead-exposed, and UWB-exposed males are shown in Table 7. Overall, 97/182 (53.3) of the pups born were male, however the proportion of males born were not different ($P > 0.1$, Table 7) for the 3 treatment groups.

The proportion of litters in which the number of male pups was equal to or exceeded the number of female pups ranged from 1/3 (33%) for the UWB-exposure group to 5/5 (100%) for the sham-exposure group. Due to the relatively small sample size, these differences were not significant ($P > 0.1$, Table 8).

Table 7. Number of male and female pups born at term to dams mated to male rats from sham-exposed dams or from dams treated with lead acetate or exposed to an UWB electromagnetic field during days 3 to 18 of pregnancy.

Treatment Group	Male		Female	
	No. Pups	(%)	No. Pups	(%)
Sham-exposed	41	(58)	30	(42)
Lead-treated	37	(53)	33	(47)
UWB-exposed	19	(46)	22	(54)

Data shown are for for n = 5 litters for sham-exposed, n = 5 litters for lead-exposed, and n = 3 litters for matings with UWB-exposed male rats.

The proportion of male pups born to females mated with sham-exposed males was not different ($P > 0.1$) than the proportion of male pups born to females mated with lead-treated or UWB-exposed males.

Table 8. **Proportion of females mated to male rats from sham-exposed dams or to males from dams treated with lead acetate or exposed to an UWB electromagnetic field during days 3 to 18 of pregnancy to produce litters in which the number of males born was equal to or exceeded the number of female offspring for that litter.**

Treatment Group	Male ≥ Female		Female > Male	
	No. Rats	(%)	No. Rats	(%)
Sham-exposed	5	(100)	0	—
Lead-treated	3	(60)	2	(40)
UWB-exposed	1	(33)	2	(67)

The proportion of female rats to remain pregnant and produce litters in which the number of female offspring exceeded the number of male offsprings at term was not affected ($P > 0.1$) by the treatment that was provided to the mother during days 3 to 18 of gestation.

Summary and Conclusions

The results obtained for these UWB-exposed rats confirm that when male embryos are exposed *in utero* to an UWB electromagnetic field from days 3 to 18 of gestation, these males are capable of fertile matings at sexual maturity. Furthermore, for these UWB-exposed dams, no other toxicity or harmful effects of UWB exposure were observed in the female or male offspring that were born and subjected to testing (Cobb, **et al.**,1996).

Previous studies performed with acute exposures using Ultrawideband sources and exposure parameters, related to, but distinct from those reported here did not find effects in rats for functional tests which included swimming performance, alterations in blood chemistries, or expression of *c-fos* protein in neural tissues (Walters **et al.**,1995). Nor were acute effects seen for UWB exposures to primates when a task paradigm was used (Sherry **et al.**,1996).

At the power settings and exposure intervals used for this study and with this Ultrawideband exposure system, exposure to the UWB field was not expected to induce heating in cells or tissues of the dam. Hence, it is presumed that the cellular

effects of UWB exposure to embryonic or fetal cells, if any, would be athermal.

It may be of interest to note that these results were obtained at a power level that approached the maximum output for this exposure system. Still, these exposures were performed at a relatively low power intensity when compared to other types of electromagnetic field sources that are used in military and civilian activities and when compared to UWB sources that are being developed.

For the conditions described here, no evidence was obtained to suggest that UWB-exposure of mated rats on days 3 to 18 of gestation altered embryonic development and the sexual differentiation of the offspring. These males appeared to have developed normally. The fact that males born to these UWB-exposed females were capable of mating, and that the fertilization rate, viability of embryos, and rates of early embryonic development among treatment groups were not different, and that mated females produced live offsprings at term, is consistent with the null hypothesis that there are no latent effects of exposure to this form of electromagnetic radiation at the intensity, frequencies, pulse rate, and for the exposure duration and developmental windows used for these rats.

It should be noted, however, that the exposures provided to these females were not initiated until 3 days after mating and did not continue throughout gestation. Furthermore, exposure were only performed on the embryos and feti resulting in the F_1 generation for these females. Hence the potential effects of UWB exposure on spermatozoal transport, survival, and/or spermatozoal selection prior to fertilization in mated rats, or to chronic and/or cumulative effects exerted on the oocytes which are destined to be released in subsequent estrous cycles, as well as other aspects of the reproductive physiology of the male and female, remain to be determined.

The lead acetate treatment provided as a positive control in this study was intermediate in dosage to that used in recent studies in rats which suggested that administration of lead acetate to males can produce demonstrable effects on reproductive performance, particularly when treatment is initiated prenatally (McGivern **et al.**,1991; Ronis, **et al.**,1996). Administration of lead acetate (0.1%) to dams during the last trimester of pregnancy (McGivern **et al.**,1991) affected the reproductive performance of both females and males, including a reduction in masculine sexual behavior during adulthood. When the effects of lead exposure administered either pre- or post-natally were compared, *in utero* exposure of males resulted in the most dramatic effects. This is consistent with the results of other studies designed to identify chemicals that cause reproductive toxicity in animals (Gulati, **et al.**,1991). In this study, most of the successful pairings of sham-, UWB- and lead-treated males resulted in fertile matings, regardless of treatment. Hence, none of the treatments provided to these rats *in utero* could be considered to have severely impaired reproductive function. The proportion of normal embryos

recovered on post-mating day 3 for all of the treatment groups was lower than expected based on prior studies with this animal model (Dooley 1988; Dooley, **et al.**,1989). The reason for this discrepancy remains to be determined.

Although, these breeding trials were based on a relatively small proportion of the males born to the female rats used for the UWB exposure trial, the number of matings provided should have been adequate to identify treatment effects of sufficient magnitude to impair fertility. The low number of matings for these UWB-exposed males was not expected. In view of the fact that only 9/31 (29%) of the pairings of UWB-exposed males with estrous females produced a fertile mating, as compared to 14/33 (42%) of the pairings with lead-exposed males, and 20/34 (59%) of the pairings with sham-exposed (control) males (data from Table 2) further studies in this area may be warranted to confirm or refute the trend for reduced copulatory activity among UWB-exposed males that is suggested by these data.

Acknowledgments

The assistance provided by Ms. Brenda Cobb, who performed the UWB exposures to these dams, behavioral testing of the progeny, and coded the males used in this phase of the Ultrawideband study is gratefully acknowledged.

References

Chapin, R. E., and. Sloane, R. A, 1997. Reproductive assessment by continuous breeding: Evolving study design and summaries of ninety studies. Environ. Health Perspect. 105 (Suppl. 1):199-205.

Cobb, B. L., Mason, P. A., Miller, S. A., Kosub, K. R., Jauchem, J., and Murphy, M. R., 1996. A teratologic study of UltraWideBand electromagnetic field exposure. Presented at: Eighteenth Annual Meeting of the Bioelectromagnetics Society, Victoria, British Columbia, Canada, June 9-14, 1996. Poster Session B: Behavior, Abstract P-160B. BEMS Abstract Book, p. 259.

Dooley, M. P., 1988. The use of eosin B to assess the viability and developmental potential of rat embryos. Dissertation, Iowa State University, Ames, Iowa, 1988.

Dooley, M. P., Pineda, M. H., and Martin, P. A., 1989. Single or intermittent exposure of rat embryos to eosin B does not affect **in vitro** development, survival after transfer, birth of live offspring, and development to weaning. 22nd Ann. Meeting Soc. for the Study of Reprod., Univ. of Missouri, Columbia, MO., August 6-9, 1989, Abstract No. 337. Biol. Reprod. Vol. 40 (Suppl. 1):160.

Dooley, M. P., Pineda, M. H., Lamont, J. W., Weber, R. J., and Moye, D. J., 1994. Continuous Exposure of rat embryos to a 1.5 g electromagnetic field (EMF) does not affect **in vitro** development and viability. Presented at: Experimental Biology 94, Anaheim, CA., April 24-28, 1994, The FASEB Journal, Vol. 8, No. 4, Part 1, p. A398, March 1994.

Dooley, M. P., Cobb, B. L., Merritt, J. H., and Jauchem, J. R., 1996. Development of rat embryos exposed to an UltraWideBand (UWB) electromagnetic field. Presented at: Eighteenth Annual Meeting of the Bioelectromagnetics Society, Victoria, British Columbia, Canada, June 9-14, 1996. Session A-8: **In Vivo** Bioeffects, Abstract A-8-1. BEMS Abstract Book, p. 30.

Frey, A. H., 1993. Electromagnetic field interactions with biological systems. FASEB J. 7:272-281.

Gulati, D. K., Hope, E., Teague, J. and Chapin, R. E., 1991. Reproductive toxicity assessment by continuous breeding in Sprague-Dawley rats: A comparison of two study designs. Fundam. Appl. Toxicol., 17:270-279.

Lamont, J. W., Weber, R. J., Dooley, M. P., Pineda, M. H., and Moye, D. J., 1994. Shielded Culture chamber and controlled uniaxial magnetic field generator for very low frequency (VLF) magnetic field exposure of cells during **in vitro** culture. Presented at: Experimental Biology 94, Anaheim, CA., April 24-28, 1994, The FASEB Journal, Vol. 8, No. 4, Part 1, p. A398, March 1994.

McGivern, R. F., Sokol, R. Z., and Berman, N. G., 1991. Prenatal lead exposure in the rat during the third week of gestation: long-term behavioral, physiological, and anatomical effects associated with reproduction. Toxicol. Appl. Pharmacol., 110:206-215.

Ronis, M. J., Badger, T. M., Shema, S. J., Roberson, P. K., and Shaikh, F., 1996. Reproductive toxicity and growth effects in rats exposed to lead at different periods during development. Toxicol. Appl. Pharmacol., 136:361-371.

Sherry, C. J., Blick, D. W., Walters, T. J., Brown, G. C., and Murphy, M. R., 1995. Lack of behavioral effects in non-human primates after exposure to ultrawideband electromagnetic radiation in the microwave frequency range. Radiat. Res., 143:93-97.

Walters, T. J., Mason, P. A., Sherry, . C., Steffen, C., and Merritt, J. H., 1995. No detectable bioeffects following acute exposure to high peak power ultra-wide band electromagnetic radiation in rats. Aviat. Space Environ. Med., 66:562-567.

Zusman, I., Yaffe, P., Pinus, H., and Ornoy, A., 1990. Effects of pulsing electromagnetic fields on the prenatal and postnatal development in mice and rats: **In vivo** and **in vitro** studies. Teratology 42:157-170.

THE EFFECT OF VISUAL SIMILARITY AND REFERENCE FRAME ALIGNMENT ON THE RECOGNITION OF MILITARY AIRCRAFT

Dr. Itiel Dror
Assistant Professor
Department of Psychology

Southampton University
Highfield, Southampton SO17 1BJ
England

Final Report for:
Summer Faculty Research Program
Armstrong Laboratory

Sponsored by:
Air Force Office of Scientific Research
Bolling Air Force Base, DC

And

Armstrong Laboratory

September, 1997

THE EFFECT OF VISUAL SIMILARITY AND REFERENCE FRAME ALIGNMENT ON THE RECOGNITION OF MILITARY AIRCRAFT

Dr Itiel Dror
Department of Psychology
Southampton University
Highfield, Southampton SO17 1BJ England

ABSTRACT

Aircraft similar in appearance (homogeneous) and dissimilar in appearance (heterogeneous) were studied at orientations consistent with the environmental frame of reference (canonical) or inconsistent with the environmental frame of reference (non-canonical). Response time data for correct identifications indicate that identification performance was better for heterogeneous than homogeneous aircraft. This performance advantage for heterogeneous aircraft was found at both the original training orientations and for novel orientations. Canonical orientations during learning produced better identification performance than non-canonical orientations. Implications for aircraft recognition training are discussed.

THE EFFECT OF VISUAL SIMILARITY AND REFERENCE FRAME ALIGNMENT ON THE RECOGNITION OF MILITARY AIRCRAFT

Dr Itiel Dror

INTRODUCTION

When teaching aircraft recognition, what cognitive processes can be utilized to maximize recognition effectiveness? In this paper, we address two such processes. First, we consider the overall visual similarity of the set of aircraft to be taught. Second, we consider the alignment of the internal reference frame of the aircraft with the environmental reference frame.

The general context in which we study these processes is that of object constancy across orientation manipulations within the picture plane. We measure recognition performance as a function of angular disparity between aircraft images presented during learning and later at test. This manipulation provides a measure of learning transfer to novel orientations. This is a crucial issue in aircraft training because aircraft are typically viewed in many more orientations than other stimulus classes. An optimal training regimen for the identification of aircraft would incorporate the least number of views necessary to achieve high object constancy across novel orientations. The number of views, and the specific views chosen, may vary depending upon the overall visual similarity of the group of aircraft to be learned, as well as the initial orientations used during training.

Visual similarity can be modeled as category membership. That is, the more dissimilar a group of objects, the "higher" level category they compose, whereas objects more similar in appearance can be considered "lower" level category members. For example, working with aircraft, a novice may classify a wide variety of aircraft as simply being "planes," whereas an Air Force pilot may identify aircraft by their specific names and even model number (F15-Eagle, or more specifically, F15c-Eagle).

Rosch, Mervis, Gray, Johnson, & Boyes-Braem (1976) suggested that expertise may interact with the basic level of categorization that people use to identify classes of objects. Since their suggestion, a growing body of evidence suggests that expertise promotes facility with category levels subordinate to the basic level. For example, Palmer, Jones, Hennessy, Unze, and Pick (1989) found that musicians and nonmusicians differed on the level at which they identified musical instruments. The musicians' identification responses were more specific than the nonmusicians ("violin" as compared to "strings," or "trumpet" as compared to "brass"). Tanaka and Taylor (1991) found that experts on birds and dogs were as fast and accurate at making subordinate level identifications (sparrow, beagle) as they were at the basic level (bird, dog). In comparison, novices on birds and dogs showed a decrement in identification performance at the subordinate level as compared to the basic level. Tanaka and Taylor (1991) concluded that increased expertise led to increased use of, and access to, subordinate level information. (See also Johnson and Mervis (1997), and Gauthier and Tarr (1997))

In our experiment, we used subjects who by self report were novices at recognizing aircraft. Thus past research suggested that their recognition for aircraft that were similar in appearance (lower category) should be

slower and less accurate than that for objects that were dissimilar in appearance (higher category). We predicted that as subjects gained expertise with the aircraft, the disparity between their identification performance on similar and dissimilar aircraft would lessen, and perhaps disappear completely.

Aircraft have a distinct axis of symmetry that is also the major axis of elongation. There are data that recognition performance is enhanced when the internal reference frame of the object is aligned with the environmental reference frame. For example, Shiffrar and Shepard (1991) presented two successive cubes on a CRT and asked subjects to determine if the rotations of the two cubes in three-dimensional space were the same or different. Both the speed and accuracy of the subjects' performance was best when the axis of symmetry of the cube was aligned with the vertical axis of the environmental reference frame. Similarly, Pani (1993) instructed subjects to predict the outcomes of various rotations of a square in three-dimensional space. Subjects' accuracy was best when the rotations where normal to both the square and the environmental reference frame (See also Appelle (1972); Corballis, Nagourney, Shetzer, & Stefanatos (1978); Friedman and Hall (1996); Hinton (1988); Parsons (1995); Pani (1994); Pani and Dupree (1994); Pani, Jeffres, Shippey, & Schwartz (1996); Pani, Williams, & Shippey (1995)).

We tested this finding with aircraft images. We predicted that when the major axis of the aircraft were aligned with the 0, 90, 180, and 270 degree orientations of the environmental reference frame, subsequent recognition performance would be better than when these reference frames were not aligned. We also tested the transfer of recognition performance as a function of object and environmental reference frame alignment. Would improved recognition performance due to aligned object and environmental frames lead to improved transfer across orientations?

Whitmore, P. G., Rankin, W. C., Baldwin, R. O., & Garcia, S. (1972) collected data relevant to the issue of learning transfer to novel orientations. They attempted to determine the minimum number of aircraft training views necessary to achieve an identification accuracy rate of 95% for novel orientations. Using slides made from scaled models, they trained subjects using regularly sequenced orientations in three-dimensional space, and then collected accuracy data for identification of slides made from models at novel orientations. Their results suggested that as few as nine well chosen views could facilitate accurate identification at 45 novel views. They reported anecdotal evidence suggesting that subjects took much longer to make identification responses when the angular disparity between novel views and test views was large.

We contend that due to the potentially severe consequences of inaccurate aircraft identification it is prudent to collect response time data on transfer of learning to novel orientations. Given enough time, accurate identification responses can be made based upon very few learning views. However, the nature of aircraft recognition precludes lengthy analysis of the target image. Thus, with this study, we focus on response time for correct responses as the primary dependent measure.

METHODS

Subjects

82 subjects were recruited through several local temporary agencies using the criteria that they 1) were between 18 and 30 years of age, 2) had at least a high school diploma or Graduate Equivalency Degree (GED), and 3) reported no previous experience with recognizing aircraft. When they arrived at the laboratory all subjects were

screened for visual acuity using a standard Schnelling Eye Chart. Only those subjects whose vision was 20/30 or better participated. All subjects were paid for their work.

Materials

Stimuli consisted of 12 high-resolution, gray-scale images of military aircraft. A "0 degree" orientation was designated for each aircraft and was a top view with the nose of the aircraft being oriented towards the top of the CRT. Thus the aircraft appeared to be standing on its tail and pointing straight up. Sixty-four images of each of the 12 aircraft were made by rotating the 0 degree image in the picture plane at increments of 5.625 degrees. When presented on the CRT in the 0 degree orientation, the height of the aircraft was approximately 10 cm. Because subjects sat approximately 60 cm from the CRT, the stimulus images subtended a visual angle of approximately 9.5 degrees.

A mask image was also generated. The mask was a circular image with a gradient fill from black to white, starting with black in the center and becoming progressively lighter along the radius, thus giving the effect of a dark centered starburst from black to gray to white across concentric circles.

Based upon the results of cluster analyses from previous experiments, and cluster analyses from pilot studies, four aircraft that were similar (Homogeneous) in appearance were chosen and four aircraft that were dissimilar (Heterogeneous) in appearance were chosen. The four Homogeneous aircraft were from the same cluster (see Figure 1), whereas the four Heterogeneous aircraft were from different clusters (see Figure 2). These eight aircraft were studied by the subjects for later identification. An additional four aircraft were chosen as distractors. Two distractors were chosen for the Homogeneous set based upon the experimenters' subjective determination that they resembled the aircraft in the Homogeneous set. Two distractors were chosen for the Heterogeneous set based upon the experimenters' subjective determination that they were as distinct as the aircraft in the Heterogeneous set. Thus there were six Homogeneous aircraft (four targets and 2 distractors) and six Heterogeneous aircraft (four targets and 2 distractors). As noted above, each of the twelve aircraft could be presented at any of 64 orientations in the picture plane.

The actual military names of the Homogeneous aircraft were Eagle, Hornet, Fulcrum, and Flanker as target stimuli with Foxbat and Falcon as the distracters. The actual military names of the Heterogeneous aircraft were Fishbed, Galab, Tomcat, and Farmer as target stimuli with Mirage and Fresco as the distracters.

A canonically-oriented set of aircraft consisted of all eight of the target aircraft described above oriented at 0, 90, 180, and 270 degrees in the picture plane. See Figure 1 for examples of aircraft at the four canonical orientations. A non-canonically-oriented set of aircraft consisted of all eight of the target aircraft described above oriented at 22.5, 112.5, 202.5, and 292.5 degrees in the picture plane. See Figure 2 for examples of aircraft at the four non-canonical orientations.

The stimuli were presented on an IBM compatible microcomputer with a high-resolution RGB CRT. Responses were made on the keyboard. Accuracy and millisecond response times were recorded by the computer. Each participant was tested in a three-sided cubicle.

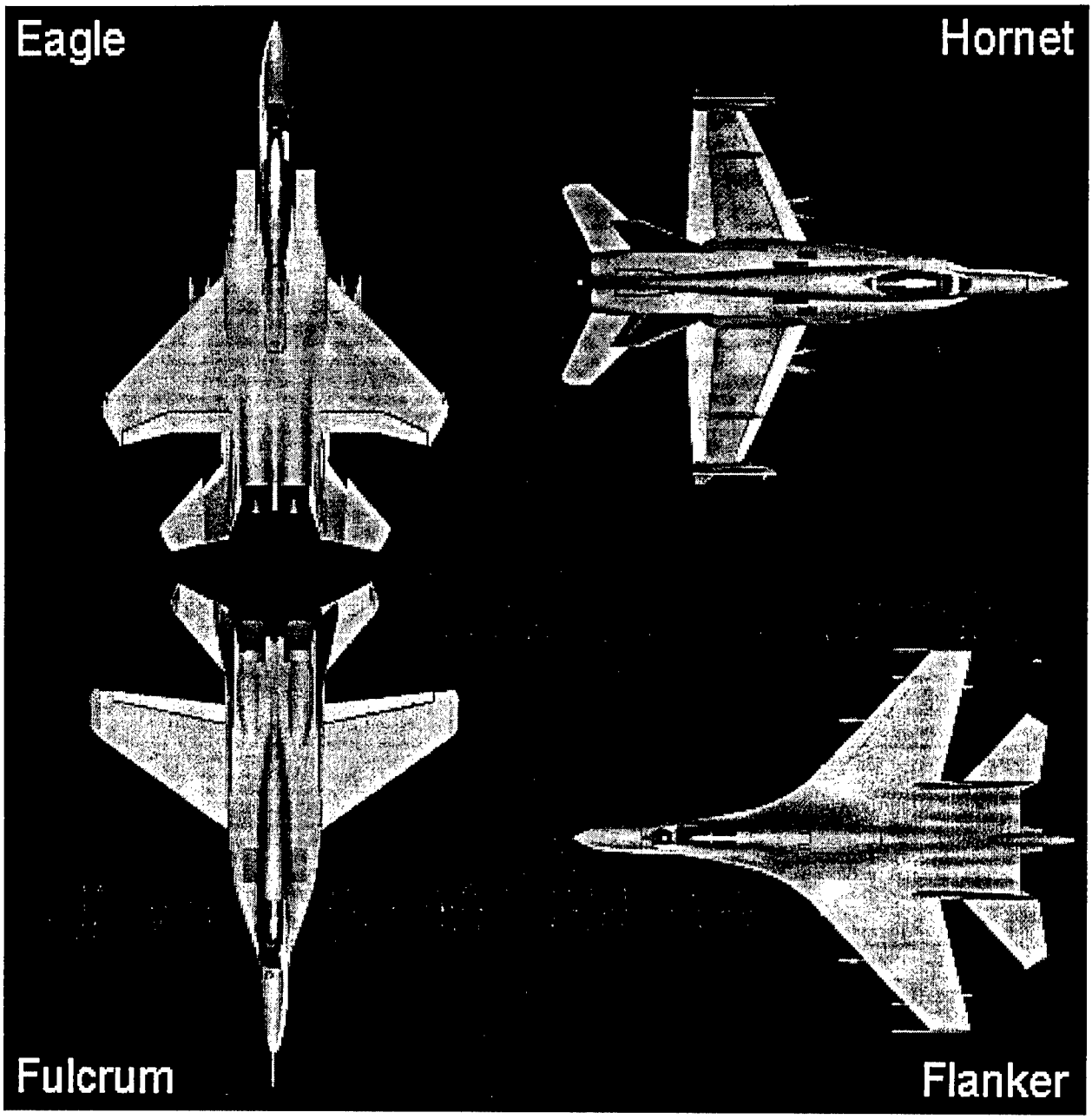

Figure 1. The four aircraft that were homogeneous in appearance, at the four canonical learning orientations, shown with their names.

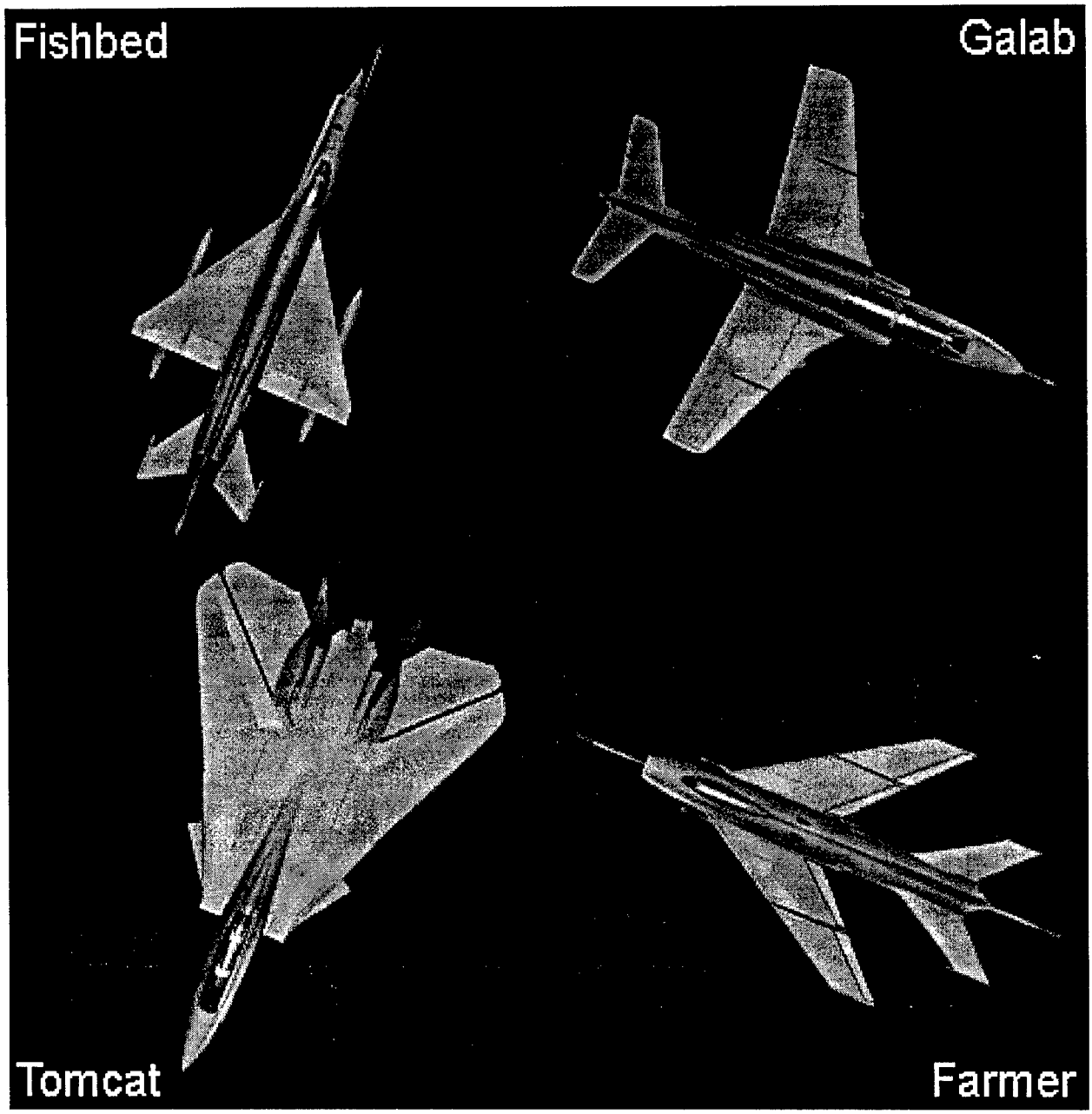

Figure 2. The four aircraft that were heterogeneous in appearance, at the four non-canonical learning orientations, shown with their names.

Design and Procedure

Pretest/Posttest. Immediately before and after the experiment all subjects completed a multiple-choice aircraft identification test. This test contained 19 aircraft including the 12 aircraft used as stimuli. Three images of an individual aircraft were presented on the CRT along with seven possible answers. Six of the answers were names of aircraft, while the seventh answer was always "none of the above." Responses were made on the keyboard using the number keys 1 - 6 for the aircraft names, and 7 for "none of the above." After a response was made, another aircraft was presented, and so on, until all 19 aircraft had been presented.

There were two forms of the test. In Form A the three images depicted the standard three views used by the Department of Defense to teach aircraft recognition. These were a side view (side), a top view (top), and a head-on view (front). In Form B all three views were oblique. In one view the aircraft was pointing towards the viewer with the nose angled up and to the right (up), in another the aircraft was pointing towards the viewer with the nose angled down and to the right (down), and in the third the aircraft was pointing away from the viewer with the nose angled up and to the right (away).

All subjects completed both forms of the test before the experiment, and again after the experiment. The order of the two versions was counterbalanced across subjects with an ABBA/BAAB design.

Aircraft Naming The experiment had two factors, each with two levels, resulting in four conditions. The first factor (Learning Orientation) varied the orientation at which the aircraft stimuli were learned. The two levels of the Learning Orientation factor were Canonical (0, 90, 180, and 270 degrees) and Non-canonical (22.5, 112.5, 202.5, and 292.5 degrees). Learning Orientation was a between-subjects factor. The second factor (Similarity) varied the degree of visual similarity among aircraft to be learned. The two levels of the Similarity factor were Homogeneous and Heterogeneous. Similarity was a within-subjects factor, and was counterbalanced across subjects. Thus the four experimental conditions were 1) Canonical and Homogeneous, 2) Canonical and Heterogeneous, 3) Non-canonical and Homogeneous, and 4) Non-canonical and Heterogeneous.

The procedure was identical for each of the four conditions. There was a Learning Phase followed by a Testing Phase. Each phase was composed of blocks of trials. Trials consisted of an aircraft stimulus both preceded and followed by a 100 ms mask. The duration of the aircraft stimulus was 5000 ms or until a response was made, whichever came first. The responses were made on keyboard keys that were labeled with the aircraft names. There was a fifth key labeled "NA" for none of the above.

Learning Phase The Learning Phase consisted of nine blocks of trials. During the first block the four aircraft were presented ten times at each of the four learning orientations. Thus there were 160 trials in the first block (4 aircraft X 4 orientations X 10 repetitions). The order of trials was randomized per subject within the block. On each trial the name of the aircraft was presented along with the aircraft image. Subjects were instructed to study the image for the full 5000 ms, and to associate the name with the aircraft. After the second mask cleared the CRT, the subjects pressed the key labeled with the correct aircraft name. Subjects were instructed to concentrate and strive for perfect accuracy because their recognition of the four planes would be tested later. Accuracy feedback was provided by a beep if an incorrect key was pressed.

The second, third, and fourth blocks of the Learning Phase were identical. During these blocks the four aircraft were presented ten times at each of the four learning orientations. Thus there were 160 trials in each block (4 aircraft X 4 orientations X 10 repetitions). The order of trials was randomized per subject per block. On each trial only the aircraft image was presented. The aircraft names were not presented. Subjects were instructed to press the key labeled with the correct aircraft name as soon as they recognized each aircraft. Subjects were instructed to respond as quickly as possible while still maintaining high accuracy. Accuracy feedback was provided by a beep if an incorrect key was pressed. After the fourth block subjects were given a ten-minute rest break.

The fifth block was identical to the first block except for the number of repetitions. The four aircraft were presented once at each of the four learning orientations. Thus there were 16 trials in the fifth block (4 aircraft X 4 orientations). The order of trials was randomized per subject within the block. On each trial the name of the aircraft was presented along with the aircraft image. Subjects were instructed to study the image for the full 5000 ms, and to associate the name with the aircraft. After the second mask cleared the CRT, the subjects pressed the key labeled with the correct aircraft name. Subjects were instructed to concentrate and strive for perfect accuracy because their recognition of the four planes would be tested later. Accuracy feedback was provided by a beep if an incorrect key was pressed.

The sixth, seventh, eighth, and ninth blocks were identical to the second, third, and fourth blocks. During these blocks the four aircraft were presented ten times at each of the four learning orientations. Thus there were 160 trials in each block (4 aircraft X 4 orientations X 10 repetitions). The order of trials was randomized per subject per block. On each trial only the aircraft image was presented. The aircraft names were not presented. Subjects were instructed to press the key labeled with the correct aircraft name as soon as they recognized each aircraft. Subjects were instructed to respond as quickly as possible while still maintaining high accuracy. Accuracy feedback was provided by a beep if an incorrect key was pressed. After the ninth block subjects were given a ten minute rest break.

Test Phase The Test Phase consisted of two blocks of trials. The first block was identical to the fifth block of the Learning Phase. The four aircraft were presented once at each of the four learning orientations. Thus there were 16 trials in the first block (4 aircraft X 4 orientations). The order of trials was randomized per subject within the block. On each trial the name of the aircraft was presented along with the aircraft image. Subjects were instructed to study the image for the full 5000 ms, and to associate the name with the aircraft. After the second mask cleared the CRT, the subjects pressed the key labeled with the correct aircraft name. Subjects were instructed to concentrate and strive for perfect accuracy because their recognition of the four planes would be tested later. Accuracy feedback was provided by a beep if an incorrect key was pressed. The order of trials was randomized per subject within the block.

The second block consisted of 320 trials during which the primary data for the experiment were collected. During the second test block the four aircraft were presented once at each of the 64 test orientations for a total of 256 presentations (4 aircraft X 64 orientations). In addition, two distractor aircraft were presented. One distractor was presented once at each of the 32 odd-numbered orientations (1, 3, 5, etc.), while the other distractor was presented once at each of the 32 even-numbered orientations (2, 4, 6, etc.), for a total of 64 distractor presentations (2 distractors X 32 orientations). The order of trials was randomized per subject within the block. On each trial only the

aircraft image was presented. The aircraft names were not presented. Subjects were instructed to press the key labeled with the correct aircraft name as soon as they recognized each aircraft. Subjects were informed that distractors had been added, and they were to press the key labeled "NA" for none of the above at the presentation of a distractor. Subjects were instructed to respond as quickly as possible while still maintaining high accuracy. Unlike all proceeding blocks in the Learning Phase and the Test Phase, no accuracy feedback was provided if an incorrect key was pressed.

The second block was preceded by 24 practice trials for the purpose of stabilizing the subjects' response time performance before the introduction of the primary experimental trials. Subjects were not informed that the first 24 trials of the second block were practice trials. For the practice trials the four aircraft were presented once at each of the four learning orientations for a total of 16 presentations (4 aircraft X 4 orientations). In addition, the two distractors were presented once at each of the 45, 135, 225, and 315 degree orientations for a total of eight presentations (2 distractors X 4 orientations). The order of the practice trials was randomized per subject.

RESULTS

All response times are expressed in milliseconds. For correct responses, medians were calculated across the four target aircraft at each orientation, for each block, for each subject. The seven blocks of the Learning Phase were analyzed separately from the final block of the Test Phase.

Learning Phase

Because there were four orientations in each of the seven learning blocks, and each subject participated in both levels of the Similarity factor, there were 56 medians per subject in the learning phase. The Similarity factor had the two levels of Homogeneous and Heterogeneous and was a within-subjects factor. The Block factor had seven levels (there were seven learning blocks) and was a within-subjects factor. The Orientation factor had four levels (there were four orientations used during learning) and was a within-subjects factor. The Learning Orientation factor had the two levels of Canonical and Non-canonical and was a between-levels factor. The design for the response time ANOVA for the Learning Phase was: ((2) Learning Orientation) X ((2) Similarity) X ((7) Block) X ((4)Orientation).

The ANOVA revealed significant main effects for Learning Orientation, $F(1, 80) = 4.54$, $p < .05$, $MSE = 545751.40$; for Similarity, $F(1, 80) = 86.83$, $p < .001$, $MSE = 110663.30.23$; for Block, $F(6, 480) = 120.80$, $p < .001$, $MSE = 14128.42$; and for Orientation, $F(3, 240) = 5.78$, $p < .01$, $MSE = 3063.52$.

As shown in Figure 3, for the Learning Orientation factor, the response time for Non-canonical presented aircraft ($M = 830$, $SE = 15.42$) was higher than the response time for Canonically presented aircraft ($M = 784$, $SE = 15.42$).

As shown in Figure 4, for the Similarity factor, the response time for Homogeneous aircraft ($M = 852$, $SE = 13.74$) was higher than the response time for Heterogeneous aircraft ($M = 761$, $SE = 9.84$).

As shown in both Figures 3 and 4, for the Block factor, the response times decreased monotonically until the fourth block, after which they held steady through the remainder of the learning phase($M1 = 905$, $SE1 = 15.41$, $M2 = 840$, $SE2 = 12.90$, $M3 = 814$, $SE3 = 11.61$, $M4 = 762$, $SE4 = 10.40$, $M5 = 770$, $SE5 = 10.47$, $M6 = 781$, SE6

= 10.08, M7 = 777, SE7 = 10.15.

For the Orientation factor, the four average response times are not meaningful because they are collapsed across the Canonical and Non-canonical orientations. Specifically, the first Orientation factor represents a collapse of performance at the 0 and 22.5 degree orientations, the second is that of the 90 and 112.5 degree orientations, the third is that of the 180 and 202.5 degree orientations, while the fourth is that of the 270 and 292.5 degree orientations. However, all terms that include the Orientation X Learning Orientation factor are meaningful because this interaction does not collapse across the Canonical and Non-Canonical factor.

The ANOVA revealed significant interactions for Similarity X Block, $F(6, 480) = 27.89$, $p < .001$, MSE = 9736.86, and Similarity X Block X Orientation, $F(18, 1440) = 1.98$, $p < .01$, MSE = 1566.85. However, the latter interaction cannot be interpreted due to the manner in which the Orientation factor is collapsed. There were no other significant interactions.

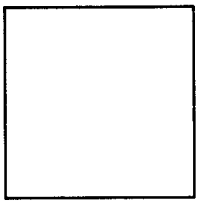

Figure 3. Response time for correct recognition of aircraft images during learning as a function of learning block. Canonical and Non-canonical learning orientations plotted separately. Error bars indicate the normalized standard error.

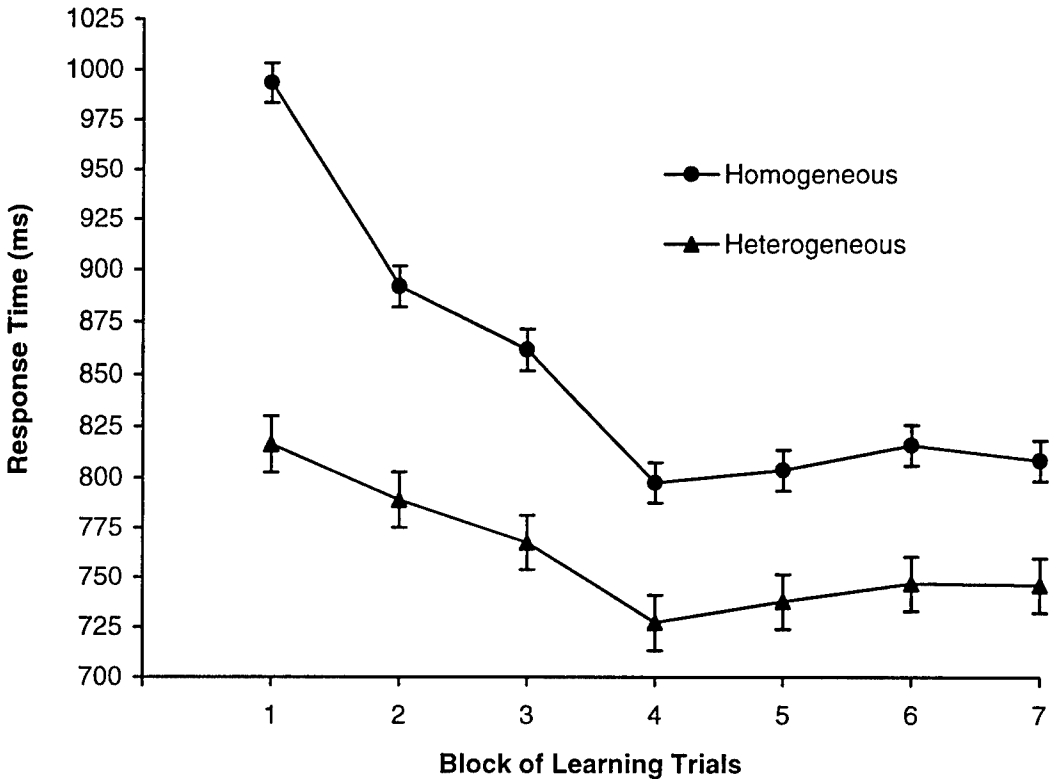

Figure 4. Response time for correct recognition of aircraft images during learning as a function of learning block. Homogeneous and Heterogeneous aircraft plotted separately. Error bars indicate the normalized standard error.

Test Phase

Because there were 64 orientations at which the aircraft were presented during the Test Phase, there were 64 medians per subject in the test phase. The 64 medians were collapsed as a function of distance from the learning orientations. Thus, all medians that were 5.625 degrees from a learning orientation were averaged, all medians that were 11.250 degrees from a learning orientation were averaged, all medians that were 16.875 degrees from a learning orientation were averaged, and so forth. Because the learning orientations were separated by 90 degrees, the maximum distance that the collapsed data could be from a learning orientation was 45 degrees. After collapsing, the data represented median response times per subject at 0.000, 5.625, 11.250, 16.875, 22.500, 28.125, 33.750, 39.375, and 45.000 degrees from a learning orientation, and made up the nine levels of the within-subjects Orientation factor. The Learning Orientation factor had the two levels of Canonical and Non-canonical and was a between-levels factor. The Similarity factor had the two levels of Homogeneous and Heterogeneous and was a within-subjects factor. The design for the response time ANOVA for the Test Phase was: ((2) Learning Orientation) X ((2) Similarity) X ((9)Orientation).

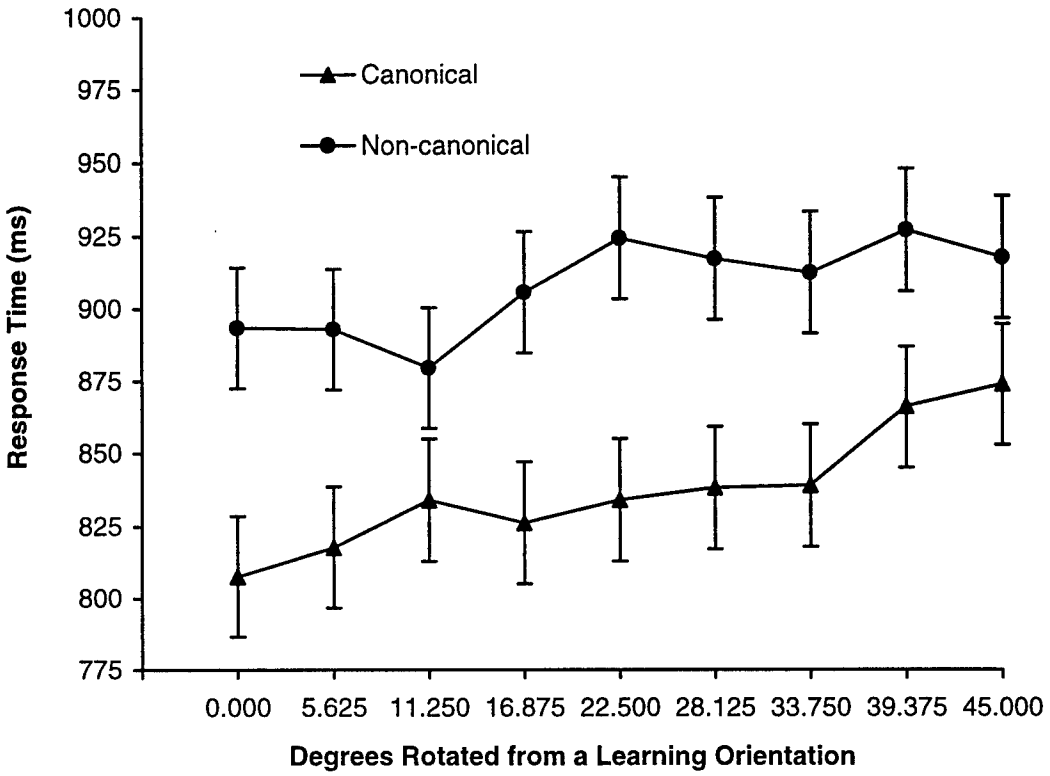

Figure 5. Response time for correct recognition of aircraft images as a function of degree rotated in the picture plane away from a learning orientation. Canonical and Non-canonical learning orientations plotted separately. Error bars indicate the normalized standard error.

The ANOVA revealed significant main effects for Learning Orientation, $F(1, 80) = 5.65$, $p < .05$, $MSE = 322875.60$; for Similarity, $F(1, 80) = 57.87$, $p < .001$, $MSE = 60913.23$; and for Orientation, $F(8, 640) = 9.88$, $p < .001$, $MSE = 4639.13$.

As shown in Figure 5, for the Learning Orientation factor, the response time for Non-canonical presented aircraft ($M = 907$, $SE = 20.92$) was higher than the response time for Canonically presented aircraft ($M = 837$, $SE = 20.92$).

As shown in Figure 6, for the Similarity factor, the response time for Homogeneous aircraft ($M = 921$, $SE = 17.82$) was higher than the response time for Heterogeneous aircraft ($M = 823$, $SE = 14.22$).

As shown in both Figures 5 and 6, for the Orientation factor, the response time tended to increase monotonically as the distance from the learning orientation increased ($M1 = 850$, $SE1 = 14.45$, $M2 = 855$, $SE2 = 14.07$, $M3 = 857$, $SE3 = 13.90$, $M4 = 866$, $SE4 = 15.77$, $M5 = 879$, $SE5 = 15.14$, $M6 = 877$, $SE6 = 15.07$, $M7 = 875$, $SE7 = 15.17$, $M8 = 896$, $SE8 = 17.14$, $M9 = 895$, $SE9 = 19.14$).

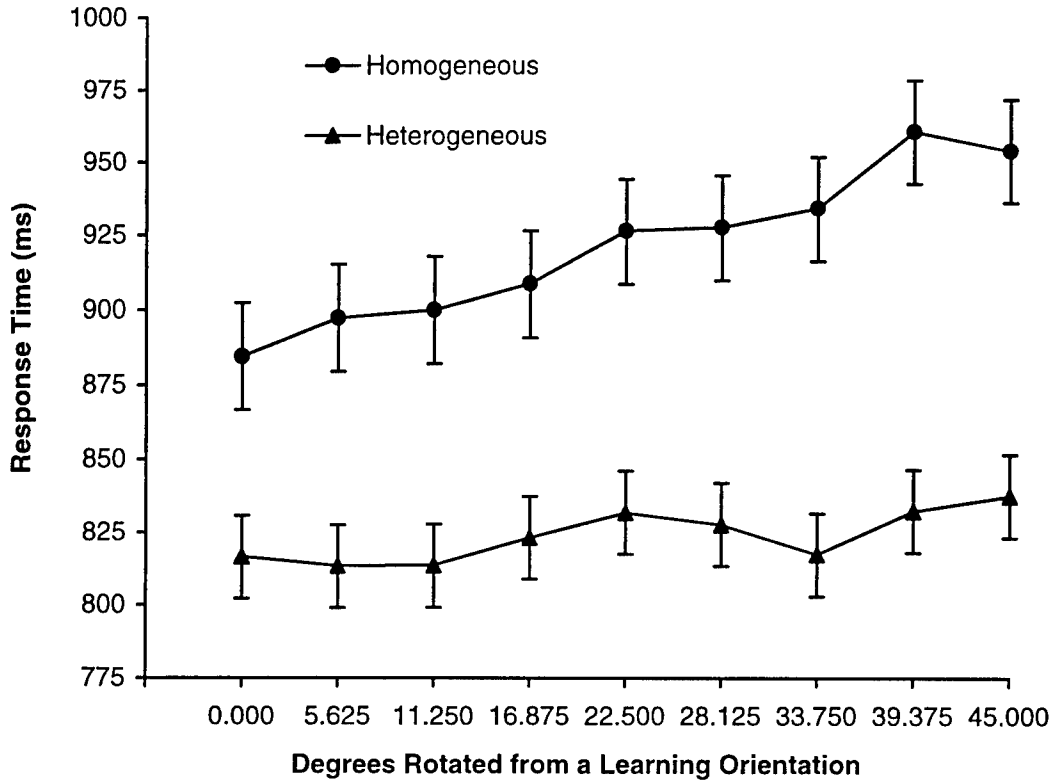

Figure 6. Response time for correct recognition of aircraft images as a function of degree rotated in the picture plane away from a learning orientation. Homogeneous and Heterogeneous aircraft plotted separately. Error bars indicate the normalized standard error.

The ANOVA revealed significant interactions for Learning Orientation X Orientation, $F(8, 640) = 2.47$, $p < .05$, $\underline{MSE} = 4639.13$, and Similarity X Orientation, $F(8, 640) = 3.06$, $p < .01$, $\underline{MSE} = 5026.07$. There was no Learning Orientation X Similarity interaction, $F(1, 80) < 1.00$.

Polynomial contrasts on the Orientation factor revealed that there was a significant linear trend, $F(1, 80) = 43.27$, $p < .001$, $\underline{MSE} = 7812.31$, with response time increasing as distance from a learning orientation increased. The sixth-order polynomial contrast was significant but could not be interpreted.

The linear component of the Orientation factor was tested between the Canonical and Non-canonical levels of the Learning Orientation factor. There was no significant linear X Learning Orientation interaction.

The linear component of the Orientation factor was tested between the Homogeneous and Heterogeneous levels of the Similarity factor. There was a significant linear X Similarity interaction, $F(1, 80) = 13.26$, $p < .001$, $\underline{MSE} = 8279.96$.

DISCUSSION

Interpretation of the results is straightforward, and the results from the Test Phase mirror those of the Learning Phase.

Discrimination between aircraft that are dissimilar in appearance is easier than between aircraft that are similar. During the Learning Phase, the Homogeneous aircraft were consistently slower to be identified than the Heterogeneous aircraft. Even after performance had leveled off around the fourth learning block, the Heterogeneous aircraft maintained a consistent advantage of approximately 65-70 ms. This difference was slightly greater at test, approximately 100 ms.

A similar pattern was found for the Learning Orientation manipulation. During the Learning Phase, the Non-canonically presented aircraft were consistently slower to be identified than the Canonically presented aircraft. Even after performance had leveled off around the fourth learning block, the Canonically presented aircraft maintained a consisted advantage of approximately 40-45 ms. This difference was slightly greater at test, approximately 70 ms.

The Orientation factor measured the transfer of recognition from the aircraft at the learning orientations to adjacent orientations in the picture plane. There was a linear decrease in recognition performance as the angular disparity increased between learning orientation and test orientation.

The average visual similarity of the set of aircraft interacted with the transfer of recognition to novel orientations. For the Heterogeneous aircraft, there was very little performance degradation as the angular disparity increased between learning orientation and test orientation. The Homogeneous aircraft generated considerably more performance degradation than the Heterogeneous aircraft for the same measure.

In contrast, there was no interaction between Learning Orientation and transfer of recognition to novel orientations. The Canonically and Non-canonically presented aircraft generated the same amount of transfer of learning.

We conclude that both average similarity of the set of aircraft and the initial orientation at which they are learned, have a powerful effect on identification performance both during learning and later at test.

The data suggest that the more distinctive the individual aircraft are within a set, the more transfer of learning will occur from the initial learning orientation to novel orientations. This in turn suggests that for distinctive aircraft fewer total views of aircraft would be needed during learning to insure accurate identification at novel orientations. In comparison, aircraft that are more similar in appearance will require more total views to insure accurate identification at novel views.

Further research is required to quantify the relationship between homogeneity of the aircraft stimulus set and the minimum number of view required to maximize recognition performance across all novel orientations. Based upon our current research (Ashworth, 1997), a mixture of oblique and accidental views (looking down any foreshortened axis) would be required. Because we have noted that the learning transfers very poorly between accidental views, all accidental views would need to be included in any training regimen, regardless of homogeneity. Thus based upon the results reported here, a savings in training time and resources could be attained by using fewer oblique views during learning of heterogeneous aircraft as compared to homogeneous aircraft.

This prescription mirrors that of Gibson (1947). In his work on aircraft recognition for the Army Air Corp, Gibson (1947) suggested that aircraft of similar appearance should be shown in pairs while students made timed discrimination responses between the pairs. He further stated that this procedure was not necessary for aircraft that were dissimilar in appearance. Thus Gibson also suggested different teaching methodologies based upon visual similarity of the aircraft.

Considering past research, (e.g., Appelle (1972); Corballis, Nagourney, Shetzer, & Stefanatos (1978); Friedman and Hall (1996); Hinton (1988); Parsons (1995); Pani (1993); Pani (1994); Pani and Dupree (1994); Pani, Jeffres, Shippey, & Schwartz (1996); Pani, Williams, & Shippey (1995); Shiffrar and Shepard (1991)) the main effect for initial learning orientation is not surprising. However, our data reveal just how powerful this effect is. For example, After four blocks of the seven-block Learning Phase, identification performance was asymptotic for both the Canonically-oriented and Non-canonically-oriented aircraft. This suggests that continued practice would not lead to equivalent performance across this manipulation.

Further, inspection of test data in Figure 3 suggests that identification performance at 22.5 degrees from a Canonically-oriented training orientation is better than that at 0.0 degrees from a Non-canonically-oriented training orientation. This means that training at the Canonical orientations and then testing at the Non-canonical orientations produces better identification than training at the Non-canonical orientations and then testing at the Non-canonical orientations! This surprising result is significant, $F(1, 80) = 4.05$, $p < .05$, $\underline{MSE} = 35868.26$.

The mechanism which drives the enhanced performance on aircraft studied at the canonical orientations is unknown. For example in his review of the reference frame literature, Palmer (1989) concludes that object recognition is mediated primarily by the intrinsic reference frame for objects whose structure clearly defines one, by an environmental reference frame for objects whose structure does not clearly define an intrinsic reference frame, with the best recognition occurring when intrinsic reference frames align with the environmental reference frame (see also Palmer, Rosch, & Chase (1981)). However Palmer does not elaborate upon why the coincidence of these two reference frames produces the best recognition performance. He simply notes that it is assumed that "there are biases toward picking other salient orientations as the reference orientation, especially gravitational vertical or the top-bottom axis of the retina" (p.127).

We concur with Shephard (1982, 1984) and Shiffrar and Shephard (1991), that this effect must ultimately derive from the invariant nature of the terrestrial gravitational field and its predictable influence on objects. Objects with primary internal axes are the most stable if their axes are either in line with gravity, or orthogonal to gravity. Objects whose primary internal axes are at oblique angles to gravity tend to topple over. Our experience with objects in the world is predominated by objects whose internal axes are normal to gravity, and thus our perceptual apparatus exploits these regularities in the world.

The results suggest that if only a very limited number of views are to used during training then views should be chosen such that the intrinsic and environmental reference frames align. Further, if the external constraints of the training regimen will allow the optimum number of views to be used, then those in which the intrinsic and environmental reference frames align should be included. As already noted, accidental views should always be included.

REFERENCES

Appelle, S. (1972). Perception and discrimination as a function of stimulus orientation: The oblique effect in man and animals. *Psychological Bulletin, 78,* 266-278.

Ashworth, A. R. S., III (1997). A comparison of oblique and accidental views for the learning of military aircraft. Manuscript in preparation.

Corballis, M. C., Nagourney, B. A., Shetzer, L. I., & Stefanatos, G. (1978). Mental rotation under head tilt: Factors influencing the location of the subjective reference frame. Perception & Psychophysics, 24(3), 263-273.

Friedman, A., & Hall, D. L. (1996). The importance of being upright: Use of environmental and viewer-centered reference frames in shape discriminations of novel three-dimensional objects. Memory & Cognition, 24(3), 285-295.

Gauthier, I., & Tarr, M. J. (in press). Becoming a greeble expert: Exploring mechanisms for face recognition. *Vision Research.*

Gibson, James, J., & Gagne, Robert, M. (1947). Research on the recognition of aircraft. In James J. Gibson (Ed.), Motion picture testing and research (pp. 113-168). *Army Air Forces Aviation Psychology Program Research Reports, Report No. 7.* U.S. Government Printing Office, Washington 25, D.C.

Hinton, G. E., & Parsons, L. M. (1988). Scene-based and viewer-centered representations for comparing shapes. *Cognition, 30,* 1-35.

Johnson, K. E., Mervis, C. B. (1997). Effects of varying levels of expertise on the basic level of categorization. *Journal of Experimental Psychology: General, 126(3),* 248-277.

Palmer, S. E. (1989). Reference frames in the perception of shape and orientation. In B. E. Shepp, S. Ballesteros (Eds.), *Object Perception: Structure and Process* (pp. 121-163). Hillsdale, NJ: Erlbaum.

Palmer, S. E., Rosch, E., & Chase, P. (1981). Canonical perspective and the perception of objects. In J. Long, A. Baddeley (Eds.), *Attention & Performance IX* (pp. 135-151). Hillsdale, NJ: Erlbaum.

Palmer, C. F., Jones, R. K., Hennessy, B. L., Unze, M. G., & Pick, A. D. (1989). How is a trumpet known? The "basic object level" concept and the perception of musical instruments. *American Journal of Psychology, 102,* 17-37.

Pani, J. R. (1993). Limits on the comprehension of rotational motion: mental imagery of rotations with oblique components. *Perception, 22,* 785-808.

Pani, J. R. (1994). The generalized cone in human spatial organization. *Spatial Vision, 8(4),* 491-501.

Pani, J. R., & Dupree, D. (1994). Spatial reference systems in the comprehension of rotational motion. *Perception, 23,* 929-946.

Pani, J. R., William, C. T., & Shippey, G. T. (1995). Determinants of the perception of rotational motion: Orientation of the motion to the object and to the environment. *Journal of Experimental Psychology: Human Perception and Performance, 21(6),* 1441-1456.

Pani, J. R., Jeffres, J. A., Shippley, G. T., & Schwartz, K. J. (1996). Imagining projective transformations: Aligned orientations in spatial organization. *Cognitive Psychology, 31,* 125-167.

Parsons, L. M. (1995). Inability to reason about an object's orientation using an axis and angle of rotation. *Journal of Experimental Psychology: Human Perception and Performance, 21(6),* 1259-1277.

Rosch, E., Mervis, C. B., Gray, W. D., Johnson, D. M., & Boyes-Braem, P. (1976). Basic objects in natural categories. *Cognitive Psychology, 8,* 382-439.

Shepard, R. N. (1982). Perceptual and analogical bases of cognition. In J. Mehler, E. C. T. Walker, & M. Garrett (Eds.), *Perspectives on mental representation* (pp. 49-67). Hillsdale, NJ: Erlbaum.

Shepard, R. N. (1984). Ecological constraints o internal representation: Resonant kinematics of perceiving, imagining, thinking, and dreaming. *Psychological Review, 91,* 417-447.

Shiffrar, M. M., & Shepard, R. N. (1991). Comparison of cube rotations around axes inclined relative to the environment or to the cube. *Journal of Experimental Psychology: Human Perception and Performance, 17(1),* 44-54.

Tanaka, J. W., & Taylor, M. (1991). Object categories and expertise: Is the basic level in the eye of the beholder? *Cognitive Psychology, 23,* 457-482.

Whitmore, P. G., Rankin, W. C., Baldwin, R. O., & Garcia, S. (1972). Studies of aircraft recognition training. *Human Resources Research Organization Technical Report 72-5,* HumRRO Division 5, Fort Bliss, Texas.

ADVANCES IN BIOLOGICALLY-BASED KINETIC MODELING FOR TOXICOLOGICAL APPLICATIONS

Brent D. Foy
Assistant Professor
Department of Physics

Wright State University
Colonel Glenn Hwy.
Dayton, OH 45435

Final Report for:
Summer Faculty Research Program
Armstrong Laboratory

Sponsored by:
Air Force Office of Scientific Research
Bolling Air Force Base, DC

and

Armstrong Laboratory

September, 1997

ADVANCES IN BIOLOGICALLY-BASED KINETIC MODELING FOR TOXICOLOGICAL APPLICATIONS

Brent D. Foy
Assistant Professor
Department of Physics
Wright State University

Abstract

Several physiological processes have been modeled and incorporated into existing pharmocokinetic models of the perfused rat liver. The kinetics of binding to proteins, membrane transport via a 4-state carrier, and the presence of serial capillary compartments in a liver have been modeled. One of the new features, protein binding kinetics, was explored through an experimental study of isolated perfused rat livers in which bromosulphophthalein (BSP) uptake and excretion was monitored at 3 different concentrations of albumin in the perfusion medium. The results indicate that the total uptake rate of an organic anion such as BSP is affected by its rate of dissociation from the protein albumin. This finding is in contrast to the usual assumption that dissociation from a protein is much faster than transport through a membrane and therefore has a negligible effect on total uptake rate.

ADVANCES IN BIOLOGICALLY-BASED KINETIC MODELING FOR TOXICOLOGICAL APPLICATIONS

Brent D. Foy

Introduction

Extrapolation of the toxicity of a chemical from a given set of experiments to different doses and/or species is an integral part of predictive toxicology. The use of models based on detailed physiological processes enhances our ability to extrapolate correctly by inherently including the non-linear dose-effect characteristics many physiological processes exhibit. In this work, three physiologically based processes have been incorporated into a model of the isolated perfused rat liver.

The first process is the explicit kinetics of a chemical binding to a protein. It is often, although not universally, assumed that the rate at which a chemical binds and unbinds from a protein is much faster than other pharmacokinetic processes such as transport through a membrane or metabolism of the chemical (Weisiger, 1985, 1991; Sorrentino, 1994). By including the explicit rates for association and dissociation, one can model those chemicals and conditions in which these rates are of the same order of magnitude as other kinetic processes. A series of experiments using isolated perfused rat livers and bromosulphophthalein (BSP) metabolism were performed to investigate this effect. These experiments indicated that the dissociation rate of BSP from albumin can be slow enough to reduce the total uptake of BSP by the liver.

The second process is the transport of a chemical through a membrane using a carrier protein. Many chemicals only pass through a plasma membrane when bound to specific membrane carrier proteins. The carrier mediated transport process can produce phenomena which can not be explained by more simplified diffusional transport descriptions of membrane transport. One of these phenomena, trans-acceleration, was simulated. The third physiological feature to be modeled was the presence of heterogeneous cells along the sinusoid of the liver. It is well-known that hepatocytes near the portal triad have different enzymatic activities than those near the central vein (Anderson, 1997). This was modeled by connecting multiple liver compartments

(with sinusoidal and cellular sub-compartments) in series via blood flow, and allowing each sub-compartment to have distinct physiological properties.

Theory

Protein-binding Kinetics

The rate at which the chemical-protein complex is formed (R_{assoc}, units μmole/hr) is given by:

$$R_{assoc} = k_{on} \cdot P_{open} \cdot C_{free} \cdot V \quad (1)$$

where k_{on} is the association rate constant ($(\mu M \cdot hr)^{-1}$), P_{open} is the concentration of open binding sites on the protein (μM), C_{free} is the concentration of free chemical (μM), and V is the volume of the compartment in which binding is occurring (L). The rate at which the chemical dissociates from the protein (R_{dissoc}, umole/hr) is given by:

$$R_{dissoc} = k_{off} \cdot CP_{bound} \cdot V \quad (2)$$

where k_{off} is the dissociation rate constant (hr^{-1}) and CP_{bound} is the concentration of the chemical-protein complex (μM). The equilibrium dissociation constant K_d (μM) is then given by:

$$K_d = \frac{k_{off}}{k_{on}}. \quad (3)$$

Carrier-Mediated Membrane Transport

The 4-state carrier transport system incorporated into the kinetic model is depicted in Fig. 1. The rate at which free carrier on side B moves to free carrier on side A (R_{BA}, μmoles/hr) is given by:

$$R_{BA} = ko_{BA} \cdot P_B \cdot V_B \quad (4)$$

where V_B is the volume of the compartment on the B side of the membrane. and the other constants are described in the figure legend. The other 3 exchange reactions have similar expressions. The equations for the rate of association and dissociation are Eqs. (1) and (2) above. Note that Eqs. (1) and (2) express concentration of protein and chemical in terms of μmoles/L, whereas the protein resides on a 2-dimensional surface for a membrane carrier. This amounts to the assumption that the compartments are well-mixed (equal concentrations of chemical throughout the compartment) with no diffusion effects near the surface. Equation 4 also

normalizes concentration to volumes instead of areas, but this is done primarily to maintain compatibility with equations (1) and (2) and the normalization does not alter the rate of transport for a given total number of carriers in a membrane.

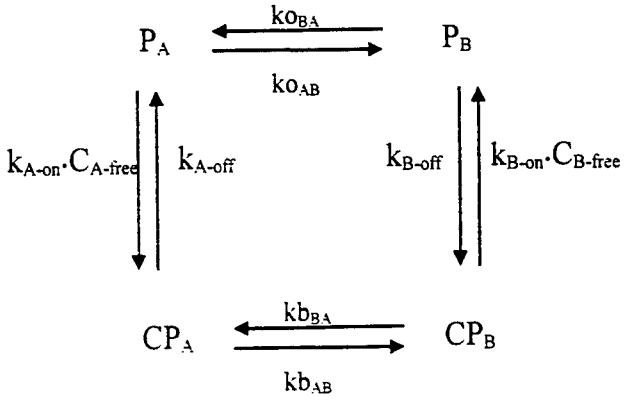

Figure 1. The 4-state carrier system. Subscripts A and B refer to the two sides of the membrane. P is the concentration of free carrier protein, CP is the concentration of the bound carrier protein, k_{on} and k_{off} are the association and dissociation constants for protein binding, ko_{AB} and ko_{BA} are the rates of exchange of free carrier protein between sides A and B (hr^{-1}), and kb_{BA} and kb_{AB} are the rates of exchange of bound carrier protein between sides A and B (hr^{-1}).

Methods

Model Implementation

The biologically-based kinetic models were coded on a PC using Advanced Computing Simulation Language (ACSL level 11, MGA Associates, Concord, MA), a numerical integration package. A schematic for the flows and reactions used in the model of the isolated perfused rat liver system is shown in Figure 2. Each of the two membranes shown in Fig. 2 has three possible transport processes: 1) non-saturable transport, to simulate a diffusion process; 2) saturable transport to phenomenologically describe transport processes (such as pore transport) which produce a maximum rate of transport regardless of concentration; and 3) explicit carrier-mediated transport. The SI membrane represents the sinusoidal membrane of the cells, and the IB membrane represents the bile membrane of the cells.

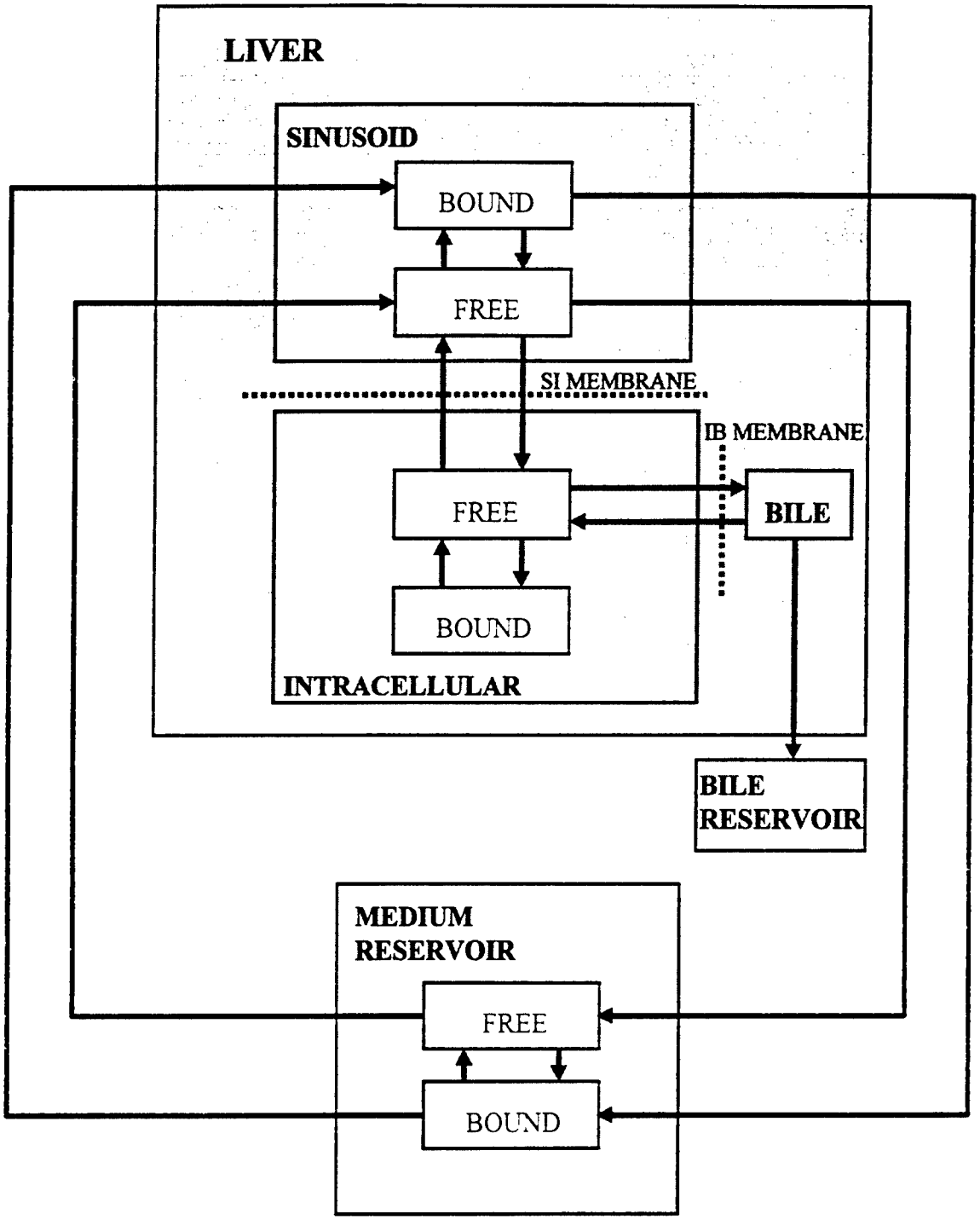

Figure 2. Schematic of the model for the isolated perfused rat liver. The free and bound chemical recirculates through the liver via the medium reservoir. Within any compartment, the free chemical can become bound and vice versa. In the intracellular space, the free parent can be excreted in the bile, which then flows to a collecting bile reservoir. Not shown is the metabolism reaction whereby parent chemical, when in the free intracellular state, can be metabolized to a metabolite chemical, which then undergoes all of the same reactions depicted in this figure, but with distinct kinetic parameters.

Simulations

Simulations to demonstrate the effect of each of the three physiological enhancements to the model were performed. Parameters common to all simulations are listed in Table 1. These values were derived for an 8g rat liver. The simulations were designed to mimic the perfused liver experiments described below, and thus used a total time of exposure to chemical of 2.5 hrs. Unless otherwise specified for a specific simulation (see Results section), each of the following processes is assumed to be inactive: metabolism, binding to protein, and transport through a membrane. When a value is specified for non-saturable membrane transport, the product of permeability times membrane area (PA) is used (units L/hr), since accurate information on membrane area for a liver is not available. Similarly, when a value is specified for saturable transport, the maximum transport rate reflects the rate for the entire membrane (μmoles/hr). When specifying values for carrier-mediated membrane transport, in addition to the constants described in Fig. 1, the transport rate is specified by the total number of carriers present in a membrane. The total number of carriers is the product of surface density of carriers (a more common measure of carrier amount) times membrane area for a whole liver.

Table 1. Physiological parameters for rat liver modeling.

Description	Value
Reservoir volume	200.0 mL
Sinusoidal volume	1.736 mL
Intracellular volume	4.664 mL
Bile canilicular volume	0.160 mL
Perfusion medium flow rate	2.7 L/hr
Flow rate of bile into bile reservoir	0.48 mL/hr

The first set of simulations explored the effect of protein binding in the liver sinusoid. The concentration of chemical in the reservoir was monitored over time, thereby providing information on the net uptake rate by the liver. The primary question is whether the net uptake

rate is primarily determined by the dissociation rate from the protein, or by the transport rate through the sinusoidal-intracellular membrane. For these simulations, the membrane transport from the intracellular space into bile was uni-directional, and occurred at a very high rate. Thus, the uptake rate would be determined solely by the dissociation rate and/or the transport rate through the membrane.

The second set of simulations explored the effect of carrier-mediated membrane transport. The phenomenon of trans-acceleration was chosen as a test case in which the data could only be explained if one uses carrier transport through the membrane. With trans-acceleration, the intracellular space is loaded with labeled chemical. The rate of label appearance outside the cells is then monitored for several different initial extracellular unlabeled concentrations of chemical. If 4-state carrier transport is occurring, then a greater extracellular concentration can produce a greater rate of appearance of label outside the cells. This finding is at odds with diffusive transport across a membrane, which would predict that the rate of label appearance outside the cell would be unchanged or slower as the extracellular concentration increases.

The third feature simulated was the importance of several liver compartments connected in series. One way serial liver compartments may manifest themselves is through sequential actions on a chemical. Specifically, for this simulation the liver was divided into two compartments. In one case, the first compartment metabolized the parent chemical (T) to a second chemical (M). Then the second compartment excreted M into bile. In the contrasting case, the two compartment were switched so that the first compartment encountered by perfusion medium was efficient at excreting M into bile, but could not metabolize T to M. The second compartment was capable of metabolizing T to M, but the M so produced would have to recirculate through the medium reservoir before it reaches the first liver compartment to be excreted into the bile. So the expected result is that the second case experiences a delayed appearance of M in the bile due to the inefficient sequence of actions by the liver compartments.

BSP Experiments

Male Fisher 344 rats weighing 200-300 g were anesthetized with ether. After surgically exposing the liver, the bile duct was cannulated, followed by separate cannulation of the portal vein. The liver was excised and placed in a dish in a temperature controlled chamber. The flow rate of the perfusion medium was set to 2.7 L/hr (45 ml/min), and the perfusion medium was oxygenated via silastic tubing with 95% O_2 / 5% CO_2. The pH was fixed to 7.4 by adjusting the oxygenation rate as necessary. After 30 minutes for stabilization, 200μL of 20 mM BSP was added. The perfusion medium was Krebs Ringer Bicarbonate plus bovine serum albumin (BSA, low endotoxin, Sigma cat. no. A2934) at 0, 1, or 4%, corresponding to 0 μM, 143 μM, and 570 μM for BSA molecular weight of 70,000 kD. A taurocholate solution (33.5 mM) was infused into the perfusion medium at 1 mL/hr to maintain bile production.

At several time points following addition of BSP (0, 2, 5, 10, 20, 30, 60, 90, 120, and 150 min), a 0.5 ml aliquot of perfusion medium was removed from the medium reservoir. The bile reservoir was collected at 30 minute time intervals. The concentration of total BSP (BSP plus metabolites containing BSP such as BSP-glutathione) in perfusion medium samples and bile samples was determined from spectral absorbance at 580 nm.

The model illustrated in Figure 2 was then applied to the BSP vs. time data of the medium reservoir and bile reservoir. In addition to the parameters in Table 1, values for protein binding kinetics and membrane transport are needed. Regarding binding of BSP to BSA, K_d was found to be 0.26 μM or less in several studies (Baker, 1966; Pfaff, 1975; Weisiger, 1984; Zhao, 1993). No direct measurement of k_{off} appears to have been made. An estimate of k_{off} of 0.053 s^{-1} has been made from application of a model to perfused liver data (Weisiger, 1984). This value is quite similar to the k_{off} value of 0.048 s^{-1} experimentally determined for binding of dibromosulfophthalein (DBSP) to BSA, despite the fact that K_d for DBSP-BSA is 2.4 μM, which is an order of magnitude higher than for BSP-BSA binding (van der Sluijs, 1987). The parameters to be used in this study to model the experimental BSP data are K_d = 0.2 μM with 1 binding site per BSA and k_{off} = 0.053 s^{-1}. The value for k_{on} is then derived from Eq. (3).

Additional, lower affinity binding sites on BSA were found to have negligible effect on the kinetics due to the low concentration of BSP relative to BSA in all experiments.

Having fixed the protein binding kinetics based on literature values, the remaining variable parameters are those describing membrane transport. Both membranes were assumed to operate via diffusional transport since this assumption enables each membrane to be described by a single variable parameter, the permeability-area product described above. The PA product for intracellular space to bile was set to a very high rate of 8.0×10^6 cm^3/s for the entire liver, while the PA product for bile back to the intracellular space was set to zero. These values may or may not be physiological but they do have the effect of letting the net rate of free BSP uptake by the liver be determined entirely by the rate of free BSP transport through the sinusoidal membrane. The PA product for the sinusoidal membrane was equal in both directions. A value of the PA product for the sinusoidal membrane which most closely matched the experimental kinetics was then found by trial and error.

A similar procedure was followed after making the assumption that the rate constants for binding of BSP to BSA were very high. This situation promotes equilibrium binding in the sinusoidal space, and tends to make membrane transport rates the limiting factor in net hepatic uptake rates.

Results

Protein Binding Simulation

Working under the assumption that only free, unbound chemical passes through the membrane, the net uptake rate of the chemical by the liver cells may be reduced by the slow release of chemical from the protein. This is most likely to occur when the protein binding rate constants k_{on} and k_{off} are small, most chemical is bound to protein, and the membrane transport rate is high. In this case, almost all of the free chemical in the sinusoid is quickly transported into the cells, and the rate of replenishment of free sinusoidal chemical depends only on the concentration of bound chemical times k_{off}. Note that under these dissociation limited conditions, the uptake rate is independent of the concentration of protein. Figure 3 shows the concentration of chemical in the reservoir vs. time for five different concentrations of binding protein under such conditions.

The three highest protein concentrations (143 μM, 570 μM, and 1140 μM) reveal nearly identical uptake rates. At the two lowest protein concentrations (0 μM and 14.3 μM), there is more chemical than protein, and consequently a much larger concentration of free chemical. This large concentration of free chemical, coupled with a high membrane permeability to free chemical, leads to a situation in which the uptake rate is actually limited by the flow rate, which determines the rate of new free chemical flowing into the sinusoid.

The contrasting situation is when the binding rate constants are high (fast) and membrane permeability is low. These conditions were used to generate Figure 4, which depicts the reservoir concentration vs. time for the same protein concentrations and same K_D as in Fig. 3. The primary feature in Fig. 4 is that the liver uptake rate (equals rate of loss of chemical from reservoir) depends on protein concentration for the 143, 570, and 1140 μM cases. This arises because lower protein concentrations lead to greater concentrations of free chemical, and more free chemical in the sinusoid means a greater transport across the membrane into the cells. Note that again in the absence of binding protein, the uptake is limited by the flow rate, even with the lower membrane permeability.

When the uptake rate is limited by the dissociation rate of the chemical from the protein, very

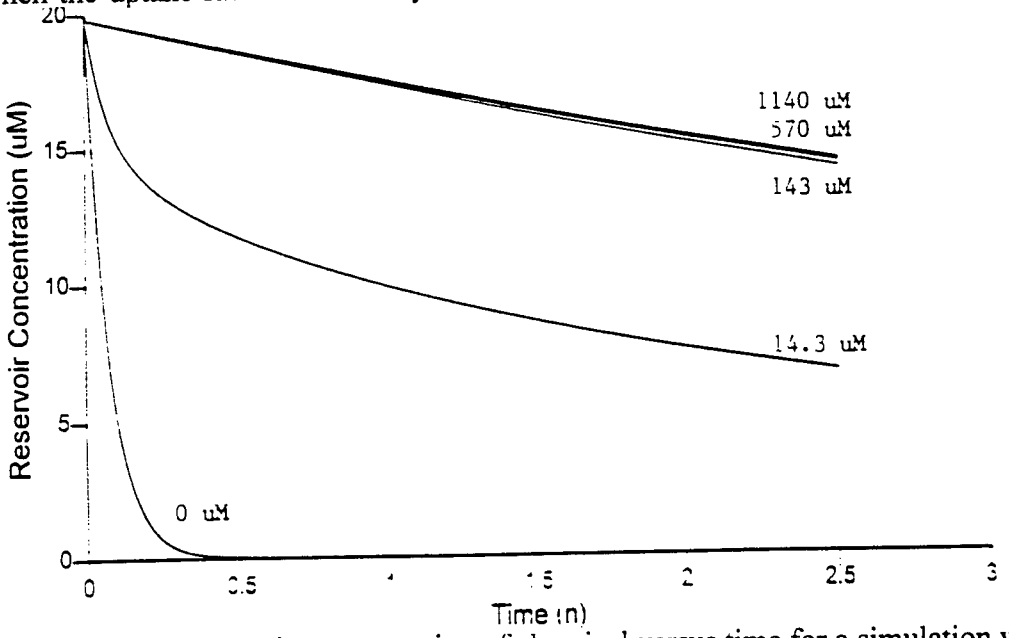

Figure 3: Reservoir concentration of chemical versus time for a simulation with protein dissociation limited uptake. Five protein concentrations were simulated - 0μM, 14.3μM, 143μM, 570μM, and 1140μM. Other parameters: k_{off} = 15 hr^{-1}, k_{on} = 250 $(hr \cdot \mu M)^{-1}$, PA =

little free chemical exists in the sinusoidal space as discussed above. The distribution of the chemical between free and bound forms is therefore not in equilibrium. By comparing the concentration of the free chemical in the sinusoid with the concentration of free chemical in the reservoir (in which the mean residence time is long enough to allow equilibrium binding of chemical to protein to occur), one can assess the extent to which protein dissociation rates are limiting total uptake rates. Table 2 includes free chemical concentrations for the simulations described in Figures 3 and 4 after 3 minutes of perfusion. One can see that under dissociation limited conditions, the free sinusoidal concentration is much lower than free reservoir concentrations.

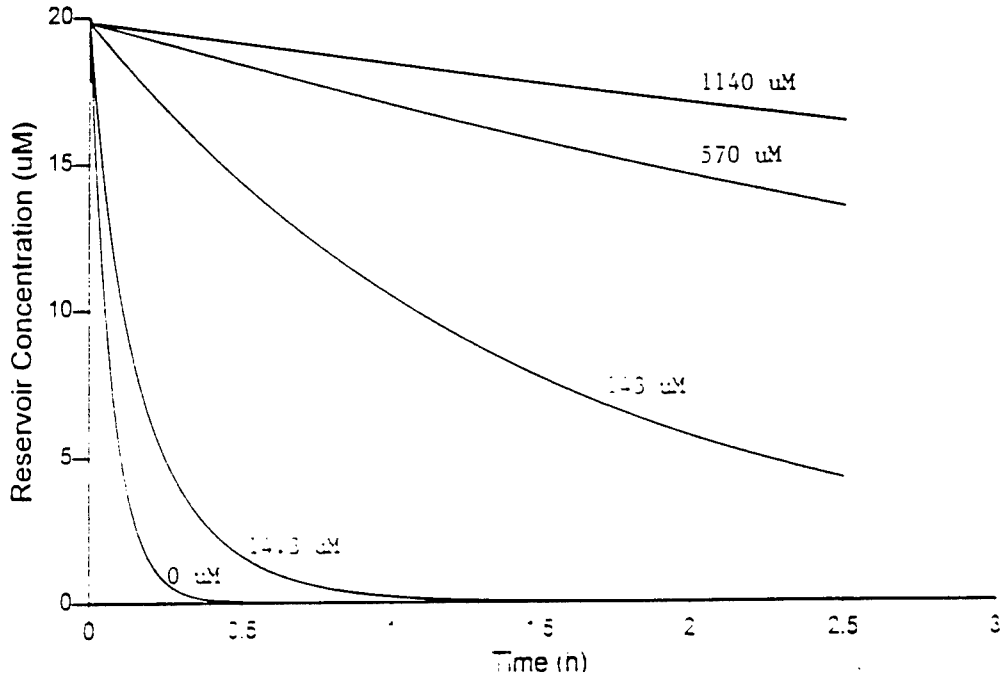

Figure 4: Reservoir concentration of chemical versus time for a simulation with membrane transport limited uptake. Five protein concentrations were simulated - 0μM, 14.3μM, 143μM, 570μM, and 1140μM. Other parameters: k_{off} = 15,000 hr^{-1}, k_{on} = 250,000 $(hr \cdot \mu M)^{-1}$, PA = 28.8 L/hr.

Table 2 Free chemical concentrations for each protein concentration. Values in μM.

	Compart.	0 μM	14.3 μM	143 μM	570 μM	1140 μM
Dissociation Limited	Sinusoid	9.7×10^{-4}	3.0×10^{-4}	0.18×10^{-4}	0.18×10^{-4}	0.18×10^{-4}
	Reservoir	10.3	3.06	9.6×10^{-5}	2.1×10^{-3}	1.1×10^{-3}
Membrane Limited	Sinusoid	9.5×10^{-2}	6.2×10^{-2}	8.8×10^{-3}	2.1×10^{-3}	1.1×10^{-3}
	Reservoir	10.2	0.90	9.3×10^{-3}	2.1×10^{-3}	1.1×10^{-3}

Carrier-mediated Membrane Transport Simulation

Carrier-mediated membrane transport can lead to the phenomenon of trans-acceleration under certain conditions. One set of parameters which can lead to trans-acceleration is for free exchange rates (ko_{AB} and ko_{BA} in Figure 1) to be smaller than bound exchange rates (kb_{AB} and kb_{BA}). This situation is illustrated in Figure 5, which shows the concentration of labeled chemical in the reservoir vs. time for 5 different initial extracellular unlabeled concentrations. This graph simulates an experiment in which the liver is pre-perfused with labeled chemical until the intracellular concentration reaches 500 μM. At time zero, the liver is switched to perfusion with unlabeled chemical at various concentrations. A purely diffusional transport process, for the same initial distribution of labeled and unlabeled chemical, would result in no alteration of efflux rate of label due to changes in extracellular concentration.

Serial Liver Compartments Simulation

An effect of the sequential processing by the liver as chemical flows from peri-portal regions to peri-venous regions is illustrated in Figure 6. The efficient sequence (A) results in a more rapid excretion of metabolite into the bile than the inefficient sequence (B).

BSP Experiments

The number of livers perfused at 570 μM, 143 μM, and 0 μM BSA, were six, three, and three respectively. A representative graph of one experiment for each BSA concentration is shown in Figure 7. Also graphed in Fig. 7 is the result of performing a simulation with the parameters described in the Methods section. A PA value of 576 L/hr produced reservoir concentration vs. time curves that closely matched data for 143 μM and 570 μM experiments. The simulation

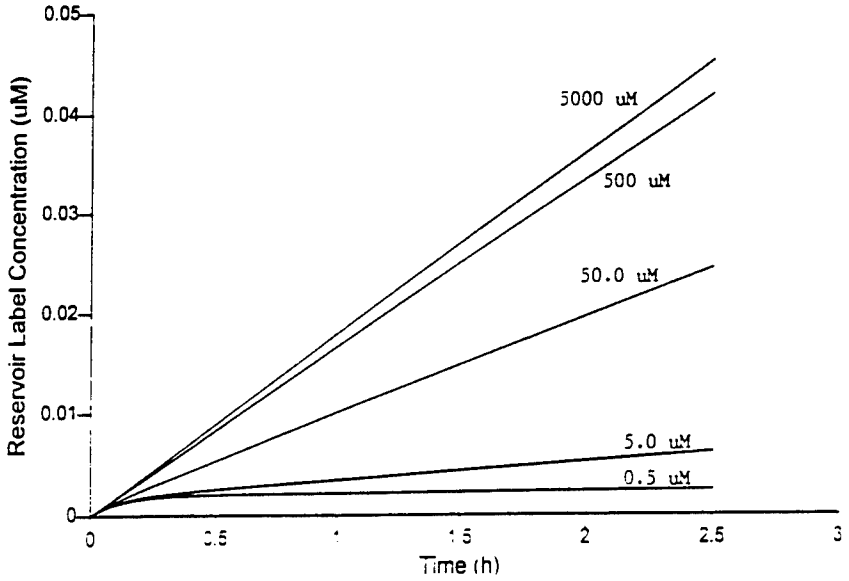

Figure 5: Reservoir label concentration of chemical versus time for a simulation demonstrating trans-acceleration. Five initial extracellular unlabeled chemical concentrations were used – 0.5μM, 5.0μM, 50μM, 500μM, and 5000μM. Other parameters: $k_{A\text{-}off} = k_{B\text{-}off} = 500{,}000\ hr^{-1}$, $k_{A\text{-}on} = k_{B\text{-}on} = 5{,}000\ (hr \cdot \mu M)^{-1}$, $ko_{AB} = ko_{BA} = 1x10^{-5}\ hr^{-1}$, $kb_{AB} = kb_{BA} = 10\ hr^{-1}$, total number of carriers = 8×10^{-4} μmoles, initial concentration of intracellular label = 500μM.

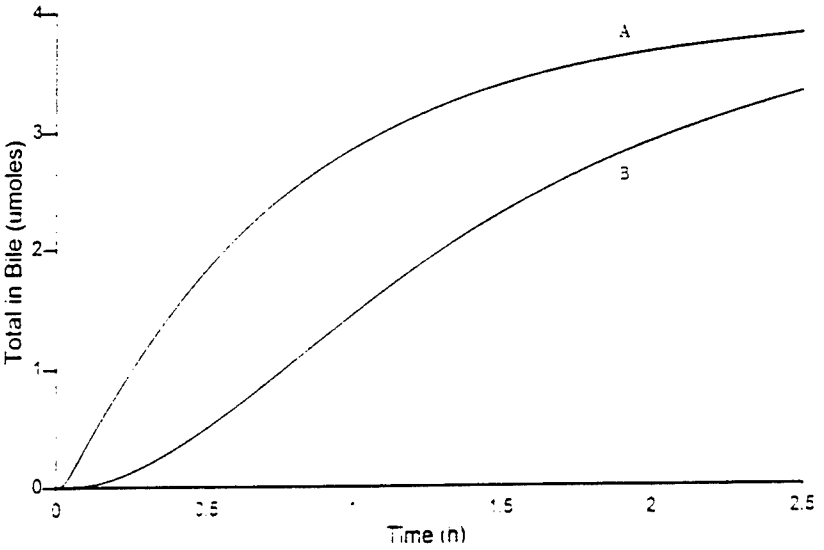

Figure 6: Cumulative biliary excretion of metabolite vs. time for two sequences of liver compartments. Both (A) and (B) sequences have PA for SI membrane of 144 L/hr in both compartments, bidirectional, for both original chemical and metabolite. In (A) sequence, the metabolism in the first compartment occurs at 100 μmoles/hr, and 0 μmoles/hr in the second compartment. The PA for metabolite only through the IB membrane is zero L/hr in the first compartment, and 7.2 L/hr in the second compartment (unidirectional, I->B). In (B) sequence, the metabolism and PA for IB membranes have the same values as for (A) sequence, but the values are switched between first liver compartment and second. The flow rate was set to 0.27 L/hr for all simulation.

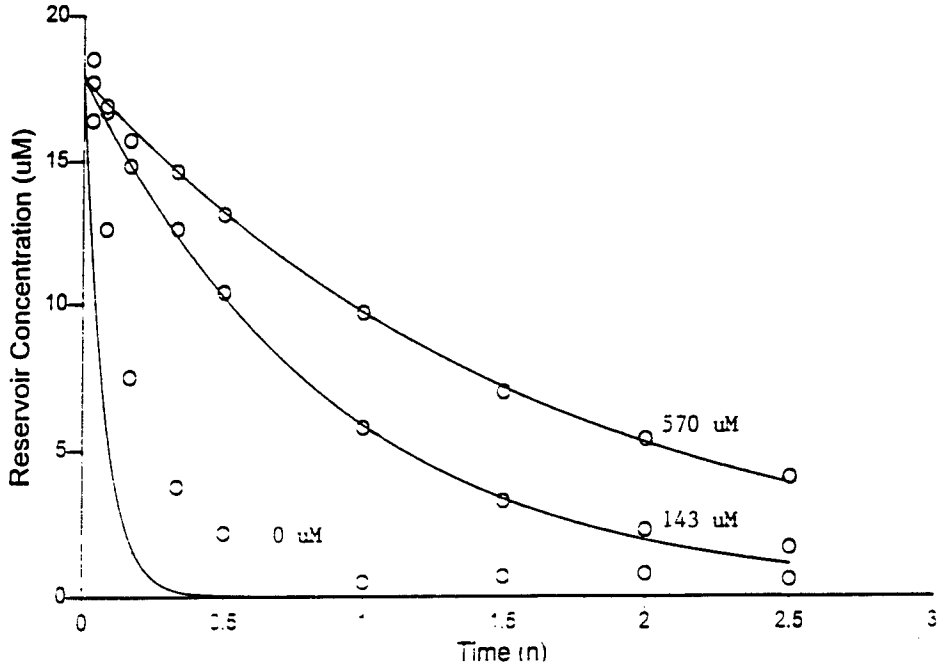

Figure 7: Total reservoir BSP concentration vs. time of experimental data (O) and simulations (lines) for the indicated protein concentrations. Other simulation parameters: k_{off} = 190 hr^{-1}, k_{on} = 950 $(\mu M\ hr)^{-1}$, PA = 576 L/hr.

curve for 0% does not closely match the experimental data. Possible reasons for this will be discussed below.

Figure 8 includes the same experimental data as Figure 7, but uses a simulation that assumes fast protein binding kinetics. It was not possible to simultaneously fit both the 143 μM and 570 μM experimental data with this assumption. Figure 8 shows the result of a simulation with parameters adjusted to closely match the 143 μM case (PA value of 173 L/hr), but which does not match the 570 μM data well. Table 3 lists the experimental and simulated rate of BSP uptake by the liver for the time period between 2 minutes and 30 minutes after exposing the liver to BSP. The slopes obtained when using dissociation limited assumptions are close to experimental slopes.

Table 3 Initial BSP uptake rates for 3 protein concentrations. Values in μmoles/min.

	0 μM	143 μM	570 μM
Experimental	0.099 ± 0.004	0.062 ± 0.004	0.028 ± 0.011
Dissociation Simul.	0.086	0.050	0.032
Fast Binding Simul.	0.086	0.053	0.017

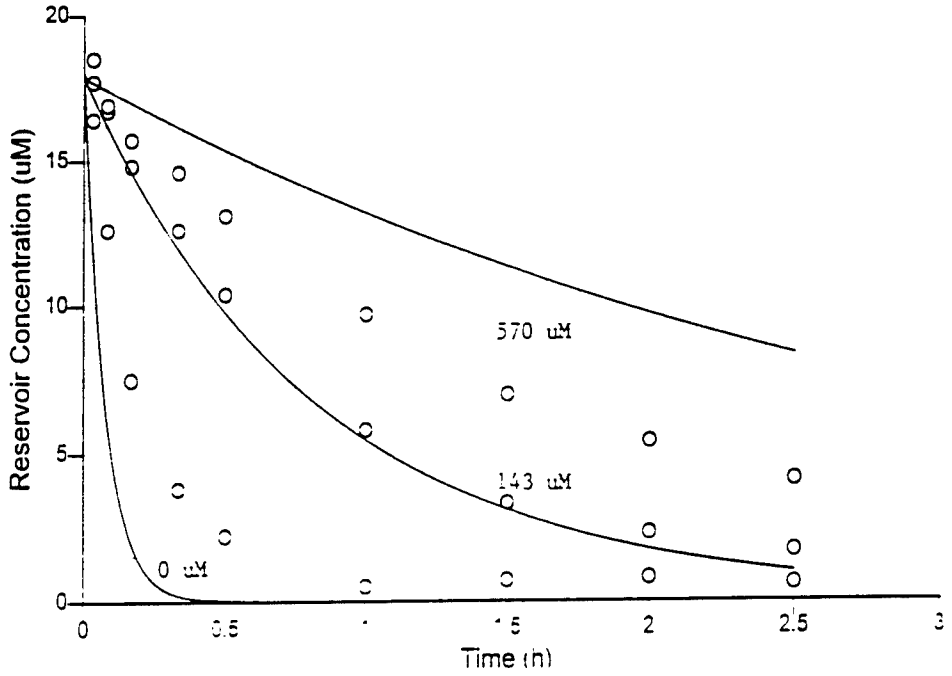

Figure 8: Total reservoir concentration vs. time of experimental data (O) and simulations (lines) for the indicated protein concentrations. Other simulation parameters: k_{off} = 190.000 hr^{-1}, k_{on} = 950.000 $(\mu M\ hr)^{-1}$, PA = 173 L/hr.

Table 4 corresponds to Table 2, but uses parameters obtained from attempting to fit the simulations to experimental data in Figures 7 and 8. The fast binding parameters produce nearly equal reservoir and sinusoidal concentrations of free BSP as expected. The dissociation limited parameters produce lower sinusoidal free concentrations than reservoir free concentrations. However, the difference in free concentrations at the higher 570 μM protein concentration is not as great as at the lower 143 μM protein concentration. The probable explanation for this will be discussed below.

Table 4. Free BSP concentrations (from simulations) at 3 minutes of perfusion time for each protein concentration. Values in μM.

	Compartment	0 μM	143 μM	570 μM
Dissociation Limited	Sinusoid	0.043	6.6×10^{-3}	3.7×10^{-3}
	Reservoir	9.2	26.9×10^{-3}	6.3×10^{-3}
Fast Binding	Sinusoid	0.14	0.024	6.2×10^{-3}
	Reservoir	9.26	0.027	6.4×10^{-3}

One consequence of failing to account for protein binding rate kinetics is that extrapolations to different doses may be inaccurate. Table 5 uses the two sets of parameters generated for Figures 7 and 8 and extrapolates the initial uptake rates (between 2 and 30 minutes after initiating BSP perfusion) under the condition of 143 μM BSA to different initial reservoir concentrations of BSP. The two sets of parameters agree well for lower BSP concentrations, but diverge at higher BSP concentrations.

Table 5. Initial uptake rates for simulations of different initial reservoir concentrations. Values in μmoles/min.

Initial Reservoir Concentration	0.2 μM	20 μM	2000 μM	20,000 μM
Dissociation Limited	5.4×10^{-4}	0.050	3.57	22.7
Fast Binding	6.2×10^{-4}	0.053	2.48	17.2

Discussion

The three extensions to the pharmacokinetic model of a perfused liver described in this work all describe physiological processes which are known to be active for some chemicals. The simulations performed each illustrate a potential set of experimental data that could only be explained through the appropriate physiological process. Explicitly including these non-linear processes can improve our accuracy in predicting toxic effects at different doses and with different species. The BSP experiments indicate that one of these processes, protein-binding kinetics, may play an important role in determining total BSP uptake.

The inclusion of more realistic physiological equations in the kinetic models necessitates an increase in the complexity of the model with a corresponding increase in the number of physiological parameters. This poses no problem for simulations, in which one can try many values for the physiological parameters. Using the physiologically based models for simulations

can be quite useful for interpreting experimental data. Even in the absence of complete knowledge of the physical parameters, one can explore the importance of various physiological processes and determine if any values for the unknown parameters provide an alternative explanation of the experimental data. However, many applications of kinetic modeling will require a reasonably good idea of the correct values for the physical parameters for the chemical and species in question. Many of the parameters incorporated in this work are experimentally challenging to obtain. The protein binding kinetic studies can be done *in vitro*, but uncertainty may still exist about the concentration of free binding sites *in vivo*, when competition of other chemicals for the same site is considered. The carrier-mediate membrane transport equations add a large number of parameters, which may require *in vitro* membrane vesicle studies. To model sequential liver compartments, one must obtain information about the transport and metabolism of a chemical in peri-portal and peri-venous hepatocytes. Such information may come from hepatocyte cultures, or from comparing anterograde and retrograde perfusion of a liver.

Regarding BSP experiments, the ability to match experimental data for 143 μM BSA and 570 μM BSA with the prediction of the model while using literature values for protein-binding parameters provides evidence that the protein-binding kinetics play a key role in determining the total liver uptake rate of BSP. The lack of correspondence between experiment and theory for the 0 μM BSA experiment may be due to a finite capacity of the membrane for transporting BSP. With 0 μM BSA, the concentration of free BSP is very high which results in a very high rate of membrane transport when using diffusion-based membrane transport. This very high rate of membrane transport in the model probably exceeds the maximum transport capacity of the plasma membrane, due to a finite number of pores or carriers for BSP.

The findings presented in Table 4 for the dissociation limited analysis (literature-based protein binding kinetics) are surprising in that they indicate a greater deviation from protein binding equilibrium for the 143 μM BSA experiment than the 570 μM BSA experiment. Intuitively, one may suppose that if the dissociation of a chemical from a protein is slow enough to reduce the total rate of uptake of the chemical by the liver, then the presence of greater amounts of protein, without additional chemical, can only lead to a greater bound fraction and a more pronounced

effect of slow dissociation. The explanation of this phenomenon (Weisiger, 1984), is that when protein concentration is high, the free concentration is indeed reduced, thereby reducing membrane transport rate into the cells. At the same time, the presence of a large concentration of protein makes the probability (and thus the net rate) of a chemical binding to the chemical somewhat higher. Thus, free chemical in the sinusoid may achieve equilibrium in its binding with the protein.

The extrapolation presented in Table 5 is one example of how the incorporation of physiological processes can improve one's predictive accuracy. Other situations may arise *in vivo* that would require the protein binding kinetic analysis to properly extrapolate to different conditions. These include variations in the competition for binding sites among several related chemicals and altered binding rate constants for a metabolite compared to the parent compound.

Future work will involve continuing to incorporate physiological processes into the liver model. Primary among these is the modeling of the complex flow paths within the liver. The model as it currently exists is suitable for simulating experiments on the order of hours. Some experiments expose the liver to a bolus of chemical for a short duration of seconds. The metabolism and excretion of the chemical under these conditions is highly dependent on the contact time the chemical has with each part of the liver. Such phenomena are probably related to the acute toxic effects some chemicals have on only discrete regions of the liver cellular structure.

References

Andersen ME, Eklund CR, Mills JJ, Barton HA, Birnbaum LS. A multicompartment geometric model of the liver in relation to regional induction of cytochrome P450s. *Toxic. Appl. Pharm.* 144: 135-144, 1997.

Baker KJ, Bradley SE. Binding of sulfobromophthalein (BSP) sodium by plasma albumin. Its role in hepatic BSP extraction. J. Clin. Invest. 45: 281-297, 1966.

Pfaff E, Schwenk M, Burr R, Remmer H. Molecular aspects of the interaction of bromosulfophthalein with high-affinity binding sites of bovine serum albumin. *Molec. Pharm.* 11: 144-152, 1975.

Sorrentino D, Zifroni, A, Van Ness K, Berk PD. Unbound ligand drives hepatocyte taurocholate and BSP uptake at physiological albumin concentration. *Am. J. Phys.* 266: G425-G432, 1994.

Van der Sluijs P, Postema B, Meijer DKF. Lactosylation of albumin reduces uptake rate of dibromosulfophthalein in perfused rat liver and dissociation rate from albumin *in vitro*. *Hepat.* 7: 688-695, 1987.

Weisiger RA, Zacks CM, Smith ND, Boyer JL. Effect of albumin binding on extraction of sulfobromophthalein by perfused elasmobranch liver: evidence for dissociation-limited uptake. *Hepat.* 4: 492-501, 1984.

Weisiger RA. Dissociation from albumin: A potentially rate-limiting step in the clearance of substances by the liver. *Proc. Natl. Acad. Aci. USA* 82: 1563-1567, 1985.

Weisiger RA, Pond S, Bass, L. Hepatic uptake of protein-bound ligands: extended sinusoidal perfusion model. *Am. J. Phys.* 261: G872-G884, 1991.

Zhao Y, Snel CAW, Mulder GJ, Pang KS. Localization of glutathione conjugation activities toward bromosulfophthalein in perfused rat liver. *Drug Metab. Dispos.* 21: 1070-1078, 1993.

MIXING AND STREAMING OF A FLUID NEAR THE ENTRANCE OF A TUBE DURING OSCILLATORY FLOW

Irwin S. Goldberg
Professor
Department of Physics and Engineering

St. Mary's University
One Camino Santa Maria
San Antonio, TX 78228-8534

Final Report for:
Summer Research Program
Armstrong Laboratory

Sponsored by:
Air Force Office of Scientific Research
Bolling Air Force Base, Washington, DC

And

Armstrong Laboratory

September 1997

MIXING AND STREAMING OF A FLUID NEAR THE ENTRANCE OF A TUBE DURING OSCILLATORY FLOW

Irwin S Goldberg
Professor
Departments of Physics and Engineering
St. Mary's University
San Antonio, Texas

Abstract:

Fluid dynamic mixing and streaming phenomena are described near the end of a semi-infinite, rigid, straight circular tube containing an incompressible Newtonian fluid. For the specific problem considered, the entrance condition flow profile resembles the sinusoidal oscillations of a flat piston at the end of the tube. Solutions to a linear approximation, involving time-harmonic Stokes flow, are obtained. The solutions to this linear approximation for velocity components and pressure are given as superpositions of developed-flow solutions plus entrance-flow solutions. The entrance-flow solutions describe entrance-flow patterns in which radial velocity components and axial velocity gradients exist near the end of the tube. These entrance-flow velocity terms decay with distance from the end of the tube. The solutions to the linear problem serve as the first-order results. These linear time-harmonic results are substituted into the nonlinear terms of a higher-order approximation to the Navier-Stokes equation, the resulting equations contain products of sinusoidal-oscillating first-order terms. These products can be equated to combinations of second-harmonic velocity oscillations in addition to time-independent steady velocity terms. These time-independent terms describe steady bi-directional streaming motion near the end of the tube. Additionally, the linear, zero-order solutions reveal a mixing phenomena with swirling secondary flow near the end of the tube.

MIXING AND STREAMING OF A FLUID NEAR THE ENTRANCE OF A TUBE DURING OSCILLATORY FLOW

Irwin S Goldberg

Introduction

A successive-approximation method is used to describe steady bi-directional streaming flow in the vicinity the end of a semi-infinite straight, rigid tube containing an incompressible Newtonian fluid. The first-order approximation is a linear approximation to a problem involving axisymmetric time-harmonic end conditions. In this approximation, the nonlinear convective acceleration terms are omitted from the Navier-Stokes equation while the linear acceleration terms containing the time derivative of velocity are retained, leading to a linear time-dependent Stokes approximation. The solution to the zero-order linear approximation, obtained by Goldberg and Folk [1], consists of the superposition of an entrance-flow contribution, which becomes negligible far from the end, plus a developed-flow contribution. An entrance length can be defined as the distance from the end, beyond which the entrance-flow contribution is less than one percent of the developed-flow contribution. Analytical results have shown that, for sinusoidal oscillating flow at very small Reynolds numbers, the entrance length in a straight rigid tube is approximately equal to one tube radius.

Methodology

To obtain a system of partial differential equations describing streaming motion, first, the nonlinear Navier-Stokes equations are expressed with the velocity components and pressure terms written as sums of mean-flow terms plus terms with time fluctuations. Next, these equations are time averaged. The resulting time-averaged partial differential equations contain expressions for mean velocity components and mean pressure plus expressions containing time averages of products of the harmonically-oscillating terms. The solution to the first-order linearized equations is used to approximate the harmonically-oscillating terms in the first-order equation.. Thus, in the first-order equations, the partial differential

equations, describing the mean flow, contain time averages of products of the sinusoidal oscillating (first-order) linear solutions. These products of sinusoidal-oscillating functions, contained in the nonlinear terms of the second-order equations, generate solutions with second-harmonic results (at twice the harmonic oscillation frequency) in addition to zero-frequency results. These zero frequency results, which are retained in the time-averaging operation, indicate a steady bi-directional streaming motion of the flow.

Equations and Boundary Conditions

Expressions containing time averages of products of harmonically-oscillating linear terms are treated as body force stresses in the first-order nonlinear approximation. For the problem involving laminar oscillatory flow at low Reynolds numbers, steady bi-directional streaming is generated by these body force stresses. For axisymmetric flow of an incompressible Newtonian fluid, the non-dimensional Navier-Stokes and continuity equations are given in cylindrical coordinates as

$$\frac{\partial U}{\partial T}+\mathrm{Re}\left(V\frac{\partial U}{\partial R}+U\frac{\partial U}{\partial Z}\right)=-\frac{\partial P}{\partial Z}+\frac{\partial^2 U}{\partial R^2}+\frac{1}{R}\frac{\partial U}{\partial R}+\frac{\partial^2 U}{\partial Z^2}\quad , \tag{1}$$

$$\frac{\partial V}{\partial T}+\mathrm{Re}\left(V\frac{\partial V}{\partial R}+U\frac{\partial V}{\partial Z}\right)=-\frac{\partial P}{\partial R}+\frac{\partial^2 V}{\partial R^2}+\frac{1}{R}\frac{\partial V}{\partial R}-\frac{1}{R^2}V+\frac{\partial^2 V}{\partial Z^2}\quad , \tag{2}$$

$$\frac{\partial U}{\partial Z}+\frac{\partial V}{\partial R}+\frac{V}{R}=0, \tag{3}$$

where dimensionless quantities are expressed with capital letters as $U = u/u_0$, $V = v/u_0$, $P = ap/(\rho v u_0)$, $Z = z/a$, $R = r/a$, $T = vt/a^2$, where u is the axial component of the velocity vector, v is the radial component of the velocity vector, p is the pressure, ρ and ν are

the density and kinematic viscosity of the fluid, a is the radius of the tube, t is time, and r and z are the radial and axial coordinates, respectively. In the above dimensionless expressions, an appropriate velocity scale factor, u_0, is introduced. For the problem considered, the scale factor, u_0, will be set equal to the maximum velocity of the oscillating entrance velocity profile . Re is the Reynolds number (defined in terms of the velocity u_0 and the tube radius, a), that is, $Re = u_0 a/\nu$. $Z=0$ designates the end of the semi-infinite tube.

The non-slip boundary conditions on the lateral surface of the rigid tube are given as

$$U(Z,R,T)|_{R=1} = 0, \qquad (4a)$$

and

$$V(Z,R,T)|_{R=1} = 0\ . \qquad (4b)$$

The end conditions, describing the velocity of the fluid at the end of the semi-infinite tube, is given in dimensionless form as

$$U(Z,R,T)|_{Z=0} = U_0(R)\ COS(WT)\ , \qquad (5a)$$

and

$$V(Z,R,T)|_{Z=0} = 0\ , \qquad (5b)$$

with the dimensionless frequency given as $W = \omega a^2/\nu$, where ω is equal to 2π times the oscillation frequency in Hz. (note: the dimensionless frequency parameter, W, is equal to the square of the commonly-used Womersley unsteadiness parameter [WOM?]) In the present study, we specify that

$$U_0(R) = \begin{cases} 1\ , & \text{when } 0 \le R < 0.98 \\ 1 - \dfrac{(R-0.98)^2}{(1-0.98)^2}\ , & \text{when } 0.98 \le R \le 1 \end{cases}\ , \qquad (5c)$$

so that the axial velocity at the end of the tube is specified to be uniform, where $U_0 = 1$, except near the walls ($0.98 \leq R \leq 1.00$) where the axial velocity parabolically approaches zero. Additionally, continuity conditions are satisfied along the central axis of the tube at R=0: that is, V and $\partial U/\partial R$ are zero at R=0. The above equations are defined for $0 \leq R \leq 1$, $0 \leq Z < \infty$, $-\infty < T < \infty$.

Equations (1) to (3) are solved using a method of successive approximations. The first-order approximation is a linear approximation with the Reynolds number, Re, set equal to zero. This first-order result will be substituted into nonlinear product terms of the second-order approximation. The equations for the second-order approximation include products of the sinusoidal-oscillating zero-order terms. The solutions to these equations contains results at twice the harmonic oscillation frequency in addition to results at zero frequency . These zero-frequency results, which are obtained from the solution to the time-averaged first order equations, show steady bi-directional streaming.

Additionally, for an appropriate range of frequencies, the velocity profiles obtained from the solutions to the linear approximation demonstrate a mixing phenomena with swirling secondary motion near the entrance.. A discussion of these streaming and mixing effects and their frequency dependence will be presented in a paper to be submitted to the Journal of Biomedical Engineering. Preprints will be available upon request.

---

[1] Goldberg, I.S. and Folk, R.T., Solutions for Steady and Non-Steady Entrance Flow in a Semi-Infinite Circular Tube at Very Low Reynolds Numbers. SIAM Journal on Applied Mathematics, Vol. 48, No. 4, pp. 770-791, 1988

A DYNAMICAL SYSTEM APPROACH IN BIOMEDICAL RESEARCH

Ramesh C. Gupta
Professor
Department of Mathematics & Statistics

University of Maine
Room 320
5752 Neville Hall
Orono, ME 04469-5752

Final Report for:
Summer Research Program
Armstrong Laboratory

Sponsored by:
Air Force Office of Scientific Research
Bolling Air Force Base, Washington, DC

And

Armstrong Laboratory

September 1997

A DYNAMICAL SYSTEM APPROACH IN BIOMEDICAL RESEARCH

Ramesh C. Gupta
Department of Mathematics & Statistics
University of Maine
Orono, ME 04469-5752

ABSTRACT

The purpose of this project is to develop statistical methods in order to improve the ability to make inferences from biomedical data using animals or human subjects. The biomedical data consist of immunological blood cell counts taken on two groups of animals; one group is exposed to radiation and the other group is not. It is assumed that these counts are associated with dynamical systems whose solutions are chaotic in nature. More specifically the cell counts are given by the dynamical system

$$p(t + 1) = c_1 p(t)(1 - p(t)) - c_2 p(t)$$

where p(t) is the proportion of normal cell counts at time t, c_1 and c_2 are constants to be determined. However, the past data suggest that
$3 < c_1 < 4$. We have a treated and a control group of animals with sample size N in each group. We are allowed to draw a blood sample from each animal. The main problem here is to examine the group differences taking into account the dynamical system described above. Further, one should compare the statistical approach that would have applied if it was not recognized that the dynamical system was at the basis of phenomenology.

In this project we study the structure of the dynamical system and develop some statistical models, incorporating the knowledge of the dynamical system to examine the group differences between the treated and the untreated group of animals.

A DYNAMICAL SYSTEM APPROACH IN BIOMEDICAL RESEARCH

Ramesh c. Gupta

1. INTRODUCTION

The United States Air Force has been interested in studying the effect of different types of radiation encountered by its personnel in space. A number of balloon and unmanned satellite flights had provided some idea of the types of radiation which would be encountered in space. These were (i) electromagnetic radiation; (2) electrons; (3) protons; and (4) nuclei of elements of higher Z numbers. For physical details and information about Z numbers, see Dalrymple et. al.(1991)

In order to study the radiation hazards of space, experiments are performed on animals as the primary biological subjects. It is, therefore, important to develop statistical methods in order to improve the ability to make inferences from biomedical data using animals or human subjects. The biomedical data consist of immunologic blood cell counts taken on two groups of animals; one group is exposed to radiation and the other group is not. It is assumed that these counts are associated with dynamical systems whose solutions are chaotic in nature. More specifically the cell counts are given by the dynamical system

$$p(t + 1) = c_1p(t)(1 - p(t) - c_2p(t),$$

where p(t) is the proportion of normal cell counts at time t, c_1 and c_2 are constants to be determined. However, the past data suggest that $3 < c_1 < 4$. We have a treated and a control group of animals with sample size N in each group. We are allowed to draw a blood sample from each animal. The main objective here is to examine the group differences taking into account the dynamical system described above.

In order to achieve the main objectives the following aspects are studied.

(1) The structure of the dynamical system and the conditions on c_1 and c_2 for the existence and stability of period 2 and period 3 solutions.

(2) In order to develop a statistical model incorporating the correlation structure between the repeated measurements, the theoretical aspects of the analysis of longitudinal data are studied. This is because, in our case, the normal assumption of the multivariate repeated measures design is not available.

(3) The method of generalized estimating equations to estimate the prameters of the model. This also involves the computational procedure due to Liang and Zeger (1986).

The analysis of the data will consist of

1. Generating data satisfying the structure of the dynamical system.
2. Developing a model incorporating the correlation structure.
3. Analysis of the data incorporating the knowledge of the dynamical system.
4. Analysis of the data in absence of the information from the dynamical system.
5. Comparison of the procedures in (3) and (4) above.
6. Studying the advantage of the dynamical system.

2. GENERAL DYNAMICAL SYSTEMS

There are many situations, in many disciplines, which can be described, at least to a crude first approximation, by a simple first order difference equation. Studies of the dynamical properties of such models usually consist of finding constant equilibrium solutions and then conducting a linearized analysis to determine their stability with respect to small disturbances: explicitly nonlinear dynamical features are usually not considered.

Recent studies have, however, shown that the very simplest nonlinear difference equations can possess an extraordinary rich spectrum of dynamical behavior, from stable points, through cascades of stable cycles, to a regime in which the behavior (although fully deterministic) is in many respects "chaotic" or indistinguishable from the sample function of a random process.

In the study of population dynamics, one wants to understand how the magnitude X_{t+1} of the population at the time t + 1 is related to the magnitude X_t of the population at time t in the preceding generation. Such a relationship may be expressed by the relation

$$X_{t+1} = \psi(X_t). \tag{2.1}$$

Biologists call the function $\psi(\cdot)$ as "density dependent" and a mathematician calls it nonlinear. In fact, the equation (2.1) is a first order nonlinear

difference equation. There are numerous applications of the equation (2.1) in various fields including genetics, epidemiology, economics and social sciences. For more examples, see May (1976).

An important example of equation (2.1) is given by

$$X_{t+1} = aX_t(1 - X_t). \tag{2.2}$$

(2.2) has been widely studied in the literature under the name logistic equation and has been applied in a number of situations, for example, see Hoppensteadt and Peskin (1992), Kelley (1991) and Mickens (1990).

Our dynamical system of blood cells is given by

$$p(t + 1) = c_1p(t)(1 - p(t)) - c_2p(t), \tag{2.3}$$

where p(t) is the proportion of normal cell count at time t. It is easily seen that (2.3) is a special case of the general system (2.1) and is more general than the logistic equation (2.2). It contains an extra term $c_2p(t)$ which we call a "death term" describing the proportion of normal blood cells which die or are destroyed. Such a phenomenon is also noticed in harvesting where $c_2p(t)$ is the harvest taken at the beginning of the $(t + 1)$th interval and $p(t + 1)$ denotes the population at the end of this interval after harvesting. For details, see Hoppenstedt and Peskin (1992).

3 . STRUCTURE OF THE DYNAMICAL SYSTEM

In order to incorporate the knowledge of our dynamical system of blood cells, we should understand the structure of the dynamical system. For this purpose Gupta (1994, 1995) and Gupta and Albanese (1997) have studied the fixed points, the period 2 and the period 3 solutions of the system which are briefly described below.

3.1 Fixed Points and Period 2 Solutions

3.1.1 Fixed Points

Suppose a dynamical system is represented by

$$y_{k+1} = f(y_k).$$

Then a is said to be a fixed point of the system if

$$f(a) = a.$$

We now present a definition of stable and unstable fixed points.

Definition. Suppose a first order dynamical system has a fixed point a. This fixed point is said to be stable or attracting if there exist an $\epsilon > 0$ such that for every y(0) satisfying

$$|y(0) - a| < \epsilon,$$

we have $\lim_{k \to \infty} y(k) = a$.

The fixed points and their stability can be obtained by using the following theorem.

Theorem 3.1.

Consider a nonlinear dynamical system

$$a(n + 1) = ra^2(n) + ba(n).$$

The two fixed points are

$$a = 0 \text{ and } a = (1 - b)/r.$$

- If $|b| < 1$, then $a = 0$ stable and $a = (1 - b)/r$ is unstable.
- If $1 < b < 3$, then $a = (1 - b)/r$ is stable and $a = 0$ is unstable.
- If $b < -1$ or $b > 3$, then both are unstable. For proof and details, see Gupta (1994) and Kelley (1991). Note that r, the coefficient of $a^2(n)$, plays no role in determining the stability of the equilibrium values of the dynamical system under consideration.

For our dynamical system of blood counts $b = c_1 - c_2$, the two fixed points are

$$a = 0 \text{ and } a = (c_1 - c_2 - 1)/c_1.$$

So

- If $-1 < c_1 - c_2 < +1$, then $a = 0$ is stable and
  $a = (c_1 - c_2 - 1)/c_1$ is unstable.
- If $1 < c_1 - c_2 < 3$, then $a = (c_1 - c_2 - 1)/c_1$ is stable and
  $a = 0$ is unstable.
- If $c_1 - c_2 < -1$ or $c_1 - c_2 > 3$, then both are unstable.

3.1.2. Period two solutions

As described before we convert our dynamical system

$$p(n + 1) = c_1p(n)(1 - p(n)) - c_2p(n)$$

by the transformation

$$z(n) = kp(n), \text{ where } k = c_1/(c_1 - c_2 - 1)$$

to

$$z(n+1) = (\lambda + 1)z(n) - \lambda z^2(n) \tag{3.1}$$

where $\lambda = c_1 - c_2 - 1$.

Consider now a more general nonlinear discrete dynamical system given by

$$\ldots u_{n+1} = Au_n + Bu_{n-1} + Cu^2_n + Du^2_{n-1} \tag{3.2}$$

where A, B, C,D are constants satisfying

$$A + B + C + D = 1.$$

As a special case when $A = 1 + \lambda$, $B = 0$, $C = -\lambda$ and $D = 0$, the resulting equation will lead to our dynamical system (3.1). For these special values of A, B, C, D, the scheme given by (3.2) is called Euler's scheme. It was shown in Gupta (1994) that the period 2 solutions a and b of (3.2) are given by

$$\left.\begin{aligned} a &= \frac{B - A - 1}{2(C - D} \\ b^2 &= a(1 - a),\ b > 0 \end{aligned}\right\} \tag{3.3}$$

For our case, substituting the values of A, B, C, D in (3.3), we get

$$a = \frac{c_1 - c_2 + 1}{2(c_1 - c_2 - 1)}$$

$$b^2 = \frac{(c_1 - c_2 + 1)(c_1 - c_2 - 3)}{2(c_1 - c_2 - 1)} > 0.$$

Now $b^2 > 0$ if $c_1 - c_2 < -1$ or $c_1 - c_2 > 1$. So the period 2 solutions of (3.1) are given by

$$Z_n = \frac{c_1 - c_2 + 1}{2(c_1 - c_2 - 1)} + (-1)^n \sqrt{\frac{(c_1 - c_2 + 1)(c_1 - c_2 - 3)}{2(c_1 - c_2 - 1)^2}}$$

Since b also has to be positive, we also should take $c_1 - c_2 > 1$.

Hence if we take $c_1 - c_2 > 3$, then $b > 0$ and $b^2 > 0$. Thus period 2 solutions exist if $c_1 - c_2 > 3$.

Stability of period of 2 solutions

Specializing to Euler's scheme $c_1 - c_2 = 1 + \lambda$, the necessary and sufficient conditions for stability are

$$2 < \lambda < \sqrt{6}$$

or

$$3 < c_1 - c_2 < 3.45.$$

For details, see Gupta (1994).

Generation of period of 2 solutions

As can be seen from equations (3.3) that period 2 solutions of equation (3.1) are of the form

$$u_n = a + (-1)^n b,\ b \neq 0$$

and are given by

$$a = \frac{\lambda + 2}{2\lambda},\ b = \pm \frac{\sqrt{\lambda^2 - 4}}{2\lambda} \tag{3.4}$$

where $\lambda = c_1 - c_2 - 1$.

Equation (3.4) is used to generate period 2 solutions of (3.1). These in turn yield the solutions to our system of blood cell data.

3.2 Period 3 Solutions

Let us consider again the general nonlinear discrete dynamical system given by

$$u_{n+1} = Au_n + Bu_{n-1} + Cu_n^2 + Du_{n-1}^2 \tag{3.5}$$

where A, B, C, D are constants satisfying

$$A + B + C + D = 1$$

As a special case, when $A = 1 + \lambda$, $B = 0$, $C = -\lambda$ and $D = 0$, the resulting equation leads to our dynamical system. For these special values of A, B, C, D the scheme given by (3.5) is called Euler's scheme. The period 3 solutions are given by

$$u_{n+3} = u_n.$$

In order to study the period 3 solutions, we proceed as follows:

For the general system given by (3.5) define

$$\alpha = \frac{D^2B + CD + AC^2}{D^3 + C^3}$$

$$\beta = \frac{AD^2 - BCD - C^2}{D^3 + C^3}$$

$$\gamma = \frac{-D^2 - ACD + BC^2}{D^3 + C^3} \tag{3.6}$$

This gives $1 + \alpha + \beta + \gamma = 0$

Let $k^2 = \frac{1}{4}\alpha^2 + \frac{1}{2}\alpha\beta + \frac{1}{2}\gamma\alpha$.

If a, b, c are the period 3 solutions of (3.5), set $a = a_1 - 1/2\alpha$, $b = b_1 - \frac{1}{2}\alpha$, $c = c_1 - 1/2\alpha$. Then a_1, b_1, c_1 are given by

(i) $a_1 = b_1 = c_1$ with $a_1^2 + 2\beta a_1 = k^2$

(ii) $a_1 = b_1 = \beta - c_1 = \pm\sqrt{k^2 - \beta^2}$

(iii) $b_1 = c_1 = \beta - a_1 = \pm\sqrt{k^2 - \beta^2}$

(iv) $c_1 = a_1 = \beta - b_1 = \pm\sqrt{k^2 - \beta^2}$.

For details, see Gupta (1994).

Special case.

Euler scheme: $A = 1 + \lambda$, $\beta = 0$, $C = -\lambda$, $D = 0$. Using (3.6), it can be verified that $\alpha = -(1 + \lambda)/\lambda$, $\beta = 1/\lambda$ and $\gamma = 0$. These in turn yield

$$k^2 = \frac{1}{4}\alpha^2 + \frac{1}{2}\alpha\beta + \frac{1}{2}\gamma\alpha = (\lambda^2 - 1)/4\lambda^2.$$

So

$$a_1 = b_1 = \pm\sqrt{k^2 - \beta^2} = \pm\sqrt{\frac{\lambda^2 - 1}{4\lambda^2} - \frac{1}{\lambda^2}} = \pm\frac{\sqrt{\lambda^2 - 5}}{2\lambda}$$

This gives

$$c_1 = \frac{1}{\lambda} \mp \sqrt{\frac{\lambda^2 - 5}{4\lambda^2}}.$$

Similarly the other two sets of solutions can be obtained.

Stability and Existence of period 3 solutions

Using the machinery developed in Ben Yu et.al. (1989) and Sleeman et.al. (1985), it was shown in Gupta (1994) that the period 3 solutions exist if $\lambda \geq 2\sqrt{2}$. It was also shown that the period 3 solution is stable for

i.e. $2.8284 \leq \lambda \leq 2.8415.$

Since, for our system $\lambda = c_1 - c_2 - 1$, we should have

$$c_1 - 3.8415 \leq c_2 \leq c_1 - 3.8284.$$

So c_1 has to be larger than 3.8415.

Period 3 solutions can be generated by taking different values of c_1 and c_2 satisfying the above inequality. For details, see Gupta (1995) and Gupta and Albanese (1997).

4. STATISTICAL APPROACH (LONGITUDINAL DATA)

In classical univariate statistics, a basic assumption is that each of a number of subjects, or experimental units, gives rise to a single measurement on some relevant variable, termed the response. In multivariate statistics, the single measurements on each subject is replaced by a vector of measurements. For example, in a univariate medical study we might measure the blood pressure of each subject, whereas in a multivariate study we might measure blood pressure, heart rate, temperature and so on. In longitudinal studies, each subject again gives rise to a vector of measurements, but these now represent the same physical quantity measured at a sequence of observation times. Thus, for example, we might measure a subject's blood pressure on each of five successive days.

Longitudinal data therefore combine elements of multivariate and time series data. However, they differ from classical multivariate data in that the time series aspect of the data typically imparts a much more highly structured pattern of interdependence among measurements than for standard multivariate data sets; and they differ from classical time series data in consisting of a large number of short series, one for each subject, rather than a single long series. Thus our problem of blood cell counts fall in the category of longitudinal data.

We shall now describe general linear models for longitudinal data.

General Linear Model

Let y_{ij}, $j = 1, 2, \ldots, n$ be a sequence of observed measurements on the ith subject, i = 1, 2, ...,m. Let t_j, $j = 1, 2 \ldots, n$, be the corresponding times at which the

measurements are taken on each unit. Associated with each y_{ij} are the values, x_{ijk}, k = 1,2,...,p of p explanatory variables. We assume that the y_{ij} are realization of a random variable y_{ij} which follow the regression model

$$y_{ij} = \beta_1 x_{ij1} + \ldots + \beta_p x_{ijp} + \epsilon_{ij} \tag{4.1}$$

where ϵ_{ij} are random sequences of lengths n associated with each of the m subjects. In the classical linear model, the ϵ_{ij} would be mutually independent $N(0, \sigma^2)$ random variables. In our context, the longitudinal structure of the data means that we expect ϵ_{ij} to be correlated within subjects.

For a formal analysis of the linear model, a matrix formulation is preferable.

Let $y_i = (y_{i1}, \ldots, y_{in})$ be the observed sequence of measurements on the ith subject and $y = (y_1, y_2, \ldots, y_m)$ the complete set of N = nm measurements from m units. Let X be an $N \times p$ matrix of explanatory variables. Let $\sigma^2 V$ be a block diagonal matrix with nonzero $n \times n$ blocks of $\sigma^2 V_0$, each representing the variance matrix for the vector of measurements on a single subject. Then the general linear model for the longitudinal data treats y as a realization of multivariate Gaussian random vector, Y, with

$$Y \sim M V N(X\beta, \sigma^2 V) . \tag{4.2}$$

For analyzing such data, the block diagonal structure of $\sigma^2 V$ is crucial. For a justification of this uniform correlation model and for other correlation models, see Diggle et. al. (1994). The estimation of β in the general linear model (4.2) may be carried out by the method of weighted least squares and by the method of maximum likelihood. For details, see Gupta (1995).

In order to overcome some of the problems associated with maximum likelihood method, a method of restricted maximum likelihood (REML) is used. For details and relative merits of MLE and REML, we refer to Gupta (1995).

ESTIMATING EQUATIONS

As has been explained before, the longitudinal data sets are comprised of repeated observations of an outcome variable and a set of covariates for each of many subjects. When the outcome variable follows a Gaussian distribution, the methods described in the previous section can be applied. However, fewer techniques are available when the outcome is not approximately Gaussian. One difficulty with the analysis of non-Gaussian longitudinal data (Discrete outcome in our case) is a lack of rich class of models such as the multivariate Gaussian for the joint distribution of y_{it} $(t = 1,2,\ldots,n_i)$. Hence in general, the likelihood methods have not been available.

The approach, due to Liang and Zeger (1986), uses working generalized linear model for the marginal distribution of y_{it}. We do not specify a form for the joint distribution of the repeated measurements. Instead, we introduce estimating equations that give consistent estimates of the regression parameters and of their variances under weak assumptions about the joint distribution. The methods proposed here reduce to maximum likelihood when the y_{it} are multivariate Gaussian. The details may be obtained from Gupta (1995). We now describe longitudual Data Analysis for discrete outcomes.

5. LONGITUDNAL DATA ANALYSIS FOR DISCRETE OUTCOMES

For discrete outcomes, current techniques are not yet as comprehensive as their analogues for Gaussian data. Regression models for discrete data are new by comparison to linear models for continuous outcomes and this in part is responsible for the lag. Logistic regression for binary outcomes was introduced in its current form by Cox in 1958; log-linear models developed in the 1950's and 1960's ; models for ordinal and

multinomial data are more recent. On the other hand, linear models for continuous responses date back to Gauss and Legendre at the start of the nineteenth century.

The discrete longitudual data problem is also harder. There is not a multivariate distribution for discrete outcomes as flexible as the multivariate Gaussian, the basis for linear model theory. For discrete data, measures of location (mean) and of dependence (covariance) are not separable as in the Gaussian case. Discrete data models which attempt to account for dependence can, therefore, be more complicated to work with.

The gap between discrete and continuous longitudual data analysis (LDA) is closing, partly as a result of two developments in statistical theory. First, regression methods for discrete and continuous univariate outcomes have been unified under the class of generalized linear models (GLM's) or quasi-likelihood models. The same approach can now be used to find linear, logistic, log-linear, survival and host-of specialized models given a single observation per subject. Second, we have experienced a resurgence of semi-parametric models where only part of the probability distribution of the data is specified. An example is the partial likelihood technique for the Cox proportional hazard model where the underlying hazard function need not be specified. Other examples include pesudo-likelihood and quasi-likelihood. These ideas have application to discrete LDA where it may be desirable to parametrically model the mean but not the dependence. We now address two questions.

1. How much dependence is there in a longitudual data set?
2. How are methods for discrete LDA differ from those of Gaussian outcomes?

In answer to the first question, the degree of dependence is small enough so that in many epidemeologic studies, even crude regression estimates which ignore the correlation are nearly optimal. It is large enough, however, so that assessments of precision of regression coefficients must take dependence into account. Zeger (1988) reviews a simple approach which uses standard regression coefficients and a robust-variance estimate. He presents some examples to determine how much correlation is in a longitudual data set. When the number of subjects is large relative to the number of observations per subject and when missing data are not an issue, the correlation is small

enough so that the ordinary least square regression coefficients are nearly as efficient in many studies. The dependence is large enough, however, to dramatically affect the estimates of percision of both the least square and maximum likelihood methods and hence the correlation must be accounted for to make correct inferences.

In response to question 2, the principal difference between the analysis of discrete and continuous longitudual data is that nonlinear models are used for regression with discrete outcomes. In non-linear models, regression structure for the mean response is not separable from the dependence among repeated measurments as it is for linear models. Zeger (1988) clarifies this point by considering some linear models and concludes that a fundamental difficulty in LDA is that the interpretations and values of regression coefficients are tied to the assumption about the nature of the time dependence. That is, regression coefficients and descriptions of dependence cannot be separated with discrete outcomes as they can in linear models.

In the following, we describe an extension of Liang and Zeger to different dispersion parameters.

EXTENSION TO DIFFERENT DISPERSION PARAMETERS

Liang and Zeger (1986) proposed an extension of generalized linear models to the analysis of longitudual data. In their formulation, a common dispersion parameter assumption across observation times is required. However, this assumption is not expected to hold in most situations. In general, the outcome may vary much across times and the conditions from which the data are collected may vary from time to time.

Park (1993) proposed a simple extension of Liang and Zeger's formulation to allow for different dispersion parameters for each time point. The extended model considered by Park (1993) was mainly used to compare the GEE approach with the ML approach for the normally-distributed responses. Park and Shin (1995) focussed on evaluating the effect of additional dispersion parameters on the estimators of the model parameters. Through a Monte Carlo simulation study, they compared the efficiency of Park's method with the Liang and Zeger's method. The extension is described as

follows:

Let t be the number of time points at which data are collected. Let $\boldsymbol{y}_i = (\boldsymbol{y}_{i1},\boldsymbol{y}_{i2},...,\boldsymbol{y}_{it_i})^T$ be the $t_i \times 1 (t_i \leq t)$ vector of responses for the i[th] subject and $\boldsymbol{x}_i = (\boldsymbol{x}_{i1}^T \boldsymbol{x}_{i2}^T,...,\boldsymbol{x}_{it_1})^T$ be the $t_i \times p$ matrix of covariate values for the i[th] subject $(i = 1,2,...,n)$. The extended marginal density of $\boldsymbol{y}_{ij}$ with different dispersion parameters over time is

$$f(y_{ij}) = \exp\left[\frac{y_{ij}\theta_{ij} - b(\theta_{ij})}{a(\phi_j)} + c(y_{ij},\phi_j)\right] \tag{5.1}$$

The mean and variance of y_{ij} are given by

$E(y_{ij}) = \mu_{ij} = b'(\theta_{ij})$

$Var(y_{ij}) = v(\mu_{ij})\ a(\phi_j)$, where $v(\mu_j) = b''(\theta_{ij})$ is the variance function and ϕ_j is possibly unknown dispersion parameters.

The possibility $\phi_j = \phi$ for all j leads to Liang and Zeger formulation. In this case for binary variables $V(\mu_{ij}) = \mu_{ij}(1-\mu_{ij})$ and $a(\phi) = 1$. For Poisson variables, $v(\mu_{ij}) = \mu_{ij}$ and $a(\phi) = 1$. The normal outcome variables, $V(\mu_{ij}) = 1$ and $a(\phi) = \phi$. The systematic part of the marginal model is

$$\eta_i = \boldsymbol{x}_i\beta \tag{5.2}$$

where $\eta_i = (\eta_{i1},\eta_{i2},...,\eta_{it_i})^T$ with $\eta_{ij} = g(\mu_{ij})$ and $\eta_{ij} = \chi_{ij}\beta$. Here $\beta = (\beta_1,\beta_2,...,\beta_\rho)^T$ is the $p \times 1$ vector of unknown parameters to be estimated and g(·) is the link parameter. Note that for binary outcome variables, $g(\mu_{ij}) = \ln(\mu_{ij}/(1-\mu_{ij}))$. If the outcome variable does not have over dispersion, then $\phi_j = 1$; otherwise ϕ_j can be used to adjust for over-dispersion. For Poisson outcome variables, $g(\mu_{ij}) = \ln(\mu_{ij})$.

Here also if the outcome variable is not overdispersed, then $\phi_j = 1$; otherwise ϕ_j can be used to adjust for over dispersion. For normal outcome variables, $g(\mu_{ij}) = \mu_{ij}$. Note that the overdispersion parameter does not only influence the marginal variance, it may also influence the mean of the response variable. In such cases, the overdispersion parameter plays a significant role in the estimation of regression parameters. This raises the necessity for a joint estimation of the regression as well as over dispersion parameters, in order to describe the marginal expectation of the outcome variable as a function of the covariates. To correct for the effect of over dispersion, Sutradher and Rao (1996) exploit a general class of joint estimating equations for the regression and over dispersion parameters.

Thus the marginal model (5.2) allows different variance parameters over time. We now briefly summarize the extended generalized estimating equations (EGEE) under the extended marginal distribution assumption (5.1) and present asymptotic theores for these equations.

Extended Generalized Estimating Equations

Let $R_i(\mathfrak{L})$ be the $t_i \times t_i$ working correlation matrix of $\boldsymbol{y}_i$ and let $\mathfrak{L}$ be an $s \times 1$ vector which fully characterizes $R_i(\mathfrak{L})$. Although the observations times and correlation matrix can differ from subject to subject, $\mathfrak{L}$ is assumed to be the same for all subjects.

Let A be a $t \times t$ diagnol matrix with $V(\mu_{ij})$ as the j^{th} diagnol element and ϕ be a $t \times t$ diagonal matrix defined by $\phi = diag(\phi_1, \phi_2, ..., \phi_t)$. Then for the i^{th} subject, the $t_i \times t_i$ working covariance matrix of $\boldsymbol{y}_i$ is given by

$$v_i = (A_i \phi_i)^{1/2} R_i(\mathfrak{L})(A_i \phi_i)^{1/2} \qquad (5.3)$$

where A_i is a $t_i \times t_i$ submatrix of A and ϕ is a $t_i \times t_i$ submatirx of ϕ. If $R_i(\mathfrak{L})$ is indeed the true correlation matrix for the $\boldsymbol{y}_i$'s, $V_i = cov(\boldsymbol{y}_i)$. The EGEE are defined by

$$\sum_{i=1}^{n} D_i^T V_i^{-1} S_i = 0 \qquad (5.4)$$

where $S_i = y_i - \mu_i$ with $\mu_i = (\mu_{i1},\mu_{i2},...,\mu_{it_i})^T$ and $D_i = \left(\frac{\partial}{\partial \beta}\mu_i\right)^T$.

The estimator of β can be obtained by iterating between quasi-likelihood methods for estimating $\mathcal{L}$ and ϕ_j, $j = 1,2,...,t$ as functions of β. The estimation process is the same as that of Liang and Zeger (1986) except that ϕ_j, $j = 1,2,...,t$ are to be estimated instead of the common ϕ.

Let $\hat{\beta}_G$ be the final solution of (5.4). Under mild regularity conditions, a slight-extension of Liang and Zeger yields that $n^{1/2}\left(\hat{\beta}_G - \beta\right)$ is asymptotically multivariate normal with zero mean and covariance matrix V_β given by

$$V_\beta = \underset{n\to\infty}{limit}\, n \left(\sum_{i=1}^{n} D_i^T V_i^{-1} D_i\right)^{-1} \left\{\sum_{i=1}^{n} D_i^T V_i^{-1} Cov(y_i) V_i^{-1} D_i\right\} \left(\sum_{i=1}^{n} D_i^T V_i^{-1} D_i\right)^{-1}$$

Note that the asymptotic variance of $\hat{\beta}_G$ depends on the dispersion parameter vector Φ, while the estimator of Liang and Zeger does not.

For a given β, $\mathcal{L}$ and Φ can be estimated from the current Pearson residuals defined by

$$\hat{r}_{ij} = \{y_{ij} - \hat{\mu}_{ij}\} / \left\{\left[\hat{V}_i\right]_{jj}\right\}^{1/2}$$

where $\hat{\mu}_{ij}$ and $\left[\hat{V}_i\right]_{jj}$ (j^{th} diagnol element of $\hat{V}_i$) depend on the current value of β. The j^{th} diagnol element of Φ is then estimated by

$$\hat{\phi}_j = \sum_{i=1}^{n} \hat{r}_{ij}^2 / n_j \qquad (5.5)$$

where n_j is the number of subjects observed at time j.

When the observation times are the same for all subjects so that $t_i = t$ and we may let $R(\alpha)$ be totally unspecified and estimate $s = t(t-1)/2$ correlations. R can be estimated by

$$\sum_{i=1}^{n} (A_i \phi_i)^{-1/2} S_i S_i^T (A_i \phi_i)^{-1/2}$$

Here estimation of ϕ is required to obtain the estimate of R, while under the common ϕ_j assumption, it is not required.

Several choices of structured $R(\mathfrak{L})$ are available which are widely applicable for longitudual data analysis, see Park and Shin (1995). One of them is the exchangeable correlation structure. Let $s = 1$ and assume that $cov(y_{ij}, y_{ij'}) = \alpha$ for all $j \neq j'$. This correlation is also called the compound symmetry correlation. Given Φ, α is estimated by

$$\hat{\alpha} = \sum_{i=1}^{n} \sum_{j>j'} r_{ij}^* r_{ij'}^* / \left\{ \sum_{i=1}^{n} \frac{1}{2} t_i (t_i - 1) \right\}$$

where $r_{ij}^* = r_{ij} / \{\phi_j\}^{1/2}$

When $\phi_1 = \phi_2 = \ldots = \phi_t = \phi$ the estimation of the common parameter ϕ is unnecessary for calculating $\hat{\beta}_G$ and $\hat{V}_\beta$. For one non-stationary dependent correlation structure and first-order autoregressive (AR-1) correlation structure, see Park and Skin (1995).

6. CONCLUSION AND FURTHER WORK

In this project we have studied the structure of the dynamical system associated with the repeated measurments on the successive counts of normal blood cells. The main problem here is to examine the group differences between the treated and the control group taking into account the dynamical system. For this end, we have explored some statistical tools dealing with the longitudual data for discrete outcomes. Further investigation will include (1) generating data satisfying the structure of the dynamical system, (2) developing an appropriate model incorporating the correlation structure, (3) analysis of the data incorporating the knowledge of the dynamical system (4) analysis of the data in the absence of the dynamical system (5) comparison of the procedures in (3) and (4) and finally (6) studying the advantages of the dynamical system.

ACKNOWLEDGEMENTS

I am thankful to Dr. Richard Albanese for supporting this project and to Mathematics Product Division of the Armstrong Laboratory for providing the necessary facilities.

REFERENCES

Ben Yu, G., B. D. Sleeman, and C. Sue Yang (1980). On the discrete logistic model of Biology. Applicable Analysis 33, 215-231.

Cullis, B. R. and C. A. McGilchrist (1990). A model for the analysis of growth data from designed experiments. Biometrics 46, 131-146.

Dalrymple, G. V., Lindsay, I. R., Mitchell, J. and Hardy, K. A. (1991). A review of USAF/NASA proton bieffects project: rationale and acute effects. Radiation Research 126, 117-119.

Diggle, P. J., K. Y. Liang, and S. L. Zeger (1994). Analysis of longitudinal data. Oxford University Press, N.Y.

Gupta, R. C. (1994). A new approach to the analysis of Biomedical data. Report submitted to Armstrong Laboratory, Brooks, AFB, TX.

Gupta, R. C. (1995). A new approach to the analysis of Biomedical data. Report submitted to Armstrong Laboratory, Brooks AFB, TX.

Gupta, R. C. and R. A. Albanese (1997). A Dynamical System Approach to the Analysis of Biomedical data. To appear in Dynamics of Continous and Discrete Impulsive Systems.

Hoppensteadt, F. C. and C. S. Peskin (1992). Mathematics in Medicine and Life Sciences. Springer Verlag, N.Y.

Kelley, W. G. (1991). Difference Equatons, Academic Press.

Liang, K. Y. and S. L. Zeger (1986). Longitudinal data analysis using generalized models. Biometrika 73, 13-22.

May, R. M. (1976). Simple mathematical models with very complicated dynamics. Nature 261, 459-467.

Mickens, R. E. (1990). Difference Equations, VanNostrand Reinhold, NY.
Park, T. (1993). A comparison of the generalized estimating equation approach with the maximum likelihood approach for repeated measurments. Statistics in Medicine 12, 1723-1732.

Park, T. and M.Shin, (1995). A practical extension of the generalized estimating equation approach for longitudual data. Communications in Statistics--Theory and Methods, 24(10), 2561-2579.

Sleeman, B. D., D. F. Griffiths, A. R. Mitchell and P. D. Smith (1985). Stable periodic solutions in nonlinear difference equations. Siam J. Science and Statistical Computation 9(3), 543-555.

Sutradhar, B.C. and Rao, P.R. (1996). On joint estimation of regression and over dispersion parameters in generalized linear models for longitudual data. Journal of Multivariate Analysis 56, 90-119.

Zeger, S. L. and K. Y. Liang (1986). Longitudinal data analysis for discrete and continuous outcomes. Biometrics 42, 121-130.

Zeger, S.L. (1988). Commentry. Statistics in Medicine 7, 161-168.

A PROTOCOL FOR DEVELOPMENT OF AMPLICONS FOR A RAPID AND EFFICIENT METHOD OF GENOTYPING HEPATITIS C VIRUS FROM CLINICAL SERUM SPECIMENTS

Dr. John Herbold
Associate Professor

School of Public Health
UT-Houston Health Science Center
Houston, TX 77030

Final Report for:
Summer Faculty Research Program
Armstrong Laboratory

Sponsored by:
Air Force Office of Scientific Research
Bolling Air Force Base, DC

And

Armstrong Laboratory

August, 1997

A PROTOCOL FOR DEVELOPMENT OF AMPLICONS FOR A RAPID AND EFFICIENT METHOD OF GENOTYPING HEPATITIS C VIRUS FROM CLINICAL SERUM SPECIMENS

Thomas R. Mertz Jr.
Graduate Student
Institute of Molecular Biology and Medicine
University of Scranton
Scranton, PA 18510
and
John R. Herbold
Associate Professor
School of Public Health
UT-Houston Health Science Center
Houston, TX 77030

Abstract

The two goals of this research project were to (1) establish a procedure to confirm the presence of Hepatitis C Virus (HCV) in serum and (2) to establish a procedure to obtain unique amplicons suitable for genotyping HCV specimens. HCV detection needed to be simple and rapid for use in a clinical laboratory setting. Genotyping of HCV is necessary for further epidemiological studies and assessment of risk to military personnel deployed worldwide. This research examines two protocols for (1) a PCR-based assay to test for HCV RNA (antigen) and (2) isolating viral RNA and preparing cDNA for a PCR-based method for genetic typing of HCV variants. Our results indicate the potential for exploring novel applications of current technology to rapidly genotype HCV variants in the clinical laboratory setting. This work will continue throughout the year at the Institute of Molecular Biology and Medicine (University of Scranton) in collaboration with the Air Force Epidemiology Research Division (Armstrong Laboratory) and the University of Texas School of Public Health.

A PROTOCOL FOR DEVELOPMENT OF AMPLICONS FOR A RAPID AND EFFICIENT METHOD OF GENOTYPING HEPATITIS C VIRUS FROM CLINICAL SERUM SPECIMENS

Thomas R. Mertz Jr. and John R. Herbold

INTRODUCTION

Hepatitis C Virus (HCV) is a single stranded RNA virus belonging to the Flaviviridae family. It is known to be the major causative agent of non-A, non-B hepatitis(Weiner et al., 1990; Choo et al., 1991). Infection can be asymptomatic, mild, chronic, and/or result in long term sequelae such as a chronic viral carrier status and potentially liver cancer. Individuals acutely infected with HCV cannot readily be differentiated on clinical or histopathologic criteria from those infected with other viral hepatitides, and, in many cases, may show no clinical manifestations. Antibody formation may not occur until several months after initial infection(Young et al., 1993). Parenteral and sexual transmission are believed to be the primary routes of infection(Houghton, 1996). Infectivity, pathogenicity, chronicity, and response to therapeutic intervention may be related to the specific HCV genotype causing infection(Hagiwara et al., 1996; Shindo et al., 1991; Versalovic et al., 1996; Yuki et al., 1997). But at present, no means is generally available to establish genotype.

Six genotypes as well as several sub-types have been elucidated after comparison of specific sequences(Parsing and Relman, 1996; Simmonds, Alberti et al., 1994; Simmonds, Holmes et al., 1993). Most work to date has focused on two distinct regions of the HCV genome: the 5′ non-coding region due to its high degree of conservation, and the NS-5 region due to its variability (Cha et al., 1991; Bukh et al., 1992b; Choo et al., 1991; O'Brien et al., 1997; Ohno et al., 1997; Okamoto et al., 1992; Pernas, 1995; Simmonds, Smith et al., 1994; Simmonds, McOmish et al., 1993). Because PCR primer selection was very important in this study, and the 5′-NCR and NS-5 region are commonly used for genotypic work, we chose one primer set from each

region using the Oligo 5.0 software package for Macintosh (Rychlik, 1996).

Reverse transcription was carried out with random primers, and thus the entire genome was amplified into DNA. This result was beneficial because it provides nucleic acid for future analysis of different areas of the genome. Also, a DNA form of the genome is more stable in storage than the RNA form.

METHODOLOGY

I. Current Clinical Laboratory Diagnostic Protocol.

Archived samples were obtained from the Air Force Epidemiological Reference Laboratory. Clinical serum samples are screened for hepatitis C antibody at the primary military medical facility by an Enzyme-Linked Immunosorbent Assay (ELISA) procedure (Abbott, 1993). ELISA positive serum samples are forwarded to the Epidemiologic Research Division for confirmation of results by repeat ELISA and a Strip Immunoblot Assay (RIBA)(Chiron, 1995; Chaudhary et al., 1993). Antibody results are provided to the attending physician for assessment in conjunction with other laboratory parameters and the clinical status of the patient.

II. Implementation of Hepatitis C Viral RNA (Antigen) Test Procedure

Our goal was to integrate an HCV antigen test procedure into the daily activities of a clinical reference laboratory so that only antigen positive samples would be subjected to HCV viral RNA isolation procedures. Samples used for antigen screening were all repeatedly reactive by ELISA and had variable (indeterminate and positive) RIBA results.

Sample sera were tested for HCV antigen using the AMPLICOR HCV Test Kit(Roche, 1993). Approval was received from Roche Molecular

Systems to participate in the RMS Research Use Certification Program for the AMPLICOR HCV Test Kit. The AMPLICOR HCV Test Kit has not been approved by the FDA, and, as such, is not used for diagnostic purposes. Specimens were prepared and tested as stated on the product insert. A 100 microliter aliquot of serum was required for each test. All necessary reagents for reverse transcription of viral RNA, amplification by PCR, and detection of the amplicon were included in the kit. Laboratory technicians and AFOSR personnel were trained by a Roche representative in the use of the kit and good laboratory practices for PCR procedures.

III. Isolation of Hepatitis C Viral RNA

Isolation of viral RNA from sera was accomplished using a commercially available kit (QIAmp Viral RNA Kit, QIAGEN Inc. #29504) in accordance with the handbook procedures. A 140 microliter aliquot of serum was required for each test. The concentration of purified RNA in each sample was determined spectrophotometrically(see Table 1) (Pharmacia Biotech Ultrospec 3000 UV/Vis Spectrophotometer). Purified RNA was either immediately reverse-transcribed or stored at -20 C until ready for use (see Methodology Section IV, Generation of Amplicons for Genotyping).

IV. Generation of Amplicons for Genotyping .

Reverse Transcriptase Polymerase Chain Reaction (RT-PCR) was accomplished using a commercially available kit (RT-PCR Kit, Stratagene Inc., #200420). RT-PCR is used to generate amplicons of complementary DNA from RNA. Random primers were used in the synthesis of cDNA. The use of random primers allowed the formation of amplicons that, collectively, represent the entire genome. Further PCR amplification with sequence-specific primers(see Methodology Section V, Selection of Sequence-Specific Primers for Genotyping) generated amplicons suitable for sequence analysis and

genotyping(Stratagene, 1997). Reverse transcriptase synthesis of first-strand cDNA requires 100 ng of RNA, according to the product insert. Volumes required ranged from 1.1-16.0 microliters based on the concentration of the previously purified RNA (Table 1).

V. Selection of Sequence-Specific Primers for Genotyping.

Specific sections in the 5'NCR and NS-5 regions were targeted based on a literature review indicating that there are two regions of the genome useful for phylogenetic analysis (Chan et al., 1992; Okamoto et al., 1996; Simmonds et al., 1994). Any sequence or primer data is in reference to Genbank accession number L02836. Potential primers (Table 2) for amplification of the NS-5 and 5'NC regions were analyzed by Oligo 5.0 for Macintosh (Rychlik, 1996). Primer selections were determined by best fit based on factors such as primer Tm matching, GC clamp design, optimal annealing temperatures, and dimer formation potential. Primers chosen for subsequent PCR are also noted in Table 2.

RESULTS AND DISCUSSION

I. Constraints of Current Clinical Laboratory Diagnostic Protocol

Requests for assessment of Hepatitis C viral antigen status have been received but there are currently no FDA approved diagnostic kits available. Additionally, research studies have indicated a variety of hepatitis C genotypes that appears to be related to infectivity, pathogenicity, chronicity, and response to therapeutic intervention. Assessment of hepatitis C viral antigen status is useful for multiple purposes. One, viral presence differentiates the active hepatitis case from patients who have been infected but are now recovered. Also, viral load is helpful when assessing response to antiviral therapy. Thirdly, viral presence coupled with epidemiologic characteristics may elucidate the natural history of hepatitis C virus infections leading to clues regarding prevention, intervention,

and therapeutic treatment. Genotyping (currently a basic research procedure) of the different viral isolates would facilitate identification and elucidation of epidemiologic patterns related to infectivity, pathogenicity, chronicity, as well as response to therapeutic intervention(Enomoto et al., 1990; Murashima et al., 1996; Murphy et al., 1994; Nagasaka et al., 1996; Matar et al., 1996; McOmish et al., 1994).

II. Implementation of Hepatitis C Viral RNA (Antigen) Test Procedure

The Roche Molecular Systems AMPLICOR HCV Test Kit was easily integrated into the daily activities of a clinical reference laboratory. It was found that the test could easily be completed within the course of a normal work day, with results usually available in 5-8 hours depending on sample size. Once FDA approval is obtained this procedure could easily be added to existing clinical reference laboratory protocols.

III. Isolation of HCV viral RNA

The QIAmp kit was chosen due to its ease of use and processing speed. The kit recovers viral RNA by passing a previously lysed sample through a column that selectively binds viral RNA. A series of washes eliminates contaminants and elutes purified RNA in water (Qiagen, 1996). Viral RNA was isolated from 50 serum samples. Purified RNA concentrations are displayed in Table 1. Some difficulty was experienced in obtaining significant quantities of purified RNA (Table 1). In order to insure greater yields, larger aliquots of serum can be processed using the QIAmp Viral RNA Kit. If greater sensitivity is desired due to low viral titer in the serum or if serum samples have undergone repeat freeze thaw cycles, it may be necessary to increase the volume of material processed through the QIAmp spin column. The procedure is outlined in the Protocol for

Large Volume Samples (Qiagen, 1996). Although the handbook suggests that the viral RNA isolation can be completed in approximately 20 minutes, we found that the time for completion depended greatly upon sample size. Thus, times for processing ten samples averaged about one hour.

IV. Generation of Amplicons for Genotyping.

RT was accomplished initially on 13 purified viral RNA samples. Samples were forwarded to the Institute of Molecular Biology and Medicine for evaluation of the primer set selected for genotyping. In some instances, it appeared that RT of purified RNA was unsuccessful. Therefore, the protocol for Synthesis of First-Strand cDNA using RT was changed as follows:

(1) Independent of the concentration of purified RNA, a 10 microliter aliquot of RNA suspension was used (RNA quantities ranged from 250-1000 ng).
(2) A master mix of buffer, Rnase Block Ribonuclease Inhibitor, dNTPs, and MMLV-RT was prepared and added in aliquots to the reactions following the 10 minute cooling period that allowed the primers to anneal to the RNA.

V. Selection of Specific Primers for Genotyping.

If the sequence data provides significant genotypic differentiation, research will be conducted into the ability to determine genotype by analysis of the amplicon melting curve during PCR (Ririe et al., 1997). This would extend greatly the speed at which genotype can be determined and practicality in a clinical reference laboratory setting.

CONCLUSION

Integration of currently available clinical test kits and standard research procedures can greatly enhance the information obtained relative to HCV infection of individuals and their clinical prognosis. The Roche HCV RNA procedure directs that a specimen diluent consisting of a bicine buffered solution containing manganese, potassium, and 0.05% sodium azide be used to resuspend the RNA pellet. The Stratagene RT procedure requires the use of RNA previously suspended in DEPC water. If the Roche test procedure diluent is compatible with the Stratagene RT procedure, or if the Roche RNA pellet could be resuspended in DEPC treated water, then the reisolation of viral RNA step could be eliminated, adding to the efficiency of the procedure. Technical Services representatives of both kit manufacturers were unable to address this issue. Parallel tests should be run to determine compatibility of the diluents with either kit for research purposes. Modification of the protocol as described resulted in generation of adequate cDNA for storage and/or transport to offsite locations for additional research procedures such as gene sequencing. The amplicons produced will be used in future sequence studies at the University of Scranton Institute of Molecular Biology and Medicine in collaboration with the Armstrong Laboratory and the University of Texas School of Public Health. If the sequence data provides significant genotypic differentiation, research will be conducted into the ability to determine genotype by analysis of the amplicon melting curve during PCR(Ririe et al., 1997). This would extend greatly the speed at which specific genotypes can be determined.

The availability of archived HCV positive sera from a broad spectrum of military personnel worldwide provides an opportunity to investigate the association between HCV genotype and risk of infection - an issue of significant military importance. The potential for widespread HCV infection in U.S. military populations parallels the issues raised when HIV was first identified (Herbold, 1986). HCV infection can be transmitted parenterally (blood

transfusion), may be transmitted sexually, can result in chronic impairment, and can result in a infectious carrier state.

Elucidation of infection patterns in U.S. military populations worldwide will depend on the identification of the predominant variants at the gene sequence level (Smith et al., 1997). This information coupled with analysis of occupational, demographic, and behavioral risk factors will enable military planners to implement effective prevention and intervention programs concomitant with the level of risk encountered (McDade & Anderson, 1996). Additionally, this information will provide valuable insight as to whether a total force HCV screening program should be implemented for this emerging infectious disease risk.

Table 1

Sample	Conc. (ng/ul)	ug used
c1	58.0	1.7241
c2	69.0	1.4493
c3	41.5	2.4096
cr4	57.0	1.7544
c5	63.0	1.5873
c6	58.4	1.7123
c7	34.6	2.8902
c8	55.0	1.8182
c9	57.2	1.7483
c10	60.6	1.6502
c11	98.6	1.0142
c12	29.1	3.4364
c13	93.6	1.0684
c14	67.0	1.4925
c15	78.5	1.2739
c16	53.5	1.8692
c17	25.5	3.9216
c18	26.8	3.7313
c19	53.7	1.8622
c20	75.6	1.3228
c21	88.0	1.1364
c22	20.9	4.7847
c23	75.3	1.328
c24	76.1	1.3141
c25	11.6	8.6207
c26	63.3	1.5798
c27	48.9	2.045
c28	79.7	1.2547
c29	86.3	1.1587
c30	11.3	8.8496
c31	82.7	1.2092
c32	32.8	3.0488
c33	46.4	2.1552
c34	0	0.000000
c35	76.1	1.3141
c36	39.7	2.5189
c37	72.9	1.3717
c38	13.2	7.5758
c39	29.1	3.4364
c40	11.4	8.7719
c41	11.4	8.7719
c42	56.4	1.773
c43	21.1	4.7393
c44	61.1	1.6367
c45	60.7	1.6474
c46	7.5	13.333
c47	28.6	3.4965
c48	6	16.667
c49	29.3	3.413
c50	27.1	3.69

Table 2

Name	Region	5' base	Polarity	5'-3' Sequence	Reference
242	NS-5	8304	-	GGCGGAATTCCTGGTCATAGCCTCCGTGAA	Chan et al, 1992
555	NS-5	8227	-	CCACGACTAGATCATCTCCG	Chan et al, 1992
243	NS-5	7904	+	TGGGGATCCCGTATGATACCCGCTGCTTTGA	Chan et al, 1992
554	NS-5	7935	+	CTCAACCGTCACTGAACAGGACAT	Chan et al, 1992
475	5'-NCR	319	+	GGAGGTCTCGTAGACCGTGC*	Okamoto et al. 1996
186	5'-NCR	751	-	ATGTACCCCATGAGGTCGGC*	Okamoto et al. 1996
O-1	NS-5	8275	+	CAGAACGACATCCGTGTT*	Oligo v 5.0 for Mac
O-2	NS-5	8769	-	GGAGTTGACTGGAGTGTGTC*	Oligo v 5.0 for Mac
				* Chosen for PCR	

REFERENCES

Abbott Laboratories. (1993). Abbott HCV EIA 2.0.

Bukh, J., Purcell, R., & Miller, R. (1992a). Importance of primer selection for the detection of hepatitis C virus RNA with the polymerase chain reaction assay. Proc Natl Acad Sci, 89:187-191.

Bukh, J., Purcell, R., & Miller, R. (1992b). Sequence analysis of the 5' noncoding region of hepatitis C virus. Biochemistry, 89:4942-4946.

Cha, T., Kolberg, J., & Irvine, B.e. (1991). Use of a Signature Nucleotide Sequence of Hepatitis C Virus for Detection of Viral RNA in Human Serum and Plasma. J Clin Micro, 29:(11). 2528-2534.

Chan, S.W., McOmish, F., & Holmes, E.C.e. (1992). Analysis of a new hepatitis C virus type and its phylogenetic relationship to existing variants. J Gen Virol, 73:1131-1141.

Chaudhray, R., Andonov, A., & MacLean C. (1993). Detection of Hepatitis C Virus Infection With Recombinant Immunoblot Assay, Synthetic Immunoblot Assay, and Polymerase Chain Reaction. J Clinical Laboratory Analysis, 7:164-167.

Chiron Corporation. (1995). Chiron RIBA HCV 2.0 SIA. 10/95 ed.

Choo, Q.L., Weiner, A.J., Overby, L.R., & et al. (1990). Hepatitis C virus: The major causative agent of viral non-A, non-B hepatitis. British Medical Bulletin, 46:(2). 423-441.

Choo, Q., Richman, K.H., Han, J., & et al. (1991). Genetic organization and diversity of the hepatitis C virus. Proc Natl Acad Sci, 88:2451-2455.

Enomoto, N., Takada, A., Nakao, T., & Date, T. (1990). There are two major types of the hepatitis c virus in Japan. Biochemical and Biophysical Research Communications, 170:1021-1025.

Hagiwara, H., Hayashi, N., Kasahara, A., & et al. (1996). Treatment with Recombinant Interferon-alpha2a for Patients with Chronic Hepatitis C: Predictive factors for Biochemical and Virologic Response. Scand J Gastroenterol, 31:1021-1026.

Herbold Jr. (1986). AIDS Policy Development Within the Department of Defense. Military Medicine, 151:(12). 623-627.

Houghton, M. (1996). Hepatitis C Viruses. In B.N. Fields, D.M. Knipe, P.M. Howley, & et al. (Eds.), Fields Virology. (pp. 1035-1051). Philadelphia: Lippincott-Raven.

Matar, G., Sharrara, H., Abdelnour, G., & Abdelnoor, A. (1996). Genotyping of Hepatitis C Virus Isolates from Lebanese Hemodialysis Patients by reverse Transcription-PCR and Restriction Fragment Length Polymorphism Analysis of 5' Noncoding Region. J Clin Micro, 34:(10). 2623-2624.

McDade, J.E., & Anderson, B.E. (1996). Molecular Epidemiology: Applications of Nucleic Acid Amplification and Sequence Analysis. Epidemiologic reviews, 18:(1). 90-97.

McOmish, F., Yap, P., Dow, B., & et al. (1994). Geographical Distribution of Hepatitis C Virus genotypes in Blood Donors: and International Collaborative Survey. J Clin Micro, 32:(4). 884-892.

Murashima, S., Sata, M., Suzuki, H., & et al. (1996). Sequence Variation of the Hypervariable Region in HCV Carriers with Normal ALT Levels: A Comparison with Symptomatic Carriers. Microbiol Immunol, 40:(12). 941-947.

Murphy, D., B.Willens. (1994). Use of the Non-Coding Region for the Genotyping of Hepatitis C Virus. J Infect Dis, 169, 473-474.

Nagasaka, A., Hige, S., Tsunematsu, I, & et al. (1996). Changes in Hepatitis C Virus Quasispecies and density Populations in Patients Before and After Interferon Therapy. J Medical Virology, 50:214-220.

O'Brien, C., Henzel, B., Wolfe, L., & et al. (1997). cDNA Sequencing of the 5' Noncoding Region (5' NCR) to Determine Hepatitis C Genotypes in Patients with Chronic Hepatitis C. Digestive Diseases and Sciences, 42:(5). 1087-1093.

Ohno, T., & et al. (1997). New Hepatitis C Virus (HCV) Genotyping System That Allows for Identification of HCV Genotypes 1a, 1b, 2a, 2b, 3a, 3b, 4, 5a, and 6a. J Clin Micro, 34:(1). 201-207.

Okamoto, H., & Kurai, K.e. (1992). Full-Length Sequennce of a Hepatitis C Virus Genome having poor homology to reported isolates: comparative dtudy of four distant genotypes. Virology, 1, 331-341.
Pernas, M., Bartolome, J., Castillo, I., & et al. (1995). Sequence of non-structural regions 3 and 5 of heptitis C virus genomes from Spanish patients: existence of a predominant variant related to type 1b. J Gen Virol, 76:415-420.

Persing, D.H., & Relman, D.A. (1996). Genotypic Detection of Antimicrobial Resistance. In D.H. Persing (Ed.), PCR Protocols for Emerging Infectious Diseases. (pp. 46-70). Washington, D.C. ASM Press.

Qiagen Inc. (1996). QIAmp Viral RNA Handbook, 6/96.

Ririe, K.M., Rasmussen, R.P., & Wittiwer, C.T. (1997). Product Differientation by Analysis of DNA Melting Curves during the Polymerase Chain Reaction. Analytical Biochemistry, 245:154-160.

Roche. (1993). Amplicor PCR Diagostics Hepatitis C Virus (HCV) Test. Instruction packet for test kit.

Rychlik, W. (1996). Oligo Primer Analysis Software v 5.0 for Mac. NBI/Genovus.

Shindo, M., Di Bisceglie, A.M., Cheung, C., & et al. (1991). Decrease in Serum Hepatitis C Viral RNA during Alpha-Interferon Therapy for Chronic Hepatitis C. Annals of Internal Medicine, 115:700-704.

Simmonds, P., Alberti, A., Alter, H.J., & et al. Editor & Hepatology 19:1321-1324. (1994). A Proposed System for the Nomenclature of Hepatitis C Viral Genotypes.

Simmonds, P., Holmes, E.C., Cha, T.A., & et al. (1993). Classification of hepatitis C virus into six major genotypes and a series of subtypes by phylogenetic analysis of the NS-5 region. J Gen Virol, 74:2391-2399.

Simmonds, P., McOmish, F., Yap, P.L., & et al. (1993). Sequence variability in the 5' non-coding region of hepatitis C virus: identification of a new virus type and restrictions on sequence diversity. J Gen Virol, 74:661-668.

Simmonds, P., Smith, D.B., McOmish, F., & et al. (1994). Identification of genotypes of hepatitis C virus by sequence comparisons in the core, E1 and NS-5 regions. J Gen Virol, 75:1053-1061.
Smith, D.B., Pathirana, S., Davidson, F., & et al. (1997). The origin of hepatitis C genotypes. J Gen Virol, 78:321-328.

Stratagene Inc. (1997). Stratagene RT-PCR Kit Instruction Manual. 17005th ed.

Versalovic, J., Swanson, D.S., & Musser, J.M. (1996). Nucleic Acid Sequencing Studies of Microbial Pathogens: Insights into Epidemiology, Virulence, Drug Resistance, and Diversity. In D.H. Persing (Ed.), PCR Protocols for Emerging Infectious Diseases. (pp. 71-86). Washington, D.C: ASM Press.

Weiner, A.J., Kuo, G., Bradley, D.W., & et al. (1990). Detection of hepatitis C viral sequences in non-a, non-b hepatitis. Lancet,335:1-3.

Young, K.K.Y., Resnick, R.M., & Myers, T.W. (1993). Detection of Hepatitis C Virus RNA by a Combined Reverse Transcription-Polymerase Chain Reaction Assay. J Clin Micro, 31:(4). 882-886.

Yuki, N., Hayashi, N., Moribe, T., & et al. (1997). Relation of Disease Activity During Chronic Hepatitis C Infection to Complexity of Hypervariable Region 1 Quasispecies. Hepatology, 25:(2). 439-444.

DEVELOPMENT OF A CONCEPTUAL DESIGN FOR AN INFORMATION SYSTEMS INFRASTRUCTURE TO SUPPORT THE *SQUDRON XXI* INIATIVE FOR THE UNITED STATES AIR FORCE

Andrew E. Jackson, Ph.D.
Assistant Professor
Department of Aeronautical Management Technology

Arizona State University East
School of Technology
6001 South Power Road-SIM Building 425
Mesa, Arizona 85206

Final Report for:
Summer Research Program
Armstrong Laboratory

Sponsored by:
Air Force Office of Scientific Research
Bolling Air Force Base, Washington, DC

And

Armstrong Laboratory

September 1997

DEVELOPMENT OF A CONCEPTUAL DESIGN FOR AN INFORMATION SYSTEMS INFRASTRUCTURE TO SUPPORT THE *SQUADRON XXI* INIATIVE FOR THE UNITED STATES AIR FORCE

Andrew E. Jackson, Ph.D.
Assistant Professor
Department of Aeronautical Management Technology
Arizona State University East

Abstract

Information processing and data delivery are crucial elements in the success of any modern organization. Squadron XXI is an initiative which is currently underway at Luke Air Force Base, Arizona, under the guidance and direction of the Air Force Research Laboratory at Williams Gateway Airport in Mesa, Arizona. The goal behind Squadron XXI is to develop and test a prototype information systems to permit all authorized users in their respective training and operational squadrons to access real-time information in support of their individual missions. The Squadron XXI information system requirements are being designed to satisfy current and future operational and training objectives for pilot training in the United States Air Force. Typical information requirements will cover scheduling and delivery of classroom instruction, simulator training, pre-flight, in-flight, and post-flight instruction, maintenance scheduling, weather data analyses, personnel qualifications, personal flight readiness certifications, and operational considerations under well defined, yet complex constraint sets. This study describes a conceptual information systems infrastructure for use at Luke Air Force Base and identifies the need for further detailed analyses to support current and future organizational and operational requirements for Air Force Pilot Training.

DEVELOPMENT OF A CONCEPTUAL DESIGN FOR AN INFORMATION SYSTEMS INFRASTRUCTURE TO SUPPORT THE *SQUADRON XXI* INIATIVE FOR THE UNITED STATES AIR FORCE

Andrew E. Jackson, Ph.D.

Introduction

The United States Air Force has embarked on an ambitious objective, to integrate a variety of disparate information sources, using existing and planned computer resources. This integrated information systems approach will be designed to provide decision-makers at all levels of the organization with the essential information they need to perform their daily missions. To address this challenging objective, Luke Air Force Base (AFB) has been selected as the site for a prototype information system development program known as Squadron XXI. The Air Force Research Laboratory (AFRL) at Williams Gateway Airport in Mesa, Arizona is developing the Squadron XXI concept. They have begun acquiring the necessary infrastructure and are identifying the necessary engineering experts who will work together to achieve the stated objectives. Squadron XXI, in its simplest terms, is an Information System (IS) which will collate, integrate, and make available a wide variety of information and data sources using an object-oriented relational database structure. The resulting information infrastructure will enable each authorized individual to access relevant, real-time information from the data warehouse to meet their individual and collective needs.

Pilot training is the primary mission at Luke and it remains the ultimate reason for the existence of most squadrons and supporting systems assigned to that location. There are some operational U.S. Air Force squadrons at Luke, however, these squadrons also support the

training function in a variety of ways. For example, the 310th Fighter Squadron at Luke is an operational squadron, which provides advanced tactical training and Night Vision Goggle training for a variety of United States and foreign military pilots. The information and data needs of the various users at Luke AFB who support the pilot training mission are similar in many respects even though their individual function may be somewhat unique at that location. This commonality drives the need to incorporate common database elements into the Squadron XXI Information System. Unique data elements must also be defined and integrated into the information support infrastructure if even a single user requires the information to perform his/her mission. Although Squadron XXI is still in the early definitional stage, several well known elements have been established which will help guide future development and integration of supporting information management systems elements. All training, scheduling and instructional support functions must be clearly established and integrated into the overall information infrastructure.

Discussion

The planning and identification of essential data processing component within the Squadron XXI Information System must be driven by the individual instructors, students, senior officers, managers, operators, technicians, and support personnel assigned to the pilot training mission. The composition and scope of these data elements are expected to be similar to data elements required at other pilot training schools, including U.S. Navy, U.S. Army, and a various civilian pilot training organizations. It is anticipated that the commonality of data elements defined for the Squadron XXI application will provide 80% or more of the data required at other

pilot training locations. This common database paradigm will therefore provide a technology transfer opportunity from the very beginning of this program.

Figure 1 (O'Brien, 1990) shows the essential role that users (*People*) serve in developing an information system. The people who are directly involved in the daily operations of the organization are best suited to identifying required information processing requirements. They may also be able to assist in defining the interface and display requirements, as candidate Squadron XXI solutions are developed and tested. Customer involvement throughout the data collection, system identification, and database development processes is essential in order for the resulting system to become and remain responsive to their needs. In this regard, a preliminary survey has been developed (see Appendix 1) to solicit essential systems data from the Subject Matter Experts (SMEs) at Luke, in preparation for the Squadron XXI system front-end needs analysis.

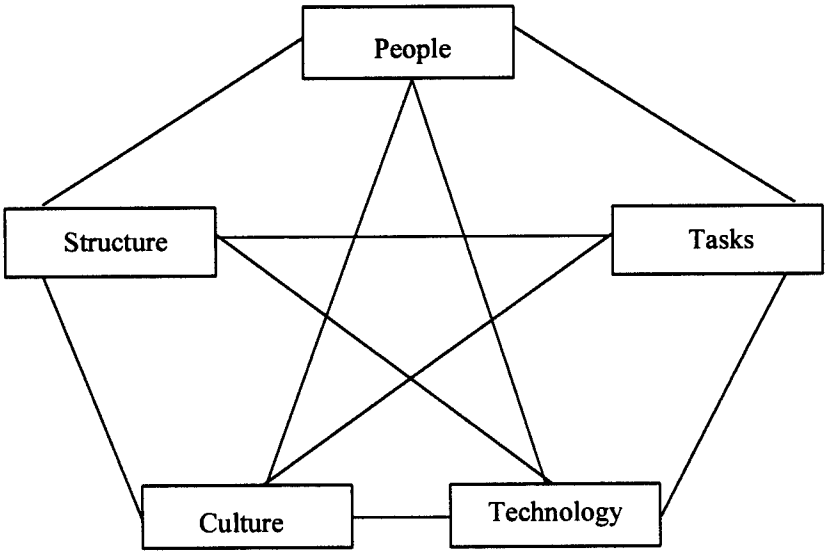

(O'Brien, 1990)

Figure 1. Five Critical Components of the Information System Development Process

Sage (1991) emphasizes the need for a structured developmental process throughout the systems life cycle (see Figure 2).

> "Human behavioral and cognitive concerns must be considered throughout all phases of system design. Systems management and integration issues are additionally of major importance in determining both the effectiveness and efficiency, and the overall functionality of system designs. To achieve a high measure of functionality, it must be possible for a system design to be produced, used, maintained, retrofitted, and retired throughout all phases of a life cycle: from need conceptualization and identification, through specification of system requirements and architectural structures, to ultimate system installation and evaluation, an ultimate operational implementation. This is a simple view of the phases of the system engineering life cycle . . . "

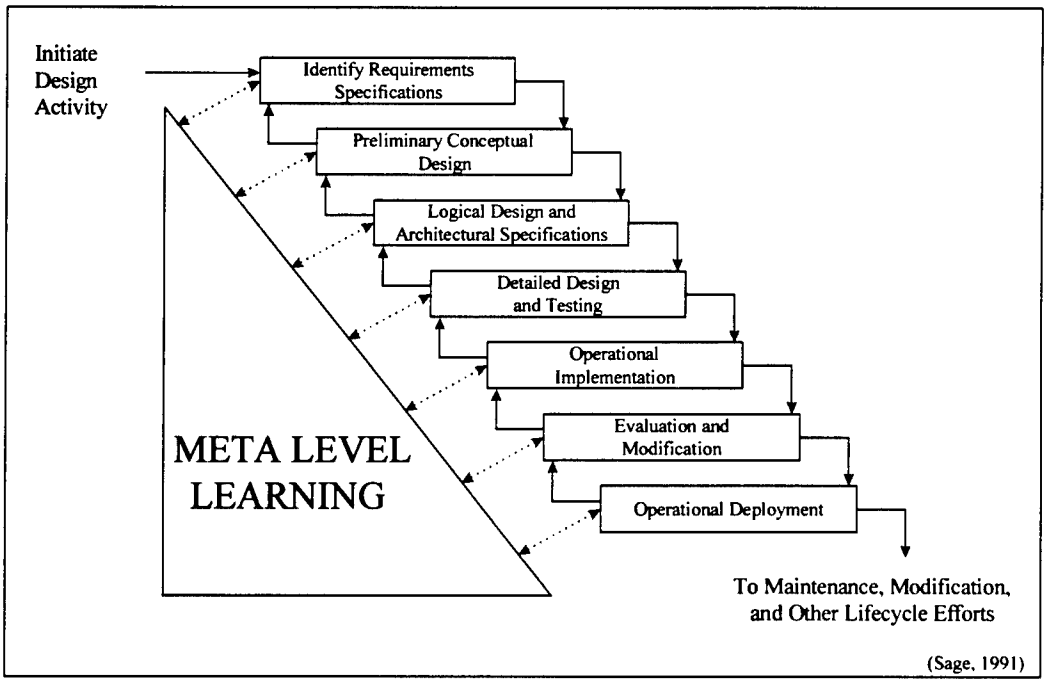

Figure 2. The decision support system design process life cycle.

The systems development life cycle should include a dedicated front-end analysis of requirements before any significant effort is expended on specific systems procurement activities and hardware integration. This front-end analysis is essential for user acceptance of the final product and for meeting the user's needs throughout the systems life cycle.

Methodology

In order to achieve the primary goals of Squadron XXI, a dedicated effort must be made to identify the various user groups and their information requirements before significant investment is made into hardware and software solutions. The need to consider existing information systems cannot be overlooked, since a significant investment has already been made in computers and systems support elements, including software, networks, and facilities. The need to integrate as much of the existing infrastructure as possible into any Squadron XXI design is a principal consideration. It is anticipated that some legacy systems may need to be integrated directly into the new information system infrastructure. During the process of evaluating alternative designs, a cost-benefit analysis will need to be performed if the cost to integrate any single component into Squadron XXI becomes too expensive. Only then can a recommendation be made to the decision-makers on which design approach is preferred.

During the front-end analysis phase and throughout the development process, the information systems analyst must attempt to define the *worst case* data processing requirements for the proposed system. Near-term data processing requirements must also include the foreseeable future to include a system design which can easily accommodate new data

processing requirements without significant reinvestment in capital equipment and the associated redevelopment costs. These design objectives are essential if newly emerging technologies and information handling methodologies are to be incorporated, as they become available. In this regard, a non-proprietary, open computer architecture and an object-oriented database design appear to be the best solution in today's information systems marketplace. A conceptual example of an open architecture is provided as Figure 3.

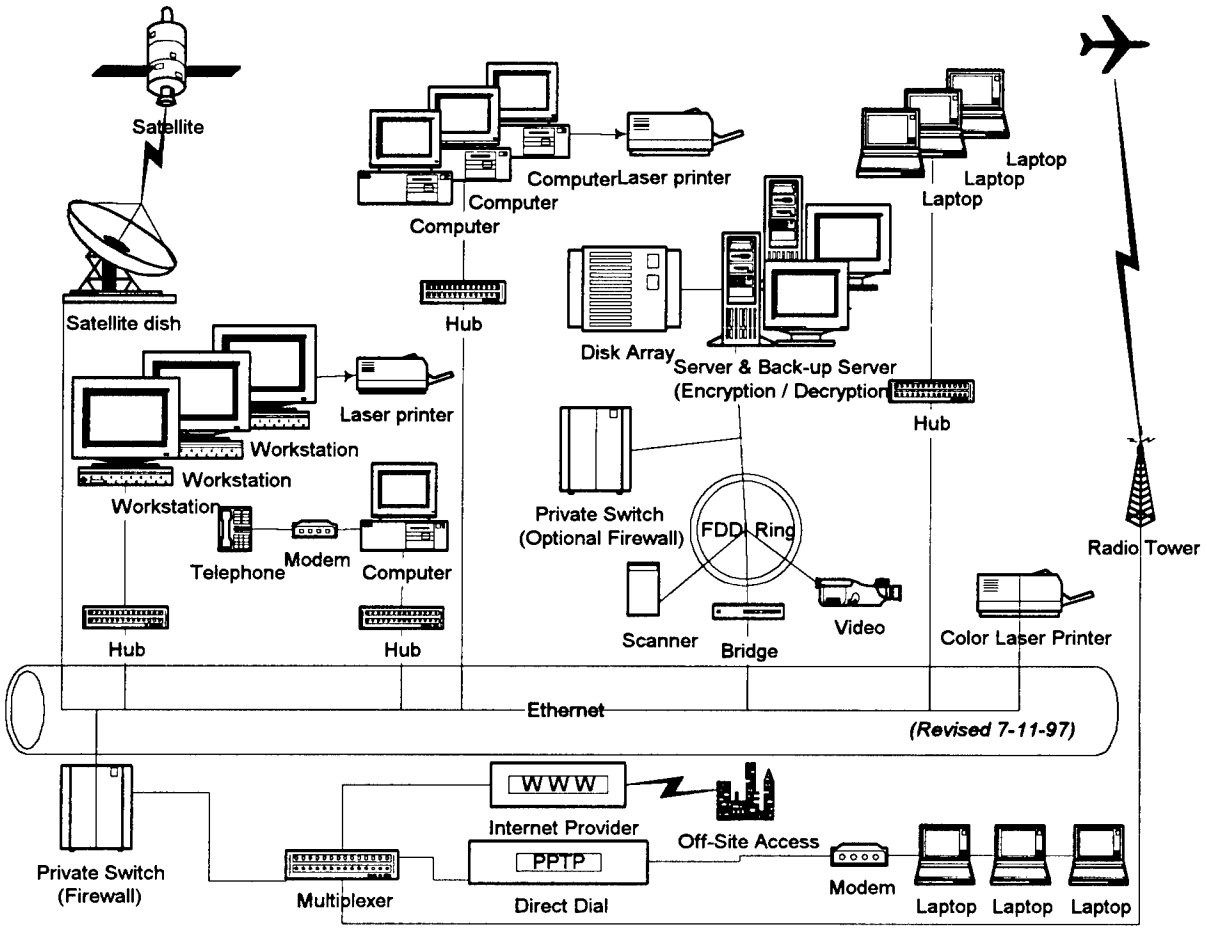

Figure 3. Conceptual Model of Squadron XXI Information System Infrastructure

In addition to the conceptual design cited above, the systems analysts must consider the sources of data, the users who have access to the data and the ways in which the available data will be used to support operational objectives. In order to accommodate these assorted (and often conflicting) design objectives, the design team must be thorough and creative in their approach to the problems. Again, the essential element is user involvement throughout the design and development process.

> "Design is the creative process through which products, processes, or systems presumed to be responsive to client needs and requirements are conceptualized or specified. There are four primary ingredients in this not uncommon definition:
>
> 1. *Design results in specifications or architecture* for a product, process or system.
> 2. *Design is a creative process.*
> 3. *Design activity is conceptual in nature.*
> 4. *A successful design must be responsive to client needs and requirements.*"
>
> (Sage, 1991)

Three different characteristics of information systems have been identified by a variety of authors, including Kroenke (1989), Sage (1991), and Schultheis, et al. (1992). Table 1 shows the three levels of information management within a specified system. It also displays the information complexity at each level of the organization, based on the individual user's organizational perspective.

Summary Classification of Information Systems

Characteristic	Operational	Tactical	Strategic Planning
Frequency	Regular, repetitive	Mostly regular	Often ad hoc
Dependability of results	Expected results	Some surprises may occur	Results often contain surprises
Time period covered	The past	Comparative	Predictive of the future
Level of Detail	Very detailed	Summaries of data	Summaries of data
Source of data	Internal	Internal and external	Mostly external
Nature of data	Highly structured data	Some unstructured data	Highly unstructured
Accuracy	Highly accurate data	Some subjective data used	Highly subjective data
Typical user	First-line supervisors	Middle managers	Top management
Level of decision	Task-oriented	Control and resource allocation-oriented	Goal-oriented

Table 1. A comparison of information systems at the operational, tactical, and strategic planning systems (Schultheis, et al., 1992).

A model similar to the one shown in Table 1 will be developed and used to classify the data element requirements for Squadron XXI. It will further be used to compose a data flow diagram enabling design engineers to meet user's information requirements in the most efficient manner possible. Weaver (1987) provides a case study approach to database design which should prove useful in establishing information processing requirements for Squadron XXI. In order to develop a well structured, efficient model for the Squadron XXI application, the

engineering team will also utilize six principles of good software design as follows: " . . . top-down partitioning, loose coupling, functional grouping for cohesion, limited span of control, managed module size, and shared modules. Following these principles increases the likelihood of achieving acceptable levels of reliability and maintainability." (Senn, 1989). Additionally, Squadron XXI information systems design modeling will benefit from a direct, yet simple approach to data analyses, data element design and information flow analyses. Software design engineers have discovered: "Great ideas are simple ideas. So is great engineering. These principles account for success stories time and time again, and they apply to virtually any field, including information systems. Simplicity also goes hand in hand with quality. Quality is associated with good design and this is in turn associated with simplicity. If a product or process is complex, it will tend to result in errors." (Senn, 1989)

The analysis team will survey the end users involved in the organization and compile a common list of data elements forming the core of the information system database. As new data elements are discovered, they will be added and integrated into the overall information model. In order to achieve this objective, the analysts must solicit information from the participating user groups according to the following guidelines.

> "What is the problem? (Define) Details of (the) Problem. How significant is the problem? What does user feel is the solution? How information systems will help. Who else knows about this and could be contacted?" (Senn, 1989).

By using a methodology like the one cited above, the analysts will be able to identify potential problems within the organization which may hamper the design and/or integration of the most

efficient IS solution. Previous efforts by Ramesh (1993) and Nullmeyer & Bruce (1991) will augment the Squadron XXI design effort. These references focus on the development of Training Management Systems (TMS) design and development issues. The TMS function at Luke Air Force Base is being filled both manually through scheduling boards, and electronically through a new scheduling management system entitled Tactical Aircrew Scheduling and Airspace Management System (TASAMS). The information contained in TASMS must be fully integrated into the Squadron XXI Information System, as well as supporting information sources, such as:

- Status of the student's academic progress
- Aircraft configuration and availability
- Weather information (brief / debrief)
- Operational support information

When the information domain is well defined and falls within the boundaries of a single department or a single building, the issues of information distribution, management, and control can easily be addressed, and satisfactory solutions readily identified. In the case of the Squadron XXI concept, the users cut across multiple organizational boundaries and may span several facilities within a geographic area. This added complexity will hamper the data collection and analysis efforts, but it is not expected that this added complexity by itself will be an insurmountable obstacle in defining user requirements. A more significant obstacle is expected to be the realm of control over computers, networks, and information database assets in multiple, large organizations similar to those found at Luke Air Force Base. One way to help overcome

this problem is to invite participants from all affected organizations to participate in the requirements definition process. This will enable the participants to identify their unique requirements and understand the common problem faced by other users in the environment. This shared tasking will simplify the integration of shared resources and allow team members to work toward a common set of design objectives.

Results

Initial results are pending receipt of surveys from SMEs at Luke AFB, however, initial indications are that a basic computer network infrastructure exists at Luke to enable prototype Squadron XXI development. This information system backbone includes an ethernet-based network, which links multiple buildings and rooms within the 56th Fighter Training Squadron at Luke AFB. There are currently 70 computers on the network consisting of mixed computer architectures from 486-66 MHz desktop and laptop computers to Pentium 200 MHz desktop instructor stations to Pentium 200 student laptop computers. Other network systems are known to exist at Luke but the scope, location, and composition of these additional computer networks are undefined at this time. The Air Force Research Laboratory is currently developing an information system testbed at Luke AFB using a Pentium-based server and 10 laptop computers. This testbed will be used to conduct research on information processing needs for the pilot training community at Luke. Additionally, it will be used as a developmental site for the contractor support team headed by Hughes Training Incorporated. The development team also includes participants from Boeing and Lockheed Martin under a teaming agreement with Hughes Training Incorporated. Arizona State University East is supporting the AFRL in the Squadron

XXI activity through graduate assistantships, faculty consultants, and task-specific contracts to meet the needs of the U. S. Air Force pilot training community.

Conclusion

Squadron XXI is an evolving concept centered on information management and data processing demands to support U. S. Air Force pilot training requirements. Since the Squadron XXI initiative is still in the early stages of development, an exact description of the final product is impossible to provide at this time. However, some design and development principles have been established. These include providing:

- Real-time access to relevant information for participants at all levels of the organization.
- On-site and off-site access to information to enhance mission planning and preparation.
- Timely updates for all decision makers to support scheduling, execution, and evaluation of all pilot training evolutions.
- Accurate and timely reporting capabilities as an integral part of the database design.

By combining structured design methodologies with the participation of current system users, the Squadron XXI team can be expected to define an appropriate solution to next-generation information processing requirements. The challenge faced by Squadron XXI is to develop a systems architecture that is responsive to the evolving needs of U. S. Air Force fighter pilots and all decision-makers throughout their respective organizations.

Appendix 1

System Name: _____

System Function: _____
(Workstation, Terminal, Server, Stand-Alone Computer, etc.)

Equipment Description:

Vendor _____

Processor _____

Memory _____

Hard Drive _____

Backup _____

I/O Devices _____

Peripheral Devices _____

Number of Like Units Installed _____

Compatible with Open Architecture Additions? Yes / No

Network Capable at This Time? Yes / No

Network Type: _____
(Ring, Bus, Star, Ethernet, FDDI, Other)

Vendor: _____

Number of Nodes? _____

Proprietary Design? Yes / No Open Architecture? Yes / No

Source Code Available? Yes / No Documentation Available? Yes / No

Type Documentation Available? _____
(Operator Handbooks, Technical Manuals, Design Documents, Software Code, etc.)

H/W Documentation? _____

S/W Documentation? _____

Network Documentation? _____

System Name: _____

Quality of Documentation Excellent Good Average Poor Very Poor

H/W Documentation? _____

S/W Documentation? _____

Network Documentation? _____

Data Requirements (Circle One):

Electronic Only **Electronic / Paper** **Paper Only**

What Defines Data Requirements? _____

System Fully Meets Customer Needs? Yes / No

Deficiencies? _____

_____

_____

_____

Point of Contact:

Name: _____

Address: _____

_____

Phone Number: _____

E-Mail Address: _____

Subject Matter Expert:

Name: _____

Address: _____

_____

Phone Number: _____

E-Mail Address: _____

System Operation Observed _____

(date)

by _____

References

Kerzner, H. (1995), Project management: A systems approach to planning, scheduling and controlling, New York: Van Nostrand Reinhold.

Kozar, K. (1989), Humanized information systems analysis and design: People building systems for people, New York: McGraw-Hill.

Kroenke, D. (1992), Management information systems, second edition, New York: McGraw-Hill.

Nullmeyer, R., and Bruce, P. (1991), Integrated aircrew training management information systems: An Organizational Perspective, Proceeding of the 13th Interservice/Industry Training System Conference, Orlando, FL.

O'Brien, J. (1994), Introduction to information systems, seventh edition, Burr Ridge, Illinois: Richard D. Irwin, Inc.

O'Brien, J. (1990), Management information systems: A managerial end user perspective, Homewood, Illinois: Richard D. Irwin, Inc.

Ramesh, R., (September 1993), Aircrew training management systems: A blueprint for design and development, final report for Summer Faculty Research Program, Armstrong Laboratory, Williams Air Force Base, Arizona.

Sage, A. (1991), Decision support systems engineering, John Wiley & Sons, Inc.: New York.

Schultheis, R., Sumner, M., and Bock, D. (1992), Management information systems: The manager's view - second edition, Irwin: Homewood, IL.

Senn, J. (1989), Analysis and design of information systems, second edition, McGraw-Hill: New York.

United States Air Force (USAF) Basic Operational Training Course F-16C/D, (May 1997), HQ AETD Syllabus F16C0B00PL, Headquarters Air Education and Training Command, Randolph Air Force Base, San Antonio, Texas.

Weaver, A. (1987), Using the structured techniques: A case study, Prentice Hall: Englewood Cliffs, NJ.

REPLICATION AND EXTENSION OF THE SCHMIDT, HUNTER, AND OUTERBRIDGE (1986) MODEL OF JOB PRFORMANCE RATINGS

Charles E. Lance
Associate Professor
Department of Psychology

The University of Georgia
Athens, GA 30602-3013

Final Report for:
Summer Research Program
Armstrong Laboratory

Sponsored by:
Air Force Office of Scientific Research
Bolling Air Force Base, Washington, DC

And

Armstrong Laboratory

September 1997

REPLICATION AND EXTENSION OF THE SCHMIDT, HUNTER, AND OUTERBRIDGE (1986) MODEL OF JOB PERFORMANCE RATINGS

Charles E. Lance
Associate professor

Department of Psychology
The University of Georgia
Athens, GA 30602-3013

Abstract

The present study tested an extension of Schmidt, Hunter, and Outerbridge's (1986) model of relationships among cognitive ability and experience, job knowledge, job proficiency and supervisor performance ratings that augmented these traditional "can-do" determinants of ratings with additional "will-do" determinants in a sample of 838 USAF first-term enlisted airmen. Results indicated a) that effects of ability and experience on job knowledge were linear, not interactive, b) that different conceptualizations of "experience" (i.e., job vs. task experience) play somewhat different roles in influencing job knowledge, job proficiency, and supervisor ratings, c) general support for the mediational roles played by job knowledge and job proficiency, and d) that supervisors' performance ratings reflect both "can-do" (i.e., technical) and "will-do" (i.e., motivational) aspects of performance. Implications and directions for future research are discussed.

REPLICATION AND EXTENSION OF THE SCHMIDT, HUNTER & OUTERBRIDGE (1986) MODEL OF JOB PERFORMANCE RATINGS

Charles E. Lance
The University of Georgia

Introduction

The field of industrial and organizational (I/O) psychology continues to grow both in terms of breadth (i.e., the number and range of topics considered as part of the field) and depth (i.e., the thoroughness with which these topics are researched)[1]. Yet despite the diversification of I/O psychology, the measurement and prediction of individual performance in organizations is a topic that is as much at the forefront of the field as it was near the turn of the 20th century (Austin & Villanova, 1992; Borman, 1991; Campbell, 1990a; Guion, 1991). Although a large number of theories have been developed concerning particular aspects of work behavior (e.g., work motivation, leadership, employee attitudes, etc., Campbell, 1990b), few general theories of work performance have been developed, especially as compared to the level of empirical efforts devoted to measuring and predicting job performance effectiveness (Campbell, Dunnette, Lawler, & Weick, 1970; Landy, Zedeck, & Cleveland, 1983; Waldman & Spangler, 1989). Recently, however, a number of studies have begun to test a series of general models of job performance and supervisory performance ratings.

Hunter (1983) developed and tested a causal model relating incumbent general cognitive ability, job knowledge, job proficiency (as measured by work sample performance), and supervisory job performance ratings. Hunter's (1983) findings from meta-analytic path analysis included: a) the effect of cognitive ability on job proficiency was largely indirect, through the mediating influence of job knowledge, b) job knowledge and job proficiency mediated effects of cognitive ability on supervisory performance ratings, and c) both job knowledge and job proficiency exerted direct effects on supervisory performance

[1] Just in the 15 years separating the publication of the first and second editions of the Handbook of industrial and organizational psychology, it grew from a "mere" 37 chapters and 1,740 pages in its first edition (Dunnette, 1976) to four volumes, 57 chapters, and 3,676 pages in its second (Dunnette & Hough, 1990, 1991, 1992; Triandis, Dunnette, & Hough, 1994).

ratings. Thus, Hunter's (1983) findings supported the idea that the major effect of cognitive ability on job proficiency was through the acquisition of job knowledge, and that supervisory rating criteria reflect job knowledge as well as actual job proficiency.

Schmidt, Hunter, and Outerbridge (1986) extended Hunter's (1983) model to include experience determinants of job knowledge, job proficiency, and supervisory performance ratings. This model (shown in Figure 1, and referred to as the "SHO Model") recognizes that job knowledge is affected positively not only by general cognitive ability, but also by the accrual of additional job experience. Like cognitive ability, the effect of job experience on job proficiency was hypothesized to be substantially mediated by job knowledge. Using portions of the same data reported by Hunter (1983), Schmidt et al. (1986) found that a) both job experience (measured as months of tenure on the present job) and cognitive ability had large direct effects on job knowledge, b) job experience and cognitive ability had direct but substantially weaker effects on job proficiency, c) job knowledge had a large direct effect on job proficiency, and d) job knowledge and job proficiency completely mediated the effects of job experience and cognitive ability on supervisory performance ratings. Schmidt et al.'s (1986) study confirmed Hunter's (1983) findings that cognitive ability's relation to job proficiency is explained substantially by the development of relevant job knowledge. Ree, Carretta, and Teachout (1995) also confirmed this finding.

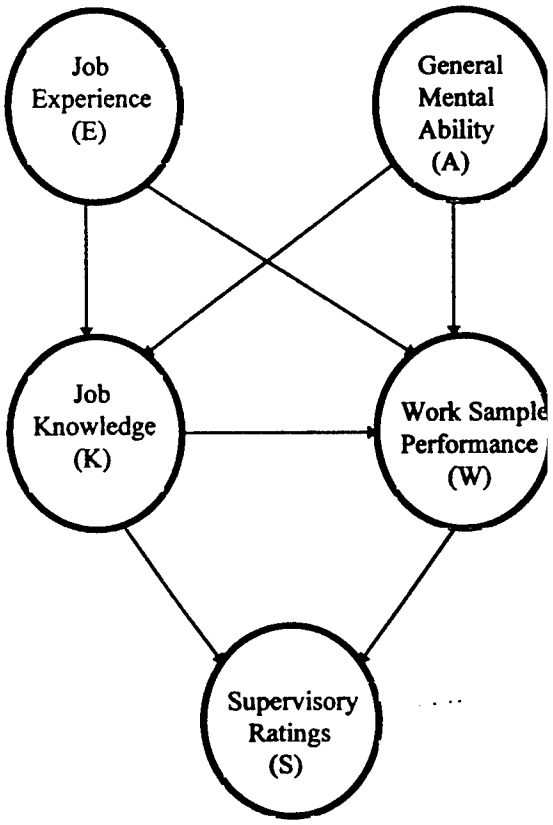

Figure 1. Schmidt, Hunter, and Outerbridge (1
model of job performance ratings.

Three other studies have extended the SHO model in various ways. For example, Pulakos, Schmitt, and Chan (1996) found that many of the basic relationships hypothesized by the SHO model were generalizable across ratee gender, ratee racial/ethnic groups, and rater level (supervisor vs. peer). In another study, Borman, White, Pulakos, and Oppler (1991) attempted to replicate Hunter's (1983) original findings. However unlike Hunter (1983), who found that job knowledge had a direct effect on supervisory

ratings as well as an indirect effect (mediated by job proficiency), Borman et al. (1991) supported a complete mediation model – the effect of job knowledge on supervisory ratings was completely mediated by job proficiency (Borman, White, & Dorsey [1995] also found support for this complete mediation model). Borman et al. (1991) also augmented Hunter's (1983) original model (a model which Borman et al. (1991) referred to as a model of "can-do" or maximal performance), with additional determinants of supervisory ratings that reflect "will-do," aspects of performance. "Will-do" determinants of supervisory ratings included measures of military awards and disciplinary actions as determined by the personality dimensions achievement orientation and dependability, respectively. As expected, supervisory ratings reflected the influences of both technical ("can-do") and motivational ("will-do") aspects of performance. Borman et al. (1995) replicated these findings and showed that they generalized to peer ratings as well.

Several conclusions are suggested by these studies. First, they suggest that both cognitive ability and job experience are important determinants of job knowledge. Second, they suggest that the effects of cognitive ability and experience on job proficiency are largely indirect, being mediated by job knowledge. These findings help establish a theoretical linkage (i.e., the development of job knowledge) between empirical relationships established in previous meta-analyses linking each of these separate predictor domains to job performance (e.g., Hunter & Hunter, 1984; Quiñones, Ford, & Teachout, 1995). That is, development of relevant job knowledge helps explain why cognitive ability and experience are related to performance. Third, studies to date indicate that most modeled relationships are generalizable across gender and racial/ethnic groups. Neither gender nor racial/ethnic status appears to play the role of a moderator of the boundary conditions of the basic relationships described by these models. Finally, Borman et al. (1991, 1995) helped further establish the importance of distinguishing between "can-do" and "will-do" aspects of performance, or what have also been referred to as technical and interpersonal proficiency (Kavanagh, Borman, Hedge, & Gould, 1987) or contextual performance (Borman & Motowidlo, 1993; Motowidlo & VanScotter, 1994).

However, several questions remain unanswered. The first concerns the form of the effects of cognitive ability and experience on job knowledge (and perhaps technical proficiency). Schmidt et al. (1986) examined only linear and additive effects. There is other evidence that suggests the effects of

experience and cognitive ability on performance are linear and additive (Schmidt, Hunter, Outerbridge, & Goff, 1988), but there also is evidence for an interactive relationship such that the relationship between cognitive ability and performance is stronger at lower levels of experience than at higher experience levels (Lance, Hedge, & Alley, 1989). This "convergence" relationship (Schmidt et al., 1988) suggests that higher ability incumbents would learn their job more quickly, but that with additional accrued experience, lower ability incumbents eventually "catch up." The first purpose of the present study was to test linear and additive versus interactive cognitive ability x experience effects on job knowledge.

The second question concerns the conceptualization of "experience" in previous studies. Schmidt et al. (1986, 1988) operationalized experience only in terms of "months-in-present-job." Quiñones et al. (1995) refer to this as a job-level time-related measure of experience. Time-in-job experience measures can be contrasted with, for example, task-level amount-related measures of the number of times tasks had been performed previously. Quiñones et al.'s (1995) meta-analysis showed that different types of experience measures bore different relationships with performance criteria: task-level and amount-related measures bore stronger relationships with criteria than alternative operationalizations of experience. The second purpose of the present study was to investigate alternative measures of experience (job-level time-related vs. task-level amount-related measures) as determinants of job knowledge and job proficiency.

The third question concerns the mediational nature of the models tested to date, and particularly the job knowledge → job proficiency → supervisory rating relationship. Earlier, Hunter (1983), Schmidt et al. (1986), and Pulakos et al. (1996) found support for a partial mediational model: job knowledge partially mediated the effect of aptitude on job proficiency, and job knowledge exerted a direct effect, as well as an indirect effect (mediated by job proficiency), on supervisory ratings. On the other hand, Borman et al. (1991, 1995) supported a complete mediational model: job knowledge completely mediated the effect of aptitude on job proficiency, and the effect of job knowledge on supervisory ratings was completely mediated by job proficiency. The third purpose of the present study was to further test these mediational roles of job knowledge and job proficiency.

Finally, recent studies (Borman et al., 1991, 1995; Pulakos et al., 1996) have modeled factors relating to motivational, as well as technical, aspects of performance as determinants of supervisory

performance ratings. These studies have supported the idea that supervisory ratings reflect both "can-do" and "will-do" aspects of performance. The final purpose of the present study was to extend these findings in comparison of the relative effects of "can-do" versus "will-do" aspects of performance on supervisory performance ratings in an independent sample.

Method

Sample

Data reported here were collected as part of the Joint Service Job Performance Measurement (JPM)/Enlistment Standards Project conducted in the 1980s and early 1990s by the U.S. Air Force (USAF) (Hedge & Teachout, 1986; Kavanagh et al., 1987; Wigdor & Green, 1991). Research participants included 1,536 first-term airmen in eight different Air Force Specialties (AFSs), that were selected to be representative of a) the four different USAF enlistment aptitude requirement areas (i.e., Mechanical, Administrative, General, and Electronics), b) various levels of occupational learning difficulty (Mumford, Weeks, Harding, & Fleishman, 1987; Weeks, 1984), and c) the number of first-term airmen populating various AFSs (i.e., the relatively more populous AFSs) in the then-current USAF enlisted occupational structure. Data reported in this study were from the four AFSs in which job knowledge measures (see below) were included as part of the JPM data collection process (Aircrew Life Support Specialist, $\underline{n} = 229$; Precision Measurement Equipment Laboratory [PMEL] Specialist, $\underline{n} = 140$; Aerospace Ground Equipment [AGE] Mechanic, $\underline{n} = 269$; Personnel Specialist, $\underline{n} = 200$).

Procedure

Briefly, each participant in the JPM project was assessed in a work sample test battery developed specifically for their AFS. In order to reduce the likelihood of ceiling effects in work sample performance, tasks were sampled from occupational survey reports so that 40% of the work sample tasks were from the 4th (i.e., most difficult) quartile of task learning difficulty, 30% were from the 3rd quartile, 20% from the 2nd quartile, and 10% were from the 1st (easiest) quartile. Work sample performance was scored as a weighted (by relative criticality) percent of task steps completed correctly as recorded by the test administrator. Participants also indicated the number of times they had performed each task on the job prior to its being administered in the work sample test ("Number of Times Performed" or "NTP"). Finally, two additional

measures reported here were collected prior to the examinee's arrival at the work sample test station: a) self-ratings of "...the amount of relevant on-the-job experience..." on each task that they would be asked to perform in the work sample test battery ("Task Experience Ratings" or "TERs:"1 = No or almost none, to 7 = A very great amount), and b) supervisory performance ratings on the same tasks ("Supervisory Ratings:" 1 = Never meets acceptable level of proficiency to 5 = Always exceeds acceptable level of proficiency). Additional details of the USAF JPM project are given in Hedge and Teachout (1992), Lance, Teachout, and Donnelly (1992), and Laue, Hedge, Wall, Pederson, and Bentley (1992).

Measures

Cognitive ability. Research participants had completed the Armed Services Vocational Aptitude Battery (ASVAB) as part of their enlistment requirements. The ASVAB contains 10 subtests which are used for personnel accession and classification decisions across the Services. The Armed Forces Qualification Test (AFQT) is a composite of the four verbal and math ASVAB subtests (Word Knowledge, Paragraph Comprehension, Arithmetic Reasoning, and Mathematics Knowledge) and is accepted as a reliable (reliability of the AFQT is estimated at .90, Earles & Ree, 1992) and valid indicator of general cognitive ability (g, Murphy, 1984; Ree & Earles, 1992). We used participants' pre-enlistment AFQT scores as measures of participants' cognitive abilities.

Job experience. Consistent with previous studies (e.g., Schmidt et al., 1986, 1988), we used the total number of months in the present assignment as the measure of job experience. Since all research participants were first-term airmen, this measure corresponded to their Total Active Federal Military Service (TAFMS, in months). Except for the occasional recording error, TAFMS is likely a nearly perfectly reliable measure of job experience. For purposes explained later, we assumed the reliability of TAFMS to be .95.

Task experience. We measured task experience as a composite of participants' reports of the number of times they had previously performed each work sample task (NTP) and their task experience ratings (TERs). Previous research (Lance et al., 1989; Lance, Parisi, Bennett, Teachout, Harville, & Welles, in press) has found that NTP ratings are markedly skewed and multimodal. We computed a transformed NTP (TNPT) as in previous studies to more approximately normalize NTP and equate its scale

with TERs as 1 = 0 NTP, 2 = 1 to 10 NTP, 3 = 11 to 20 NTP, 4 = 21 to 50 NTP, 5 = 51 to 100 NTP, 6 = 101 to 800 NTP, and 7 = 801 to 999 NTP. For each task, task experience was computed as the mean of TNTP and TER. Overall, task experience (TaskExp) was measured as the mean task experience across all work sample tasks attempted (mean Cronbach's alpha across the four samples = .729).

Job knowledge. Written multiple choice job knowledge tests were developed specifically around the tasks that were included in each AFS's work sample test battery, and were administered to participants prior to the work sample test administration. For example, sample job knowledge items tied to the AGE Mechanic work sample task "Splice electrical system wiring" included "What splicing method requires the use of a barrel splice?" "What is meant by crimping a connector?" and "When is it necessary to apply flux to a connector before soldering?" The number of items in the job knowledge tests ranged between 93 (PMEL Specialist) to 159 (AGE Mechanic). Job knowledge test scores (JKTSs) were computed as the percentage of items answered correctly (mean Cronbach's alpha across the four samples = .704).

Job proficiency. As mentioned earlier, work sample test items were scored as a weighted percentage of task steps completed correctly. We measured job proficiency as the mean work sample test item score across all work sample items performed (mean Cronbach's alpha = .581).

Supervisor ratings. Supervisory ratings were measured as the mean task performance rating corresponding to tasks included in the work sample test battery (mean Cronbach's alpha = .887).

Motivational aspects of performance. Two indices related to "will-do" aspects of performance (previously reported by Borman et al., 1991) were available from participants' personnel records. Disciplinary actions was coded from Unfavorable Information Files (UIF) as 0 = None, 1 = Minor infraction, 2 = Moderate infraction, or 3 = Serious infraction leading to court-martial. Awards was measured as the number of military awards and commendations received. As with TAFMS, we assumed that except for infrequent coding errors and perhaps processing delays, these measures also would be nearly perfectly reliable. Thus we estimated their reliabilities at .95.

Aptitude x experience cross-products. In order to test aptitude x experience interaction hypotheses, we created two cross-product terms for analyses by a) centering AFQT, TAFMS, and TaskExp scores (i.e., calculating scores' deviations about their respective means), and b) multiplying corresponding

deviation scores. These deviation cross products (i.e., AFQT*TAFMS and AFQT*TaskExp) carry the appropriate interaction terms necessary to test moderator hypotheses.

Analyses

Consistent with previous research (e.g., Borman et al., 1991; Hunter, 1983; Schmidt et al., 1986), we computed meta-covariances for analysis (Jöreskog & Sörbom, 1993). Specifically, we a) computed correlations (rs) and standard deviations (SDs) among study variables in each sample, b) transformed rs to zs, c) calculated sample-size weighted mean zs and SDs across samples, d) backtransformed the mean zs to rs and e) input the mean rs and SDs to the LISREL 8.14 program for analysis of the meta-covariance matrix. Also consistent with previous research, the models we tested were manifest variable models. Nevertheless, we chose to correct for attenuation in model parameter estimates due to measurement error by fixing a) the factor loading of each observed measure on its underlying construct (i.e., elements in LISREL's Λ_Y matrix) to the square root of its estimated reliability (i.e., $[r_{YY'}]^{1/2}$), and b) the variables' residual variances (i.e., elements of LISREL's Θ_ε matrix) to $(1-r_{YY'})*\sigma^2_{Yi}$, where σ^2_{Yi} refers to the observed measures' variances (see Bollen, 1989; Farkas & Tetrick, 1989; Williams & Hazer, 1986). We chose not to correct for range restriction on the exogenous variables because a) incumbent populations usually are restricted on cognitive ability due to pre-employment selection on g-related selectors, b) research participants' experience levels were within the ranges studied previously by Schmidt et al. (1988), and c) the numbers of disciplinary actions taken and the numbers of awards given are truly restricted in the population from which our samples were obtained (first-term airmen).

Models tested. We performed two sets of analyses in parallel, with experience operationalized in terms of Job Experience and Task Experience, respectively. In each set we performed a series of nested model comparisons as recommended by Williams and Holahan (1994) and others. Beginning with the most restrictive model, we fit an uncorrelated factors model which, since each variable was operationalized using a single indicator, corresponded to a Null model (i.e., $\Sigma(\Theta) = \sigma^2_{Yi}*I$). Second, we fit a Structural Null model, in which covariances among exogenous variables (Aptitude, Experience, the AxE Interaction, Disciplinary Actions, and Awards) were free parameters to be estimated, but no causal effects were estimated between them and the endogenous variables (Job Knowledge, Job Proficiency, and Supervisory

Ratings), or among the endogenous variables.[2] The difference in model fit between the Null and Structural Null models provides an assessment of the interrelatedness of the exogenous variables. Third, we fit a complete mediation model that included Linear Effects Only from Aptitude and Experience to Job Knowledge, from Job Knowledge to Job Proficiency, and from Job Proficiency, Disciplinary Actions and Awards to Supervisory Ratings. The difference in fit between the Structural Null and Linear Effects Only models provides an assessment of the viability of causal connections proposed by Borman et al. (1991). Fourth, we fit a Complete Mediation model that included the additional effect of the AxE interaction on Job Knowledge. The difference in fit between the Linear Effects Only and Complete Mediation models evaluates possible Aptitude x Experience interactive effects on Job Knowledge. Fifth, we fit a Partial Mediation model that included the additional linear effects of Aptitude and Experience on Job Proficiency and Supervisory Ratings. The difference in fit between the Complete Mediation and Partial Mediation models tests whether Job Knowledge completely mediates the effects of Aptitude and Experience on Job Proficiency and Supervisory Ratings (as suggested by Borman et al., 1991), or whether there are direct effects as well (as suggested by Schmidt et al., 1986). Finally, we fit a Saturated Structural model to determine whether there existed direct AxE interaction effects on either Job Proficiency or Supervisory Ratings.

Model fit. We evaluated overall model fit in terms of a) the overall χ^2 statistic, b) the standardized root mean squared residual (RMSR) of the difference between the sample and reproduced covariance matrices, c) Bentler and Bonett's (1980) normed fit index (NFI), and d) Bentler's (1990) comparative fit index (CFI). We also evaluated differences in models' fit in terms of the difference χ^2 statistic ($\Delta\chi^2$).

[2] Consistent with Jaccard and Wan (1995), however, the covariances between the AxE interaction term and its constituent linear terms were restricted equal to zero.

Table 1

Study Variables' Standard Deviations and Intercorrelations

Variable	SD	Intercorrelations								
		1	2	3	4	5	6	7	8	9
1. Incumbent Aptitude	17.02	1.00								
2. Task Experience	.65	.01	1.00							
3. Aptitude x Task Exp.	11.40	-.10*	.01	1.00						
4. Job Experience	10.73	.13*	.39*	-.04	1.00					
5. Aptitude x Job Exp.	183.80	.00	-.04	.41*	-.02	1.00				
6. Job Knowledge	.11	.24*	.23*	-.07	.22*	-.02	1.00			
7. Job Proficiency	1.18	.16*	.28*	-.03	.31*	-.04	.38*	1.00		
8. Disciplinary Actions	.32	-.05	-.02	.01	-.04	.02	-.05	-.08	1.00	
9. Number of Decorations	.25	-.02	.04	-.03	.26*	-.08	.09	.08	-.06	1.00
10. Supervisor Ratings	.66	.05	.24*	.03	.22*	-.05	.21*	.27*	-.11*	.15*

* $p < .01$

Results

Study variables' standard deviations (SDs) and intercorrelations are shown in Table 1. The correlation between Aptitude and Task Experience was negligible ($r = .01$), but the positive correlation between Aptitude and Job Experience ($r = .13$) indicates some tendency for lower-aptitude airmen to select out (or be separated from) of the USAF over the first term of enlistment. Second, the relatively low correlation between Job and Task Experience ($r = .39$) supports the idea that they reflect different Experience constructs (Quiñones et al., 1995). Third, low correlations between the AxE interactions and their constituent terms indicate that mean-centering effectively isolated the interaction components of interest. Fourth, "can-do" aspects of performance (i.e., Aptitude and Experience) were largely unrelated to "will-do" aspects of performance (i.e., Disciplinary Actions and Awards). The one exception was a positive relationship between Job Experience and Awards, indicating that longer-tenured airmen had longer windows of opportunity to receive one or more awards. Finally, endogenous variables were significantly correlated with their putative causes.

Table 2

Overall Model Goodness-of-Fit Indices

		Job Experience Model				Task Experience Model			
	df	χ^2	RMSR	NFI	CFI	χ^2	RMSR	NFI	CFI
Saturated Structural	6	4.82	.014	.99	1.00	17.20	.028	.95	.97
Partial Mediation	8	5.97	.016	.98	1.00	19.01	.029	.95	.97
Complete Mediation	13	41.81*	.036	.89	92	54.96*	.045	.84	.87
Linear Effects Only	14	42.28*	.038	.89	.92	56.69*	.046	.84	.87
Structural Null	20	319.00*	.130	.18	.18	346.26*	.130	.02	.00
Null	28	390.60*	--	--	--	353.03*	--	--	--

Note. RMSR = Standardized root mean squared residual, NFI = normed fit index, CFI = comparative fit index.

- $p < .001$.

Table 2 shows overall goodness of fit statistics for the Job and Task Experience models tested. All indications were that the Partial Mediation model provided the best fit to the data: the χ^2 statistics were nonsignificant for both the Job and Task Experience models, RMSRs were below .03, and NFIs and CFIs were larger than .95 in both cases. More specific model comparisons indicated that a) exogenous variables were significantly interrelated for the Job Experience model (Null vs. Structural Null models $\Delta\chi^2(8) = 71.60$, $p < .001$), but not for the Task Experience model ($\Delta\chi^2(8) = 6.77$, $p > .05$). Both models supported hypotheses of mediated linear relationships of the form hypothesized by Borman et al. (1991) (Structural Null vs. Linear Effects Only models $\Delta\chi^2(6) = 276.72$, $p < .001$ and 289.57; $p < .001$, for the Job and Task Experience models, respectively), but neither supported Aptitude x Experience interactive effects on Job Knowledge (Linear Effects Only vs. Complete Mediation models $\Delta\chi^2(1) = .47$, $p > .05$, and 1.73; $p > .05$, for the Job and Task Experience models, respectively). Both models also supported the ideas that Job Knowledge only partially (and not completely) mediates effects of Aptitude and Experience on other endogenous variables (Complete Mediation vs. Partial Mediation models $\Delta\chi^2(5) = 35.84$, $p < .001$, and 35.95; $p < .001$, for the Job and Task Experience models, respectively), and that there were no Aptitude x Experience interaction effects on either Job Proficiency or Supervisor ratings (Partial Mediation vs. Saturated Structural models $\Delta\chi^2(2) = 1.15$, $p > .05$, and 1.81; $p > .05$, for the Job and Task Experience

models, respectively). Nevertheless, somewhat different patterns of results were obtained for the Job versus Task Experience models.

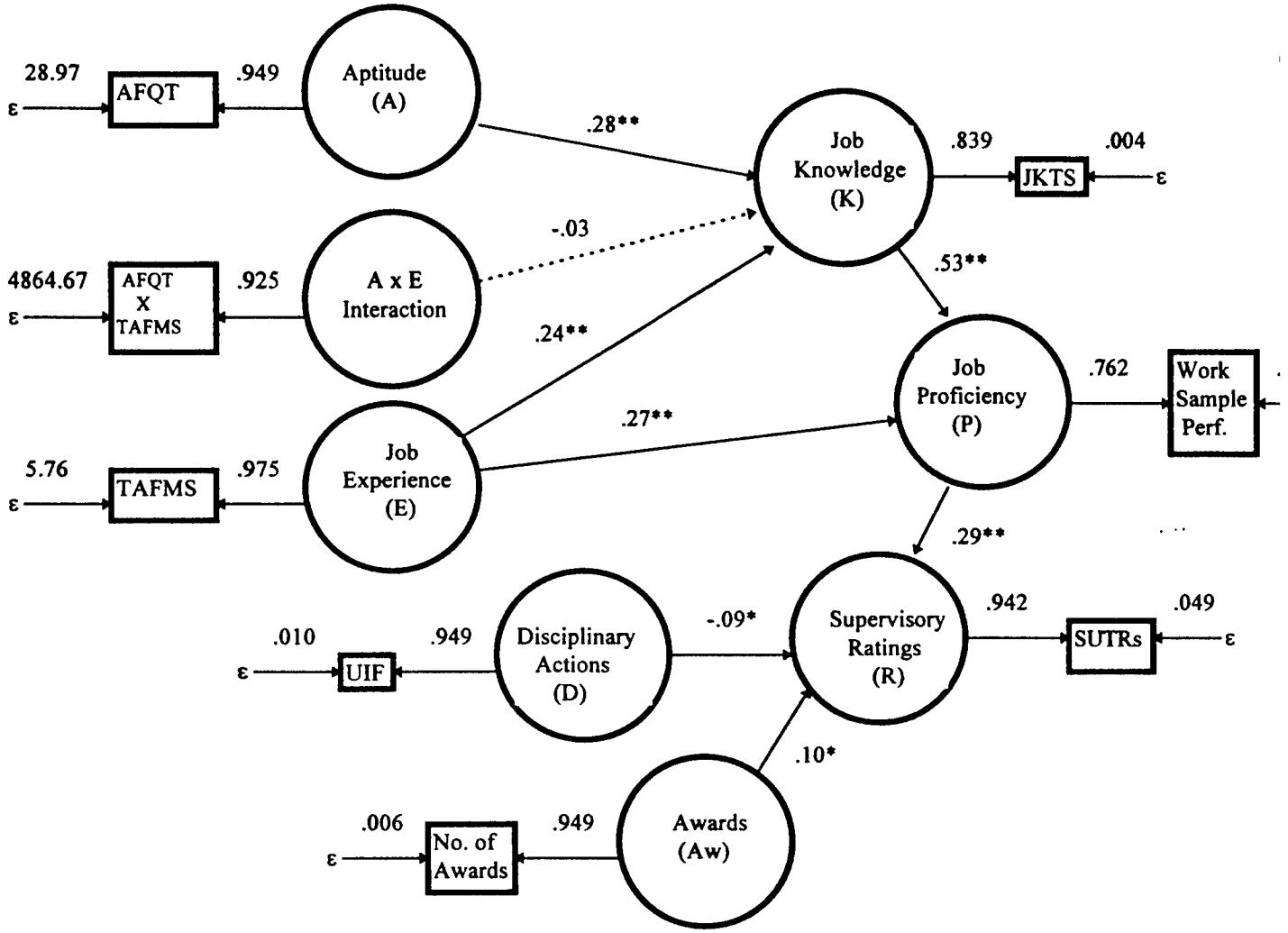

Figure 2. Results for Job Experience Model.

Figures 2 and 3 show standardized structural parameters (path coefficients) for the Job and Task Experience models, respectively. Results shown for the Job Experience model in Figure 2 are largely consistent with previous tests of similar models. As in Schmidt et al. (1986) and Borman et al. (1991), results support the idea that Job Knowledge mediates exogenous variables' effects on Job Proficiency and Supervisor Ratings. Also, as in Borman et al. (1991), Supervisor Ratings reflect the influence of both

"can-do" aspects of performance (i.e., Job Proficiency) and "will-do" aspects (i.e., Disciplinary Actions and Awards). Also consistent with Schmidt et al. (1986) Job Experience had a direct effect on Job Proficiency as well as an indirect effect through Job Knowledge. Thus, results indicate that the primary benefit of Cognitive Ability is in terms of facilitating learning the job, whereas Job Experience benefits both job learning and actual proficiency in performing job duties.

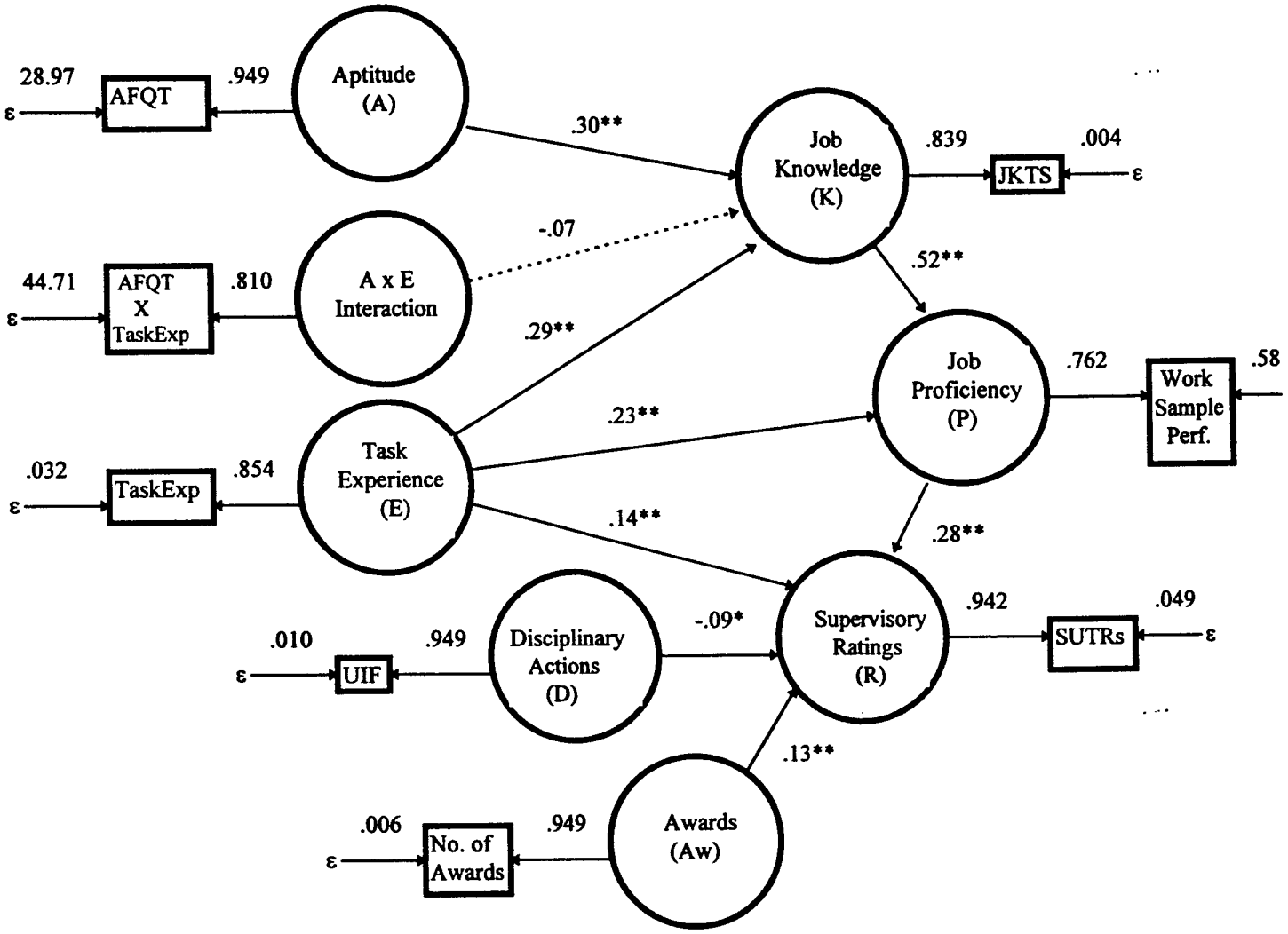

Figure 3. Results for Task Experience Model.

Results for the Task Experience model (shown in Figure 3) are similar for the Job Experience model but here Task Experience plays a larger role: in addition to enhancing Job Knowledge and Job Proficiency, Task Experience also had a direct effect on Supervisory Ratings. Thus Task Experience, as it is tied more closely to the tasks actually performed on the job (vs. simply the length of time spent on the job), appears to facilitate learning the job (i.e., enhances Job Knowledge), enhance Job Proficiency directly (from increased opportunities to perform job tasks), and affect Supervisor Ratings.

Discussion

The first purpose of this study was to test the form of the effects of cognitive ability and experience on job knowledge. Although there is some evidence of ability x experience interactive effects on performance (Lance et al., 1989), the present findings supported other empirical literature which indicates only linear and additive effects (e.g., McDaniel et al., 1988). Failure to detect significant ability x experience interaction effects may reflect general difficulties in the detection of moderated relationships in nonexperimental data (McClelland & Judd, 1993), or that these effects are, in fact, linear in the population. Failure to detect ability x experience interaction effects might also be attributable to direct range restriction on ability due to the USAF's selection of participants, in part, on the basis of their AFQT scores. One other possibility is that participants' mean level of experience (all participants were in their first term of enlistment) was too short for the proposed interactive effects (i.e., a "convergence" relationship, McDaniel et al., 1988) to unfold. Future research should investigate possible aptitude x experience interaction effects in samples with broader ranges of aptitude and over longer mean lengths of employee tenure to test these possibilities.

The second purpose of this study was to test whether different conceptualizations of "experience" played different roles in determining job knowledge, job proficiency, and supervisor ratings. Job and Task Experience were only modestly intercorrelated (r = .39), supporting the idea that they reflect different underlying Experience (i.e., time-related vs. amount-related) constructs. Yet, their operational roles in determining outcome variables were similar. Both exerted direct effects on Job Knowledge and Job Proficiency. We see these beneficial effects of Experience as arising from increased declarative knowledge

(effects on Job Knowledge) and procedural knowledge and skill (effects on Job Proficiency) (Campbell, 1990a). However, only Task Experience had a direct effect on Supervisory Ratings that was not mediated by actual Job Proficiency. This may reflect a tendency for supervisors to bias ratings in favor of incumbents who perform certain tasks more often, or the possibility that higher performers are more readily called upon to perform job tasks than are poorer performers (Ford, Quiñones, Sego, & Sorra, 1992). We see these as additional questions for future research.

The third purpose of this study was to test the mediational roles of job knowledge and job proficiency. Results were partially supportive of earlier research. As discussed in the previous paragraph, effects of Experience were only partially mediated by job knowledge and job proficiency, and this is consistent with Schmidt et al.'s (1986) previous findings. And consistent with Borman et al.'s (1991, 1995) work (but not Schmidt et al.'s), a complete mediational model was supported for the Aptitude → Job Knowledge → Job Proficiency → Supervisory Rating relationships. This supports the ideas that a) the primary benefit of aptitude is increased job knowledge through enhancement of declarative knowledge, b) declarative knowledge (Job Knowledge) facilitates the acquisition of procedural knowledge and skills (manifested in Job Proficiency), and c) Supervisor Ratings reflect how well incumbents do their jobs (Job Proficiency) and not what they know about it (Job Knowledge).

The final purpose of this study was to test effects of "can-do" and "will-do" aspects of performance on Supervisory Ratings. While the effects of the former generally were larger, both were significant. This points to the importance of considering "extra-role" behaviors or "contextual performance" (Borman & Motowidlo, 1993; Motowidlo & VanScotter, 1994) as well as "in-role" behaviors in models of job performance and performance rating (Campbell, 1990a). Future research should continue ongoing efforts at taxonomies of extra-role behaviors to complement existing models of prescribed work behaviors.

References

Austin, J. T., & Villanova, P. (1992). The criterion problem: 1917-1992. Journal of Applied Psychology, 77, 836-874.

Bentler, P. M. (1990) Comparative fit indices in structural models. Psychological Bulletin, 107, 238-246.

Bentler, P. M., & Bonett, D. G. (1980). Significance tests and goodness-of-fit in the analysis of covariance structures. Psychological Bulletin, 88, 588-600.

Bollen, K. (1989). Structural equations with latent variables. New York: Wiley.

Borman, W. C. (1991). Job behavior, performance, and effectiveness. In M. D. Dunnette & L. M. Hough (Eds.), Handbook of industrial and organizational psychology (2nd ed.) (Vol. 2) (pp. 271-326). Palo Alto, CA: Consulting Psychologists.

Borman, W. C., & Motowidlo, S. J. (1993). Expanding the criterion domain to include elements of contextual performance. In N. Schmitt & W. C. Borman (Eds.), Personnel selection in organizations (pp. 71-98). San Francisco: Jossey-Bass.

Borman, W. C., White, L. A., & Dorsey, D. W. (1995). Effects of task performance and interpersonal factors on supervisor and peer performance ratings. Journal of Applied Psychology, 80, 168-177.

Borman, W. C., White, L. A., Pulakos, E. D., & Oppler, S. H. (1991). Models of supervisory job performance ratings. Journal of Applied Psychology, 76, 863-872.

Campbell, J. P. (1990a). Modeling the performance prediction problem in industrial and organizational psychology. In M. D. Dunnette & L. M. Hough (Eds.), Handbook of industrial and organizational psychology (2nd ed.) (Vol. 1) (pp. 687-732). Palo Alto, CA: Consulting Psychologists.

Campbell, J. P. (1990b). The role of theory in industrial and organizational psychology. In M. D. Dunnette & L. M. Hough (Eds.), Handbook of industrial and organizational psychology (2nd ed.) (Vol. 1) (pp. 39-73). Palo Alto, CA: Consulting Psychologists.

Campbell, J. P., Dunnette, M. D., Lawler, E. E., & Weick, K. E. Jr. (1970). Managerial behavior, performance and effectiveness. New York: McGraw-Hill.

Dunnette, M. D. (Ed.), (1976). Handbook of industrial and organizational psychology. Chicago: Rand McNally.

Dunnette, M. D., & Hough, L. M. (Eds.) (1990). Handbook of industrial and organizational psychology (2nd. Ed.) (Vol. 1). Palo Alto, CA: Consulting Psychologists.

Dunnette, M. D., & Hough, L. M. (Eds.) (1991). Handbook of industrial and organizational psychology (2nd. Ed.) (Vol. 2). Palo Alto, CA: Consulting Psychologists.

Dunnette, M. D., & Hough, L. M. (Eds.) (1992). Handbook of industrial and organizational psychology (2nd. Ed.) (Vol. 3). Palo Alto, CA: Consulting Psychologists.

Earles, J. A., & Ree, M. J. (1992). The predictive validity of ASVAB for training grades. Educational and Psychological Measurement, 52, 721-725.

Farkas, A. J., & Tetrick, L. E. (1989). A three-wave longitudinal analysis of the causal ordering of satisfaction and commitment on turnover decisions. Journal of Applied Psychology, 74, 855-868.

Ford, J. K., Quiñones, M. A., Sego, D. J., & Sorra, J. (1992). Factors affecting the opportunity to perform trained tasks on the job. Personnel Psychology, 45, 511-527.

Guion, R. M. (1991). Personnel assessment, selection, and placement. In M. D. Dunnette & L. M. Hough (Eds.), Handbook of industrial and organizational psychology (2nd ed.) (Vol. 2) (pp. 327-397). Palo Alto, CA: Consulting Psychologists.

Hedge, J. W., & Teachout, M. S. (1986). Job performance measurement: A systematic program of research and development. (AFHRL-TP-86-37). Brooks AFB, TX: Air Force Human Resources Laboratory, Training Systems Division.

Hedge, J. W., & Teachout, M. S. (1992). An interview approach to work sample criterion measurement. Journal of Applied Psychology, 77, 453-461.

Hunter, J. E. (1983). A causal analysis of cognitive ability, job knowledge, job performance, and supervisory ratings. In F. Landy, S. Zedeck, & J. Cleveland (Eds)., Performance measurement and theory (pp. 257-266). Hillsdale, NJ: Erlbaum.

Hunter, J. E., & Hunter, R. F. (1984). Validity and utility of alternative predictors of job performance. Psychological Bulletin, 96, 72-98.

Jaccard, J., & Wan, C. K. (1995). Measurement error in the analysis of interaction effects between continuous predictors using multiple regression: Multiple indicator and structural equation approaches. Psychological Bulletin, 117, 348-357.

Jöreskog, K. G., & Sörbom, D. (1993). LISREL 8 user's guide. Chicago, IL: Scientific Software.

Kavanagh, M. J., Borman, W. C., Hedge, J. W., & Gould, R. B. (1987). Job performance measurement in the military: A classification scheme, literature review, and directions for research. (AFHRL-TR-87-15). Brooks AFB, TX: Air Force Human Resources Laboratory, Manpower and Personnel Division.

Lance, C. E., Hedge, J. W., & Alley, W. E. (1989). Joint relations of task proficiency with ability, experience, and task difficulty: A cross-level, interactional study. Human Performance, 2, 249-272.

Lance, C. E., Parisi, A. G., Bennett, W. Jr., Teachout, M. S., Harville, D. L., & Welles, M. L. (in press). Moderators of skill retention interval/performance decrement relationships in eight U.S. Air Force enlisted specialties. Human Performance.

Lance, C. E., Teachout, M. S., & Donnelly, T. M. (1992). Specification of the criterion construct space: An application of hierarchical confirmatory factor analysis. Journal of Applied Psychology, 77, 437-452.

Landy, F. L., Zedeck, S., & Cleveland, J. (1983). Performance measurement and theory. Hillsdale, NJ: Erlbaum.

Laue, F. J., Hedge, J. W., Wall, M. L., Pederson, L. A., & Bentley, B. A. (1992). Job performance measurement system development process. (AL-TR-1992-0120). Brooks AFB, TX: Armstrong Laboratory, Human Resources Directorate, Technical Training Research Division.

McClelland, G. H., & Judd, C. M. (1993). Statistical difficulties of detecting interactions and moderator effects. Psychological Bulletin, 114, 376-390.

McDaniel, M. A., Schmidt, F. L., & Hunter, J. E. (1988). Job experience correlates of job performance. Journal of Applied Psychology, 73, 327-330.

Motowidlo, S. J., & VanScotter, J. R. (1994). Evidence that task performance should be distinguished from contextual performance. Journal of Applied Psychology, 79, 475-480.

Mumford, M. D., Weeks, J. J., Harding, F. D., & Fleishman, E. A. (1987). Measuring occupational difficulty: A construct validation against training criteria. Journal of Applied Psychology, 72, 578-587.

Murphy, K. R. (1984). Armed Services Vocational Aptitude battery. In D. J. Keiser & R. C. Sweetland (Eds.), Test critiques. Kansas City, MO: Test Corporation of America.

Pulakos, E. D., Schmitt, N., & Chan, D. (1996). Models of job performance ratings: An examination of ratee race, ratee gender, and rater level effects. Human Performance, 9, 103-119.

Quiñones, M. A., Ford, J. K., & Teachout, M. S. (1995). The relationship between work experience and job performance: A conceptual and meta-analytic review. Personnel Psychology, 48, 887-910.

Ree, M. J., Carretta, T. R., & Teachout, M. S. (1995). Role of ability and prior knowledge in complex training performance. Journal of Applied Psychology, 80, 721-730.

Ree, M. J., & Earles, J. A. (1992). Intelligence is the best predictor of job performance. Current Directions in Psychological Science, 1, 86-89.

Schmidt, F. L., Hunter, J. E., & Outerbridge, A. N. (1986). Impact of job experience and ability on job knowledge, work sample performance, and supervisory ratings of job performance. Journal of Applied Psychology, 71, 432-439.

Schmidt, F. L., Hunter, J. E., Outerbridge, A. N., & Goff, S. (1988). Joint relation of experience and ability with job performance: Test of three hypotheses. Journal of Applied Psychology, 73, 46-57.

Triandis, H. C., Dunnette, M. D., & Hough, L. M. (Eds.) (1994). Handbook of industrial and organizational psychology (2nd. Ed.) (Vol. 4). Palo Alto, CA: Consulting Psychologists.

Waldman, D. A., & Spangler, W. D. (1989). Putting together the pieces: A closer look at the determinants of job performance. Human Performance, 2, 29-59.

Weeks, J. (1984). Occupational learning difficulty: A standard for determining the order of aptitude requirement minimums. (AFHRL-SR-84-26). Brooks AFB, TX: Air Force Human Resources Laboratory, Manpower and Personnel Division.

Wigdor, A. K., & Green, B. F. Jr. (Eds). (1991). Performance assessment for the workplace. Washington, DC: National Academy Press.

Williams, L. J., & Hazer, J. T. (1986). Antecedents and consequences of satisfaction and commitment in turnover models: A reanalysis using latent variable structural equation methods. Journal of Applied Psychology, 71, 219-231.

Williams, L. J., & Holahan, P. J. (1994). Parsimony-based fit indices for multiple-indicator models: Do they work? Structural Equation Modeling, 1, 161-189.